Characterisation of potential regulators of PAMP-triggered immunity

A thesis submitted to the University of East Anglia for the degree of Doctor of Philosophy

Roda Niebergall

The Sainsbury Laboratory

John Innes Centre

Norwich, UK

September 2012

Abstract

An essential part of plant innate immunity is the perception of pathogen-associated molecular patterns (PAMPs) through surface-localised pattern-recognition receptors (PRRs). EFR and FLS2 are well characterised PRRs, which recognise the bacterial elongation factor Tu and flagellin, respectively. A variety of downstream responses upon PAMP perception have been described. However, it is still poorly understood how EFR- and FLS2-dependent signalling is mediated. Here, I used two different approaches in order to identify novel components of both signalling pathways.

First, I characterised seven candidate genes of a predicted flagellin-dependent gene expression network, which are predicted to regulate each other's expression in a flagellin-dependent manner, and therefore, are potentially involved in the FLS2 signalling pathway. Further characterisation revealed that mutation of at least three of the seven candidate genes was affecting flg22-mediated signalling.

In addition, I characterised a predicted protein phosphatase 2C (PP2C), which had been identified in a yeast two-hybrid screen with the EFR cytoplasmic domain and was therefore referred to as PIE (PP2C-interacting with EFR). Using Co-IP experiments, I confirmed that PIE associates with EFR *in planta*. Furthermore, PIE also associates with FLS2 and BIK1, a co-regulator of both PRRs, *in planta.* Interestingly, PIE dissociates from both the EFR and FLS2 complexes upon PAMP perception. PIE expressed *in planta* and in *E. coli* exhibits protein phosphatase activity and we showed that PIE dephosphorylates EFR, FLS2 and BIK1 *in vitro*. As expected from bio-informatic predictions, I confirmed that PIE is phosphorylated upon PAMP perception. Furthermore, I demonstrated that EFR and FLS2 kinase activities are partially required for PIE phosphorylation. Both *PIE* overexpression and *pie* knock-down lines display reduced PAMP-triggered responses, indicating that an optimal *PIE* expression level is required for proper induction of signalling. All together, these results imply that PIE is a novel regulator of the EFR and FLS2 signalling pathway.

TABLE OF CONTENTS

List of Figures

List of Tables

Acknowledgements

Pursuing a Ph.D. is both a painful and exciting journey. There are weeks filled with frustration, solitude and self-doubt. And then along the way there are this short moments of pure beauty that make it all worth it. And then by the time I finally reached my destination, I realized that in the end, I never travelled alone. Because after all a Ph.D. is a team effort and I would like to express my gratitude to all those, who “travelled” with me.

First of all, I would like to thank my supervisor, Dr Cyril Zipfel, who constantly offered his advice, shared his knowledge and “pushed” me in the right direction. Without your enthusiasm the PIE-story would have never made it so far.

I would also like to thank the two other members of my supervisory committee, Dr Silke Robatzek and Prof. Dr Sophien Kamoun. You constantly made me aware of the weaknesses of my project but always offered a helping hand. Your doors were always open and you were more than happy to discuss my work with me.

I am also grateful for the help of all CZ lab members. Everyone one of you has their own character and it was a pleasure to work with you guys. I am particular thankful for everyone who helped to develop the PIE-story: Vardis, Daniel, Alberto….

I especially would like to thank Alberto, Jacqui, Cecile and Rosa, who patiently helped to correct my Thesis. I would have been lost without you guys.

Lena, thanks for being my office mate - it was a pleasure to share the Berlin office with you. And also many thanks to Frederikke for home-cooked meals and movie nights.

And because there is also a life outside of the lab, I would like to thank my family and friends, but especially my father - you always made me aware of what really matters in life. You are my biggest supporter!

Abbreviations

ABA	Abscisic acid
ABA3	ABA DEFICIENT 3
ABI	ABA-INSENSITIVE
ACA	AUTOINHIBITED CA^{2+}-ATPASE
ACS	ACC-synthase
AD	Activation domain
ADP	Adenosine diphosphate
AHA	ARABIDOPSIS H^{+}-ATPase
AP2C	Arabidopsis phosphatase 2C
*At*PP2-B6	*Arabidopsis thaliana* PHLOEM PROTEIN 2-B6
ATP	Adenosintriphosphat
At	*Arabidopsis thaliana*
*At*MIN7	*A. thaliana* HopM1 interactor 7
AP2C	ARABIDOPSIS PHOSPHATASE 2C
ARF	ADP ribosylation factor
ANS	ANTHOCYANIDIN SYNTHASE
Avr	Avirulence
Ax21	Activator of XA21-mediated immunity
BAK1	BRI1 ASSOCIATED KINASE 1
BAPTA	1,2-bis(o-aminophenoxy)ethane- N,N,N',N'-tetraacetic acid
BD	Binding domain
BIK1	Botrytis-induced kinase
BIP3	BINDING PROTEIN 3
BKI1	BRI1 KINASE INHIBITOR 1
BKK1	BAK1-LIKE 1
BR	Brassinosteroids
BRI1	BRASSINOSTEROID INTENSIVE 1
BSMT1	S-ADENOSYLMETHIONINE-DEPENDENT METHYL-TRANSFERASE 1
C4H	CINNAMATE 4-HYDROXYLASE
CaM	Calmodulin
CAPS	Cleaved amplified polymorphic sequence
CBL	Calcineurin B-like
CC	Coiled-coil
CDPK	Calcium-dependent protein kinase
Cf9	*Cladosporium fulvum* resistance gene 9
CERK1	CHITIN ELICITOR RECEPTOR KINASE 1
CEBiP	Chitin elicitor binding protein
DFR	DIHYDROFLAVONOL 4-REDUCTASE
CLV1	CLAVATA 1
CNGC2	Cyclic nucleotide-gated cation channel 2
COI1	CORONATINE INSENSITIVE 1
Co-IP	Co-Immunoprecipitation
COR	Coronatine
CPS	Cold shock protein
CTR1	CONSTITUTIVE TRIPLE RESPONSE 1
DAMP	Damage-associated molecular pattern
DAR	DA1-RELATED
DTT	Dithiothreitol
EAR	ERF-associated Amphiphilic Repression
EDS1	ENHANCED DISEASE SUSCEPTIBILITY 1
EDTA	Ethylenediaminetetraacetic acid
EGF	Epidermal growth factor

eGFP	Enhanced green fluorescent protein
EGTA	Ethylene glycol tetraacetic acid
EHD	EH domain
EFR	EF-TU RECEPTOR
ERF104	ETHYLENE RESPONSE FACTOR 104
EF-Tu	Elongation factor Tu
EIL	EIN2-like proteins
EIN3	ETHYLENE-INSENSITIVE 3
EIX	Ethylene-inducing xylanase
ER	Endoplasmic reticulum
ET	Ethylene
ETI	Effector-triggered immunity
ETS	Effector-triggered susceptibility
FLS2	FLAGELLIN-SENSING 2
FRK1	FLG22-INDUCED RECEPTOR-LIKE KINASE 1
G3Pp4	GLYCEROL-3-PHOSPHATE PERMEASE 4
GA	Giberellic acid
GAI	GA-INSENSITIVE
GBP	GLUCAN BINDING PROTEIN
GCN5	GENERAL CONTROL NON-REPRESSIBLE 5
GEF	Guanine nucleotide exchange factor
GFP	Green fluorescent protein
GPA1	G PROTEIN ALPHA SUBUNIT 1
GPI	glycosylphosphatidyl-inositol
GSL5	GLUCAN SYNTHASE-LIKE 5
GST	Glutathione S-transferase
HA	Hemagglutinin
HAB1	HOMOLOGY TO ABA-INSENSITIVE 1
HLH	Helix-loop-helix
HR	Hypersensitive response
HrpZ	Hairpin
HypSys	Hydroxyproline-rich systemins
ICS1	ISOCHORISMATE SYNTHASE 1
IP	Immunoprecipitation
JA	Jasmonic acid
JA-Ile	Jasmonoyl–isoleucine
JAZ	JASMONATE ZIM-domain-containing
KAPP	Kinase associated protein phosphatase
Km	Michaelis constant
Le	*Lycopersicon esculentum*
LecRK-V.5	LECTIN RECEPTOR KINASE-V.5
LIM	Lin11, Isl-1 and Mec-3
LPS	Lipopolysaccharide
LRR	Leucine-rich repeat
LysM	lysine motif
MAP-kinase	Mitogen-activated protein kinase
MBP	maltose binding protein
MEKK	Mitogen-activated protein kinase kinase
MKP	MPK phosphatase
MP2C	MEDICAGO PHOSPHATASE 2C
NADPH	Nicotinamide adenine dinucleotide phosphate
NAC	Petunia NAM and *Arabidopsis* ATAF1, ATAF2, and CUC2
NASC	Nottingham Arabidopsis Stock Centre
NaF	Sodium fluoride
$NaVO_3$	Sodium metavanadate

NB	Nucleotide binding
NDR1	NON-RACE-SPECIFIC DISEASE RESISTANCE
NOS	Reactive nitrogen species
NPR1	NONEXPRESSER OF PR GENES 1
Nt	*Nicotiana tabacum*
OG	Oligogalacturonides
Os	Oryza sativa
OST1	OPEN STOMATA 1
PAMP	Pathogen-associated molecular pattern
PAD4	PHYTOALEXIN DEFICIENT 4
PAPP2C	PHYTOCHROME-ASSOCIATED PROTEIN PHOSPHATASE TYPE 2C
PBL	AVRPPHB SUSCEPTIBLE 1-like
PEPR	Pep-receptor
PGIP	Polygalacturonaseinhibiting protein
PGN	Peptidoglycan
PIA1	PP2C INDUCED BY AVRRPM1
PIE	PP2C-INTERACTING WITH EFR
PLL	POLTERGEIST-like
PMR4	POWDERY MILDEW RESISTANT 4
POL	POLTERGEIST
PP1	Protein phosphatases type 1
PP2A	Protein phosphates 2A
PP2B	Protein phosphates 2B
PP2C	Protein phosphates 2C
PP2CA	PROTEIN PHOSPHATASE 2CA
PPM	Mg^{2+}-dependent protein phosphatases
PPP	Phosphoprotein phosphatases
PR	Pathogenesis-related
PRR	Pattern-recognition receptor
PTI	Pattern-triggered immunity
Pto	*Pseudomonas syringae* pv. *tomato*
PTP	Protein tyrosine phosphatase
PUB	PLANT U-BOX
qRT-PCR	quantitative real-time polymerase chain reaction
R	Resistance
RALF	Rapid alkalinization factor
RIN4	RPM1-INTERACTING PROTEIN 4
RbohD	Respiratory burst oxidase homologues D
RGL	RGA-LIKE1
RGA	REPRESSOR OF GA1-3
RLK	Receptor-like kinase
RLK5	RECEPTOR-LIKE PROTEIN KINASE 5
RLP	Receptor-like protein
RNP	Ribonucleoprotein
RPW8.2	RESISTANCE TO POWDERY MILDEW 8.1
ROS	Reactive oxygen species
RPM1	RESISTANCE TO P. SYRINGAE PV MACULICOLA
RPS	RESISTANT TO P. SYRINGAE
SA	Salicylic acid
SAG101	SENESCENCE ASSOCIATED GENE 101
SAR	Systemic acquired resistance
SCF	Skp1-Cullin-F-box-protein complex
SDS-PAGE	SDS-PAGE (sodium dodecyl sulphate- polyacrylamide gel electrophoresis

SERK	SOMATIC EMBRYOGENESIS RECEPTOR-LIKE KINASE
SID2	SA INDUCTION DEFICIENT 2
SR160	SYSTEMIN RECEPTOR 160kDa
T3SS	Type 3 secretion system
TAL	Transcription Activator-Like
TBS	Tris buffered saline
TF	Transcription factor
TG	Tris/Glycine
TLR	Toll-like receptors
TIR	Toll/interleukin-1 receptor
TM	Transmembrane domain
UPA	UPREGULATED BY AVRBS3
VBF	VIP1-BINDING F-BOX PROTEIN
VIP1	VirE2-INTERACTING PROTEIN 1
WAK	Wall-associated kinase
WIN2	HOPW1-1-INTERACTING PROTEIN 2
WUS	WUSCHEL
XB	XA21-binding protein
Xoo	*Xanthomonas oryzae* pv. *oryzae*
Zm	*Zea maize*

Chapter 1: General introduction

1.1 Plant pathogen interactions- A broad overview

Plants are constantly exposed to a variety of potential pathogens. However, infection is only observed between a limited combination of plants and pathogens. In most cases, this is due to the fact that the plant does not support the pathogen's life style, consequently, they are called non-hosts (Thordal-Christensen, 2003). In addition, plants exhibit different constitutive defence mechanisms, which prevent microbes from entering and colonizing tissues. This includes pre-formed physical barriers, like the rigid cell wall and wax layers, or chemical barriers, like antimicrobial compounds (Thordal-Christensen, 2003; Nuernberger and Lipka, 2005). However, some pathogens manage to overcome these constitutive defence mechanisms and are able to invade their host plant by penetration of epidermal surfaces, through secretion of cell wall degrading enzymes or by entering through natural openings, such as stomata (Melotto et al., 2008). At this stage, invading pathogens face a multi-layered immune system that perceives attempted invasions and activates a variety of host defence responses.

An essential part of basal immunity is the perception of conserved pathogen structures, the so-called pathogen-associated molecular patterns (PAMPs) (Medzhitov and Janeway, 2002). In addition, plants are able to indirectly detect pathogen attack through perception of damage-associated molecular patterns (DAMPs), which are endogenous molecules that are released from the plant itself during infection (Boller and Felix, 2009). Recognition of PAMPs and DAMPs by surface-localised pattern-recognition receptors (PRRs) triggers a wide variety of defence responses and ultimately results in PAMP-triggered immunity (PTI). Pathogens thus evolved mechanisms to avoid host recognition or to suppress host defence responses, largely through the secretion of virulence effectors. Bacterial effectors are mostly secreted via the type-III secretion system (T3SS) into the cytoplasm of the host cells to induce effector-triggered susceptibility (ETS) (Chisholm et al., 2006; Jones and Dangl, 2006; Dodds and Rathjen, 2010). In turn, plants evolved resistance (R) proteins that detect directly or indirectly the presence or activity of these effectors. The recognition of pathogen effectors is often associated with localized cell death surrounding the infection site, a

phenomenon known as the hypersensitive response (HR), and results in effector-triggered immunity (ETI) (Jones and Dangl, 2006).

The dynamic evolutionary interplay between plants and their pathogens is illustrated by the zigzag model (Figure 1.1) (Jones and Dangl, 2006). According to this model, plants developed an immune system with increased sensitivity to trigger defence responses with increased intensity, while pathogens continuously evolved new mechanism to perturb these defence mechanisms.

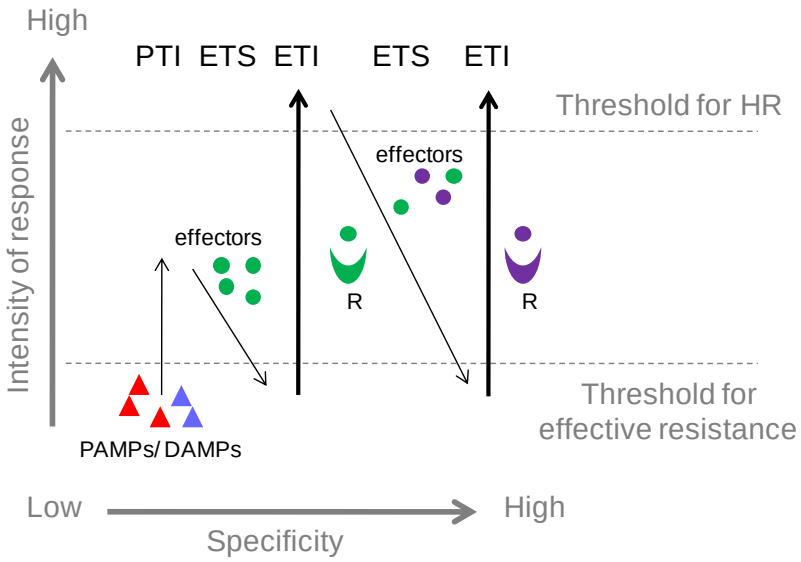

Figure 1.1: A zigzag model describes the "evolutionary arm-race" between plants and their surrounding pathogens
Plants recognize PAMPs and DAMPs through PRRs, resulting in PAMP-triggered immunity (PTI). In turn, successful pathogens deliver effectors that interfere with PTI, leading to effector-triggered susceptibility (ETS). Consequently, plants evolved R proteins, which detect effectors or sense their action and activate effector-triggered immunity (ETI). This "arm-race" proceeds when pathogens gain new effectors that help to suppress ETI. In turn, natural selection favours new plant R proteins that can recognize newly acquired effectors. Adapted from Jones and Dangl, 2006.

1.2 PAMPs, DAMPs and their respective PRRs

PAMPs are highly conserved molecular structures that are characteristic for a whole class of microorganisms and are generally essential for microbial survival (Medzhitov and Janeway, 2002). PAMPs are usually absent from the host organism, allowing the host to recognize them as non-self. However, since PAMPs are not only unique to pathogens but are also produced by non-pathogenic microorganisms, they are also referred to as MAMPs

(microbe-associated molecular patterns) (Mackey and McFall, 2006; He et al., 2007).

Recently, a second class of elicitors has been described, the so-called damage-associated molecular pattern. DAMPs are endogenous molecules that are thought to arise from the plant itself during pathogen attack, *e.g.* by degradation of the cell wall or by cleavage of precursor proteins to smaller peptides (Matzinger, 2002; Yamaguchi et al., 2006; Lotze et al., 2007). Thus, the perception of DAMPs enables plants to indirectly detect pathogens by monitoring events that occur during an infection.

PAMP and DAMP recognition activates a similar set of defence responses, indicating a partial convergence in the corresponding signalling pathways (Krol et al., 2010; Postel et al., 2010; Schulze et al., 2010). Both elicitors are perceived by surface-localized PRRs. Most plant PRRs are transmembrane receptor-like kinases (RLKs) or receptor-like proteins (RLPs) (Monaghan and Zipfel, 2012). RLKs and RLPs both contain an N-terminal ecto-domain, which provides the specific ligand recognition site, and a single-stranded transmembrane (TM) domain (Albert et al., 2010a; Monaghan and Zipfel, 2012). While RLKs also contain an intracellular kinase domain, RLPs have only a short cytosolic domain without an obvious signalling domain. Therefore, RLPs must most likely form a complex with signalling-capable proteins, such as RLKs (Albert et al., 2010a; Monaghan and Zipfel, 2012). So far only few PAMP-PRR pairs have been well characterised (Figure 1-2) and each will be discussed below.

1.2.1 Flagellin and FLS2

Flagellin, the main component of bacterial flagella, acts as a PAMP in vertebrates and most of the higher plants (Felix et al., 1999; Ramos et al., 2004). However, the flagellin-perception systems of animals and plants recognise different epitopes of the protein, indicating that the corresponding receptors evolved independently (Ausubel, 2005; Zipfel and Felix, 2005; Boller and Felix, 2009).

In most plant species, the flg22 epitope, which represents 22 amino acids of the conserved N-terminus of flagellin, is sufficient to activate defence

responses including callose deposition, ethylene (ET) accumulation, production of reactive oxygen species (ROS) and seedling growth inhibition (Felix et al., 1999; Gómez-Gómez et al., 1999; Asai et al., 2002). Notably, pre-treatment with flg22 also reduces susceptibility to the pathogenic bacterium *Pseudomonas syringae* pv. *tomato* (*Pto*) DC3000 (Zipfel et al., 2004). The *Arabidopsis* flagellin receptor FLS2 (FLAGELLIN SENSITIVE 2) was identified in a screen for mutants with reduced flg22-induced seedling growth inhibition, and cross-linking experiments confirmed that FLS2 exhibits flg22-binding affinity (Figure 1.2) (Gómez-Gómez and Boller, 2000; Chinchilla et al., 2006). In addition, FLS2 orthologues have been found in other plant species including *N. benthamiana,* tomato and rice (Hann and Rathjen, 2007; Robatzek et al., 2007; Takai et al., 2008). FLS2 is a leucine-rich repeat receptor-like kinase (LRR-RLK) with 28 extracellular LRRs, a transmembrane domain and an intracellular kinase domain (Gómez-Gómez et al., 1999). According to the similarity of the protein kinase domains, *Arabidopsis* LRR-RLKs have been divided into different families and FLS2 was placed in family LRR XII, which has ten members (Shiu and Bleecker, 2001). A systematic site-directed mutagenesis approach demonstrated that the LRRs 9 to 15 are required for flg22 binding; however, the exact binding site is still unknown (Dunning et al., 2007; Albert et al., 2010b; Helft et al., 2011; Mueller et al., 2012).

Surprisingly, it was reported that FLS2 also perceives high concentrations of CLV3, an endogenous peptide that regulates stem-cell homeostasis in the shoot apical meristem, and Ax21, a PAMP from *Xanthomonas oryzae* pv. *oryzae* (Danna et al., 2011; Lee et al., 2011). However, these results are highly controversial and were recently challenged, as two independent studies failed to reproduce these observations (Mueller et al., 2012; Segonzac et al., 2012).

1.2.2 EF-Tu and EFR

Elongation factor Tu (EF-Tu) is one of the most conserved and abundant bacterial proteins (Jeppesen et al., 2005). However, EF-Tu was shown to be recognised as a PAMP specifically in *Brassicaceae* species, suggesting that

EF-Tu perception is an innovation in this plant family (Kunze et al., 2004). PAMP activity of EF-Tu was assigned to its N-terminus and the synthetic peptides elf18 and elf26, which represent the first 18 or 26 amino acids of the N-terminus, are sufficient for activation of defence responses (Kunze et al., 2004).

In *Arabidopsis,* EF-Tu is recognised by the LRR-RLK EFR (EF-TU RECEPTOR) that as FLS2 belongs to the subfamily XII of LRR-RLKs (Figure 1.2) (Zipfel et al., 2006). EFR and FLS2 display a similar structure; however, EFR contains only 21 LRRs instead of 28 (Boller and Felix, 2009). Notably, by systematically swapping domains of FLS2 and EFR, it could be demonstrated that LRR7 to LRR21 of EFR are required for elf18 binding (Albert et al., 2010b).

As FLS2, EFR is highly glycosylated but both receptors differ in their requirement for components regulating protein folding, glycosylation and quality control in the endoplasmic reticulum (ER-QC) (Li et al., 2009; Nekrasov et al., 2009; Saijo et al., 2009; Häweker et al., 2010). CRT3 (CALRETICULIN3) and UGGT (UDP-GLUCOSE:GLYCOPROTEIN GLUCOSYL-TRANSFERASE) were identified as important components of EFR quality control, whereas an ER protein complex compromising SDF2 (STROMAL-DERIVED FACTOR-2), heat shock protein 70 (HSP70) BiP (LUMINAL BINDING PROTEIN), and the HSP40 ERdj3B was shown to regulate EFR biogenesis (Li et al., 2009; Lu et al., 2009; Nekrasov et al., 2009; Saijo et al., 2009; Häweker et al., 2010). While mutants of many of these components do not accumulate functional EFR, and therefore display strongly impaired elf18-responsiveness, their responses to flg22 are not affected (Li et al., 2009; Nekrasov et al., 2009; Saijo et al., 2009; Häweker et al., 2010). Since EFR may have evolved more recently than FLS2, it was implied that its amino acid sequence might be less capable of folding properly in the absence of ER-QC components.

Elf18 treatment induces a similar set of defence responses as flg22 (Zipfel et al., 2006). In addition, *Arabidopsis efr* mutants are more susceptible to *Agrobacterium tumefaciens* transformation and to weakly virulent strains of *Pto* DC3000, illustrating the importance of EF-Tu perception in defence against bacteria (Zipfel et al., 2006; Nekrasov et al., 2009). Expression of

AtEFR in *N. benthamiana* and tomato, which lack an endogenous EF-Tu perception system, confers elf18-responsiveness and increases resistance to bacterial pathogens (Zipfel et al., 2006; Lacombe et al., 2010). This demonstrates that downstream signalling components are conserved between plant families and more importantly that heterologus expression of PRRs can confer broad-spectrum disease resistance.

1.2.3 Ax21 and XA21

XA21 was identified more than 15 years ago as a locus conferring resistance to the Gram negative bacterium *Xanthomonas oryzae* pv. *oryzae* (*Xoo*) in rice (Song et al., 1995). However, its matching ligand was only recently identified as the type I-secreted sulphated protein Ax21 (activator of XA21-mediated immunity) (Figure 1.2) (Lee et al., 2009). Ax21, which is involved in quorum sensing, is conserved in all *Xanthomonas* species and was therefore classified as a novel PAMP (Lee et al., 2009; Han et al., 2011a; Han et al., 2011b). The 17 amino acid tyrosine sulphated peptide $AxY^{S}22$, which is derived from the N-terminal region of Ax21, is sufficient to trigger XA21-mediated resistance in rice (Lee et al., 2009). Tyrosine sulfation of Ax21 is critical for its recognition by XA21, as unmodified peptides do not elicit XA21-mediated defence responses (da Silva et al., 2004; Lee et al., 2009).

XA21 is a LRR-RLK of subfamily LRR XII and displays structural similarity to EFR and FLS2 (Shiu and Bleecker, 2001). Recently, the ER-localised chaperon *Os*BiP3 (Oryza sativa BINDING PROTEIN 3) was reported to regulate XA21 processing and stability (Park et al., 2010). Transgenic lines overexpressing *OsBiP3* display significantly decreased XA21 accumulation and consequently, XA21-mediated immunity is compromised in these lines (Park et al., 2010). This indicates that XA21, like EFR, is sensitive to disturbance in the ER quality control machinery.

1.2.4 CERK1, a multifunctional PRR?

Chitin, the main component of fungal cell wall, acts as a potent elicitor of defence during plant-fungal interactions (Felix et al., 1993). Chitin is a long-

chain polymer of a N-acetylglucosamine and is recognized as a PAMP in a wide range of plant species of both monocots and dicots (Shibuya and Minami, 2001).

In rice, chitin perception requires the RLK *Os*CERK1 (CHITIN ELICITOR RECEPTOR KINASE 1) and the RLP *Os*CEBiP (CHITIN ELICITOR-BINDING PROTEIN) that form a heteromeric complex upon chitin treatment (Kaku et al., 2006; Wan et al., 2008; Shimizu et al., 2010; Sharfman et al., 2011). Both proteins contain LysM (lysine motif) domains that were shown to be essential for chitin binding (Figure 1.2) (Iizasa et al., 2010; Liu et al., 2012).

In *Arabidopsis, At*CERK1 is the primary PRR for chitin recognition (Figure 1.2) (Miya et al., 2007; Wan et al., 2008; Iizasa et al., 2010; Petutschnig et al., 2010). A recent study demonstrated that chitin perception induces *At*CERK1 dimerisation, which is essential for the formation of active receptor complexes (Liu et al., 2012). The *Arabidopsis* genome also encodes three proteins that share similarity with *Os*CEBiP (Shinya et al., 2012; Wan et al., 2012). However, mutation of these genes has no significant effect on chitin-induced responses, demonstrating that they are not required for chitin signalling in *Arabidopsis* (Shinya et al., 2012; Wan et al., 2012). Instead, LYK4 (LysM-containing receptor-like kinase 4) was shown to be additionally required for chitin signalling, indicating that different plants may employ different LysM proteins to perceive this PAMP (Wan et al., 2012).

Recently, it was reported that *At*CERK1, together with the LysM domain-containing proteins LYM1 and LYM3, is also involved in the perception of peptidoglycans (PGNs) (Figure 1.2), which are cell wall components of Gram positive and Gram negative bacteria (Willmann et al., 2011). PGN is a bacterial N-acetylglucosamine oligomer, which is structurally similar to chitin (Heijenoort, 2001). PGN-induced responses are abolished in the *cerk1* mutant (Willmann et al., 2011). In addition, *cerk1* mutant plants are hyper-susceptible to *Pto* DC3000 infection (Gimenez-Ibanez et al., 2009). This further confirms the involvement of *At*CERK1 in PGN perception and consequently immunity to bacterial infection.

A recent study demonstrated that in rice LYP4 and LYP6 (Lysin Motif-Containing Proteins 4 and 6), orthologues of *Arabidopsis* LYM1 and LYM3,

function as additional chitin receptors and that both proteins are also required for PGN perception (Liu et al., 2012). Thus, *At*CERK1 and LYP4/LYP6 function as promiscuous PRRs for different PAMPs.

1.2.5 EIX and *Le*Eix1/2

EIX, an ethylene-inducing xylanase from the fungus *Trichoderma viride,* triggers ethylene biosynthesis, electrolyte leakage, PR (PATHOGENESIS-RELATED) gene expression and HR in tomato and tobacco (Fuchs et al., 1989; Bailey et al., 1990; Bailey et al., 1993; Ron et al., 2000; Elbaz et al., 2002). The enzymatic activity of EIX is not required for induction of defence responses, indicating that the protein *per se* functions as an elicitor (Enkerli et al., 1999; Furman-Matarasso et al., 1999).

In tomato, the two leucine-rich repeat receptor-like proteins (LRR-RLPs) *Le*Eix1 and *Le*Eix2 were identified as EIX-binding proteins (Figure 1.2) (Ron and Avni, 2004). However, transient overexpression of both proteins revealed that only *Le*Eix2 mediates EIX-induced responses (Ron and Avni, 2004). Notably, *Le*Eix1 and *Le*Eix2 form a heteromeric complex upon EIX perception and overexpression of *LeEix1* attenuates EIX-induced responses (Bar et al., 2010). Since the expression of *LeEix1* is also upregulated upon EIX treatment, it was suggested that perception of this PAMP might mimic *LeEix1* overexpression (Bar et al., 2010). Therefore, it was hypothesised that *Le*Eix1 associates with *Le*Eix2 upon EIX perception to attenuate downstream signalling (Bar et al., 2010).

1.2.6 GBP, an extracellular glucan binding protein

1,3-β-branched heptaglucoside derived from the cell wall of *Phytophtora sojae* is recognized as a PAMP by members of the *Fabaceae* family (Mithöfer et al., 2000; Fliegmann et al., 2004). A potential PRR, the β-glucan binding protein (GBP), was identified in soybean (Figure 1.2) (Mithöfer et al., 2000; Fliegmann et al., 2004; Fliegmann et al., 2005). However, since GBP mainly localises in the extracellular space, it is unclear how this protein mediates intracellular signalling (Fliegmann et al., 2004). Furthermore, since

GBP-related proteins have also been identified in plant species outside of the *Fabaceae* family, it was suggested that GBP is essential but not sufficient for downstream signalling (Mithöfer et al., 2000; Fliegmann et al., 2004). Therefore, an additional receptor component, which is involved in transmembrane signalling, still needs to be identified.

1.2.7 *At*Peps and PEPR1/2

The synthetic DAMP *At*Pep1, a 23 amino acid long peptide, represents the C-terminus of a putatively cytoplasmic protein encoded by *PROPEP1* (Huffaker et al., 2006). *At*Pep1 is part of a peptide family containing the six potential paralogues, *At*Pep2 to *At*Pep7 (Huffaker et al., 2006). *At*Pep1 perception triggers similar responses as flg22 and elf18, including ROS production, seedling growth inhibition and expression of defence-related genes (Huffaker et al., 2006; Krol et al., 2010; Yamaguchi et al., 2010). In addition, pre-treatment with *At*Pep1 induces resistance against *Pto* DC3000 (Yamaguchi et al., 2010).

The LRR-RLK PEPR1 (PEP1 RECEPTOR 1) was identified as an *At*Pep receptor by chemical cross-linking experiments (Yamaguchi et al., 2006). However, since T-DNA insertion mutants of *PEPR1* are only partially impaired in *At*Pep1-induced responses, it was speculated that another receptor is involved in *At*Pep1 perception (Krol et al., 2010; Yamaguchi et al., 2010). Indeed, PEPR2 was recently demonstrated to act as an additional *At*Pep1 receptor (Figure 1.2) (Krol et al., 2010; Yamaguchi et al., 2010). The *pepr1 pepr2* double mutant is completely insensitive to *At*Pep1, indicating that both receptors contribute to *At*Pep1 perception (Krol et al., 2010; Yamaguchi et al., 2010). Binding assays revealed that in addition to *At*Pep1, PEPR1 also recognizes *At*Pep2 to *At*Pep6, while PEPR2 also recognizes *At*Pep2 (Yamaguchi et al., 2010).

Notably, the *At*Pep orthologue *Zm*Pep1 is recognized as a DAMP in maize (Huffaker et al., 2011). This demonstrates that peptides of the Pep family have a conserved function across plant species as endogenous regulators of innate immunity.

1.2.8 Oligogalacturonides and WAK1

A second group of well characterised DAMPs are oligogalacturonides (OGs), which are released from the plant cell wall during fungal infections or wounding (De Lorenzo et al., 2011). OGs were initially reported to regulate several aspects of plant growth and development such as root and flower formation (Marfà et al., 1991; Darvill et al., 1992; Bellincampi et al., 1993). However, OGs also induce a variety of immune responses, including the expression of defence-related genes, ROS production and callose deposition (Aziz et al., 2004; Ferrari et al., 2007; Denoux et al., 2008; Galletti et al., 2008). Pre-treatment with OGs also protects grapevine and *Arabidopsis* leaves from infection by the necrotrophic fungus *Botrytis cinerea* (Aziz et al., 2004; Ferrari et al., 2007).

The *Arabidopsis* wall-associated kinase WAK1, which consists of an ectodomain containing EGF (epidermal growth factor)-like repeats, a kinase domain and a transmembrane domain, is able to bind OGs *in vitro* (Decreux et al., 2006). Based on lethality and redundancy problems, the possibilities to study the function of WAK1 by reverse genetics are limited (Wagner and Kohorn, 2001). However, using a domain swapping approach, it could be confirmed that WAK1 is able to bind OGs and to induce downstream responses *in planta* and therefore is a PRR for OGs (Figure 1.2) (Brutus et al., 2010).

1.2.9 Examples of orphan PAMPs and DAMPs

Although several PRRs have been identified, the receptors for many elicitors remain unknown. This includes well characterised PAMPs such as lipopolysaccharides (LPS), Pep13 and cold shock protein (CPS).

Lipopolysaccharides are major components of the outer membrane of Gram negative bacteria and elicit defence responses in different plant species of both monocots and dicots (Boller and Felix, 2009). PAMP activity was assigned to the lipid A part, and its elicitor activity depends on its acetylation and phosphorylation pattern (Silipo et al., 2010).

Pep13, a highly conserved epitope of a secreted transglutaminase from the oomycete *Phytophthora sojae*, acts as a strong elicitor of defence responses in parsley and potato (Nürnberger et al., 1994; Brunner et al., 2002). Although a high-affinity binding site for Pep13 was detected in parsley membranes, the Pep13 receptor is still unknown (Boller and Felix, 2009).

The bacterial cold-shock protein, which accumulates upon rapid cooling in bacteria, acts as a PAMP in different members of the *Solanaceae* family (Felix and Boller, 2003). CPS elicitor activity was assigned to the highly conserved RNA-binding motif RNP-1 (ribonucleoprotein-1) (Felix and Boller, 2003).

Several DAMPs are primarily synthesised as protein precursors, which are cleaved into the active elicitor upon biotic stress (Yamaguchi and Huffaker, 2011). A prominent example is systemin, a *Solanaceae*-specific peptide, which is released upon wounding from the precursor prosystemin to induce defence responses (Constabel et al., 1998). The receptor-like kinase SR160 (SYSTEMIN RECEPTOR 160 kDa), which was later shown to function as a receptor for brassinosteroids, exhibits systemin binding affinity (Scheer and Ryan, 2002; Holton et al., 2007). However, *sr160* mutant plants still display systemin-induced response, indicating that SR160 is not the systemin receptor (Holton et al., 2007; Lanfermeijer et al., 2008; Malinowski et al., 2009).

RALF (RAPID ALKALINIZATION FACTOR) was identified in an alkalinisation assay, originally developed to search for systemins in tobacco (Pearce et al., 2001a). Notably, the RALF precursor contains a dibasic RR motif that is recognized by specific serine-proteases for release of the active peptide (Olsen et al., 2002). Like systemin, RALF is able to activate mitogen-activated protein kinases (MAPKs) and to induce medium alkalinisation in cell culture, suggesting a potential role in plant defence responses (Pearce et al., 2001a). However, recent results indicate that RALF peptides, which exist in a variety of species, are primarily involved in developmental processes (Bedinger et al., 2010). Potential components of the *Le*RALF receptor complex were identified in experiments using photoaffinity labelled RALF peptides in tomato; however, the *bona fide* receptor remains unknown (Scheer et al., 2005).

Hydroxyproline-rich systemin (HypSys) peptides, which are derived from a preproHypSys precursor, induce the expression of defence-related genes in different members of the *Solanaceae* family (Pearce et al., 2001b; Pearce and Ryan, 2003; Pearce et al., 2007; Chen et al., 2008; Pearce et al., 2009). Furthermore, overexpression of *preproHypSys* enhances resistance to *Helicoverpa armigera* larvae in tobacco (Ren and Lu, 2006).

These peptides are examples of the vast diversity of DAMPs that can elicit plant defence but for which putative receptors still need to be discovered.

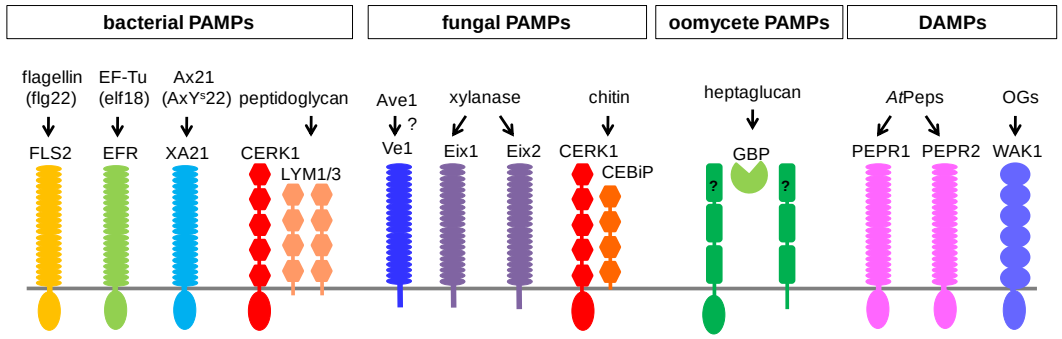

Figure 1.2: Plant pattern recognition receptors with known ligands
The LRR-RLKs FLS2, EFR and XA21 recognise the bacterial PAMPs flagellin, elongation factor Tu or the type-I secreted peptide Ax21, respectively. The LysM-domain containing proteins LYM1, LYM3 and CERK1 mediate perception of bacterial peptidoglycans. Ave1 is a putative ligand for the tomato LRR-RLP Ve1; however, direct binding has not yet been confirmed. The tomato LRR-RLPs *Le*Eix1 and *Le*Eix2 both bind the fungal PAMP xylanase, while the LysM-RLP CEBiP and the LysM-RLK CERK1 are part of the chitin perception system in rice. In *Arabidopsis,* CERK1 is sufficient for chitin perception. In legumes, an extracellular β-glucan-binding protein (GBP) binds *Phytophthora* heptaglucoside; however, it is yet unknown how this protein transmits intracellular signalling. The DAMPs *At*Peps and oligogalacturonides are perceived by the LRR-RLKs PEPR1 and PEPR2 and the RLK WAK1, respectively. Figure adapted from Monaghan and Zipfel, 2012.

1.3 Signalling events downstream of PAMP and DAMP perception

PAMP perception induces a variety of events, starting with the formation of active receptor complexes and subsequently, induction of downstream signalling (Figure 1-4). Early PAMP-induced responses include ion fluxes across the plasma membrane, changes in protein phosphorylation, ROS production, MAPK activation and transcriptional reprogramming.

Furthermore, callose deposition and synthesis of defence-related hormones are observed upon elicitor treatment.
In addition, several mechanisms have been described, which negatively regulate these defence responses, in order to block constitutive signalling.

1.3.1 Positive regulation of PAMP receptors complexes

The formation of active receptor complexes is the first detectable event after PAMP perception. In the current model, upon ligand binding, the two well characterised PRRs EFR and FLS2 may undergo conformational changes and post-translational modifications allowing them to heteromerize with downstream signalling components (Figure 1.3) (Boller and Felix, 2009).
An important signalling partner of several PRRs is the LRR-RLK BAK1 (BRI1-ASSOCIATED KINASE), which belongs to the family of SERK (SOMATIC EMBRYOGENESIS RECEPTOR-LIKE KINASE) LRR-RLK proteins (Hecht et al., 2001; Albrecht et al., 2008). BAK1 was initially identified as an interactor and positive regulator of the brassinosteroid (BR) receptor BRI1 (BRASSINOSTEROID INSENSITIVE 1), which regulates many aspects of growth and development (Li et al., 2002; Nam and Li, 2002). However, later studies revealed that BAK1 also heteromerizes with the PAMP receptors FLS2 and EFR in a ligand-dependent manner (Figure1-3) (Chinchilla et al., 2007; Heese et al., 2007; Roux et al., 2011). *Bak1* mutants display reduced responses to elf18 and flg22, indicating that its association with EFR and FLS2 positively regulates both PAMP signalling pathways (Chinchilla et al., 2007; Heese et al., 2007). But since BAK1 is not involved in ligand perception (Chinchilla et al., 2007), it was defined to function as a co-regulator, rather than a co-receptor. Heteromerization of FLS2 and EFR with BAK1 triggers auto- and transphosphorylation events, leading to activation of downstream signalling (Figure 1-3) (Chinchilla et al., 2007; Schulze et al., 2010; Schwessinger et al., 2011).
Interestingly, *bak1* null mutants are also compromised in their responsiveness to several other PAMPs and DAMPs, including LPS, PGN and *At*Pep1, indicating that BAK1 regulates additional PRRs (Shan et al., 2008; Krol et al., 2010). Indeed, it was recently reported that BAK1 also

interacts with PEPR1 and PEPR2, as well as with *Le*Eix2 (Bar et al., 2010; Postel et al., 2010). However, *bak1* null mutants still respond marginally to flg22 and elf18 elicitation, raising the possibility of redundancy with other members of the SERK family. In fact, it was recently demonstrated that additional SERK proteins are recruited into the FLS2 and EFR complex in a ligand dependent manner (Roux et al., 2011). It was further shown that BKK1/SERK4 (SOMATIC EMBRYOGENESIS RECEPTOR-LIKE KINASE/BAK1-LIKE 1) acts partially redundantly with BAK1 as a major regulator of FLS2-, EFR-, and PEPR1/2-mediated signalling (Figure1-3) (Roux et al., 2011).

The membrane-associated cytoplasmic kinases BIK1 (BOTRYTIS-INDUCED KINASE1) and related PBL (AVRPPHB SUSCEPTIBLE 1-like) proteins were reported to function as positive regulators of both flg22- and elf18-induced responses (Lu et al., 2010b; Zhang et al., 2010). BIK1 associates constitutively with FLS2 and potentially also with BAK1 (Figure 1.3) (Lu et al., 2010b; Zhang et al., 2010). Following flg22 perception, BAK1 phosphorylates BIK1, which subsequently phosphorylates FLS2 and BAK1 and partially dissociates from the FLS2 complex (Figure1-3) (Lu et al., 2010b; Zhang et al., 2010). Notably, BIK1 is also phosphorylated upon elf18 treatment and associates with EFR in un-elicited cells (Figure1-3) (Zhang et al., 2007). *Bik1 pbl1* mutants are compromised in PAMP-triggered defence responses, further confirming their role as positive regulators of PTI (Lu et al., 2010b; Zhang et al., 2010; Laluk et al., 2011).

In rice XB3, an E3 ubiquitin ligase, acts as a positive regulator of XA21-dependent signalling. XB3 was shown to associate with XA21 *in vitro* and *in planta.* Furthermore, transgenic lines with reduced *Xb3* expression display decreased XA21 levels and are compromised in their resistance to *X. oryzae* pv. *oryzae* (Wang et al., 2006). This indicates that XB3 is required for proper XA21 accumulation and consequently for XA21-mediated resistance (Wang et al., 2006).

1.3.2 Negative regulation of PAMP receptors complexes

PRRs and their co-regulators are under tight regulation to attenuate and fine tune signalling; as well as to avoid constitutive receptor activation in the absence of pathogens.

A well characterised example is XA21 that is inactivated by XB24 and XB15 (XA21-BINDING PROTEIN 24 and 15) (Park et al., 2008; Chen et al., 2010b). Prior to PAMP perception, XA21 associates with the ATPase XB24, which promotes phosphorylation of XA21 on specific serine and threonine residues and thereby maintains XA21 in an inactive state (Chen et al., 2010b). Notably, XA21 activity is compromised when *Xb24* is over-expressed, confirming its role as a negative regulator (Chen et al., 2010b). XB24 was further shown to disassociate from XA21 upon ligand perception to facilitate receptor activation and induction of downstream responses (Figure 1-3) (Chen et al., 2010b). XA21-mediated signalling is in turn attenuated by the protein phosphatase 2C (PP2C) XB15 (Park et al., 2008). XB15, which displays similarity to the POLTERGEIST-type PP2Cs from *Arabidopsis*, associates with XA21 to induce its dephosphorylation and consequently inactivation (Figure 1.3) (Park et al., 2008). *Xb15* silencing lines display spontaneous cell death and constitutive expression of defence-related genes, illustrating the importance of negative regulation of defence signalling pathways (Park et al., 2008).

In *Arabidopsis,* the KINASE-ASSOCIATED PROTEIN PHOSPHATASE (KAPP) was shown to associate with FLS2 and to negatively regulate flg22-triggered signalling (Gómez-Gómez et al., 2001). However, since KAPP also associates with several other plant RLKs (Braun et al., 1997; Williams et al., 1997; Gómez-Gómez et al., 2001; Shah et al., 2002), the specificity of these interactions is questionable.

Recently, the two closely related E3 ubiquitin ligases PUB12 and PUB13 (PLANT U-BOX 12 and 13) were identified as negative regulators of the FLS2 signalling pathway (Figure 1.3) (Lu et al., 2011). PUB12 and PUB13 constitutively associate with BAK1 and are recruited into the FLS2 complex upon ligand-induced BAK1-FLS2 heteromerization (Figure1.3) (Lu et al., 2011). Notably, PUB12 and PUB13 poly-ubiquitinate FLS2 and thereby

promote flg22-induced FLS2 degradation (Lu et al., 2011). In accordance with these observations, *pub12/13* mutant plants display elevated flg22-triggered responses and enhanced resistance to *Pto* DC3000 (Lu et al., 2011; Li et al., 2012b). However, it remains to be determined whether a similar mechanism attenuates signalling of other BAK1-interacting PRRs, such as EFR. Furthermore, in contrast to XA21, it is yet unclear how constitutive activation of FLS2 and EFR is blocked in the absence of their ligand.

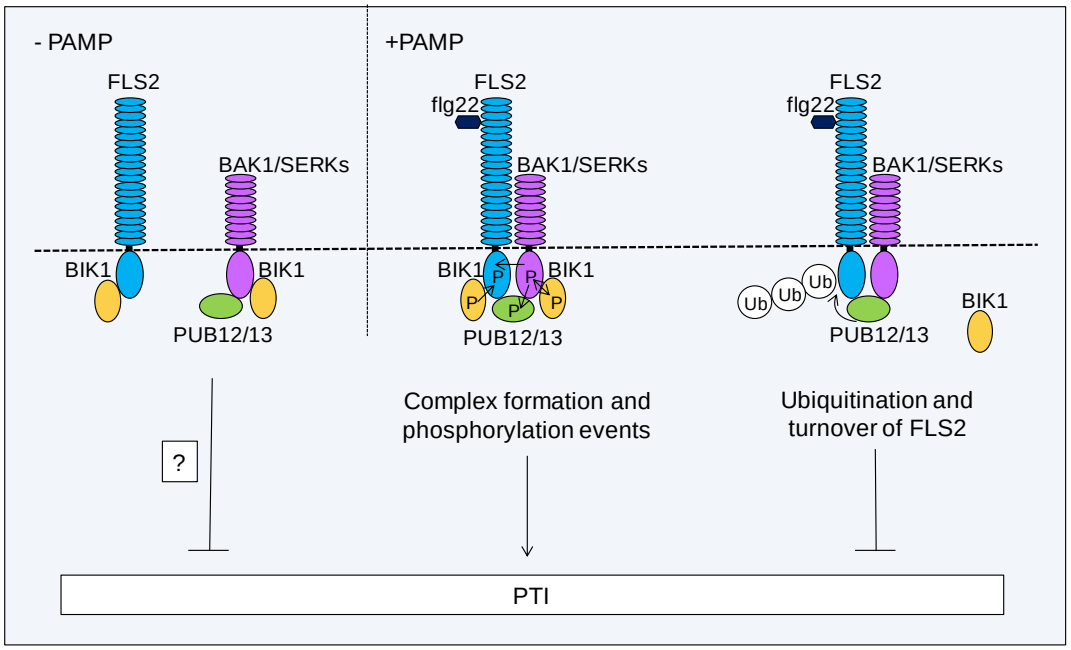

Figure 1.3: FLS2 activation is under both positive and negative regulation
BIK1, as well as other related PBLs, interacts constitutively with FLS2 and BAK1. Upon flg22 perception, BAK1 heteromerises with FLS2 and transphosphorylates BIK1 and the E3 ligases PUB12 and PUB13. In turn, BIK1 transphosphorylates BAK1 and FLS2. These phosphorylation events activate FLS2 signalling, resulting in PTI. PUB12 and PUB13 catalyse FLS2 poly-ubiquitination and thereby promote its degradation and attenuation of signalling. The direction of phosphorylation and ubiquitination events are indicated by arrows, phosphorylated proteins are marked with a P and poly-ubiquitinated proteins with Ub.

1.3.3 Phosphorylation events in response to PAMP perception

Treatment with calyculin A and okadaic acid, two potent inhibitors of protein phosphatases 1 and 2A, was shown to mimic the action of elicitors and induces a rapid medium alkalinisation, accumulation of PR proteins and

ethylene production (Raz and Fluhr, 1993; Felix et al., 1994). In contrast, PAMP-induced responses are blocked in cells pre-treated with the protein kinase inhibitor K-252a (Felix et al., 1991). These observations demonstrate the importance of phosphorylation events in PTI. Interestingly, phosphorylation of PRRs was shown to regulate distinct processes. Using a site-directed mutagenesis approach, four potential FLS2 phosphorylation sites were identified. Although $FLS2^{T867V}$, $FLS2^{T1040A}$, $FLS2^{T1072A}$ and $FLS2^{S878A}$ are not affected in their flg22 binding capacity, all four mutants display altered PAMP-triggered responses (Robatzek et al., 2006). In addition, flg22-mediated endocytosis of $FLS2^{T867V}$ is strongly reduced (Robatzek et al., 2006). Furthermore, while phosphorylation events are required for several downstream signalling events (Asai et al., 2002; Robatzek et al., 2006; Schulze et al., 2010; Schwessinger et al., 2011), they are not required for the association of BAK1 with EFR and FLS2 (Schulze et al., 2010; Schwessinger et al., 2011). Consequently, treatment with the kinase inhibitor K-252a does not prevent complex formation (Schulze et al., 2010).

Targeted mutagenesis of predicted XA21 phosphorylation sites indicated that Ser^{686}, Thr^{688} and Ser^{689} are required for XA21 protein stability (Xu et al., 2006a). In contrast, Ser^{697} appears to be critical for the interaction with XB15, since $XA21^{S697A}$ fails to associate with this PP2C (Park et al., 2008).

In addition to PRRs, a high number of potential downstream signalling components are differentially phosphorylated upon PAMP perception, indicating that this post-translational modification also plays an essential role in signal transduction (Benschop et al., 2007; Nühse et al., 2007).

1.3.4 Ion fluxes

One of the earliest detectable responses upon PRR activation is an extracellular alkalinisation caused by ion fluxes across the plasma membrane (Boller and Felix, 2009). These include an increased influx of H^+ and Ca^{2+} ions and an efflux of K^+ ions and anions (Jabs et al., 1997; Pugin et

al., 1997; Garcia-Brugger et al., 2006; Jeworutzki et al., 2010; Ranf et al., 2011).

It was reported that the cation channel CNGC2 (CYCLIC NUCLEOTIDE GATED CHANNEL 2) mediates Ca^{2+} influx in response to LPS and Pep1 perception (Ali et al., 2007; Qi et al., 2010). In contrast, the plasma membrane-localised Ca^{2+} ATPases ACA8 (AUTOINHIBITED $CA2^{+}$-ATPASE, ISOFORM 8) and ACA10 were shown to contribute to the flg22-elicited Ca^{2+} burst (Figure 1.4) (Frei dit Frey et al., 2012). Importantly, ACA8 associates with FLS2, implying a direct link between flg22 perception and calcium signalling (Frei dit Frey et al., 2012). However, although pharmacological studies indicate that calcium channels also play an important role in mediating elf18- and flg22-induced calcium influx, the identity of these channels is still unclear (Jeworutzki et al., 2010; Kwaaitaal et al., 2011; Ranf et al., 2011). Notably, it was recently implied that ionotropic glutamate receptor (iGluR)-like channels might play a role in flg22-, elf18- and chitin-triggered responses (Kwaaitaal et al., 2011). Consequently, treatment with iGluR inhibitors was reducing PAMP-triggered Ca^{2+} influx as well as several downstream responses including MAPK activation and defence gene expression (Kwaaitaal et al., 2011). However, genetic evidence that confirms these observations is so far still missing.

Changes in cytosolic Ca^{2+} concentrations are perceived by calcium-binding proteins including calmodulins (CaMs), calcium-dependent protein kinases (CDPKs) and calcineurin B-like (CBL) proteins that contain Ca^{2+}-binding EF-hand motifs (Reddy and Reddy, 2004). CaMs and CBLs do not possess enzymatic activity and need to convey the calcium signal via conformational changes to target proteins. In contrast, CDPKs belong to a plant-specific class of serine/threonine protein kinases that exhibit direct calcium binding properties (Wurzinger et al., 2011).

Several calcium-binding proteins have been shown to regulate plant defence responses. In tobacco cell cultures expressing the R protein Cf9 (*Cladosporium fulvum* resistance gene 9), recognition of the fungal effector Avr9 (*C. fulvum* avirulence gene 9) results in rapid phosphorylation and activation of *Nt*CDPK2 (Romeis et al., 2000; Romeis et al., 2001). Furthermore, plants silenced for *NtCDPK2* are compromised in the induction

of the Avr9/Cf-9-dependent HR (Romeis et al., 2001). In *Arabidopsis,* CPK1 positively regulates SA accumulation and thereby contributes to resistance against fungal and bacterial pathogens (Coca and San Segundo, 2010). In addition, several *Arabidopsis* CDPKs are activated upon flg22 perception in a Ca^{2+}-dependent manner (Boudsocq et al., 2010). Using a functional genomic screen, the closely related CDPK4, 5, 6 and 11 were identified as important positive regulators of PAMP-induced ROS burst and a subset of transcriptional changes (Figure 1.4) (Boudsocq et al., 2010).

1.3.5 The oxidative burst

PAMP treatment induces a rapid transient oxidative burst within few minutes of treatment (Nicaise et al., 2009). This includes the production of reactive oxygen and reactive nitrogen species (ROS and NOS, respectively) (Ma and Berkowitz, 2007). ROS, such as peroxides or oxygen ions, can act as antibiotic agents, as well as secondary messengers to induce various defence responses (Apel and Hirt, 2004). Furthermore, ROS have been shown to inhibit pathogen invasion by strengthening the cell wall via oxidative cross-linking (Apel and Hirt, 2004).

In *Arabidopsis,* PAMP-induced ROS production is mainly mediated by the membrane-localized NADPH oxidase RbohD (RESPIRATORY BURST OXIDASE HOMOLOGUE D) (Figure 1.4) (Nühse et al., 2004; Zhang et al., 2007). Interestingly, RbohD is phosphorylated in response to flg22 perception, and this phosphorylation is required for its activity (Benschop et al., 2007; Nühse et al., 2007).

ROS production was implied to be downstream of elicitor-induced calcium burst and is inhibited by Ca^{2+}-chelators such as EGTA (ethylene glycol tetraacetic acid) and BAPTA (1,2-bis(o-aminophenoxy)ethane- N,N,N',N'-tetraacetic acid), and by Ca^{2+}-channel blockers, such as La^{3+} (Tavernier et al., 1995; Kadota et al., 2004; Segonzac et al., 2011). Notably, flg22-induced ROS production is strongly impaired in a *cpk4/5/6/11* quadruple mutant, indicating that CPK4, 5, 6 and 11 play partially redundant roles in regulating RbohD (Figure1.4) (Boudsocq et al., 2010).

1.3.6 Activation of mitogen-activated protein kinases

Activation of MAPK cascades occurs within 5-10 minutes upon PAMP perception (Boller and Felix, 2009). MAPK signalling relies on sequential phosphorylation events between three protein types: a MAP kinase kinase kinase (MAPKKK or MEKK), a MAP kinase kinase (MAPKK or MKK) and a MAP kinase (MPK) (Pedley and Martin, 2005).

In *Arabidopsis*, a complete MAPK cascade comprising MEKK1-MKK4/5-MPK3/6 was initially proposed to be involved in flg22-triggered signalling (Asai et al., 2002). However, later studies revealed that MEKK1 is not required for activation of MPK3/6, but rather activates MPK4 (Ichimura et al., 2006; Nakagami et al., 2006; Suarez-Rodriguez et al., 2007; Gao et al., 2008). Thus, the MEKK upstream of MPK3/6 is still unknown. Flg22-induced activation of MPK4 is dependent on MKK1 and MKK2 (Figure 1.4) (Mészáros et al., 2006; Gao et al., 2008; Qiu et al., 2008). In addition, MPK11, a close homologue of MPK4, was recently identified as an additional component of FLS2 signalling (Figure 1.4) (Bethke et al., 2011). MPK4 was originally described as a negative regulator of salicylic acid (SA)-mediated resistance but as a positive regulator of ethylene- and jasmonic acid (JA)-dependent defence responses (Petersen et al., 2000; Brodersen et al., 2006). However, it was recently shown that the R protein SUMM2 guards the MPK4 pathway (Zhang et al., 2012). This explains why *mekk1* and *mpk4* mutation leads to constitutive defence activation and why MEKK1 and MPK4 were proposed as negative regulators. Genetic analysis of double mutants with *summ2* revealed that the MEKK1-MKK1/2-MPK4 pathway rather regulates PTI positively (Kong et al., 2012).

MPK3 and MPK6 were reported to phosphorylate and subsequently deactivate the ethylene biosynthesis enzyme 1-amino-cyclopropane-1-carboxylic acid (ACS) (Liu and Zhang, 2004; Yoo et al., 2008; Bethke et al., 2009; Li et al., 2012a). This observation could explain how PAMP perception induces ethylene accumulation (Felix et al., 1999).

MAPK cascades can be negatively regulated by MPK phosphatases (MKPs) (Bartels et al., 2010). In *Arabidopsis,* MKP2 interacts with MPK3 and MPK6 to regulate oxidative stress and pathogen defense responses (Lumbreras et

al., 2010). *mkp2* mutant plants display reduced disease symptoms after infection with the biotrophic pathogen *Ralstonia solanacearum,* while the susceptibility to the necrotrophic fungus *B. cinerea* is increased (Lumbreras et al., 2010). This indicates that MKP2 has different functions in the regulation of responses to biotrophic and necrotrophic pathogens (Lumbreras et al., 2010). In addition, MKP1 and PTP1 (protein tyrosine phosphatase 1) act as repressors of MPK3/MPK6-dependent stress signalling (Bartels et al., 2009; Anderson et al., 2011; González Besteiro et al., 2011). *mkp1 ptp1* double mutants exhibit an increased resistance to *Pto* DC3000 (Bartels et al., 2009). Recently, it was shown that *mkp1* mutant plants also display enhanced PAMP-induced responses (Anderson et al., 2011).

Furthermore, several PP2Cs have been demonstrated to deactivate MAPK cascades. For instance, AP2C1 (ARABIDOPSIS PHOSPHATASE 2C1) and AP2C3/PP2C5 interact with MPK3, MPK4 and MPK6 to regulate various processes, including plant defence responses (Schweighofer et al., 2007; Brock et al., 2010). Notably, *AP2C1* overexpression enhances susceptibility to the necrotrophic fungus *B. cinerea* (Schweighofer et al., 2007).

1.3.7 Transcriptional reprogramming

PAMP perception induces massive transcriptional reprogramming. For example, in *Arabidopsis* more than 1,000 genes are differentially expressed after flg22 treatment (Navarro et al., 2004; Zipfel et al., 2004; Denoux et al., 2008). A similar set of genes is regulated by elf18 and a partial overlap was also observed with PGN or chitin (Zipfel et al., 2006; Gust et al., 2007; Wan et al., 2008). This indicates at least a partial convergence in the corresponding signalling pathways.

Interestingly, the expression of genes, encoding RLKs, including EFR, FLS2, BAK1 and BKK1, is induced upon PAMP perception (Zipfel et al., 2004; Zipfel et al., 2006; Postel et al., 2010). Furthermore, downstream signalling components such as MPK3, MEKK1 and MKK4 are similarly induced upon PAMP treatment (Navarro et al., 2004; Zipfel et al., 2004).

Important transcriptional changes are regulated downstream of MAPK activation by WRKY-type transcription factors (Figure 1.4) (Eulgem and Somssich, 2007; Pandey and Somssich, 2009). For instance, in *Arabidopsis* WRKY22 and WRKY29 act as positive regulators downstream of MPK3/6 (Asai et al., 2002), while MPK4 regulates gene expression by interacting with WRKY25 and WRKY33 (Zheng et al., 2007). In contrast, WRKY18, WRKY40 and WRKY60 function as negative regulators of basal resistance against bacterial and fungal pathogens (Xu et al., 2006b; Pandey et al., 2010).

In rice *Os*WRKY62 functions as a negative regulator of XA21-mediated resistance (Peng et al., 2008). Notably, it was recently reported that XA21 is cleaved upon $AxY^{S}22$ perception to release the intracellular domain (Park and Ronald, 2012). The XA21 intracellular domain carries a functional nuclear localisation signal and is consequently imported in the nucleus, where it associates with *Os*WRKY62 (Park and Ronald, 2012). However, it is yet to be determined whether XA21 directly phosphorylates *Os*WRKY62, leaving the role of this interaction unclear.

In addition, CDPKs play an important role in transcriptional reprogramming in plant innate immune signalling. Using a functional genomic screen and genome-wide gene expression profiling, it was demonstrated that CDPK4, 5, 6 and 11 act synergistically and independently of MAPKs to induce defence gene expression (Figure 1.4) (Boudsocq et al., 2010).

1.3.8 Receptor endocytosis

Ligand-induced receptor endocytosis has been well studied in yeast and animal cells, while its occurrence in plants has only recently been described (Geldner and Robatzek, 2008). Notably, ligand-mediated endocytosis has been observed with several PRRs (Ron and Avni, 2004; Robatzek et al., 2006; Chen et al., 2010a). For instance, upon flg22 perception, membrane resident FLS2 is rapidly internalized into intracellular vesicles that are likely trafficked for degradation (Figure 1.4) (Robatzek et al., 2006). Interestingly, FLS2 endocytosis requires kinase activities as the receptor internalisation is completely abolished in presence of the general kinase inhibitor K-252a (Robatzek et al., 2006). In addition, mutation of a potential phosphorylation

site on FLS2 impairs its endocytosis, indicating that FLS2 phosphorylation and endocytosis may be connected (Robatzek et al., 2006). FLS2 also possesses a PEST-like sequence, which is required for ubiquitin-triggered receptor endocytosis (Robatzek et al., 2006). Mutation of this motif impairs FLS2 endocytosis and compromises flg22-induced seedling growth inhibition (Robatzek et al., 2006). This indicates that endocytosis may negatively affect the FLS2 signalling pathway.

Similar to FLS2, *Le*Eix2 endocytosis is induced by ligand perception (Bar and Avni, 2009). *Le*Eix2 contains a conserved endocytosis signal within the cytoplasmic domain and mutation of this motif results in abolishment of HR in response to EIX (Ron and Avni, 2004). *Le*Eix2 internalization is negatively regulated by both *Le*Eix1 and the EH domain-containing protein EHD2 (Bar and Avni, 2009; Bar et al., 2010). Since association with both proteins also reduces EIX-induced responses, it was further implied that endocytosis positively regulates *Le*Eix2 signalling (Bar and Avni, 2009; Bar et al., 2010).

These examples illustrate that receptor endocytosis has diverse functions: While it is yet unclear whether FLS2 can signal from endosomes or whether flg22-triggered signalling is terminated by receptor internalisation, *Le*Eix2-dependent signalling is enhanced (Miaczynska et al., 2004; Geldner and Robatzek, 2008; Sharfman et al., 2011).

1.3.9 Stomatal closure

Stomata present, in addition to natural wound sites, major entry points for many plant pathogens. Thus, PAMP-induced stomatal closure is an effective mechanism to restrict pathogen growth (Melotto et al., 2008).

In *Arabidopsis,* biotic stress-induced stomatal closure relies on ABA (abscisic acid) signalling components such as the guard cell-specific OST1 (OPEN STOMATA 1) kinase, ABA3 (ABA DEFICIENT 3) and GPA1 (G PROTEIN ALPHA SUBUNIT 1); as well as RbohD (Merlot et al., 2002; Melotto et al., 2006; Mersmann et al., 2010; Zeng and He, 2010; Macho et al., 2012). Furthermore, the plant defence hormone salicylic acid (SA) and the SA signalling component NPR1 (NONEXPRESSER OF PR GENES 1) are required for PAMP-induced stomatal closure (Zeng and He, 2010).

Stomatal opening is mainly driven by an uptake of cations and a subsequent water influx. In *Arabidopsis,* the two plasma membrane-localized proton pumps AHA1 (ARABIDOPSIS H^+-ATPASE ISOFROM 1) and AHA2 are involved in generating the required electrochemical gradient (Merlot et al., 2007; Liu et al., 2009; Haruta et al., 2010). Interestingly, AHA1 and AHA2 are differentially phosphorylated upon flg22 perception and a gain-of-function mutation in *AHA1* results in enhanced flg22-triggered responses (Benschop et al., 2007; Nühse et al., 2007; Liu et al., 2009). This indicates that AHA1 regulates stomatal closure upon PAMP perception (Figure 1.4). AHA1 and AHA2 were also recently reported to associate with RIN4 (RPM1-INTERACTING PROTEIN 4), an important regulator of PTI and ETI (Mackey et al., 2002; Kim et al., 2005; Liu et al., 2009). *RIN4* overexpression enhances H^+-ATPase activity and consequently prevents stomatal closure, while the *rin4* knock-out mutant exhibits decreased H^+-ATPase activity (Liu et al., 2009). Therefore, RIN4 was implied to function as a positive regulator of AHA1/2.

Furthermore, the *Arabidopsis* L-type lectin receptor kinases LecRK-VI.2 and LecRK-V.5 have be described as regulators of stomatal immunity (Desclos-Theveniau et al., 2012; Singh et al., 2012). However, while in *lecrk-VI.2-1* PAMP-induced stomatal closure is impaired and the susceptibility to *Pto* DC3000 is enhanced, *lecrk-V.5* displays constitutive stomatal closure and increased resistance to *Pto* DC3000 (Desclos-Theveniau et al., 2012; Singh et al., 2012). Thus, both proteins play contrasting roles in PAMP-induced stomatal closure.

1.3.10 Callose deposition

One of the late PAMP-induced responses is the accumulation of callose, a plant *β*-1,3-glucan polymer, between the cell wall and the plasma membrane (Figure1-4) (Gómez-Gómez et al., 1999). In *Arabidopsis,* GLUCAN SYNTHASE-LIKE 5/POWDERY MILDEW RESISTANT 4 (GSL5/PMR4) mediates callose deposition in response to the perception of PAMPs and fungal pathogens (Jacobs et al., 2003; Nishimura et al., 2003; Kim et al., 2005). In addition, *pmr4* mutant plants display increased susceptibility to the

non-virulent *Pto* DC3000 *hrcC*$^{-}$ mutant, which lacks a functional type-III secretion system (Kim et al., 2005). The altered resistance is partially dependent on SA signalling as *pmr4* mutants display constitutive expression of SA-induced genes (Nishimura et al., 2003). However, reduction of SA levels in *pmr4* plants still allows slightly increased growth of the non-adapted bacterium *P. syringae* pv. *phaseolicola* (Ham et al., 2007). This suggests that PMR4-dependent callose deposition contributes to antibacterial immunity.
Interestingly, *rbohD* mutant plants display reduced callose accumulation after flg22 and OG treatment (Zhang et al., 2007; Galletti et al., 2008), indicating that callose deposition may be dependent of ROS production.

1.3.11 The hypersensitive response

According to their lifestyle, plant pathogens are classified as biotrophs, necrotrophs and hemibiotrophs (Glazebrook, 2005). While biothrophs feed on living host cells, necrotrophs derive nutrients from dead or dying cells. In addition, many pathogens behave as both biotroph and necrotroph, depending on the stage of their life cycle and the environmental conditions. Thus, they are referred to as hemi-biotrophs. Since biotrophs depend on living cells, an effective defence against these pathogens is the Hypersensitive Response (HR), a rapid development of programmed cell death in the region surrounding the infection sites (Mur et al., 2008). However, several examples illustrate that HR is not necessary essential for resistance. For instance, while HR responses are abolished in *dnd1 (defence, no death 1)* and *dnd2*, both mutants display an increased bacterial resistance (Clough et al., 2000; Jurkowski et al., 2004; Genger et al., 2008). Hence, cell death itself is not sufficient to limit pathogen growth in these mutants.
The HR is associated with several physiological changes such as ion fluxes and the production of reactive oxygen species (Ma and Berkowitz, 2007; Mur et al., 2008). Although HR is mostly linked to ETI, cell death responses can also be induced by PAMP perception. For instance, flagellin from *Pseudomonas avenae* was reported to induce cell death in suspension-cultured rice cells, while flagellin from *Pseudomonas syringae* pvs. *glycinea*

and *tomato* induce HR in their non-hosts *N. tabacum and N. benthamiana* (Che et al., 2000; Taguchi et al., 2003; Hann and Rathjen, 2007; Naito et al., 2008). Notably, silencing *NbFLS2* abolished the flagellin-induced HR, indicating that the flagellin receptor, or a closely related molecule, is capable of mediating HR in *N. benthamiana* (Hann and Rathjen, 2007).

1.3.12 Hormone signalling in relation to PTI and general defence

The phytohormones ethylene, salicylic acid and jasmonic acid are important regulators of plant defence responses (Robert-Seilaniantz et al., 2011). However, recent studies revealed that also several other hormones including brassinosteroids, abscisic acid, auxin, giberellic acid and cytokinin influence disease resistance outcomes (Robert-Seilaniantz et al., 2011; Albrecht et al., 2012; Belkhadir et al., 2012).

Hormonal cross-talk in defence responses

JA and ET signalling are generally associated with resistance to necrotrophic pathogens, whereas SA-dependent defence mainly contributes to resistance against biotrophic and hemibiotrophic pathogens (Glazebrook, 2005). SA is also involved in the establishment of systemic acquired resistance (SAR), a broad-spectrum resistance triggered by local infection (Grant and Lamb, 2006). Although SA and ET/JA defence response pathways act mostly antagonistically, as the activation of one often suppresses the activation of the other, synergistic interactions have also been reported (Schenk et al., 2000; Kunkel and Brooks, 2002; Beckers and Spoel, 2006). An important regulator of the cross-talk between the two pathways is MPK4 (Petersen et al., 2000; Brodersen et al., 2006). *mpk4* mutant plants display elevated SA levels and constitutive expression of SA-induced genes, whereas the expression of JA responsive genes is impaired (Petersen et al., 2000; Brodersen et al., 2006). This indicates that MPK4 positively regulates JA-mediated responses, but acts as a negative regulator of SA signalling or that in the *mpk4* mutants SUMM2 activation promotes SA accumulation and thus, downregulation of JA signalling.

Salicylic acid

A central regulator of the SA signalling pathway is NPR1, which mediates induction of SA-responsive genes, including *PR-1* (Dong, 2004). Notably, it was reported very recently that NPR1 directly binds SA and was therefore implied to function as a SA receptor (Wu et al., 2012). However, another study demonstrated that the closely related NPR3 and NPR4 but not NPR1 exhibit SA binding affinity (Fu et al., 2012). Furthermore, NPR3 and NPR4 were shown to function as adaptors for an E3 ubiquitin ligase to mediate SA-dependent degradation of NPR1 (Fu et al., 2012). Thus, further investigation must be undertaken, to explain these apparently contradictory results.

Jasmonic acid

JA mediates defence against necrotrophic pathogens; however, JA was also recently implied to play a role in SAR (Robert-Seilaniantz et al., 2011). Most JA responses are mediated through the F-box protein CORONATINE INSENSITIVE1 (COI1) (Xie et al., 1998; Browse, 2009; Fonseca et al., 2009; Sheard et al., 2010). *Coi1* mutant plants display elevated SA levels and exhibit enhanced susceptibility to necrotrophic pathogens such as *Alternaria brassicicola* and *B. cinerea* (Thomma et al., 1998; Kloek et al., 2001).

Using mutational and transcriptional approaches, a family of JASMONATE ZIM domain-containing (JAZ) proteins was identified that represses JA signalling (Thines et al., 2007; Yan et al., 2007; Chini et al., 2009). JAZ proteins interact with COI1 and the basic helix-loop-helix (bHLH) transcription factor MYC2, a key regulator of JA-induced plant defence responses (Melotto et al., 2006; Katsir et al., 2008). Perception of JA leads to COI1-mediated degradation of JAZs and relieves repression on MYC2 to facilitate activation of JA-responsive genes (Robert-Seilaniantz et al., 2011).

Ethylene

In *Arabidopsis,* ethylene is perceived by five different receptors that repress ET signalling in absence of the hormone (Stepanova and Alonso, 2009). An important component of this signalling pathway is the protein kinase CTR1 (CONSTITUTIVE TRIPLE RESPONSE 1), which negatively regulates the ET signalling pathway (Stepanova and Alonso, 2009). CTR1 is inactivated by

ET, resulting in de-repression of downstream components such as EIN2 (ETHYLENE INSENSITIVE 2), a key regulator of ET signalling, or the transcription factor EIN3 (ETHYLENE-INSENSITIVE 3) (Stepanova and Alonso, 2009). It was recently reported that EIN3 and the EIN3-like proteins EIL1 and EIL2 directly promote *FLS2* expression by binding to the *FLS2* promoter (Boutrot et al., 2010). Consequently, ethylene-insensitive mutants are impaired in flg22-triggered responses such as stomatal closure and ROS production (Boutrot et al., 2010; Mersmann et al., 2010). Since, flg22 perception induces ET synthesis and EIN3 accumulation (Felix et al., 1999; Chen et al., 2009), it was hypothesised that flg22-induced ethylene production could maintain FLS2 levels in a positive feedback loop (Boutrot et al., 2010).

Brassinosteroids

Brassinosteroids play an important role in the regulation of plant growth and development (Yang et al., 2011). In addition, BR perception was also shown to have both positive and negative effects on plant immunity. For instance, treatment with brassinolide, which is the most active brassinosteroid, increases resistance to a wide range of biotrophic pathogens (Robert-Seilaniantz et al., 2011). In contrast, two independent studies recently demonstrated that activation of BR signalling inhibits PTI responses (Albrecht et al., 2012; Belkhadir et al., 2012). However, it is still controversial whether BAK1 is required for this cross-talk. Albrecht et al. (2012) demonstrated that BR modulates PTI response downstream or independently of the FLS2-BAK1 complex and therefore through BAK1-independent mechanisms. In contrast, Belkhadir et al. (2012) provided evidence that BR signalling modulates PTI through both BAK1-dependent and independent mechanisms. Based on their results BRI1 activation inhibits PAMP signalling through antagonistic recruitment of BAK1. Therefore, further investigations must be carried out to explain these contradictory results.

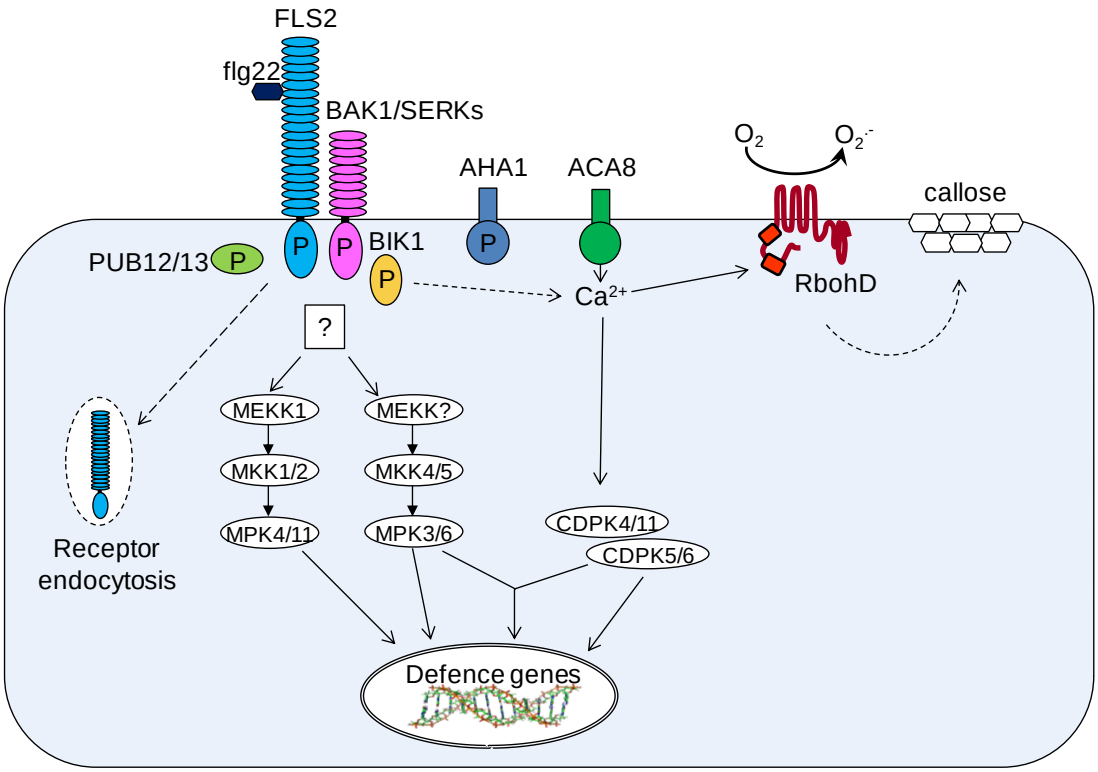

Figure 1.4: Current model of the FLS2 signalling pathway in *Arabidopsis*
Flg22 perception leads to rapid phosphorylation of AHA1, which was implied to facilitate PAMP-induced stomatal closure. Ca^{2+} influx, which is partially mediated by the ATPase ACA8, induces the activation of of Ca^{2+}-dependent protein kinases and RbohD, which is required for PAMP-triggered ROS burst. Flg22 perception also leads to the activation of at least two MAPK cascades. Both cascades regulate synergistically and independently of CDPK4/5/6 and 11 the expression of defense-related genes. Flg22 perception also induced FLS2 endocytosis and potentially attenuates the FLS2 signalling pathway. Phosphorylated proteins are marked with a P.

1.4 Effector-triggered susceptibility

To counteract PTI, plant pathogens evolved mechanisms to secrete and deliver effector proteins into host cells that interfere with plant innate immunity. Effectors that successfully suppress pathogen recognition or defence responses are then called virulence effectors (Feng and Zhou, 2012). Many Gram negative bacteria use the type III-secretion system to inject effectors into host cells (He et al., 2007). Therefore, mutant strains which lack a functional type III-secretion system exhibit reduced pathogenicity (Fouts et al., 2003).

In addition, pathogens produce different phytotoxins that affect plant immunity. Well characterised examples are coronatine (COR), which

promotes stomata opening and suppresses SA-dependent host defences, and the lipopeptides syringomycin and syringopeptin, which affect the membrane integrity of host cells (Grgurina et al., 2002; Brooks et al., 2005).
A variety of effectors and their effect on the host targets have been reported and a few examples are described below (Figure 1.5).

1.4.1 Effectors targeting PAMP-receptor complexes

Several virulent effectors target PRRs and their co-regulators to successfully promote disease (Figure1.5). A well characterised example is the type III-secreted effector AvrPtoB from *P. syringae* that interacts with FLS2, CERK1 and BAK1 (Göhre et al., 2008; Shan et al., 2008; Gimenez-Ibanez et al., 2009). The C-terminal E3 ligase domain of AvrPtoB was implied to mediate poly-ubiquitination of FLS2 and CERK1 and thus, to induce the degradation of both PRRs (Göhre et al., 2008; Gimenez-Ibanez et al., 2009). However, enzymatic activity of AvrPtoB is not required for inhibition of BAK1 kinase activity (Shan et al., 2008) and it was recently implicated that AvrPtoB inhibits BAK1 through competitive interference at the substrate-binding site (Cheng et al., 2011). Thereby, AvrPtoB effectively blocks immune reponses.
Early PAMP signalling events are also suppressed by the type III-secreted effector AvrPto, which acts as a kinase inhibitor (Xing et al., 2007). AvrPto was shown to associate with the kinase domains of the PRRs EFR and FLS2, as well as with their co-regulator BAK1 (Shan et al., 2008; Xiang et al., 2008; Xiang et al., 2010; Zhang et al., 2010). Furthermore, the AvPto-BAK1 interaction was reported to suppress flg22-triggered BAK1-FLS2 heterimerization (Shan et al., 2008). Consistently, in plants inoculated with *Pto* DC3000 Δ*avrPto*Δ*avrPtoB,* an increased FLS2-BAK1 association was detected compared to *Pto* DC3000-inoculated plants (Shan et al., 2008). However, recent results indicate that FLS2 is preferentially targeted by AvrPto and that BAK1 is most likely not a target of AvrPto *in vivo* (Xiang et al., 2010). Additionally, it was implied that the AvrPto-FLS2 interaction does not affect BAK1-FLS2 heteromerization, but rather blocks FLS2 kinase activity to prevent phosphorylation of BIK1 (Xiang et al., 2008; Xiang et al.,

2010; Zhang et al., 2010). Thus, the identity of preferential targets of AvrPto, as well as the exact outcome of these interactions, is still unclear.

BIK1 and several other PBLs are degraded by the type III-secreted effector AvrPphB from *P. syringae* (Figure 1.5) (Zhang et al., 2010). Stable AvrPphB expressing transgenic plants display reduced ROS production and callose deposition in response to different PAMPs, confirming that this effector successfully suppresses PTI (Zhang et al., 2010). Recently, it was shown that BIK1 is also targeted by AvrAC, a type III effector from *Xanthomonas campestris* pv. *campestri* (Feng and Zhou, 2012). AvrAC uridylylates conserved phosphorylation sites in the activation loop of BIK1 and thereby blocks its kinase activity (Feng and Zhou, 2012).

1.4.2 Effectors targeting MAPK cascades

The two *P. syringae* effectors HopAI1 and HopF2 effectively suppress PAMP-induced MAPK activation (Figure 1-5). HopF2, which exhibits mono-ADP-ribosyltransferase activity, ribosylates MKK5 *in vitro* and thereby, inhibits its kinase activity (Wang et al., 2010). Consequently, HopF2 successfully interferes with PAMP-triggered defence responses and promotes pathogen virulence. Intriguingly, HopF2 is associated with the plasma membrane and also suppresses flg22-induced phosphorylation of BIK1 (Wu et al., 2011). However, direct interaction between HopF2 and BIK1 could not be detected (Wu et al., 2011). Thus, it remains unclear whether HopF2 directly targets BIK1.

The *Pseudomonas* effector HopAI1, which displays phosphothreonine lyase activity, was reported to deactivate MPK3 and MPK6 by dehydroxylating a phospho-threonine in the activation loop preventing potential rephosphorylation (Zhang et al., 2007). HopAI1-mediated inactivation of MAPKs results in suppression of PAMP-induced gene expression and callose deposition (Zhang et al., 2007). Recently, it was reported that HopAI1, as well as AvrB, target MPK4 to block its kinase activity (Cui et al., 2010; Zhang et al., 2012).

1.4.3 Effectors targeting nuclear components

TAL (Transcription Activator-Like) effectors (TALEs) are DNA-binding proteins, which are found in the Gram negative bacterial pathogens *Xanthomonas* spp. and *Ralstonia solanacearum* (Scholze and Boch, 2011). The N-terminal region of TALEs contains secretion and translocation signals for the T3SS, while the C-terminal region contains a nuclear localization signal and a transcriptional activation domain (Boch and Bonas, 2010). The most prominent characteristic of TALEs is their central domain, which consists of tandem nearly identical repeats that recognize and bind specific DNA sequences (Boch et al., 2009; Moscou and Bogdanove, 2009).
TALEs mimic eukaryotic transcription factors (TFs) and are able to activate gene expression in host cells (Kay et al., 2007; Römer et al., 2007). A well characterized TAL protein is AvrBs3 from *Xanthomonas campestris* pv. *vesicatoria*, which induces mesophyll cell hypertrophy in susceptible pepper varieties (Marois et al., 2002). AvrBs3 was shown to induce the expression of *UPA20 (UPREGULATED BY AVRBS3 20)*, a gene encoding a basic helix–loop–helix-type TF that regulates cell expansion (Figure 1-5) (Kay et al., 2007). AvrBs3 binds to a conserved element in the *upa20* promoter, the UPA box, via its central repeat region (Kay et al., 2007). In resistant pepper varieties, AvrBs3 is recognized by the resistance protein Bs3 (Römer et al., 2007). The promoter of *Bs3* contains a *UPA* box, which is bound by AvrBs3 (Römer et al., 2007; Römer et al., 2009). Consequently, this effector directly promotes the expression of the corresponding R protein.

Another effector that modulates host transcription is XopD, a T3SS effector from *Xanthomonas campestris.* XopD contains a helix-loop-helix domain required for DNA binding and two conserved EAR (ERF-associated Amphiphilic Repression) motifs required to repress SA- and JA-induced gene expression *in planta* (Kim et al., 2008). XopD was recently reported to target the transcription factor *At*MYB30, which is a positive regulator of plant defense responses (Figure1.5) (Raffaele et al., 2008; Canonne et al., 2011). XopD specifically interacts with *At*MYB30 via its HLH domain to suppress the transcriptional activation of *At*MYB30 target genes (Canonne et al., 2011).

Thereby, XopD successfully inhibits plant defense responses and promotes disease (Canonne et al., 2011).

1.4.4 Re-opening the gates: How pathogens overcome stomatal closure

Stomata are major entry point for plant pathogens and thus, PAMP-induced stomatal closure is an effective defence mechanism. However, some virulent pathogens evolved strategies to re-open stomata to facilitate their entry into the plant leaf. For instance, virulent *P. syringae* strains secrete the phytotoxin coronatine, which represses ABA-mediated stomatal closure (Melotto et al., 2006). COR structurally mimics the bioactive jasmonate JA-Ile (jasmonoyl-isoleucine) and was shown to bind to the JA receptor COI1 (Katsir et al., 2008). Association between COI1 and JA-Ile or COR promotes degradation of JAZ proteins and release of the transcription factor MYC2 (Katsir et al., 2008). Recently, it was reported that the COR-dependent release of MYC2 activates the expression of three NAC (petunia NAM and *Arabidopsis* ATAF1, ATAF2, and CUC2) domain-containing transcription factors (Zheng et al., 2012). These transcription factors then repress the SA biosynthesis gene *ICS1 (ISOCHORISMATE SYNTHASE 1)* and activate the SA metabolism gene *BSMT1 (S-ADENOSYLMETHIONINE-DEPENDENT METHYL-TRANSFERASE 1),* resulting in reduced SA levels (Zheng et al., 2012). These observations confirm that COR regulates stomatal closure by inhibiting SA signalling.

In addition to COR, a secreted small molecule from the bacterial pathogen *Xanthomonas campestris* pv. *campestris* was shown to suppress stomatal closure (Gudesblat et al., 2009). The production of this bacterial factor is under the control of the *rpf*/DSF (diffusible signal factor) gene cluster (Gudesblat et al., 2009); however, the exact identity of the molecule is still unclear.

1.4.5 Effectors targeting vesicle trafficking

The *P. syringae* effector HopM1 was shown to accumulate in the trans-Golgi network/early endosomes of host cells, where it mediates degradation of *At*MIN7 (*A. thaliana* HopM1 interactor 7) (Figure 1.5) (Nomura et al., 2006; Nomura et al., 2011). *At*MIN7, which belongs to the adenosine diphosphate (ADP) ribosylation factor (ARF) guanine nucleotide exchange factor (GEF) protein family, is a key component of vesicle trafficking (Tanaka et al., 2009; Nomura et al., 2011). Notably, *atmin7* mutant plants display reduced flg22-triggered callose deposition, confirming the involvement of *At*MIN7 in PTI (Nomura et al., 2011). Interestingly, activation of ETI by the *Pseudomonas* effectors AvrRpt2, AvrPphB and HopA1 blocks HopM1-dependent *At*MIN7 destabilization, indicating that *At*MIN7 is also required for ETI (Nomura et al., 2011).

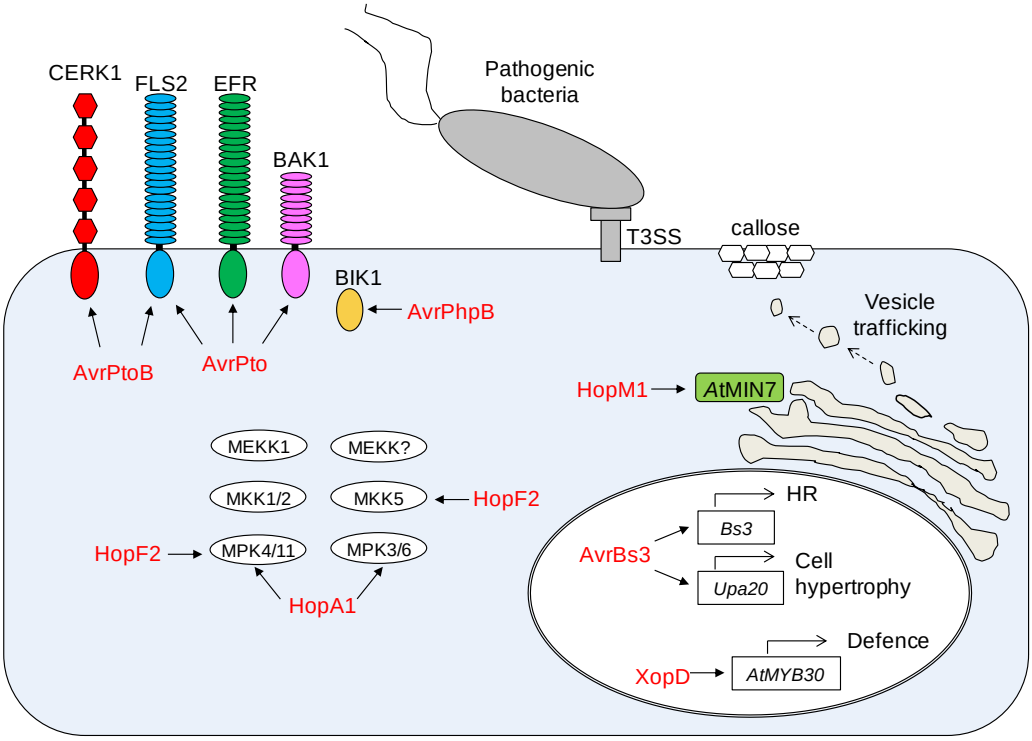

Figure 1.5: Type III-secreted effectors target different components of PAMP-triggered signalling
Many Gram negative phytopathogenic bacteria deliver virulent effectors into a host cell via a type-III secretion system. Here, the effectors target PTI signalling components to induce effector-triggered immunity. For instance, three effectors from *P. syringae*, AvrPtoB, AvrPto and AvrPphB, target components of PAMP receptor complexes to block downstream signalling. HopF2 and HopA1 both target different parts of MAPK cascades. In addition, AvrBs3 and XopD from *Xanthomonas campestris* regulate the expression of defense-related genes, while the *P. syringae* effector HopM1 targets *At*MIN7, a component of vesicle trafficking.

1.5 Effector-triggered immunity

The second layer of plant's immune system is based on the recognition of pathogen effectors through resistance proteins, which results in effector triggered immunity (Chisholm et al., 2006; Jones and Dangl, 2006).

1.5.1 Gene-for-gene concept, guard hypothesis and decoy model

More than 60 years ago, Harold Flor defined the gene-for-gene hypothesis, which is based on his observations of the interaction between flax and the flax rust fungus. According to this model, disease resistance in plants commonly requires two components: an avirulence (*Avr*) gene from the pathogen and a matching resistance (*R*) gene in the host (Flor, 1971). For instance, the avirulence factor AvrL567 from flax rust was shown to interact with the flax R protein L6 *in planta* to induce an HR-like necrotic response (Dodds et al., 2006).

However, direct interaction has only been observed between few R proteins and effectors and it was suggested that effectors might also be recognized via indirect interactions. Consequently, a guard hypothesis was formulated, which postulates that R proteins monitor the target (guardee) of a pathogen effector and thus, detect effectors via their effect on the host molecules (Dangl and Jones, 2001). A classic example for an indirect interaction is RIN4 that is guarded by the R proteins RPM1 (RESISTANCE TO P. SYRINGAE PV MACULICOLA 1) and RPS2 (RESISTANT TO P. SYRINGAE 2) (Mackey et al., 2002; Axtell and Staskawicz, 2003; Mackey et al., 2003). RIN4 is a target of the *P. syringae* effectors AvrRpt2, AvrRpm1 and AvrB. AvrRpt2, a cysteine protease, can degrade RIN4, while AvrRpm1 and AvrB can induce phosphorylation of RIN4 (Mackey et al., 2002; Axtell and Staskawicz, 2003; Mackey et al., 2003). RIN4 cleavage and phosphorylation activates RPM1 and RPS2, which leads to ETI and restriction of bacterial growth (Mackey et al., 2002; Axtell and Staskawicz, 2003; Mackey et al., 2003).

An extension of the guard hypothesis, the decoy model, implies that a guardee can evolve into a decoy. The decoy mimics the effector target to attract the effector and thus, to triggers its recognition through a decoy-associated R protein (van der Hoorn and Kamoun, 2008). However, in contrast to the guardee, the decoy does not necessarily have a function in defence signalling. An example is the serine/threonine kinase Pto, which may act as a decoy for targets of the *P. syringae* effector AvrPto (Zipfel and Rathjen, 2008). AvrPto is a kinase inhibitor, which was shown to bind and block several PRRs (Shan et al., 2008; Xiang et al., 2008). However, AvrPto also associates with Pto and consequently competes with the PRRs for AvrPto binding (Xing et al., 2007). Thereby it mediates the association of AvrPto and the R protein Prf and consequently triggers immunity (Mucyn et al., 2006).

1.5.2 General structure of R proteins

NB-LRRs, which contain a nucleotide binding domain (NB) and a C-terminal LRR domain, are the most common R proteins (Lukasik and Takken, 2009). The central NB site is part of the NB-ARC domain, an ATPase domain that is also found in apoptosis related proteins in animals (Lukasik and Takken, 2009). The NB-ARC domain of R proteins was implied to function as a molecular switch in which the ADP (Adenosine diphosphate) bound state represents the ‘off’ and the ATP (Adenosine triphosphate) the ‘on’ state (Takken and Goverse, 2012).

Based on their N-terminal domain, NB-LRRs can be divided into two subclasses, the coiled-coil (CC) and Toll/interleukin-1 receptor (TIR) proteins (Chisholm et al., 2006). TIR-NB-LRRs share structural and functional similarities to the TOLL immune receptor in *Drosophila* and Toll-like receptors (TLR) in mammals (Caplan et al., 2008). The CC and TIR domains were shown to mediate protein-protein interactions but might also contribute to pathogen recognition (Lukasik and Takken, 2009).

Well characterised members of the NB-LRR class include the CC-NB-LRR RPM1 and the TIR-NB-LRR RPS4 (RESISTANT TO P. SYRINGAE 4) that

recognise the *P. syringae* effectors AvrRpm1/AvrB and AvrRPS4, respectively (Bisgrove et al., 1994; Grant et al., 1995; Hinsch and Staskawicz, 1996).

A second important class of R genes encodes extracellular LRR (eLRR) proteins, which include RLPs, RLKs and PGIPs (polygalacturonaseinhibiting protein) (Fritz-Laylin et al., 2005). This class of R proteins contains several tomato RLPs, which confer resistance to the leaf-mould fungus *Cladosporium fulvum.* The best-studied example is Cf9, which confers resistance to *C. fulvum* expressing Avr9*,* a small cysteine-rich peptide that is secreted in the host during infection (Hammond-Kosack and Jones, 1997). Since the cytoplasmic domain of Cf-9 lacks a potential signalling domain, it was suggested that Cf-9 associates with other signalling components to activate defence responses (Rivas and Thomas, 2002).

1.5.3 ETI signalling pathways

The presence of either a CC or TIR domain typically determines whether an NB-LRR-mediated resistance response requires NDR1 (NON-RACE-SPECIFIC DISEASE RESISTANCE) or the EDS1/PAD4/SAG101 complex (ENHANCED DISEASE SUSCEPTIBILITY 1/PHYTOALEXIN DEFICIENT 4/SENESCENCE ASSOCIATED GENE 101), respectively (Eitas and Dangl, 2010).

EDS1, PAD4 and SAG101 display homology to eukaryotic lipases (Rivas, 2012). However, lipid-related enzymatic activity has not been reported for these proteins and their biochemical mode of action remains unknown (Rivas, 2012). EDS1 associates with both PAD4 and SAG101. But while the EDS1-PAD4 complex is found in cytoplasm and nucleus, the EDS1-SAG101 complex is exclusively present in the nucleus (Feys et al., 2005). Activation of TIR-NB-LRRs leads to increased nuclear accumulation of EDS1, which regulates transcriptional reprogramming of SA-induced and defence-related genes (García et al., 2010). Notably, it was demonstrated that EDS1

interacts with different transcription factors (García et al., 2010). In contrast, cytoplasmic EDS1 was implied to mediate pathogen-induced cell death (García et al., 2010). In addition to its role in ETI, EDS1 is also a major regulator of basal resistance (Feys et al., 2005; Wiermer et al., 2005).
Recently, two independent studies demonstrated that EDS1 is targeted by the bacterial effectors HopA1 and AvrRps4, which are detected by the TIR-NB-LRRs RPS4 and RPS6, respectively (Bhattacharjee et al., 2011; Heidrich et al., 2011). Consequently, it was hypothesised that the main function of EDS1 is to regulate basal immunity, while its function in ETI (partially) originates from being guarded by TIR-NB-LRRs (Bhattacharjee et al., 2011).

NDR1 was shown to regulate a variety of immune responses; however, its molecular function remains elusive. NDR1 was first shown to be required for resistance to both bacterial and fungal pathogens in a non-race-specific manner (Century et al., 1995). Furthermore, NDR1 plays a role in the activation of several CC-NB-LRRs (Aarts et al., 1998).
Recently, it was shown that NDR1 associates with RIN4, which is required for signalling mediated by the three CC-NB-LRR proteins RPM1, RSP2, and RPS5 (Day et al., 2006). The NDR1–RIN4 interaction is required for activation of RPS2-mediated resistance and it was implied that the association with RIN4 may physically link NDR1 to different R proteins (Day et al., 2006).

1.6 Overview of this Thesis

The perception of PAMPs is essential for the induction of basal defence responses. Two well described PAMP receptors are EFR and FLS2, which perceive bacterial elongation factor Tu and flagellin, respectively. A variety of downstream responses occurring upon perception of both PAMPs have been described. However, it is still poorly understood how EFR- and FLS2-dependent signalling is mediated and how activation of both receptor complexes is regulated. To gain further insight into these mechanisms, two approaches were used. In Chapter 3, I describe a predicted flg22-dependent gene expression network, which was generated using publicly available

microarray data. Candidates of this network are predicted to regulate each other‘s expression in a flg22-dependent manner and therefore, play a potential role in the FLS2 signalling pathway. Using different biological assays, I tested if seven candidates corresponding to the predicted main regulators of this gene expression network are required for flg22-induced responses. Importantly, I could identify that three of these genes are genetically involved in PTI signalling.

In Chapter 4, I present the preliminary characterisation of three proteins that were identified in a yeast two-hybrid screen with the EFR cytoplasmic domain. In order to test whether these proteins might play a role in the EFR signalling pathway, I examined whether they localise in the same subcellular compartments as EFR and whether they associate with EFR *in planta.*

In Chapter 5, the most promising of these three candidates, a predicted PP2C-type phosphatase referred to as PIE (PP2C-interacting with EFR), is extensively studied. Using biochemical and genetically approaches, I showed that PIE is involved in PAMP-triggered signalling.

Chapter 2: Material and Methods

2.1 DNA methods

2.1.1 Isolation of genomic DNA

The following described method gives a crude preparation of genomic DNA that was used for genotyping. Two big leaves of mature *Arabidopsis thaliana* plants or 2-4 14-day old old seedlings were grinded in 400 µl extraction buffer [200 mM Tris (pH 7.5), 250 mM NaCl, 25 mM EDTA, 0.5% SDS] and spun down for 5 minutes at 13.000 rpm. The supernatant was transferred in new tubes and 300 µl Isopropanol was added. The solutions were mixed by vortexing and afterwards spun down for 5 minutes at 13.000 rpm. The supernatant was discarded and the DNA pellet was washed with 70 % Ethanol. The DNA was dried at room temperature and dissolved in 100 µl water.

Genomic DNA that was used for cloning was extracted using the DNeasy Plant Mini Kit (Qiagen) as described in the provided manual.

2.1.2 Isolation of cDNA

RNA was extracted and cDNA was synthesized as described below in section 2.3.1 and 2.3.3. The cDNA was used for cloning PCRs, semi and real-time quantitative PCR.

2.1.3 Plasmid isolation from *E. coli*

Three ml LB cultures containing the appropriate antibiotics were inoculated with a single *E. coli* colony and incubated over night at 37°C with shaking. On the next day the cultures were spun down for one minute at 13.000 rpm and the cell pellet was resuspended in 300 µl GET buffer [50 mM glucose, 10mM EDTA, 25 mM Tris-HCl (pH 8)]. 300 µl 1% SDS/ 0.2 M NaOH were added and the solutions were mixed by inverting the tube for several times. After incubation for 5 minutes at room temperature, 300 µl KAcF [147 g Potassium Acetate and 25.5 ml Formic Acid in a final volume of 500 ml] were added and solutions were mixed by inverting the tube. Reactions were incubated for 5 minutes at room temperature and afterwards centrifuged at 13.000 rpm for 10 min. The supernatant was carefully transferred in new tubes and 500 µl isopropanol were added. Solutions were mixed by vortexing and centrifuged at 13.000 rpm for 10 minutes. DNA pellets were washed in 400 µl 70% EtOH, dried for 10 minutes at room temperature and resuspended in 40 µl H_2O containing 1 µl 200 ug/ml RNAseA (Promega).

2.1.4 PCR methods

All in this study used primers were ordered from Sigma-Aldrich and used in 10 µM concentration. dNTPS were purchased from Invitrogen and if not stated otherwise, used in a 2 mM concentration.

2.1.4.1 High-fidelity PCR

6.5 µl water
2 µl dNTPs
0.5 µl Primer 1
0.5 µl Primer 2
0.5 µl Phusion High Fidelity DNA Polymerase (Finnzymes)
5 µl High Fidelity Buffer (Finnzymes)
10 µl DNA
Reactions were incubated in a Themocycler running the temperature program described in Table 2.1.

Table 2.1: High-fidelity PCR thermal program

Step	Temperature	Time period of step	number of cycles
Initial denaturation	98 °C	2 minutes	1 x
Denaturation	98 °C	45 seconds	30 x
Annealing	55-62°C*	45 seconds	
Extension	72 °C	1-3 minutes**	
Final extension	72 °C	5 minutes	1 x

* The annealing temperature was set according to the melting temperature of the used cloning primers.
** The elongation time was set according to the length of the desired PCR fragment (with around 30 seconds per kilo base pair).

2.1.4.2 Colony PCR

A single *E. coli* or *A. tumefaciens* colony was inoculated in a PCR mix containing 12 µl water, 2 µl Standart Taq buffer (New England Bio Labs, NEB), 2 µl forward and reverse primer, 2 µl dNTPs and 0.1 µl Taq DNA Polymerase (NEB). Reactions were incubated in a Themocycler running the the programm described in Table 2.2.

Table 2.2: Colony PCR thermal program

Step	Temperature	Time period of step	number of cycles
Initial denaturation	95 °C	2 minutes	1 x
Denaturation	95 °C	45 seconds	30 x
Annealing	50°C	45 seconds	
Extension	72 °C	3 minutes	
Final extension	72 °C	5 minutes	1 x

2.1.4.3 Genotyping PCR

DNA for genotyping PCRs was extracted as described in 2.1.1. Primers were designed using the program “T-DNA primer Design” on the SIGnAL website (http://signal.salk.edu/tdnaprimers.2.html) and ordered from Sigma. Per

reaction 1 µl DNA was mixed with 0.1 µl Taq DNA Polymerase (NEB), 2 µl forward and reverse primer, 2 µl Standart Taq buffer (NEB), 2 µl dNTPs, 10.9 µl water. Reactions were incubated in a Themocycler running the following temperature cycle (Table 2.3).

Table 2.3: Genotyping PCR thermal program

Step	Temperature	Time period of step	Number of cycles
Initial denaturation	94 °C	3 minutes	1x
Denaturation	94 °C	15 seconds	2 x
Annealing	65°C	30 seconds	
Extension	72 °C	2 minutes	
Denaturation	94 °C	15 seconds	1 x
Annealing	63 °C	30 seconds	
Extension	72 °C	2 minutes	
Denaturation	94 °C	15 seconds	2 x
Annealing	62 °C	30 seconds	
Extension	72 °C	2 minutes	
Denaturation	94 °C	15 seconds	1 x
Annealing	60 °C	30 seconds	
Extension	72 °C	2 minutes	
Denaturation	94 °C	15 seconds	2 x
Annealing	59 °C	30 seconds	
Extension	72 °C	2 minutes	
Denaturation	94 °C	15 seconds	1 x
Annealing	57 °C	30 seconds	
Extension	72 °C	2 minutes	
Denaturation	94 °C	15 seconds	2 x
Annealing	56 °C	30 seconds	
Extension	72 °C	2 minutes	
Denaturation	94 °C	15 seconds	40 x
Annealing	55 °C	30 seconds	
Extension	72 °C	2 minutes	
Final extension	72 °C	5 minutes	1 x

2.1.4.4 Genotyping *da1-1* mutants using CAPS

Da1-1 mutants were genotyped using CAPS (cleaved amplified polymorphic sequence) as described in Li et *al.* 2008. Therefore, DNA was extracted and amplified as described in 2.1.1 and 2.1.4.3. 6 µl PCR product were mixed with 2 µl Buffer 2 (NEB), 0.2 µl BSA (NEB), 12 µl water and 0.5 µl *Mlu*I (NEB). Reactions were incubated for 5 hours at 37 °C and restriction fragments were separated in 2 % agarose gels. Only wild-type but not *da1-1* DNA fragments carry the *Mlu*I restriction site in the *DA1* gene and therefore, only this DNA is cut by the enzyme, releasing a fragment of ~ 540 bp.

2.1.5 DNA sequencing

Per reaction 4 µl DNA, 3 µl water, 1 µl ABI Big Dye Terminator Ready Reaction Mix Ver. 3.1 (Invitrogen), 1.5 µl 5x sequencing buffer and 0.5 µl primer were mixed and incubated in a Thermocycler running the program described in Table 2.4. Reactions were submitted to The Genome Analysis Centre (Norwich, UK). Sequencing results were analysed with Vector NTI ContigExpress.

Table 2.4: Thermal program for DNA sequencing

Step	Temperature	Time period of step	number of cycles
Initial denaturation	96 °C	1 minutes	1 x
Denaturation	96 °C	10 seconds	30 x
Annealing	50 °C	5 seconds	
Extension	72 °C	4 minutes	
Final extension	15 °C	∞	1 x

2.1.6 Agarose gel separation

DNA fragments were separated by electrophoresis. Depending on the fragment size 1-2% Agarose gels were prepared in 1 x TAE [40 mM Tris, 20 mM NAOAc, 1 mM EDTA, pH 7.9] containing 1 µg/ml ethidium bromide (Sigma). 0.1 vol of 10 x loading buffer [50% (w/v) glycerol, 50 mM EDTA, 10 x TAE, 0.25 % (w/v) 64 bromophenol blue, 0.25% (w/v) xylene cyanol] were added to the DNA samples and gels were run at 10 - 100 V until the desired separation was achieved. Results were analysed using a short wavelength UV transilluminator (GelDoc 1000, BioRad).

2.1.7 DNA elution from Ararose gels

For gel elution of DNA fragments, DNA was visualised on a long wavelength UV transilluminator (TM40, UVP) and the desired fragment was excised using a razor blade. DNA was then eluted using the Marchery Nagel Nucleospin Extract-Kit as described in the providers manual. DNA was eluted in 50 µl water.

2.2 Bacterial cloning-general overview

For cloning either the classical “cut and paste” method or the GATEWAY technology (Invitrogen) was used. DNA fragments were amplified by high fidelity PCR. PCR fragments were separated on agarose gels and eluted. After cloning inserts in the primary/entry vector, the identity of cloned fragments was confirmed by colony PCR (2.1.4.2), restriction test-digest (2.2.1) and DNA sequencing (2.1.5).

2.2.1 Restriction digests

For a test digest, 4 µl DNA were mixed with 14 µl water, 2 µl restriction buffer, 0.2 µl enzyme and if required 0.2 µl BSA [10 mg/ml]. For subcloning, 12 µl DNA were mixed with 14 µl water, 3 µl buffer, 0.5 µl enzyme and if required 0.5 µl BSA [10 mg/ml]. Reactions were incubated at 37°C for 3 to 14 hours. Restriction fragments were separated by Agarose gel-electrophoresis. All in this study used enzymes were purchased from NEB or Roche and used with the by the provider indicated buffer.

2.2.2 Transformation of plasmids in chemically competent *E. coli* by heat shock

Per reaction 5 µl DNA were mixed with 50 µl chemical competent cells and incubated on ice for 10 minutes. Heat shock was performed at 42 °C for 45 seconds. After adding 300 µl LB, cells were incubated with shaking at 37 °C for 1 hour and plated on selection plates (LB with relevant antibiotic). Plates were incubated for 12-16 hours at 37 °C.

2.2.3 Transformation of plasmids in *Agrobacterium tumefaciences* by electroporation

Per reaction 2 µl DNA were mixed with 15 µl electro-competent cells and 40 µl 10% glycerol in electroporation cuvettes with a width of 1 mm. After incubation for 10 minutes on ice, cells were transformed by electroporation using a Bio-Rad electroporator (Bio-Rad) with the following settings: 1800 V with a capacity of 25 µF over 200 Ω resistance. After adding 300 µl LB, cells were incubated with shaking at 28°C for 1 hour and plated on selection plates (LB with relevant antibiotic). Plates were incubated for 2-3 days at 28°C.

2.2.4 Classical “cut and paste” cloning

For this method inserts were first subcloned in pGEM-T Easy (Promega), amplified in *E. coli* and then cloned in the destination.

2.2.4.1 Poly(A)-tailing

25 µl gel eluted PCR product were mixed with 3 µl Standard Taq buffer (NEB), 2 µl dNTPs and 0.2 µl Taq DNA Polymerase (NEB). Reactions were incubated for 20 minutes at 72°C.

2.2.4.2 Subcloning in pGEM-T Easy

Per reaction 3 µl poly(A)-tailed PCR product were mixed with 5 µl 2x Ligation buffer (Promega), 1 µl pGEM-T Easy (Promega) and 1 µl T4 Ligase (Promega). Reactions were incubated over night at 4°C and plasmids were transformed in chemical competent cells as described above. Transformants

were selected on LB plates containing Carbencilin. Positive tranformants were selected by colony PCR. Plasmids were extracts from *E. coli* as described in 2.1.3 and the identity of the insert was confirmed by restriction digest (2.2.1) and sequencing (2.1.5). Insert were the cloned in the destination vector (2.2.4.3).

2.2.4.3 Cloning in the destination vector

Desired insert were released from pGEM-Teasy (Promega) by restriction digest. Therefore, 12 µl DNA were mixed with 14 µl water, 3 µl buffer, 0.5 µl enzyme, and if required 0.5 µl BSA [10 mg/ml]. For the vector digest 4 µl and 22 µl water were used instead. Reactions were incubated at 37°C for 3 to 14 hours. Restriction fragments were separated by agarose gel-electrophoresis. 6.5 µl of gel eluted insert were mixed with 2 µl of gel eluted vector, 1 µl ligation buffer (NEB) and 0.5 µl T4-ligase (NEB). Ligations were incubated over night at 4 °C. Plasmids were then transformed in chemical competent cells as described in 2.2.2 and selected on the appropriate antibiotics.

2.2.5 GATEWAY cloning

For GATEWAY cloning, all forward cloning primers contained a CACC extension at the 5'-end. Inserts were amplified by cloning PCR, gel eluted and ligated in pENTR-D-TOPO (Invitrogen) by combining 0.5 µl vector solution, 0.5 µl 6x salt solution (Invitrogen) and 3 µl of DNA fragment solution. The reaction was incubated for 30 min at room temperature. The whole reaction volume was used to transform *E. coli* ONE-SHOT chemically competent cell (Invitrogen) as described in 2.2.2. Transformants were selected on LB containing Kanamycin.

2.2.5.1 GATEWAY LR-reaction

To clone inserts from pENTR D-TOPO into a destination vector, the GATEWAY LR reaction technology was used. Destination vector were either selected from the pGWB or pEARLY GATE series (Nakagawa *et al*., 2007; Earley *et al*., 2006). 1 µl pENTR was mixed with 3 µl destination vector, 4 µl 1xTris-EDTA (pH 8.0) and 2 µl LR clonase II (invitrogen). Reactions were incubated for 16 hours at room temperature. The LR clonase was inactivated by adding 1 µl Proteinase K (Invitrogen) and incubation for 10 minutes at 37 °C. 3 µl of the reaction were used to transform ONE SHOT chemical competent cells (Invitrogen). pEARLY vector transformants were selected on LB contain Kanamycin. For vectors of the pGWB series, transformants were selected on LB containing Kanamycin and Hygromycin.

Table 2.5: Vector backbones used in this study

Vector	Source/Reference	Used for
pGEM-Teasy	Promega	subcloning
pENTR-D-TOPO	Invitrogen	subcloning
pGWB11 (C-term. FLAG)	Nakagawa et al., 2007	*in planta* expression
pGWB14 (C-term. HA)	Nakagawa et al., 2007	*in planta* expression
pK7WGF2,0 (N-term. eGFP)	Karimi et al. 2005	*in planta* expression
pK7FWG2,0 (C-term. eGFP)	Karimi et al. 2005	*in planta* expression
pGEX-4T1 (N-term. GST)	GE Healthcare	*E. coli* expression
pOPINM (His/MBP)	Berrow et al., 2006	*E. coli* expression

Table 2.6: Plasmids used in this study

Description	backbone	Vector insert	Reference/cloned by
Plant expression vectors			
35S::EFR-GFP-His	pEarleyGate103	EFR CDS	Cloned by Yasu Kadota
35S::FLS2-GFP-His	pEarleyGate103	FLS2 CDS	Cloned by Benjamin Schwessinger
35S::BRI1-GFP-His	pEarleyGate103	BRI1 CDS	Cloned by Benjamin Schwessinger
35S::BIK1-eGFP	pK7FWG2,0	BIK1 CDS	Cloned by Cecile Segonzac
35S::PIE-FLAG	pGWB11	CDS At3g12620	-
35S::PIE-eGFP	pK7FWG2,0	CDS At3g12620	-
35S::MYB32-eGFP	pK7FWG2,0	CDS At4g34990	-
35S::MYB32-HA	pGWB14	CDS At4g34990	-
35S::PP2C-58-eGFP	pK7FWG2,0	CDS At4g28400	-
35S::PP2C-58-FLAG	pGWB11	CDS At4g28400	-
***E. coli* expression vectors**			
PIE-GST	pGEX-4T1	CDS At3g12620	-
GST	pGEX-4T1	-	-
EFR-MBP	pOPINM	EFR CD (682-1031aa)	Schwessinger et al., 2011
EFR (kinase dead)-MBP	pOPINM	EFR (D849N) CD	Schwessinger et al., 2011
FLS2-MBP	pOPINM	FLS2 CD (840-1173aa)	Schwessinger et al., 2011
FLS2 (kinase dead)-MBP	pOPINM	FLS2 (D977N) CD	Schwessinger et al., 2011
BIK1-MBP	pOPINM	BIK1 CDS	Cloned by Lena Stransfeld

Table 2.6 (continued): Plasmids used in this study

BIK1 (kinase dead)-MBP	pOPINM	BIK1 CDS (K105A and K106A)	Cloned by Lena Stransfeld
BAK1-MBP	pOPINM	BAK1 CD (256-615aa)	Schwessinger et al., 2011
BAK1 (kinase dead)-MBP	pOPINM	BAK1 (D418N) CD	Schwessinger et al., 2011
BRI1-MBP	pOPINM	BRI1 CD (814-1196aa)	Schwessinger et al., 2011

2.3 RNA work

2.3.1 RNA Isolation

For each RNA sample four 14-day old seedlings were frozen in liquid Nitrogen. Plant tissues were grinded and 1 ml TRI reagent (Sigma) was added. Samples were mixed by vortexing and incubated for 5 minutes at room temperature. 200 µl Chloroform were added and samples were mixed by vortexing, incubated at room temperature for 5 minutes and spun down for 20 minutes at 13.000 rpm. 500 µl of the upper phase solution were transferred into new tubes and 500 µl Isopropanol were added. Samples were mixed by vortexing and spun down for 20 minutes at 13.000 rpm.The supernatant was discarded and the pellets were washed with 400 µl 70 % Ethanol. Pellets were dried for 10 minutes at room temperature. RNA were dissolved in 30 µl RNase free water by incubating for 5 minutes at 53 °C. RNA concentrations were determined using a Nanodrop.

2.3.2 DNase treatment

DNase treatment was performed using the TURBO DNA-free kit (Ambion) as described in the provided manual. Therefore 30 µl RNA were mixed with 3 µl buffer and 1 µl DNase (Ambion). DNase treatment was performed for 30 minutes at 37°C. The DNase was inactivated by adding 4 µl Inactivation Reagent.

2.3.3 Reverse transcription PCR

RT reactions were performed using Superscript II (Invitrogen) or Superscript III (Invitrogen) as described in the provided manuals. For each 20 µl reaction 2-5 µg RNA were used. For all reaction Oligo (dT_{15})-primers were used. At the end of the cDNA synthesis, the cDNA samples were diluted by adding 60-80 µl water.

2.3.4 Quantitative real-time PCR

qRT-PCR assays were performed using SYBRgreen (Sigma). 10 µl SYBRgreen were mixed with 6.5 µl water, 1.5 µl cDNA and 1 µl each forward

and reverse primer. Samples were incubated in a Chromo 4 Thermal Cycler (MJ Reaserch) or CFX96 Real Time System Thermal Cycler (Bio-Rad) running the program described in Table 2.7. Samples values were normalized with the value from qRT-PCRs with the housekeeping gene (At5g15400) and wild type (Col-0 or La-*er* untreated).

Table 2.7: Quantitative real-time PCR thermal program

Step	Temperature	Time period of step	number of cycles
Initial denaturation	95 °C	4 minutes	1x
Denaturation	94 °C	10 seconds	40 x
Annealing	60 °C	15 seconds	
Extension	72 °C	17 seconds	
read plate			
Final extension	72 °C	10 minutes	1 x
Melting curve from 65 °C to 95 °C, read every Δ 0.5 °C, hold 1 second			

2.3.5 Calculation of qRT-PCR primer efficiency

To calculate the primer efficiency of all qRT-PCR primers, a standard curve was made using serial dilutions of cDNA (1:1, 1:2, 1:4, 1:16). The measured Ct (Cycle Threshold) values were plotted against the log value of the corresponding cDNA dilution. The efficiency of each primer set was determined using the equation E=10 (-1/slope). Primers with efficiency between 1.95 and 2.05 were selected for quantitative analysis.

2.4 Protein work

2.4.1 General methods

2.4.1.1 Protein separation by one-dimensional polyacrylamide gel electrophoresis

For all polycrylamid gel electrophoresis the Mini-PROTEAN Tetra Electrophoresis System (Bio-Rad) was used. Stacking and resolving gels were prepared as described by Laemli, 1970. Gels were run in Mini-PROTEAN III gel tanks (Bio-Rad) filled with SDS-running buffer [25 mM Tris, 250 mM glycine, pH 8.3, 0.1% SDS]. The gel electrophoresis was performed in a continuous buffer system at 90 V till the proteins reached the separating gel and then with 150 V till the desired separation was reached. To determine the molecular size of the separated proteins, in all gels 10 ul of Page Ruler Prestained Protein Ladder (Thermo Scientific) or Pretsained Protein Marker (NEB) was included.

2.4.1.2 Semi-dry blotting of acrylamid gels

Four Whatman papers and two fiber pad were equilibrated for 5 min in pre-chilled transfer buffer [25mM Tris, 192mM glycine, 20% (v/v) methanol, pH 8.3]. The PVDF membranes (BioRad) were activated by incubation for 1 min in methanol. To assemble the transfer sandwiches one fiber pad and two Whatman papers were stacked on the anodic electrode panel of the gel holder cassette (clear side). The activated membrane was transferred on the blotting paper and the gel was placed on top. Air bubbles were carefully removed. Two Whatman papers and another sponge were placed on top and air bubbles were again carefully removed. The cathode panel of the gel holder cassette (black side) was placed onto the transfer stack and the transfer cassette was closed. Proteins were either transferred for 2 hours at 90 V or over night at 30 V.

2.4.1.3 Coomassie staining

To stain on the membrane bound proteins, membranes were incubated for 5-30 minutes in Coomassie stain solution [0.5% (w/v) Coomassie brilliant blue R-250, 50% (v/v) methanol, and 7.5 glacial acetic acid] and de-stained for 30 minutes with de-stain solution [20% (v/v) methanol, 5% (v/v) acetic acid].

2.4.1.4 Immunodetection

PVDF transfer membranes containing immobilised proteins were blocked for one hour at room temperature with 0.1 % TBS-T buffer [0.5M NaCl, 200mM Tris-HCl, 0.1 % (v/v) Tween-20] containing 5 % dried skimmed milk powder (w/v) with gentle shaking. The membranes were then incubated with the primary antibodies (Table 2.8) in 0.1 % TBST buffer containing 5 % dried skimmed milk powder (w/v) for 1 hour at RT or O/N at 4°C. The membranes were washed three times for 10 min with 0.1 % TBS-T buffer and incubated for 1 hour at RT with 0.1 % TBST buffer containing 5% dried skimmed milk powder (w/v) containing the secondary antibodies (Table 2.8) covalently coupled to horseradish peroxidase (HRP). The membrane was washed three times for 10 min each with 0.1 % TBST buffer. Peroxidase signal of the secondary antibody-HRP conjugate was then detected with ECL (Amersham Biosciences) as described in the provided manual. The membranes were exposed onto ECL Hyperfilm (Amersham Biosciences) or Fuji Medical X-Ray Film (Fuji). Film exposure ranged from 10 sec to 12 hours.

Table 2.8: Antibodies used in the study

Antibody	Company	Origin	Working Dilution
α-HA-HRP	Santa Cruz	Rabbit	1:2000
α-GFP	Torrey Pines/AMS	Rabbit	1:5000
α-His	Novagen	Mouse	1:1000
α-FLS2	Eurogentec	Rabbit	1:1000
α -BAK1	Eurogentec	Rabbit	1:1000
α –Rabbit (A0545)	Sigma	Goat	1:5000
α -Mouse (A0168)	Sigma	Goat	1:15000
α-GST	Upstate	Rabbit	1:5000
α-FLAG (F3165)	Sigma	Rabbit	1:5000
α-Phospho-Tyrosine	Cell Signaling	Mouse	1:2000
α-Phospho-Serine	abcam	Rabbit	1:1000
α-Phospho-Threonine	Cell Signaling	Rabbit	1:1000

2.4.1.5 Phos-tag SDS-PAGE

This Protocol was kindly provided by the group of Prof. Dr Roger Innes (Indiana University, USA).

SDS-gels were prepared as as described in section 2.4.1.1., but the separation gel was additionally supplemented with 50 nM Phos-tag (AAL-107, Wako Pure Chemical Industries, Ltd., Japan) and 50 nM $MnCl_2$. Gel electrophoresis was performed as described in section 2.4.1.1. When the desired separation was reached, the SDS-gels were incubated for 10 minutes in transfer buffer (section 2.4.1.2) containing 1 mM EDTA and afterwards for 10 minutes in transfer buffer without EDTA. GELS were transferred as described in section 2.4.1.2.

2.4.2 Expression of recombinant proteins in *Nicotiana benthamiana*

Agrobacterium tumefaciens cultures were grown at 28 °C overnight in 100 ml LB-liquid medium containing the relevant antibiotics. Cells were harvested by centrifugation at 3.500 rpm and resuspended in 10 mM $MgCl_2$, 10 mM MES, 150 µM Acetosyringone. The suspensions were set to OD_{600nm} = 0.9. The solution were incubated with shaking at room temperature and infiltrated in four week old *N. benthamiana* leaves using a 1 ml needleless syringe. All samples were taken two days post infiltration.

1 M MES buffer: 19.62 g MES were hydrate in 80 ml water. The pH was set to pH 6.3 with KOH, fill up with water to 100 ml. Solutions were filter sterilized and stored at -20 °C.

0.1 M Acetosyringone: 200 mg Acetosyringone were dissolved in 10 ml ethanol. Solutions were stored at -20 °C.

2.4.3 Protein extraction from *Nicotiana benthamiana* and *Arabidopsis thaliana*

Plant material was grinded in liquid nitrogen with pre-chilled pestle and mortar and transfer in pre-chilled tubes. 1 ml cold extraction buffer was added per g of plant material and incubate for 20 minutes on ice. Extracts were centrifuged for 20 min at 15.000 rpm and 4 °C (Sorvall RC-5B centrifuge with SM-24 rotor). The extracts were filtered through Bio-Spin exclusion columns (Bio-Rad) in 15 ml falcon tubes. Protein concentrations were determined using the Bio-Rad Protein Assay Kit (Bio-Rad). All samples were diluted to an equal protein concentration in 15 ml Falcon tubes or 1.5 ml Lobind protein tubes (Eppendorf). For crude extract preparation 300 ul were transferred in separate tubes and mixed with 100 ul 4x LDS-buffer and 10 mM DTT.

Extraction buffer for *Arabidopsis thaliana*

150 mM Tris pH 7.5, 150 mM NaCl, 10% Glycerol, 10 mM EDTA, 5 mM DTT, 1% protease inhibitor (Sigma), 1% IPEGAL CA-630 (Sigma) (v/v), for band shift assay in addition: 1 mM Sodium Molybdate, 1 mM NaF

Extraction buffer for *Nicotiana benthamiana*

150 mM Tris pH 7.5, 150 mM NaCl, 10% Glycerol, 10 mM EDTA, 1mM Sodium Molybdate, 1mM NaF, 2% (w/v) PVPP, 10 mM DTT, 1% protease inhibitor (Sigma), 1% IPEGAL CA-630 (Sigma) (v/v)

2.4.4 Protein Immunoprecipitation

For Immunoprecipitation the desired beads (as described below) were added to the plant extract and reactions were incubated on a roller mixer for up to 4 hours at 4 °C. Beads were the collected by centrifuging for 30 seconds at 500 g. Beads were four times washed with washing buffer [150 mM Tris pH 7.5, 150 mM NaCl, 10% Glycerol, 10 mM EDTA, 5 or 10 mM DTT, 0.5 % IPEGAL CA-630 (Sigma)]. After the last washing, remaining supernatant was carefully removed with a needle fitted on a syringe. If not stated otherwise, proteins were eluted from the beads by adding 40 µl 2x LDS-buffer (Invitrogen) + 10 mM DTT. Proteins were denaturated by incubating for 10 minutes at 90 °C, centrifuged for 5 minutes at 13.000 rpm and separated on SDS-gels.

2.4.4.1 α-GFP and α-HA Immunoprecipitation

To each plant extract 40 µl GFP-Trap (Chromotek) or 40 ul anti-HA Affinity Matrix (Roche) were added.

2.4.4.2 α-FLAG Immunoprecipitation

Per sample 40 µl ANTI-FLAG M2 Affinity Gel (Sigma), three times washed in extraction buffer, were blocked for 10 minutes at room temperature in 1 ml extraction buffer containing 400 ug BSA and added to the protein extracts.

2.4.4.3 FLAG elution

After the incubation the beads were washed as described in 2.4.4 and eluted in 40 µl elution buffer [150 mM Tris pH 7.5, 150 mM NaCl, 10% Glycerol, 10 mM EDTA, 10mM DTT, 1% protease inhibitor (Sigma), 0.2 M FLAG peptide (Sigma)] by strong mixing for 10 minutes at room temperature. Beads were collected by centrifugation for 30 seconds at 2.000 rpm and supernatant containing the eluted proteins was transferred into new tubes. Elution was repeated for two times and the eluted proteins were concentrated using StrataClean resin (Stratagene). Therefore 30 µl StrataClean resin was added to the eluted proteins, extracts were mixed and incubated for 10 minutes at room temperature. The to StrataClean resin bound proteins were collected by centrifugation for 1 min at 13.000 rpm. Supernatants were removed and concentrated proteins were eluted by adding 60 µl 2x LDS-buffer (Invitrogen) + 10 mM DTT (Sigma).

2.4.5 Expression of recombinant of proteins from pBAD-Myc/His and pGEX4T1

Full length coding sequence of At3g12620 was cloned into pGEX4T1 (GE Heathcare) to express GST-tagged proteins and transformed in *E. coli* BL21 expression cells. A single colony of the expression cells was inoculated in 5 ml Lb medium contain Carbencilin and grown over night with shaking at 37 °C. On the next day the overnight cultures were transfer in 100 ml LB cultures and cells were grown with shaking at 37 °C till OD_{600nm}=0.6-0.9. Expression of proteins encoded by pGEX4T1 was induced by adding 0.1 mM IPTG. Cultures were incubated with shaking at 18 °C and 1 ml samples were taken after 0, 1, 5 and 20 hours after induction. Cells were peleted by centrifugation for 1 minute at 16.000 g, mixed with 40 µl 1x LDS buffer (Invitrogen) and 10 mM DTT. Proteins were denaturated by incubation for 10 minutes at 90 °C. Proteins were separated by SDS-gel electrophoresis and either stained with Simply Blue Safe Stain (Invitrogen) as described in the provided manual or transferred on PDVF membranes and detected with α-GST antibodies.

2.4.6 Purification of GST-tagged proteins

A single colony of BL21 cells containing pGEX4T1 encoding PIE-GST was inoculated in 5 ml L-medium with Carbencilin and incubated over night at 37 °C with shaking. On the next day a 1 little culture was inoculated with the overnight culture and bacteria was grown at 37 °C with shaking till OD_{600nm}=0.6-0.9. Protein expression was induced by adding 1 mM IPTG and cultures were incubated at 18 °C for 16 hours. On the next day cells were harvested and resuspended in 10 ml BugBuster Protein Extraction Reagent (Novagen) + 0.5 mM DTT+ 1 % protease inhibitor (Sigma) and incubated for 20 minutes on ice. Cells were sonicated for 7-times 20 seconds with each

one minute in between and extracts were spun down for 20 minutes with 20.000 g at 4 °C. The supernatant was filtered through Bio-Spin exclusion columns (Bio-Rad) in 50 ml falcon tubes and 1: 2 diluted with column buffer [20 mM Tris pH 7.5, 0.3 M NaCl, 1 mM EDTA, 0.1 % SDS]. GST-tagged proteins were then purified using a FPLC-system (Amersham) with GSTrap FF Columns (GE Healthcare). Therefore the GST-Trap columns were equilibrated with 5 column volumes of binding buffer [140 mM NaCl, 2.7 mM KCl, 10 mM Na2HPO4, 1.8 mM KH2PO4, pH 7.2]. Diluted cell lysates were applied on the GST-trap columns. Columns were washed with 5 volumes of binding buffer and GST-tagged proteins were eluted with 5 volumes of binding buffer elution buffer [50 mM Tris-HCl, pH 8.0 and 10 mM reduced glutathione]. Eluted proteins were concentrated in Amicon Ultra-4 Centrifugal Filter devices (Milipore) by centrifugation for 10-60 minutes at 10.000 g till a final volume of 200 µl to 1 ml was reached. Proteins were frozen in liquid nitrogen and stored at -80 °C.

2.4.7 Purification of MBP-tagged proteins

A single colony of BL21 cells containing pOPINM with the desired fragment was inoculated in 5 ml LB with Carbencilin and incubated over night at 37 °C with shaking. On the next day, a 1 little culture was inoculated with the overnight culture and bacteria were grown at 37 °C with shaking till OD_{600nm}=0.6-0.9. Protein expression was induced by adding 1 mM IPTG and cultures were incubated at 18 °C for 16 hours. On the next day cells were harvested and resuspended in 10 ml BugBuster Protein Extraction Reagent (Novagen) + 0.5 mM DTT+ 1 % protease inhibitor (Sigma) and incubated for 20 minutes on ice. Cells were sonicated and extracts were spun down for 20 minutes with 20.000 g at 4 °C. The supernatant was then transferred into 50 ml falcon tubes and 1: 2 diluted with column buffer [20 mM Tris pH 7.5, 0.3 M NaCl, 1 mM EDTA, 0.1 % SDS]. The extraction columns were prepared by adding 8 ml of amylase resin beads (NEB) into 20 ml-Poly-Prep Columns (Bio-Rad). The columns were then washed with 3 volumes of water, 3 volumes of 0.1 % SDS, 1 volume of water and 3 volumes column buffer. The diluted lysate was applied to the prepared columns. After the lysate was passing through the columns, columns were washed with 8 volumes of column buffer. Proteins were eluted with 3 ml elution buffer [20 mM Tris pH 7.5, 0.2 M NaCl, 1 mM EDTA, 0.1 % SDS and 10 mM maltose]. Proteins were concentrated in Amicon Ultra-4 Centrifugal Filter devices (Milipore) by centrifugation for 10-30 minutes at 10.000 g till a final volume of 200 µl to 1 ml was reached. Proteins were frozen in liquid nitrogen and stored at -80 °C.

2.4.8 *In vitro* interaction assays

To test for *in vitro* interaction, all proteins were expressed in *E. coli* and extracted as previously described. The protein concentrations were determined using Bio-Rad Protein Assay Kit (Bio-Rad). 2 µg of the proteins

were mixed in total volume of 40 µl *in vitro* buffer [20 mM Tris pH7.5, 0.2 M NaCl, 1 mM EDTA, 0.1 % SDS, 2 mM DTT, 1 % Tween]. 10 µl were used for detection of proteins in the input and mixed with 2 mM DTT and 4 µl 4x LDS-buffer (Invitrogen). The remaining 30 µl were diluted with *in vitro* buffer to a final volume of 1 ml. Per reaction 50 µl Amylose resin beads (NEB), three-times washed in 1 ml *in vitro* buffer, were added to the proteins. Reactions were incubated for 2 hours on a rolling shaker at 4 °C. Beads were washed for four times in 1 ml *in vitro* buffer. Proteins were eluted in 50 µl *in vitro* buffer containing 10 mM maltose and incubated with shaking at room temperature. Beads were collected by centrifugation for 1 minute at 13.000 rpm. 45 µl supernatant was transferred into new tubes. 2 mM DTT and 15 µl 4x LDS-buffer were added. The protein extracts from input and pull down were denaturated for 10 minutes at 90 °C. Protein solutions were equally divided on two 10 % SDS-gels, separated by gel electrophoresis, transferred onto PVDF membranes as previously described and proteins were detected with α-His and α-GST antibodies.

2.4.9 Enzymatic assays

2.4.9.1 Phosphatase treatment

To dephosphorylate PIE, FLAG-tagged PIE was co-expressed with EFR-GFP in *Nicotiana benthamiana* as described in 2.4.2. Band shift was triggered by treatment with 100 nM elf18 for 20 minutes. PIE-FLAG was extracted and immunoprecipitated as described in 2.4.3. Beads were washed as described 2.4.3 and 300 µl water and 30 µl buffer 3 (NEB) were added. Solutions were mixed thoroughly and equally dived in three tubes. The first tube was used as a control and no phosphatase was added. To the second and third reaction 4 µl calf intestinal phosphatase (CIP, NEB) were added. To the third tube in addition different phosphatase inhibitors [50 mM NaF, 50 mM EDTA, 10 mM $NaVO_3$] were added. Reactions were incubated for 1 hour at 37 °C. Then 30 µl 4xLDS buffer (Invitrogen) were added. Proteins were denaturated by incubation for 10 minutes at 90 °C, centrifuged for 5 minutes at 13.000 rpm and separated on 12 % SDS-gels.

2.4.9.2 PP2C activity assays

PIE phosphatase activity was measured according to the instructions provided by the manufacturer by using a Serine/Threonine Phosphatase Assay System (Promega, 2009). PIE-FLAG was transiently expressed in *N. benthamiana* as described in section 2.4.2. Proteins were extracted from 0.5 g of agro-infiltrated tissue with 1.5 ml buffer as described in section 2.4.3 and purified by FLAG IP as described in section 2.4.4. Alternatively, PIE-GST was expressed in *E. coli* and purified as described in section 2.4.6. 1 µg of extracted protein was used per reaction. PP2C activity was measured in 1x

PP2C buffer in a final volume of 50 ul. The colour was allowed to be developed for 15 min, and the absorbance was measured at 600 nm with a plate reader (Varioscan). The reaction was inhibited with 50 mM sodium fluoride (NaF) or 25 mM EDTA.
PP2C buffer (5x): 250 mM imidazole (pH 7.2), 1 mM EGTA, 25 mM $MgCl_2$, 0.1 % β-mercaptoethanol, 0.5 mg/ml BSA

2.4.9.2 *In vitro* phosphatase assay

For autophosphorylation experiments 1 µg of MBP-fusion proteins were incubated in 30 µl kinase buffer [50 mM Tris, pH 7.5, 10 mM $MgCl_2$, 10 mM MnCl2, 1 mM DTT] containing 1 µM unlabeled ATP and 183 kB of $\gamma^{[32P]}$ATP (6,000 Ci/mmol) (PerkinElmer Life Science) for 30 min at 30°C with shaking at 900 rpm. For the dephosphorylation assay the ^{32}P-labeled proteins were washed with PP2C buffer and incubated with GST or PIE-GST for 30 minutes. The reaction was stopped by adding 10 µl 2x LDS buffer and boiling for 5 minutes. Proteins were separated by SDS-PAGE. Gels were transferred to PVDF, which were stained with Coomassie brilliant blue and destained. For the autoradiography, the dried membrane was exposed to an image plate. The amount of incorporated ^{32}P was quantified using the AIDA image analysis software. Values are represented as percentage of the negative control.

2.5 Cell biological assays

To determine the subcellular localisation of fluorescent-tagged proteins, *Nicotiana benthamiana* leaf tissue transiently overexpressing the indicated proteins, or transgenic *Arabidopsis* plants, were analysed with a Leica SP5 Confocal Microscope (Leica Microsystems, Germany). Plasmolysis was induced by incubated leaf slices in 2 M Sorbitol solution.

2.7.1 Growth condition of plants for different biological assay

2.7.1.1. Plants grown on soil

Arabidopsis thaliana plants were grown as at 20 °C with a 10 hour photoperiod and 65 % humidity with 2 plants per pot (7 x 7 cm) for ROS assay and 4 plants per pot (9 x 9 cm) for bacterial growth assay. *Nicotiana benthamiana* plants were grown at an average temperature of 24 °C with 45-65 % relative humidity under long day conditions (16 hours light).

2.6 Plant material and growth conditions

Table 2.9: *Arabidopsis thaliana* lines used in the study

Lines	Mutated locus	Description	reference/ source or NASC code
Col-0	-	Columbia 0, wild-type	-
La-*er*	-	Landsberg erecta, wild-type	-
efr fls2	AT5G20480 AT5G46330	double T-DNA insertion mutant	Nekrasov et al., 2009
atpp2-b6-1 (SALK_064440)	At2g02310	T-DNA insertion	N564440
atpp2-b6-2 (SALK_107367)		T-DNA insertion	N607367
g3pp4 (SALK_071338)	At4g17550	T-DNA insertion	N659964
da1-1	At1g19270	EMS mutant	Li et al., 2008
DA1 COM		EMS mutant complemented with genomic sequence	
tcp15-3 (SALK_011491)	At1g69690	T-DNA insertion	N511491
tcp14-3 tcp15-3 (SALK_011491; SM_3_19812)	At3g47620 At1g69690	double T-DNA insertion mutant	Prof. Michael Bevan/ Caroline Smith (JIC)
atpp2c-73-1 (SALK_042824)	At5g27930	T-DNA insertion	N659830
atpp2c-73-2 (SALK_028649)		T-DNA insertion	N528649
ralfl23-1 (SALK_064994)	At3g16570	T-DNA insertion	N564994
ralfl23-2 (SALK_000027)		T-DNA insertion	N661237
*ralfl23-3 (*SALK_135682)		T-DNA insertion	N635682
DELLA quintuple (rgat, gai-t6, rgl1-1, rgl2-1, rgl3-1)	At1g14920	pentuple T-DNA insertion mutant	Cheng et al, 2004
pie-1 (SALK_036920)	At3g12620	T-DNA insertion	N536920
pie-2 (SALK_016641)		T-DNA insertion	N516641
pie-3 (WiscDsLoxHs095_12C)		T-DNA insertion	N909115
pK7FWG2,0-At3g12620-eGFP, T3, line 17-2	At3g12620	PIE-FLAG; *PIE* overexpression line	generated by M. Smoker (The Sainsbury Lab)
pGWB11-At3g12620-eGFP, T3, line 2-3	At3g12620	PIE-eGFP; *PIE* overexpression lines	generated by M. Smoker (The Sainsbury Lab)
pGWB11-At3g12620-eGFP, T3, line 4-7	At3g12620	PIE-eGFP; *PIE* overexpression line	generated by M. Smoker (The Sainsbury Lab)

2.7.1.2 Plants grown on plates

Sterile seeds were sown on plates containing Murashige-Skoog (MS) salts medium (Duchefa), 1% sucrose, and 1% agar, incubated for 2 days at 4°C and then grown at 20 °C with a 16 hour photoperiod.

2.7.2 Arabidopsis seed sterilisation

Seeds were gas sterilized in a desiccator with 100 ml sodium hypochlorite solution (chlorine bleach) and 3 ml 37 % HCl. After a treatment time of 4 to 8 hours, seeds were dried in a sterile hood for 1 hour.

2.7.3 Generating stable transgenic *Arabidopsis* lines

Transgenic *Arabidposis* lines were generated be floral dip method (Clough and Bent, 1998). Transformants were the selected on MS-media with Kanamycin.

2.7.4 Generation of multiple Arabidopsis mutants by crossing

Individual flowers of mature *Arabidopsis* plants were emasculate using fine tweezers and fresh pollen from donor stamens was patted onto each single stigma. Mature siliques containing F1 seed were harvested. Success of crossing was confirmed by genotyping and plants containing desired mutations of both parents were grown as described above and allowed to self-pollinate. Plants homozygous for both desired mutations were again selected by genotyping.

2.7 Biological assays

2.8.1 PAMPs

Flg22 and elf18 peptides were purchased from Peptron. BL was purchased from Xiamen Topusing Chemical.

2.8.1 ROS assay

Eight leaf discs (4 mm diameter) of four 4 week-old plants were sampled using a cork borer and floated overnight in 200 µl sterile water in a white 96-well plate (Greiner, Germany). The following day the water was replaced with 100 µl solution containing 17 mg/ml (w/v) luminol (Sigma), 10 mg/ml horseradish peroxidase (Sigma) and 100 nM elf18 or 100 nM flg22 per well. Luminescence was measured using a Varioskan Flash (Thermo Scientific) multi plate reader.

2.8.1 Seedling growth inhibition

Seeds were surface-sterilized as described in 2.7.2, sown on MS media, stratified for 2 days at 4 °C and grown for 5 days at 20 °C. Five-day old

seedlings were transferred into 24-well plates (with 2 seedlings per well) containing 500 µl liquid MS with or without the indicated amount of peptide and incubated for seven days. Dry weight of six replicates per treatment was measured using a precision scale (Sartorius).

2.8.2 PAMP-induced gene expression

Seeds were surface-sterilized as described, sown on MS media, stratified for 2 days at 4°C and grown for 5 days at 20°C. Five-day-old seedlings were transferred into 24-well plates (with 2 seedlings per well) containing 500 µl liquid MS and grown for another week. The night before the PAMP-treatment, in the well remaining MS was replaced with 500 µl fresh MS solution. On the next day 500 µl MS containing 200 nM flg22 or elf18 were added. Samples were taken 0 minutes, 30 minutes, 1 hour and 3 hours after treatment. For each treatment 4 seedling were pooled and frozen in liquid Nitrogen. RNA extraction (2.3.1), cDNA synthesis (2.3.3) and qRT-PCRs (2.3.4) were performed as previously described. The expression of each marker gene was normalized to the expression of the housekeeping gene At5g15400 and plotted relative to the wild type (Col-0 or La-*er*) steady-state expression level.

2.8.3 Bacterial growth assay

Pseudomonas syringae pv. *tomato* DC3000 and *P. syringae* pv. *tabaci* 6605 (*Pta*) (Table 2.10) were grown over night in Kings B medium supplemented with appropriate antibiotics. Cells were harvested by centrifugation for 10 minutes at 35.000 rpm and resuspended in sterile water to OD_{600nm} = 0.2 (for *Pto* DC3000 Δ*AvrPto/*Δ*AvrPto* and *Pto* DC3000 *COR*$^-$*)* and OD_{600nm} = 0.02 (for *Pto* DC3000, 0.002 for *Pta*). Prior to spraying, Silwett L-77 was added to the bacterial solutions to a final concentration of 0.04 % (v/v).

For *Pseudomonas syringae:* Four week-old plants were sprayed with bacterial solutions till all leaves were well covered and additional solution was dripping off.

For *Pseudomonas syringae* pv. *tabaci:* Two leaves per plants of three-weeks old plants were syringe infiltrated with a needleless syringe.

Three days after infection samples were taken using a cork-borer (2 mm). Per genotype from four plants each two leave disc were taken. Leaf discs were ground in 1 ml 10 mM $MgCl_2$, diluted and plated on TSA with appropriate selection. Plates were incubated at 28 °C. Colonies were counted two days later.

2.8.4 Flg22-induced resistance

As described in 2.8.3 but with the following modifications. Three leaves per plants were infiltrated with water or 1 µM flg22. One day later the plants were

sprayed (OD_{600nm}=0.02) with *Pto* DC3000. Leaf samples were taken 2 days after infection.

Table 2.10: Summary of pathogens used in the study

Strain		Description	Reference
Pseudomonas syringae pv. *tomato* (Pto) DC3000	wild type	-	Whalen *et al*., 1991
	Cor-,	coronatine mutants	Melotto *et al*., 2006
	ΔavrPto/ ΔavrPtoB	strain lacking the effectors ΔavrPto/ΔavrPtoB	Lin and Martin, 2005
P. syringae pv. *tabaci* 6605 (Pta)	-	-	Shimizu *et al*., 2003

2.8 Overview media and antibiotics

All recipes are for the scale of 1 liter. Solutions were all sterilized by autoclaving.

2.9.1 LB (Lysogeny broth)

10 g tryptone, 5 g yeast extract, 10 g NaCl, pH 7.0. For solid medium, 10g agar was included.

2.9.2 King's B

20 g Peptone, 1.5g Heptahydrated Magnesium Sulfate, 1.5g Potassium Hydrogen Phosphate, 10mL glycerol. pH7.0. For solid medium, 10 g agar

2.9.3 TBA (Trypticase soy agar)

15 g Tryptone, 5 g Soytone - enzymatic digest of soybean meal, 5 g NaCl, 10 g Agar

2.9.4 MS (Murashige Skoog)

4.3 g MS salts, 0.59 g MES, 0.1 g myo-inositol, 1 ml of 1000x MS vitamin stock, 10 g sucrose pH was adjusted to 5.7 with KOH . For solid medium, 8 g phytoagar

2.9.5 YEPD (Yeast Extract Peptone Dextrose)

20 g Bacto peptone 20 g, 10 g Yeast extract, 20 g Dextrose

2.9.6 Antibodies

All antibodies were used in the following final concentrations
Kanamycin: 50 µg/ml for bacteria and plants
Carbencilin: 100 µg/ml for bacteria

Spectinomycin: 100 µg/ml for bacteria
Rifampicin: 50 µg/ml for bacteria
Gentamicin: 25 µg/ml for bacteria
Hygromycin: 40 µg/mL for plants and 100 µg/ml for bacteria

2.9 Data analysis

All statistical analysis was performed using the Graph Pad Prism software. Here, the student t-test was used to analyse the values of two sample groups while the ANOVA Tukey test was used to analyse the values of three or more sample groups.

Chapter 3: Characterisation of a flg22-dependent gene expression network

3.1 Introduction

An essential part of plant innate immunity is the perception of PAMPs by surface-localised pattern recognition receptors. A well described example is the recognition of the bacterial PAMP flagellin, the main component of the flagellum, by the LRR-RLK FLS2 (Felix et al., 1999; Gómez-Gómez and Boller, 2000; Chinchilla et al., 2006). In *Arabidopsis thaliana*, flg22, a 22-amino-acid epitope of flagellin, is sufficient to activate an onset of detectable responses including ROS production, ion fluxes and MAPK activation (Felix et al., 1999; Gómez-Gómez and Boller, 2000; Nühse et al., 2000). Furthermore, expression profiling revealed that flg22 perception induces up- or down-regulation of more than 1,000 genes in *Arabidopsis* (Navarro et al., 2004; Zipfel et al., 2004; Denoux et al., 2008). Many of these gene expression changes are controlled downstream of MAPK and CDPK activation by WRKY-type transcription factors (Asai et al., 2002; Boudsocq et al., 2010). For example, WRKY22 and WRKY29 act as positive regulators downstream of MPK3/6 (Asai et al., 2002), while MPK4 regulates gene expression by interacting with WRKY25 and WRKY33 (Zheng et al., 2007; Qiu et al., 2008). Additionally, it was recently shown that also CDPK4, 5, 6 and 11 act synergistically and independently of the MAPKs to induce the expression of defence-related genes (Boudsocq et al., 2010).

To gain further insight into the underlying transcriptional regulation of genes that are differentially expressed upon flg22 perception, expression data from plants treated with this PAMP were used to build a putative transcriptional regulatory network. Candidates of this so-called flg22-dependent gene expression network are predicted to regulate each other‘s expression in a flg22-dependent manner and therefore are potentially involved in the FLS2-signalling pathway. In order to assess the genetic requirement of selected genes for flg22-triggered responses, I characterized available mutants with different bioassay.

3.2 Results

3.2.1 Identification of potential regulators of flg22-dependent gene expression

Note: All data analysis to generate the flg22-dependent gene expression network was performed by Dr Daniel MacLean (Head of Bioinformatics, The Sainsbury Laboratory).

Publicly available microarray data from AtGenExpress Visualization Tool (Schmid et al., 2005), which was generated from 5-week old *Arabidopsis thaliana* Col-0 plants treated with water or 1 µM flg22 for 1 or 4 hours, was used to identify genes that are up- or down-regulated upon flg22 perception. In order to determine whether these genes regulate each other's expression, the partial correlation coefficient was calculated for each pair of transcripts. Here, the partial correlation coefficient is describing the relationship between two genes, while withdrawing the effect of other genes on their relationship (Opgen-Rhein and Strimmer, 2007). The thereby identified regulatory effects can be indirect, e.g. through the action of proteins, metabolic changes or effects on the cell environment, or direct, e.g. in cases where the regulator encodes a transcription factor that directly controls the expression of the regulated gene (Figure 3.1).

Around 120 significant regulatory relationships were identified and the genes involved in these interactions were used to build the nodes of the flg22-dependent gene expression network (Figure 3.2). Genes that were predicted to regulate each other's expression were connected, whereat the line intensity represents the strength of the regulation (Opgen-Rhein and Strimmer, 2007). Seven genes of this network were predicted to be involved in a higher number of interactions, and were classified as main regulators (Table 3.1 and Figure 3.2, in green). These genes were selected for further characterization to confirm a potential involvement in the FLS2 signalling pathway.

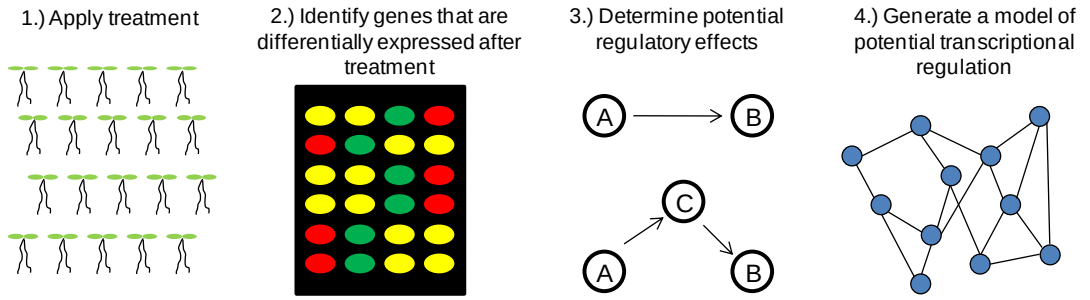

Figure 3.1: General strategy for building a transcriptional regulatory network
(1) Apply different treatments to cells/organism in order to elicit responses. (2) After the treatment, the expression level of many transcripts is measured. (3) The partial correlation coefficient of all pairs of transcripts is calculated to determine whether genes directly or indirectly regulate each other's expression. (4) Based on these relationships, a model is built that described the transcriptional control of the system.

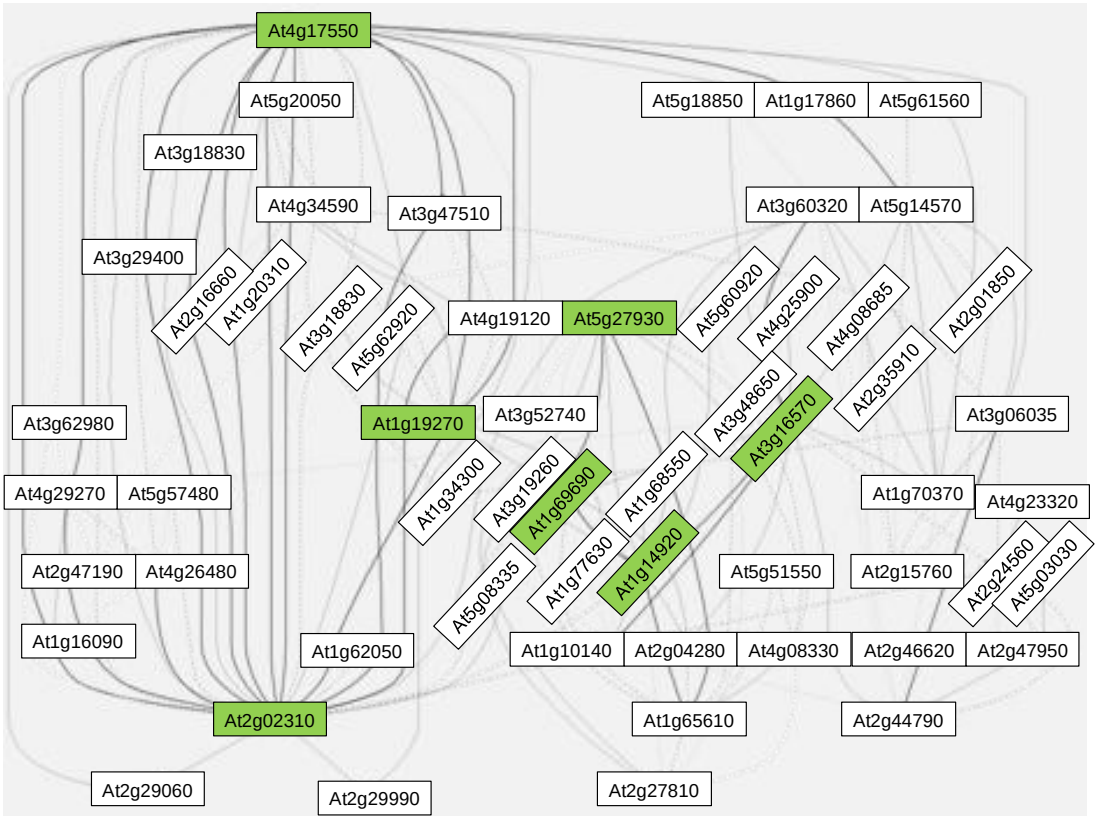

Figure 3.2: A flg22-dependent gene expression network
The predicted transcriptional regulatory network was generated by analysing publicly available microarray data from AtGenExpress Visualization Tool (http://jsp.weigelworld.org/expviz/expviz.jsp). Fifty-six genes were identified that are predicted to regulate each other's expression in a flg22-dependent manner. The genes are presented as the nodes of the network. The line intensity represents the strength of the regulation. The seven predicted main regulators of the network are indicated in green.

Table 3.1: Predicted main regulators of the flg22-dependent gene expression network
Seven genes that were predicted to be involved in a higher number of interactions were classified as main regulators. AGI number, name and the gene(s) that they are predicted to regulate are indicated.

AGI	Name	Predicted to regulate
At2g02310	*At*PP2-B6, PHLOEM PROTEIN 2-B6	At1g19270
At4g17550	G3Pp4, GLYCEROL-3-PHOSPHATE PERMEASE 4	At1g19270
At5g27930	PP2C-73	-
At3g16570	RALFL23, RAPID ALKALINIZATION FACTOR LIKE 23	At1g69690
At1g19270	DA1	At1g69690
At1g69690	TCP15	-
At1g14920	GAI, GIBBERELLIC ACID INSENSITIVE	At1g69690 At3g16570

3.2.2 Validation of the predicted flg22-dependent gene expression network by qRT-PCR

Prior to the characterisation of the seven candidate genes, the predicted network was validated by confirming that the expression of these genes is regulated by flg22 treatment, as indicated by the microarray data. Relative expression levels of all candidate genes were determined by qRT-PCR with gene-specific primers and cDNA from *Arabidopsis thaliana* seedlings treated with 1 µM flg22 for 0, 1 or 4 hours. The efficiency of the PAMP treatment was determined by confirming that two well known flg22-induced genes, *WRKY22* and *FRK1 (FLG22-INDUCED RECEPTOR-LIKE KINASE 1)*, were up-regulated after the treatment (data not shown). Gene expression of all seven candidates was quantified in three biological replicates and the measured induction values were normalized to the expression of the housekeeping gene At5g15400.

The qRT-PCR results confirmed that the expression of all seven candidate genes is activated or repressed as indicated by the microarray data (Figure 3.3 and Table 3 in Appendix). Next, I compared the rate of induction or repression that was measured by qRT-PCR or predicted by microarray analysis. In order to have an additional dataset to compare the qRT-PCR results to, I also included values from the *Arabidopsis* eFP Browser database (Winter et al., 2007) (Figure 3.3 and Table 3 in Appendix). Since both

microarray datasets were generated from 5-week old *Arabidopsis thaliana* Col-0 plants treated with 1 µM flg22, they are expected to predict similar induction values.

For most genes, including *GAI*, *RALFL23*, *TCP15* and *PP2C-73,* the two microarray databases and the qRT-PCRs showed similar induction values (Figure 3.3 A-D). For *DA1* and *G3Pp4* both microarrays predicted different induction values than the qRT-PCRs. Here, the values determined by qRT-PCR were lower than the microarray results (Figure 3.3 E and F). Both microarray databases predicted significantly different values for *AtPP2-B6* (Figure 3.3 G). Here, only qRT-PCRs results and the data from the *Arabidopsis* eFP Browser indicated a similar induction rate (Figure 3.3 G).

In summary, the qRT-PCR results confirmed the tendency of induction or repression for most genes, as indicated by microarrays. Furthermore, since expression values from seedlings were compared to the induction values in mature plants, it can be concluded that the flg22-dependent gene expression was robust and independent of the developmental stage of the plant.

3.3.2 Characterization of the predicted seven main regulators of the flg22-dependent gene expression network

PAMP-triggered signalling pathways consist of a complex network of connected as well as distinct events, beginning with ligand perception and receptor activation and leading to numerous detectable responses (Nicaise et al., 2009). Therefore, it is evident that a wide variety of outputs needs to be assessed to elucidate whether a protein is involved in any of these events. Instead of characterizing all seven candidates extensively, I pre-selected the most promising candidates by measuring two flg22-triggered outputs, ROS production and seedling growth inhibition, in available candidate mutants. Both assays can be easily used to characterize a high number of plants. Additionally, it is possible to identify mutants that are only involved in one specific output of PAMP-triggered signalling.

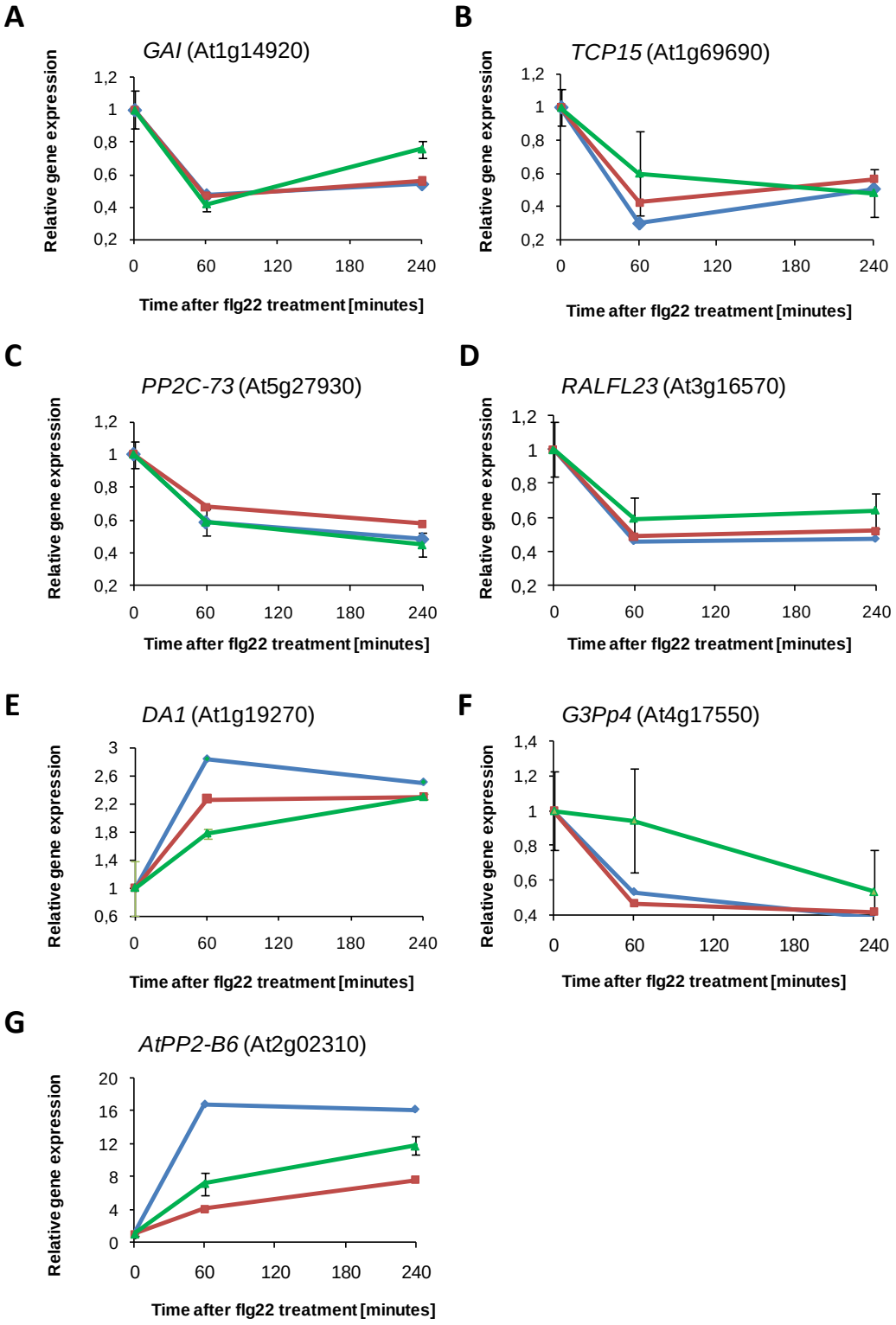

Figure 3.3: **Relative flg22-dependent gene expression of the seven predicted main regulators of the flg22-dependent gene expression network**
(A-G) Gene expression was determined by qRT-PCR (green) with gene specific-primers and cDNA generated from *Arabidopsis thaliana* seedlings treated with 1 µM flg22 (time point zero, 60 and 240 minutes). Expression values were normalized to the expression of the housekeeping gene At5g15400 and plotted relative to expression levels at time point 0. Results are average ± standard error with n=4. In addition, publicly available microarray data from eFP Browser (red) and AtGene Express (blue), generated from 5-week old *Arabidopsis thaliana* Col-0 plants treated with 1µM flg22, were included in each graph for comparison.

3.3.2.1 PHLOEM PROTEIN 2-B6 (AtPP2-B6)

AtPP2-B6 (PHLOEM PROTEIN 2-B6) encodes an uncharacterised protein that carries a putative F-Box and a PP2-like domain, which is highly similar to the PP2 domain of cucumber lectins (Dinant et al., 2003). The *Arabidopsis* genome encodes 30 PP2-like domain containing proteins that were, based on their overall domain structure, divided into two subgroups (Dinant et al., 2003). *At*PP2-B6 belongs to subgroup II, which contains two characterised members: *At*PP2-B9 and *At*PP2-B14 (Figure 3.4) (Dinant et al., 2003).

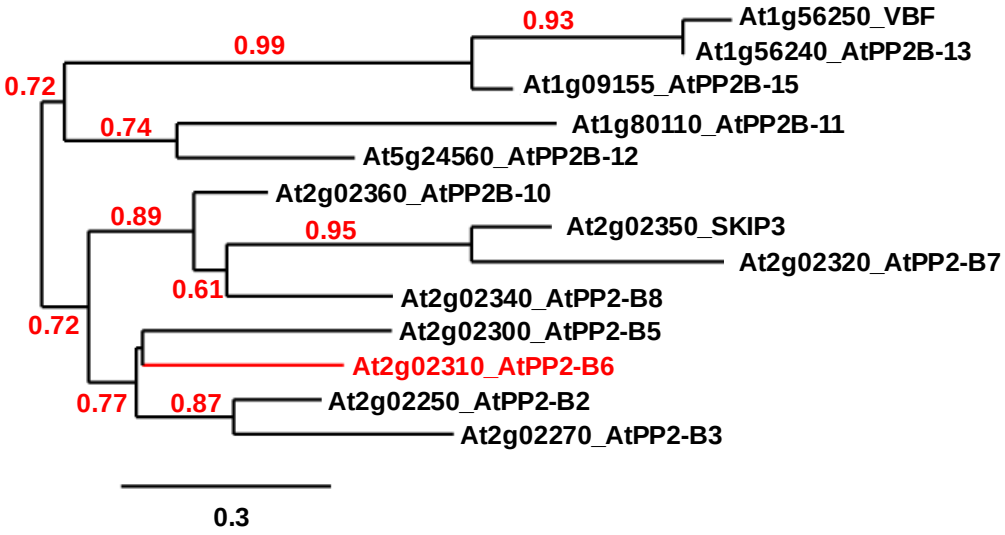

Figure 3.4: *At*PP2-B6 is part of subgroup II of *Arabidopsis* PP2-like domain containing proteins
Phylogenetic tree of subgroup II of *Arabidopsis* PP2-like proteins. *At*PP2-B6 is marked in red. The phylogenetic tree was generated using full-length amino acid sequences. MUSCLE was used for the alignment, PhyML for the phylogeny and TreeDyn for drawing the tree (www.phylogeny.fr). The horizontal branches are drawn to scale as indicated by the scale bar (bar = substitution/site rate of 0.3 %), and their length indicates the level of divergence among sequences. Bootstrap values are indicated in red above nodes.

*At*PP2-B9 interacts with the SCF (Skp1-Cullin-F-box-protein complex) subunit ASK1 (ARABIDOPSIS SKP1 HOMOLOGUE 1) in yeast two-hybrid assays and was therefore called SKIP3 (SKP1 INTERACTING PARTNER 3) (Farras et al., 2001). The second characterised member, *At*PP2-B14, is also referred to as VIP1-BINDING F-BOX PROTEIN (VBF) (Zaltsman et al., 2010). VBF interacts with ASK1, as well as with the putative transcription

factor VIP1 (VirE2-INTERACTING PROTEIN 1) and the *Agrobacterium tumefaciens* virulence protein VirE2, two components of the T-DNA nucleoprotein complex (Zaltsman et al., 2010). VBF mediates the targeted proteolysis of both VIP1 and VirE2 and thereby promotes the integration of the T-DNA into the plant genome (Zaltsman et al., 2010).

The closest homologue of *At*PP2-B6 is *At*PP2-B5 (Figure 3.4) and both proteins share around 50 % amino acid identity (Figure 3.5).

```
AtPP2-B5        MGQKHGVDTRGKGAEFCG----CWEILTEFINGSS-------ASFDDLPDDCLAIISSFT  49
AtPP2-B6        MGQKLGVDSRQKIRQVLGSSSKVQKHDVESIGGGGGEIVPGHSPFDDLPEDCISNIISFT  60

AtPP2-B5        STPRDAFLAALVSKSFGLQFNSDSVWEKFLPPPDYVSLLPKSRVFSSKKELYFALC-DPF 108
AtPP2-B6        S-PRDVCVSASVSKSFAHAVQCDSIWEKFLP-SEYESLIPPWRVFSSKKDLYFTLCYDPV 118

AtPP2-B5        PNHNGKMSFRLDKASGKKCVMLSAKKLLISRVVNPKYWKWISIPESRFDEVPELLNIDSF 168
AtPP2-B6        LVEDGKKSFWLETASGKKCVLLAAKELWITGGNNPEYWQWIELCESSFEKVPELLNNRSF 178

AtPP2-B5        DIRGVLNTRIISPGTHYSAYIVYTKTSHFNGFQTSPIQAGVGFQRHGMSKTFIRFD---- 224
AtPP2-B6        QMGGSMSTQILSLGTHYSVYIVYKIKDERHGLRDLPIQVGVGFKGQEMPKQFICFDESTD 238

AtPP2-B5        ------------SKKRQDGWMEAKIGDFYNEGGLIGFNLIEVSVVDVARYPHMNMKSG-L 271
AtPP2-B6        KTKEWPKKKLMKSKKRGDGWMEAEIGDFFNDGGLMGFDEVEVSIVDVTSP---NLKCGVM 295

AtPP2-B5        IEGIEFRPKDSR 283
AtPP2-B6        IEGIEFRPKDCQ 307
```

Figure 3.5: Alignment of *At*PP2-B6 and its closest homologue *At*PP2-B5
Multiple alignments were generated with Muscle 3.7. Amino acid similarity was determined according to BLOSUM62. In yellow: max similarity (3.0), in blue: medium similarity (1.5). The predicted F-Box domain is underlined (http://pfam.sanger.ac.uk), the predicted PP2-like domain is double underlined (http://pfam.sanger.ac.uk).

In order to test whether *AtPP2-B6* plays a role in the FLS2 signalling pathway, two *atpp2-b6* T-DNA insertion lines were obtained from NASC (Nottingham Arabidopsis Stock Centre) and homozygous mutants were characterised (Figure 3.6 A). Both tested *atpp2-b6* mutants displayed wild-type-like flg22-triggered ROS production and seedling growth inhibition (Figure 3.6 B and C). However, since both tested T-DNA lines contain only a T-DNA insertion at the 3'-UTR of the gene, the *At*PP2-B6 protein level might not be affected. Since, T-DNA lines that carry a T-DNA insertion in the beginning of the gene were not available; the gene could alternatively be silenced by RNAi. Furthermore, it would be of interest to test the effect of *AtPP2-B6* overexpression on flg22-induced responses.

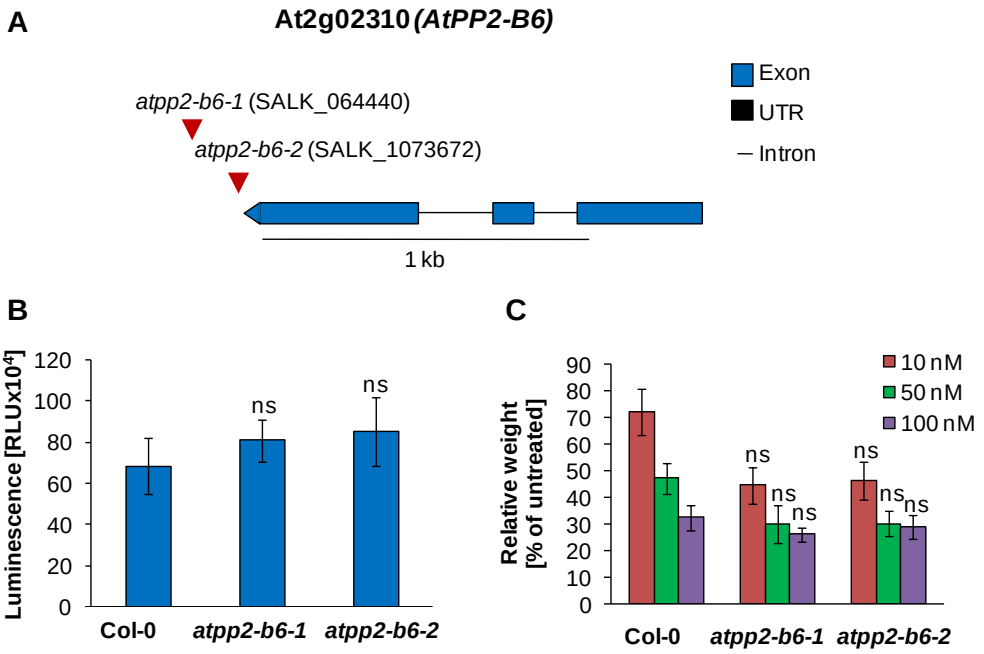

Figure 3.6: Both tested *attpp2-b6* lines display wild-type flg22-triggered responses
(A) *atpp2-b6-1* and *atpp2-b6-2* carry a T-DNA insertion in the 3'-UTR of *AtPP2-B6* (www.arabidopsis.org). (B) Total ROS production represented as relative light units (RLU) in Columbia (Col-0), *atpp2-b6-1* and *atpp2-b6-2* after elicitation with 100 nM flg22. Results are average ± standard error with n=8. This experiment was repeated three times with similar results, (C) Seedling growth inhibition in response to increasing concentrations of flg22 in Columbia (Col-0), *atpp2-b6-1* and *atpp2-b6-2*. Values are represented as percentage of fresh weight of untreated seedlings. Results are average ± standard error with n=6. This experiment was repeated two times with similar results. ns indicates that values were not significantly different from that of wild-type.

3.3.2.2 GLYCEROL-3-PHOSPHATE PERMEASE 4 (G3Pp4)

G3Pp4 (GLYCEROL-3-PHOSPHATE PERMEASE 4) belongs to a family of putative organic phosphate transporters that consists of five members (G3Pp1 to 5) (Figure 3.7) (Ramaiah et al., 2011).

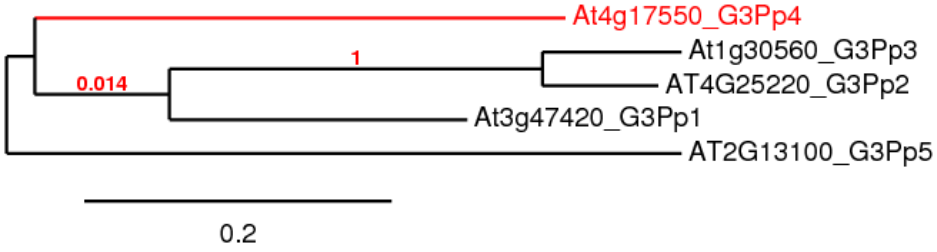

Figure 3.7: G3Pp4 belongs to a family of putative organic phosphate transporter
Phylogenetic tree of *Arabidopsis* phosphate transporters. G3Pp4 is marked in red. The phylogenetic tree was generated using full-length amino acid sequences. MUSCLE was used for the alignment, PhyML for the phylogeny and TreeDyn for drawing the tree (www.phylogeny.fr). The horizontal branches are drawn to scale as indicated by the scale bar (bar = substitution/site rate of 0.2 %), and their length indicates the level of divergence among sequences. Bootstrap values are indicated in red above nodes.

While G3Pp2 and G3Pp3 share a high percentage of sequence similarity, the other family members, including G3Pp4, only share around 50 % amino acid identity (Figure 3.8).

```
G3Pp3           MASWTSSEFLYEEVKPPGIHFLERFRRSGKLSFKQYQAMVFVLTFIAYIAFHATRKPNSI 60
G3Pp2           MASWTSSQFLYEETKPWGIQFLEKFKRSGRLSFKQYQALVFILTFVAYIAFHAARKPNSI 60
G3Pp1           MGSLMQSEPEMEK-KPIGIRFLERIKGS-KLSYSAYQAIVLIVTFLAYASYHAARKTTSI 58
G3Pp4           MAMNSKRK------TPPGIALLRRVRGR-NWSPKTFRYAILFITFIAYACYHASRKPSSI 53
G3Pp5           MQSRIVGL-------APAFSLFPNLNTP-HKTFTFHQILVLITFTAYASFHASRKPPSI 52

G3Pp3           VKGTLSEQPTGH-----------------------------FKGADKGGWAPFDGPDGT 90
G3Pp2           VKGTLSAS-----------------------------------TIEGGWAPFDGPDGT 83
G3Pp1           VKSALDPQSPDTGLNSL-----------------LLRFTSFGSSVKEEGGWAPFNGPDGT 101
G3Pp4           VKSVLHPDSSTKPPQEHNSDKIYPWPMGNVFVKREIGDIDEVLLHRKSKGWEPFNGKDGT 113
G3Pp5           VKSVLGPPSLNS-------------------------------SSIDNGWAPFNGTQGT 80

G3Pp3           ALLGQIDLAFLSVYAVGMFVAGHLGDRLDLRTFLTIGMVGTGVCTALFGVAFWANIHAFY 150
G3Pp2           ALLGQIDLAFLSVYAVGMFVAGHLGDRLDLRTFLTIGMIGTGLFTALFGVAFWANFHSFY 143
G3Pp1           VLLGEIDVAFLAVYAFGMYFAGHLGDRMNLRIFLTVGMIGTGLFTSLFGVGYWGNIHSFY 161
G3Pp4           SRLGEIDVAFLACYSIGMYVAGHLGDSLDLRLFLTWGMIGSGFFVGLFGMGYFWNIHAFW 173
G3Pp5           KRLGELDLAFLSSYALGMYFAGHLGDRIDLRYFLVFGMMGSGILTLVFGLGYWMNVHTLG 140

G3Pp3           YFLAIQTLAGWFQSIGWPCVVAVLGNWFDKKRRGVIMGVWSAHTSLGNIIGTLIATGLLK 210
G3Pp2           YFLAVQVMAGLFQSIGWPCIVAVLGNWFDKKRRGMIMGVWSAHTSLGNIAGSLIASGLLR 203
G3Pp1           YFLIMQMLAGLFQSSGWPSVVAVVGNWFNKKKRGLIMGIWNAHTSVGNITGSLIAAAMLR 221
G3Pp4           FFLVMQMAAGLFQATGWPSVVAVVGNWFGKRKRGLIMGIWNAHTSVGNICGSLIAAGVLE 233
G3Pp5           FYMSVQIVCGLFQSIGWPCVVSVVGNWCGKEKRGLIMGLWNSHTSVGNILGSVIASSVLD 200

G3Pp3           FGWGWSFVGPALLITFLGIVVYLFLPVNPHAV---------------EAERDGSEVDSTM 255
G3Pp2           YGWGWSFLGPAFLMTFLGIVVYLFLPVNPPTV---------------EAERDGTEIDSTM 248
G3Pp1           YGWGWSFVVPGVIIVVIGLVNYAFLPVSPENV---------------GAERDEVLDSSSE 266
G3Pp4           YGWGWSFIAPGFVMSLGGVLVYLFLAAYPEDVGFPDINSNSGKFIKRKRDVEEEEEEVEE 293
G3Pp5           FGWGWSFVLPGVLVLVSGVVVFMFLVVSPNDLG---------------FEELGKEIEIEM 245

G3Pp3           RLGDTIT-ESFLSSRTS-----TGFD--RRAVGFLAAWKIPGVAPFAFCLFFTKLVSYTF 307
G3Pp2           RLGDTIT-ESLLESRMS-----TGFD--RKAVGFMAAWKIPGVAPFAFCLFFTKLVSYTF 300
G3Pp1           KIGNSVN-EPLLLSSSD-----SETDDKKRAVGFIEAWRIPGVAPFALCLFFAKLVAYTF 320
G3Pp4           DLGTDVEGDGEGSSGSG-----SGYEN-KRSVGLLQACMIPGVIPFALCLFFSKLVAYTF 347
G3Pp5           SLGENVE-ESLRKHEAEGAVLLENVDDSSFAIGFLEAWRLPGVAPYAFCLFFSKLVAYTF 304
G3Pp3           LYWLPFYVSQTEIGGEQLSQETSGNLSTLFDVGGVVGGILAGYFSDQLDGRAITAGGFIY 367
G3Pp2           LYWLPFYVSHNMIGGEYLSEETSGNLSTIFDVGGVVGGVLAGYISDQLNGRAITAAGFMY 360
G3Pp1           LYWLPFYVSHTAIEGEYLSDETAGNLSTMFDVGGVVGGIMAGYISDRIGARAITAASFMY 380
G3Pp4           LYWLPFYLSQTTIGGEYVSVKTAGNLSTLFDVGGIVGGILCGYISDKFKARATTAAAFMY 407
G3Pp5           LYWLPYYLRHTAVAGVNLSHKTAGILSTVFDVGGVLGGISAGFISDKIKARALTSITFLA 364

G3Pp3           LTIPALFLYRIYGHVSMTINIILMFVAGLFVNGPYALITTAVAADLGTHKSLKGNARALA 427
G3Pp2           LAIPALFLYRVFGHISLTINVILMFTSGVFIIGPFALITTAVSADLGTHKSLKGNARALA 420
G3Pp1           CSIPALFFYRSYGHVSLLANASLMFLTGMLVNGPYALITTAVSADLGTHSSLKGNSRALA 440
G3Pp4           AAIPAMLVYHSYGGVSQTVNILLMMVAGLFVNGPYALITTAVSADLGTHKSLQGDSRALA 467
G3Pp5           LSIPALIMYRVYGSVSMFINIVLMFISGLLVNGPYALITTAVAADLGTQDSIKGNGRALA 424

G3Pp3           TVTAIIDGTGSVGAAIGPVLTGYIAAI-SWDAVFYMLMTAALISGLLLTTLIIEEVKTLL 486
G3Pp2           TVSAIIDGTGSVGAAIGPVLTGYISAI-SWDAVFYMLMTAALISGLLLTKLIIAEVKALL 479
G3Pp1           TVTAIIDGTGSVGAAVGPLLTGYISSRGSWTAVFTMLMGAAFVAGLLLTRLVMAEVAEKI 500
G3Pp4           TVTAIIDGTGSAGAALGPLLTGFLSTLG-WQAVFYMLVVGALCAGLLLTRLVIAEIREKL 526
G3Pp5           TVTAIIDGTGSVGAALGPLLAGYISSRG-WNSVFFMLIVSIFFAGLFLVRLAKSEINTMR 483

G3Pp3           YGSSEEDHEVAAAS-TSRPPIDVLI 510
G3Pp2           FGSEDEVAASSSSPPASRPPIDVLV 504
G3Pp1           AESRPSEECRSPVDYVQDHVMEV-- 523
G3Pp4           GYVDEEVPASEPLLTDRR------- 544
G3Pp5           SG--ELIASSVP------------- 493
```

Figure 3.8: Alignment of *Arabidopsis* G3Pp proteins
Multiple alignments were generated with Muscle 3.7. Amino acid similarity was determined according to BLOSUM62. In yellow: max similarity (3.0), in blue: medium similarity (1.5).

g3pp4 knock-down mutant plants display a phosphate starvation phenotype in both presence and absence of phosphorus, including a significant increase of lateral root length (Ramaiah et al., 2011). Therefore, it was implied that G3Pp4 plays a role in maintenance of phosphorus homeostasis (Ramaiah et al., 2011).

In order to determine whether *G3Pp4* is involved in PAMP-triggered responses, I characterised the previously described *g3pp4* T-DNA insertion mutant line that I obtained from NASC (Figure 3.9 A) (Ramaiah et al., 2011). The *g3pp4* mutant did not display altered flg22-triggered responses in seedling growth inhibition and ROS assays (Figure 3.9 B and C), indicating that G3Pp4 may not be involved in the regulation of these PTI outputs.

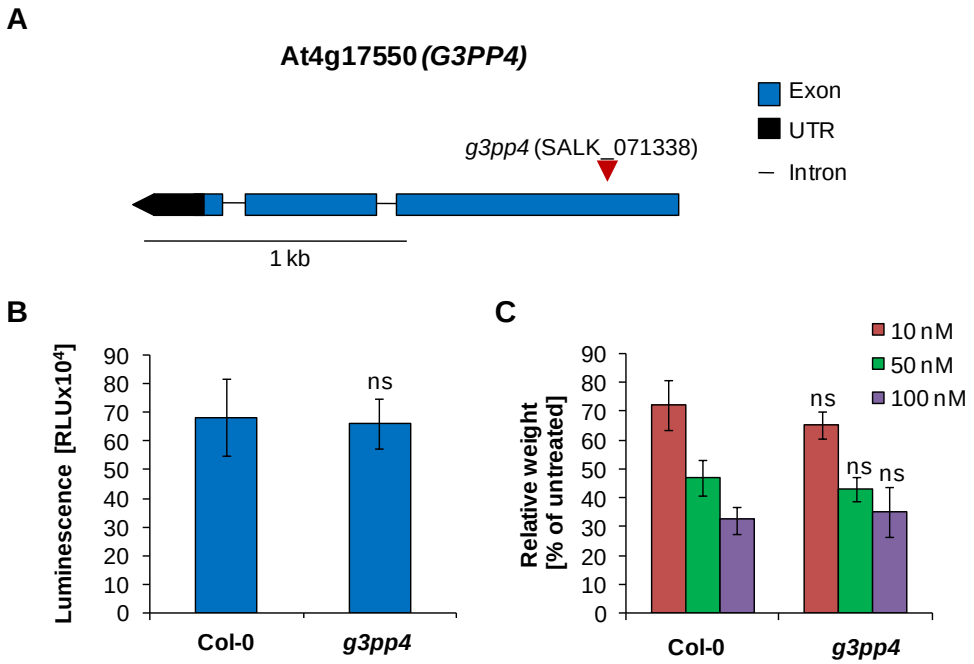

Figure 3.9: *g3pp4* displays wild-type flg22-triggered responses
(A) The *g3pp4* mutant carries a T-DNA insertion in the first exon of *G3PP4* (www.arabidopsis.org). (B) Total ROS production represented as relative light units (RLU) in Columbia (Col-0) and *g3pp4* mutant plants after elicitation with 100 nM flg22. Results are average ± standard error with n=8. This experiment was three times repeated with similar results. (C) Seedling growth inhibition in response to increasing concentrations of flg22 in Columbia (Col-0) and *g3pp4* mutant seedlings. Values are represented as percentage of fresh weight of untreated seedlings. Results are average ± standard error with n=6. This experiment was two times repeated with similar results. ns indicates that values were not significantly different from that of wild-type.

3.3.2.3 TCP15

TCPs belong to a plant specific family of basic helix-loop-helix transcription factors that was named after the three transcription factors TEOSINE

BRANCHED1 from *Zea mays,* CYCLOIDEA from *Anthirridium majus* and PCF from *Oryza sativia* (Cubas et al., 1999). Different members of the TCP family are involved in cell proliferation, growth and organ identity (Cubas et al., 1999). *TCP15* belongs to a small subclade that includes *TCP8, TCP14, TCP22* and *TCP23* and that is clustered on chromosome 1 (Figure 3.10). The closest homologue of TCP15 is TCP14 (Figure 3.10 and 3.11), and both proteins act redundantly in the promotion of cell proliferation in young internodes (Kieffer et al., 2011).

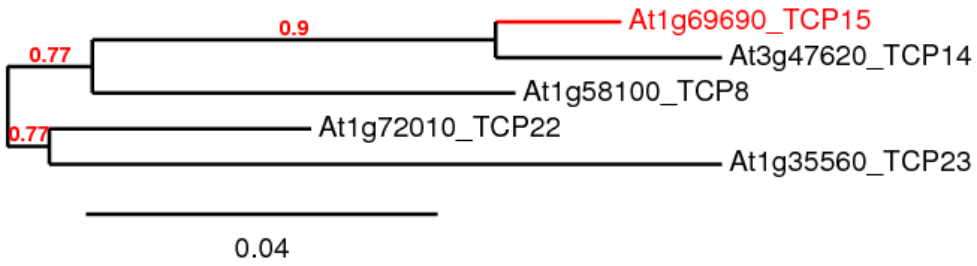

Figure 3.10: TCP15 and its closest homologues belong to a subclade of a plant specific family of basic helix-loop-helix transcription factors
Sub-clade of *Arabidopsis* TCP proteins. TCP15 is marked in red. The phylogenetic tree was generated using full-length amino acid sequences. MUSCLE was used for the alignment, PhyML for the phylogeny and TreeDyn for drawing the tree (www.phylogeny.fr). The horizontal branches are drawn to scale as indicated by the scale bar (bar = substitution/site rate of 0.04 %), and their length indicates the level of divergence among sequences. Bootstrap values are indicated in red above nodes.

```
TCP15           ------------MD--------------PDPDHNHRPNFPLQLLDSS----------TSS 24
TCP14           MQKPTSSILNVIMDGGDSVGGGGGDDHHRHLHHHHRPTFPFQLLGKHDPDDNHQQQPSPS 60

TCP15           SSTSLAIIS-----TTSEPNSEP------------------------KKPPPKRTSTKDR 55
TCP14           SSSSLFSLHQHQQLSQSQPQSQSQKSQPQTTQKELLQTQEESAVVAAKKPPLKRASTKDR 120

TCP15           HTKVEGRGRRIRMPAMCAARVFQLTRELGHKSDGETIEWLLQQAEPAVIAATGTGTIPAN 115
TCP14           HTKVDGRGRRIRMPALCAARVFQLTRELGHKSDGETIEWLLQQAEPSVIAATGTGTIPAN 180

TCP15           FTSLNISLRSSRSSLS-AAHLRTTPSSYY----------------------FHSPHQS- 150
TCP14           FTSLNISLRSSGSSMSLPSHFRSAASTFSPNNIFSPAMLQQQQQQQRGGGVGFHHPHLQG 240

TCP15           ----------------MTHHLQHQHQVRPKNESHSSSSSS---------------SQLLD 179
TCP14           RAPTSSLFPGIDNFTPTTSFLNFHNPTKQEGDQDSEELNSEKKRRIQTTSDLHQQQQQHQ 300

TCP15           HNQMGNYLVQST-AGSLPTSQSPATAP--FWS----------SGDNTQN--LWAFNINPH 224
TCP14           HDQIGGYTLQSSNSGSTATAAAAQQIPGNFWMVAAAAAAGGGGGNNNQTGGLMTASIGTG 360

TCP15           HSG-----------VVAGDVYNPNSGGSGGG---SGVHLMNFAAPIALFSGQP-LASG-- 267
TCP14           GGGGEPVWTFPSINTAAAALYRSGVSGVPSGAVSSGLHFMNFAAPMAFLTGQQQLATTSN 420

TCP15           ----------YGGGGGGGEHSHYGVLAALNAAYRPVAETGNHNNNQQNRDGDHHHNHQE 317
TCP14           HEINEDSNNNEGGRSDGGGDHHNTQRHHHHQQQHHHNILSGLNQYGRQVSGDSQASGSLG 480

TCP15           DGSTSHHS- 325
TCP14           GGDEEDQQD 489
```

Figure 3.11: Alignment of TCP15 and its closest homologue TCP14
Multiple alignments were generated with Muscle 3.7. Amino acid similarity was determined according to BLOSUM62. In yellow: max similarity (3.0), in blue medium similarity: (1.5). The predicted TCP domain is underlined (http://pfam.sanger.ac.uk).

tcp15 tcp14 double mutant plants display a significant reduction in inflorescence height and pedicel length (Kieffer et al., 2011; Li et al., 2012c). Using a dominant negative approach it could be further demonstrated that TCP15 is a regulator of organ growth and cell differentiation, and plants expressing TCP15 fused to the EAR repressor domain display a reduced size and altered leaf and inflorescence morphology (Uberti-Manassero et al., 2012). Furthermore, leaves of this mutant contain smaller and less differentiated cells (Uberti-Manassero et al., 2012).

To determine whether *TCP15* is involved in flg22-triggered signalling, I determined PTI responses in the previously described double knock-out mutant *tcp15 tcp14* as well as the *tcp15* single mutant (both mutants were provided generously by Prof. Michael Bevan, John Innes Centre, UK) (Figure 3.12 A and B).

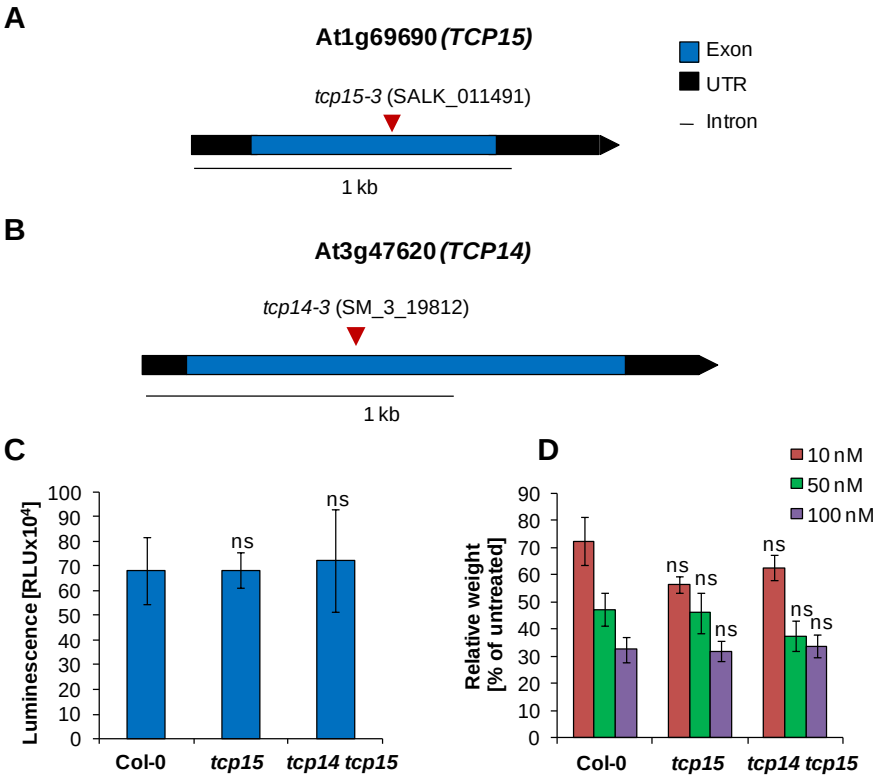

Figure 3.12: *tcp15* single and *tcp14 tcp15* double mutants display wild-type flg22-triggered responses

(A and B) *tcp15-3* and *tcp14-3* carry a T-DNA insertion in the exon (www.arabidopsis.org). (C) Total ROS production represented as relative light units (RLU) in Columbia (Col-0), *tcp15-3* and *tcp14-3 tcp15-3* after elicitation with 100 nM flg22. Results are average ± standard error with n=8. This experiment was three times repeated with similar results. (D) Seedling growth inhibition in response to increasing concentrations of flg22 in Columbia (Col-0), *tcp15-3 and tcp14-3 tcp15-3*. Values are represented as percentage of fresh weight of untreated seedlings. Results are average ± standard error with n=6. This experiment was two times repeated with similar results. ns indicates that values were not significantly different from that of wild-type.

Flg22-triggered ROS production and seedling growth inhibition were comparable to wild-type responses in both tested mutants, indicating that *TCP15* is not involved in the FLS2 signalling pathway or at least in the regulation of these two PTI outputs (Figure 3.12 C and D)

3.3.2.4 Protein phosphatase 2C-73 (PP2C-73)

PP2Cs (Protein Phosphatases 2C) are monomeric enzymes that belong to the serine/threonine phosphatases. The *Arabidopsis* genome encodes 76 predicted PP2Cs that have been subgrouped according to their amino acid sequence and PP2C-73 has been placed in subgroup E (Figure 3.13) (Schweighofer et al., 2004).

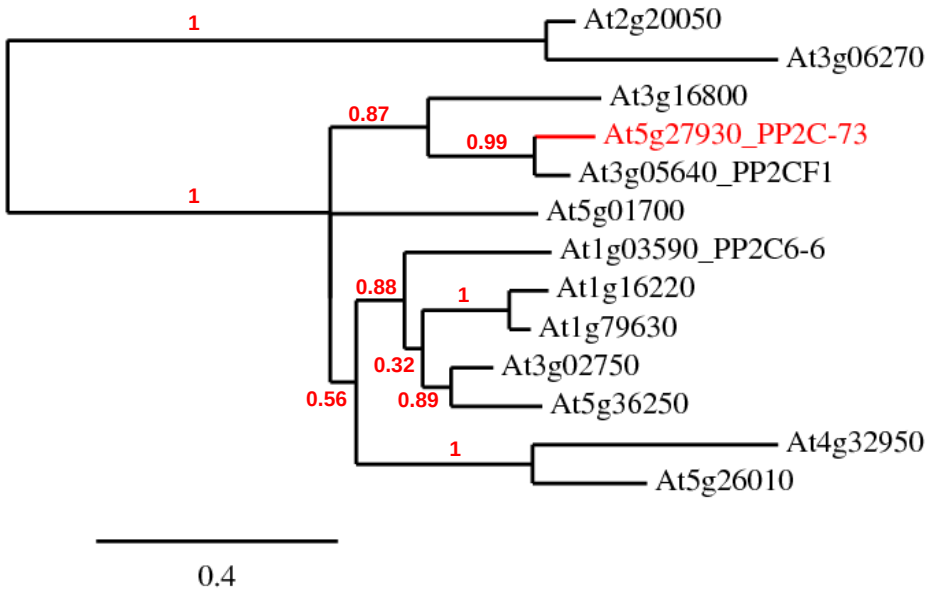

Figure 3.13: PP2C-73 and its closest homologue PP2CF1 belong to the PP2C subgroup E
Phylognetic tree of subgoup E of *Arabidopsis* PP2Cs. PP2C-73 is marked in red. The phylogenetic tree was generated using full-length amino acid sequences. MUSCLE was used for the alignment, PhyML for the phylogeny and TreeDyn for drawing the tree (www.phylogeny.fr). The horizontal branches are drawn to scale as indicated by the scale bar (bar = substitution/site rate of 0.4 %), and their length indicates the level of divergence among sequences. Bootstrap values are indicated in red above nodes.

So far only two members of subgroup E have been characterised: *At*PP2C6-6 and *At*PP2CF1. *At*PP2C6-6 was found to interact with the histone acetyltransferase GCN5 (GENERAL CONTROL NON-REPRESSIBLE 5)

(Servet et al., 2008). Furthermore, since *atpp2c6-6* T-DNA insertion mutants display enhanced acetylation of H3K14 and H3K27, the targets of GNC5, *At*PP2C-6-6 was implied to function as a negative regulator of GCN5 activity (Servet et al., 2008).

Overexpression of *AtPP2CF1*, the closest homolog of *PP2C-73* (Figure 3.13 and Figure 3.14), results in plants with increased biomass production (Hiroki et al., 2010). Although it was confirmed that *AtPP2CF1* encodes an active PP2C-type phosphatase, it is yet unclear how this proteins regulates the plant development (Sugimoto et al., 2011).

```
PP2C-73         MGHFSSMFNGLARSFSIKKVKN-NNGNCDAKEAADEMASEAKKKELILKSSGYVNVQGSN 59
PP2CF1          MGHFSSMFNGIARSFSIKKAKNINSSKSYAKEATDEMAREAKKKELILRSSGCINADGSN 60

PP2C-73         NLASLFSKRGEKGVNQDCALVWEGFGCQEDMIFCGIFDGHGPWGHYVAKQVRNSMPLSLL 119
PP2CF1          NLASVFSRRGEKGVNQDCAIVWEGYGCQEDMIFCGIFDGHGPWGHFVSKQVRNSMPISLL 120

PP2C-73         CNWQKILAQATL-EPELDLEGSNKKISRFDIWKQSYLKTCATVDQELEHHRKIDSYYSGT 179
PP2CF1          CNWKETLSQTTIAEP--D-----KELQRFAIWKYSFLKTCEAVDLELEHHRKIDSFNSGT 172

PP2C-73         TALTIVRQGEVIYVANVGDSRAVLAMESDEGSLVAVQLTLDFKPNLPQEKERIIGCKGRV 239
PP2CF1          TALTIVRQGDVIYIANVGDSRAVLATVSDEGSLVAVQLTVDFKPNLPQEEERIIGCNGRV 232

PP2C-73         FCLDDEPGVHRVWQPDAETPGLAMSRAFGDYCIKEYGLVSVPEVTQRHISTKDHFIILAS 299
PP2CF1          FCLQDEPGVHRVWQPVDESPGLAMSRAFGDYCIKDYGLVSVPEVTQRHISIRDQFIILAT 292

PP2C-73         DGIWDVISNQEAIEIVSSTAERPKAAKRLVEQAVRAWKKKRRGYSMDDMSVVCLFLHSSS 359
PP2CF1          DGVWDVISNQEAIDIVSSTAERAKAAKRLVQQAVRAWNRKRRGIAMDDISAVCLFFHSSS 352

PP2C-73         SS-SLSQHHHAMTILK 373
PP2CF1          SSPSL----------- 358
```

Figure 3.14: Alignment of PP2C-73 and PP2CF1
Multiple alignments were generated with Muscle 3.7. Amino acid similarity was determined according to BLOSUM62. In yellow: max similarity (3.0), in blue: medium similarity (1.5). The predicted PP2C domain is underlines (http://pfam.sanger.ac.uk).

To determine whether PP2C-73 is involved in PAMP-triggered signalling, I characterised two *atpp2c-73* mutants that carry a T-DNA insertion in the first exon and the 3'-UTR of *AtPP2C-73,* respectively (Figure 3.15 A). Both mutants did not display significantly altered flg22-triggered responses in seedling growth inhibition and ROS assays (Figure 3.15 B and C). However, since PP2C-73 and *At*PP2CF1 share more than 70 % amino acid identity (Figure 3.14), they may act redundantly. Therefore, it would be necessary to generate *atpp2c-73 atpp2cf1* double mutants to further assess whether this candidate is involved in flg22-mediated signalling.

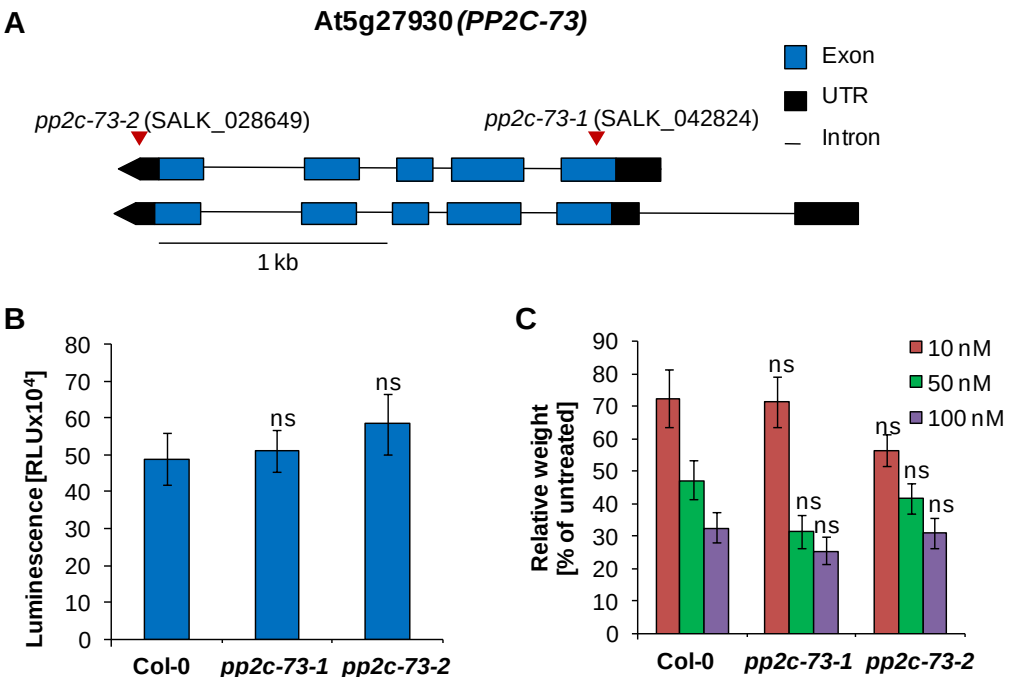

Figure 3.15: *pp2c-73* mutants display wild-type flg22-triggered responses
(A) *pp2c73-1* carries a T-DNA in the third exon, *pp2c73-2* carries a T-DNA in the 3'-UTR of *PP2C-73* (www.arabidopsis.org). (B) Total ROS production represented as relative light units (RLU) in Columbia (Col-0), *pp2c73-1 and pp2c73-2* after elicitation with 100 nM flg22. Results are average ± standard error with n=8. This experiment was three times repeated with similar results. (C) Seedling growth inhibition in response to increasing concentrations of flg22 in Columbia (Col-0), *pp2c73-1 and pp2c73-2*. Results are represented as percentage of fresh weight of untreated seedlings. Results are average ± standard error with n=6. This experiment was two times repeated with similar results. ns indicates that values were not significantly different from that of wild-type.

3.3.2.5 RAPID ALKANILIZATION FACTOR-like 23 (RALFL23)

RALF-like (RALFL) peptides share high amino acid sequence similarity with RALF (RAPID ALKALINIZATION FACTOR), a peptide that was discovered in an alkalinisation assay, originally developed to search for systemin orthologous in tobacco (Pearce et al., 2001a). Like systemin, RALF is able to activate MAP kinases and to induce medium alkalinisation in tobacco cell culture (Pearce et al., 2001a). The RALF precursor contains a signal peptide, indicating that it is likely to be secreted (Pearce et al., 2001a). In addition, the protein contains a dibasic RR motif that is recognized by specific serine-proteases for release of the active peptide (Olsen et al., 2002). Although so far no RALF receptor has been identified, it is anticipated that these peptides are ligands for receptor-mediated responses. This idea is mainly supported by the fast medium alkalinisation that peaks at less than five minutes after adding the peptide to cell-suspension cultures. In addition, experiments with

photoaffinity labelled RALF peptide led to the discovery of potential components of a RALF receptor complex in tomato (Scheer et al., 2005). The *Arabidopsis* genome contains 34 different *RALFL* genes, which all consist of a single exon (Olsen et al., 2002). Since the genes display varying expression profiles (Olsen et al., 2002; Cao and Shi, 2012), it is likely that the RALFL peptides convey signals involved in a range of physiological processes (Wu et al., 2007; Srivastava et al., 2009; Covey et al., 2010; Mingossi et al., 2010).

The expression of *RALFL23* is down-regulated upon BL treatment and it was suggested that this peptide might be involved in BR signalling (Srivastava et al., 2009). Notably, *RALFL23* overexpression results in reduced BL-induced hypocotyl elongation (Srivastava et al., 2009). In addition, this mutant displays reduced shoot growth and develops smaller leaves (Srivastava et al., 2009). RALFL23, as well as its close homologues RALFL22, RALFL33 and RALFL1, carries a predicted site-1-protease recognition site that is identical to the recognition site in the membrane-associated transcription factor bZIP17, which is cleaved by the serine-protease S1P (Site-1 Protease) in response to salt stress (Sakai et al., 1998; Srivastava et al., 2009) (Figure 3.16 and 3.17). It could be confirmed that S1P also cleaves RALFL23 *in vitro* (Srivastava et al., 2009). Furthermore, crossing *35S::RALFL23* to a *s1p* mutant reverted the overexpression phenotype, confirming the importance of S1P for RALFL23 processing (Srivastava et al., 2009).

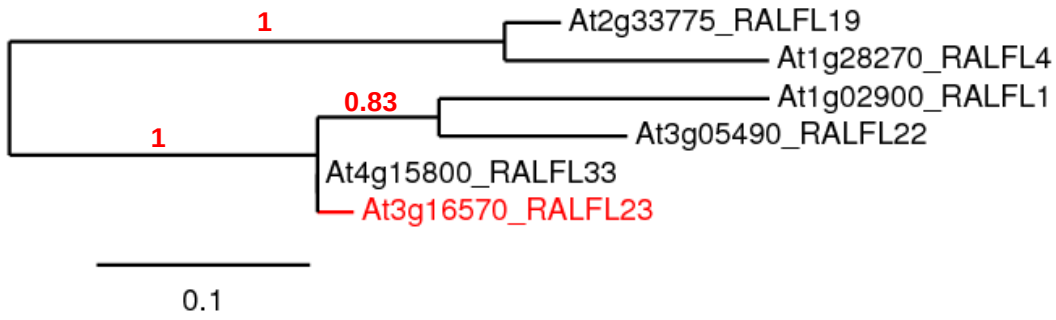

Figure 3.16: RALFL23 and its closest homologues
Phylogenetic tree of RALFL23 and its closest homologues. RALFL23 is marked in red. The phylogenetic tree was generated using full-length amino acid sequences. MUSCLE was used for the alignment, PhyML for the phylogeny and TreeDyn for drawing the tree (www.phylogeny.fr). The horizontal branches are drawn to scale as indicated by the scale bar (bar = substitution/site rate of 0.1 %), and their length indicates the level of divergence among sequences. Bootstrap values are indicated in red above nodes.

```
RALFL1          MDKSFTLFLTLTILVVFIISSPPVQAGFANDLGGVAWATTGDNGSGCHGSIAEC--IGAE 58
RALFL22         MTNTRAIYAVIAILAI-VISAVESTGDFGDSLD-FVRAGSSSLFSGCTGSIAEC--IAEE 56
RALFL23         MRGLSRNSGAAAIFAILLILAVHNWSVAVSSQSTEFAGDFPPFETECRGTIAECSVSAAL 60
RALFL33         MRGLSTKP----VAIIIAILTVHFLFAAVTSQS---SGDFVPIESKCNGTIAECSLSTAE 53

RALFL1          --------------EE-EMDSEINRRILATTKYISYQSLKRNSVPCSRRGASYYNCQNGA 103
RALFL22         --------------EEMEFDSDISRRILAQKKYISYGAMRRNSVPCSRRGASYYNCQRGA 102
RALFL23         GDGGDLFYGGGEMGEEFEMDSEINRRILATRRYISYGALRRNTIPCSRRGASYYNCRRGA 120
RALFL33         --------------EEFEMDSEINRRILATTKYISYGALRRNTVPCSRRGASYYNCRRGA 99

RALFL1          QANPYSRGCSKIARCRS- 120
RALFL22         QANPYSRGCSTITRCRR- 119
RALFL23         QANPYSRGCSAITRCRRS 138
RALFL33         QANPYSRGCSAITRCRR- 116
```

Figure 3.17: Alignment of RALFL23 and its closest homologues, RALFL22, RALFL33 and RALFL1
Multiple alignments were generated with Muscle 3.7. Amino acid similarity was determined according to BLOSUM62. In yellow: max similarity (3.0), in blue medium: similarity (1.5). The double underlined sequences indicate the presumptive site-1-protease recognition site, the underlined sequences represent predicted signal peptides and the arrow indicates the actual cleavage site in RALF23 (Srivastava et al., 2009).

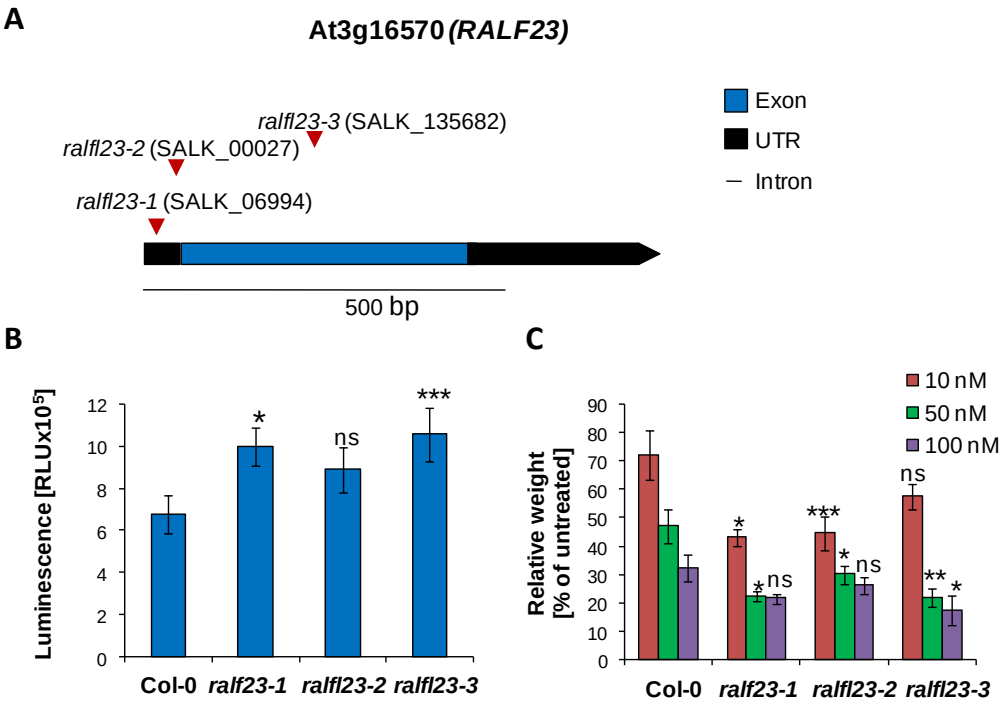

Figure 3.18: *ralfl23* mutants display enhanced flg22-triggered responses
(A) *ralfl23-1* carries a T-DNA insertion in the 5'-UTR of *RALFL23*, *ralfl23-2* and *ralfl23-3* carry a T-DNA insertion in the exon of *RALFL23* (www.arabidopsis.org). (B) Total ROS production represented as relative light units (RLU) in Columbia (Col-0) and *ralfl23* mutant plants after elicitation with 100 nM flg22. Results are average ± standard error with n=8. This experiment was three times repeated with similar results. (C) Seedling growth inhibition in response to increasing concentrations of flg22 in Columbia (Col-0) and *ralfl23* mutant seedlings. Results are represented as percentage of fresh weight of untreated seedlings. Results are average ± standard error with n=6. This experiment was two times repeated with similar results. Asterisks indicate significant differences compared with wild-type values at P>0.05 (*), P>0.01 (**) or P>0.001 (***). ns indicates that values were not significantly different from that of wild-type.

In order to determine whether RALFL23 is involved in the FLS2 signalling pathway, *ralfl23* T-DNA insertion mutants were obtained from NASC. *ralfl23-1* carries a T-DNA insertion in the 5'-UTR of *RALFL23*, while *ralfl23-2* and *ralfl23-3* carry a T-DNA insertion in the exon (Figure 3.18 A). In both assays, all three tested mutants displayed enhanced flg22-triggered responses in seedling growth inhibition and ROS assays (Figure 3.18 B and C). These results indicate that RALFL23 may be involved in flg22-mediated signalling.

3.3.2.6 GIBBERELLIC ACID INSENSITIVE (GAI)

GAI (GIBBERELLIC ACID INSENSITIVE) is one of the five *Arabidopsis* DELLA transcription factors (Figure 3.19) that are negative regulators of the giberellic acid (GA) signalling pathway (Harberd et al., 2009). GAI, RGA (REPRESSOR OF GA1-3), RGL1 (RGA-LIKE1), RGL2 and RGL3, which carry an N-terminal DELLA domain, as well as a C-terminal GRAS domain (Figure 3.20), block the expression of GA-induced genes in absence of the pyotohormone (Harberd et al., 2009). Upon GA perception the DELLA proteins are poly-ubiquitinated by the E3 ubiquitin ligase complex $SCF^{SLY1/GID2}$ and subsequently, the degradation of these transcription factors reliefs the repression of GA-responsive genes (Harberd et al., 2009).

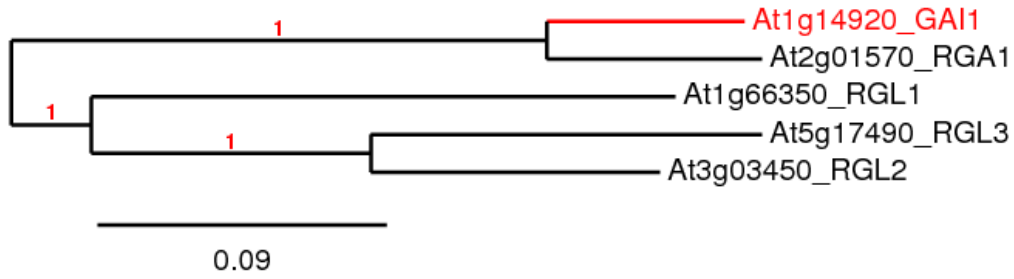

Figure 3.19: GAI is one of the five *Arabidopsis* DELLA domain-containing proteins
Phylogenetic tree of the five *Arabidopsis* DELLA proteins. GAI is marked in red. The phylogenetic tree was generated using full-length amino acid sequences. MUSCLE was used for the alignment, PhyML for the phylogeny and TreeDyn for drawing the tree (www.phylogeny.fr). The horizontal branches are drawn to scale as indicated by the scale bar (bar = substitution/site rate of 0.09 %), and their length indicates the level of divergence among sequences. Bootstrap values are indicated in red above nodes.

Figure 3.20: Alignment of the five *Arabidopsis* DELLA transcription factors
Multiple alignments were generated with Muscle 3.7. Amino acid similarity was determined according to BLOSUM62. In yellow: max similarity (3.0), in blue: medium similarity (1.5). The predicted DELLA domain is underlined (http://pfam.sanger.ac.uk), the predicted GRAS domain is double underlined (http://pfam.sanger.ac.uk).

The five DELLA transcription factors have both distinct and overlapping functions in the regulation of plant development. While RGA and GAI repress stem elongation (Dill and Sun, 2001; King et al., 2001), RGL2 inhibits seed

germination (Lee et al., 2002). In addition, RGA, RGL1, and RGL2 regulate floral development (Cheng et al., 2004; Tyler et al., 2004; Yu et al., 2004). Interestingly, the DELLA *quadruple* mutant, which lacks GAI, RGA, RGL1 and RGL2, displays a reduced flg22-triggered seedling growth inhibition (Navarro et al., 2008). Consistently, mutants that stabilize one or more DELLAs show increased flg22-sensitivity (Navarro et al., 2008). Additionally, flg22 treatment affects the accumulation of RGA by delaying its GA-mediated degradation, indicating that DELLA stabilization contributes to flg22-induced growth inhibition (Navarro et al., 2008).

DELLAs also regulate ROS production in response to abiotic stress by promoting the expression of ROS detoxification enzymes (Achard et al., 2008). Consequently, the DELLA *quintuple* mutant, which lacks all five DELLA transcription factors, exhibits higher basal ROS levels that are further increased upon salt stress (Achard et al., 2008). The DELLA *quadruple* mutant also displays enhanced susceptibility to different pathogens including the necrotrophic fungus *Botrytis cinerea* and the hemibiotrophic bacterium *Pto* DC3000 (Navarro et al., 2008). This enhanced pathogen growth seems to be mainly caused by elevated SA levels and therefore a suppression of JA/ET-dependent gene expression (Navarro et al., 2008). Consistently, the enhanced *Pto* DC3000 growth was reverted when *gai* was crossed to the JA-insensitive *coi1-16* mutant (Navarro et al., 2008).

Since it was reported that the DELLA *quadruple* mutant displays reduced flg22-sensitivity in seedling growth inhibition, I wanted to test whether also the flg22-induced ROS production is affected. Therefore, I characterised the DELLA *quintuple* mutant, which lacks all five DELLA transcription factors (kind gift from Prof. Nicolas Harberd, University of Oxford, UK) (Fu et al., 2004). As previously reported, DELLA *quintuple* mutant plants displayed reduced seedling growth inhibition with all tested flg22 concentrations (Figure 3.21 B). In addition, this mutant also produced significantly less flg22-triggered ROS (Figure 3.21A). Although this result is consistent with the reduced flg22-sensitivity in seedling growth inhibition, it is contrary to the observed enhanced ROS production induced by abiotic stress (Achard et al., 2008). While it has been shown that DELLA *quintuple* mutants plants display enhanced expression of genes encoding ROS detoxification enzymes

(Achard et al., 2008), it is possible that the flg22-triggered ROS production is too high to be reverted through increased enzyme production.

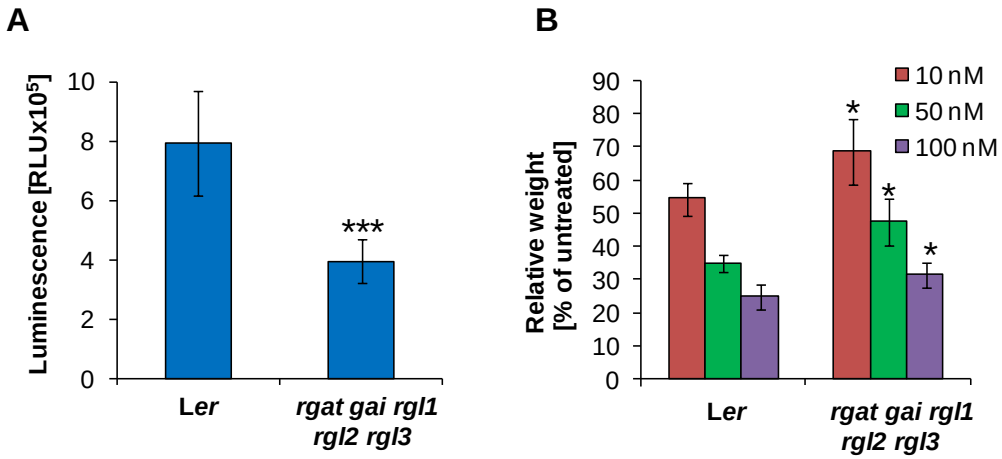

Figure 3.21: DELLA *quintuple* mutants display reduced flg22-triggered response
(A) Total ROS production represented as relative light units (RLU) in Landsberg *erecta* (L*er*) and DELLA *quintuple* (*rgat gai rgl1 rgl2 rgl3*) after elicitation with 100 nM flg22. Results are average ± standard error with n=8. (B) Seedling growth inhibition in response to increasing concentrations of flg22 in Landsberg *erecta* (L*er*) and DELLA *quintuple* (*rgat gai rgl1 rgl2 rgl3*). Results are represented as percentage of fresh weight of untreated seedlings. Results are average ± standard error with n=6. Asterisks indicate significant differences compared with wild-type values at P>0.05 (*) or P>0.001 (***). These experiments were two times repeated with similar results.

3.3.2.7 DA1

DA1, as well as its close homologues, the *DA1-RELATED (DAR)* genes (Figure 3.22), encode predicted ubiquitin receptors (Li et al., 2008). DA1 carries a predicted LIM-domain and a ubiquitin interaction motif (Figure 3.23) (Punta et al., 2012). LIM-domains, which are named after their initial discovery in the proteins Lin11, Isl-1 and Mec-3, have been shown to mediate protein-protein interactions (Bach, 2000).

DA1 has previously been described as a negative regulator of seed morphogenesis and organ growth (Li et al., 2008). The *da1-1* mutant, which carries a single-nucleotide glycine to alanine (G/A) transition causing a point mutation in a conserved amino acid (Figure 3.24 A), displays increased seed and organ size including enlarged flowers, leaves and siliques (Li et al., 2008). Furthermore, *da1-1* plants undergo a longer phase of proliferative growth (Li et al., 2008). Since no direct interactor of DA1 has yet been identified and since the *da1-1* mutation does not affect the ubiquitin binding

affinity, the underlying molecular mechanism how this protein regulates cell proliferation is still unknown (Li et al., 2008).

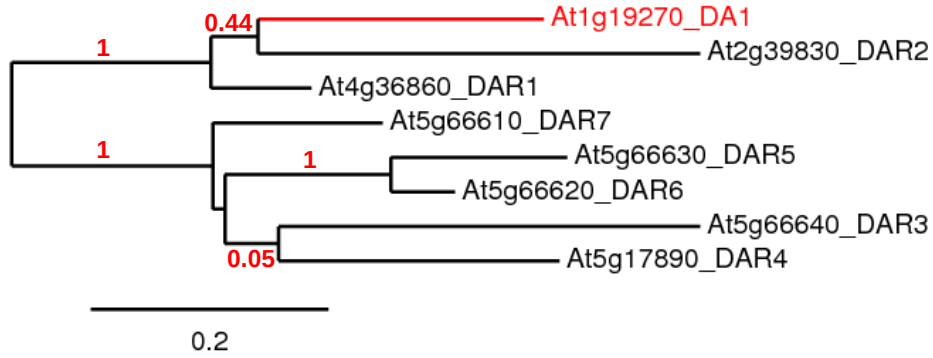

Figure 3.22: DA1 and DA1-related (DAR) proteins are predicted ubiquitin receptors
Phylogenetic tree of *Arabidopsis* DA1 and DA1-related proteins. DA1 is marked in red. The phylogenetic tree of *Arabidopsis* was generated using full-length amino acid sequences. MUSCLE was used for the alignment, PhyML for the phylogeny and TreeDyn for drawing the tree (www.phylogeny.fr). The horizontal branches are drawn to scale as indicated by the scale bar (bar = substitution/site rate of 0.2 %), and their length indicates the level of divergence among sequences. Bootstrap values are indicated in red above nodes.

```
DA1             MGWFNKIFKGSNQRLRVG--NNKHNHNVYYDNYPTASHDDEPSAADTDADNDEPHHTQEP 58
DAR1            MGWLTKILKGSSHKFSDGQCNGRYREDRNLEGPRYSAEGSDFDKEEIECAIALSLSEQEH 60

DA1             STSEDNTS------------NDQENEDIDRAIALSLLEENQEQTSISGKYSMPVDEDEQL 106
DAR1            VIPQDDKGKKIIEYKSETEEDDDDEDEDEEYMRAQLEAAEEEERRVAQAQIEEEEKRRA 120

DA1             ARALQESMVVGNSPRHKSGSTYDNGNAYGAGDLYG----NGHMYGGGNVYANGDIYYPRP 162
DAR1            EAQLEETEKLLAKARLEEEEMRRSKAQLEEDELLAKALQESMNVGSPPRYDPGNILQPYP 180

DA1             ITFQMDFRICAGCNMEIGHGRFLNCLNSLWHPECFRCYGCSQPISEYEFSTSGNYPFHKA 222
DAR1            FLIPSSHRICVGCQAEIGHGRFLSCMGGVWHPECFCCNACDKPIIDYEFSMSGNRPYHKL 240

DA1             CYRERYHPKCDVCSHFIPTNHAGLIEYRAHPFWVQKYCPSHEHDATPRCCSCERMEPRNT 282
DAR1            CYKEQHHPKCDVCHNFIPTNPAGLIEYRAHPFWMQKYCPSHERDGTPRCCSCERMEPKDT 300

DA1             RYVELNDGRKLCLECLDSAVMDTMQCQPLYLQIQNFYEGLNMKVEQEVPLLLVERQALNE 342
DAR1            KYLILDDGRKLCLECLDSAIMDTHECQPLYLEIREFYEGLHMKVEQQIPMLLVERSALNE 360

DA1             AREGEKNGHYHMPETRGLCLSEEQTVSTVRKRSKHGTG-KWAGNITEPYKLTRQCEVTAI 401
DAR1            AMEGEKHGHHHLPETRGLCLSEEQTVTTVLRRPRIGAGYKLIDMITEPCRLIRRCEVTAI 420

DA1             LILFGLPRLLTGSILAHEMMHAWMRLKGFRTLSQDVEEGICQVMAHKWLDAELAAGSTNS 461
DAR1            LILYGLPRLLTGSILAHEMMHAWLRLNGYPNLRPEVEEGICQVLAHMWLESETYAGSTLV 480

DA1             NAASSSSS---SQGLKKGPRSQYERKLGEFFKHQIESDASPVYGDGFRAGRLAVHKYGLR 518
DAR1            DIASSSSSAVVSASSKKGERSDFEKKLGEFFKHQIESDSSSAYGDGFRQGNQAVLKHGLR 540

DA1             KTLEHIQMTGRFPV 532
DAR1            RTLDHIRLTGTFP- 553
```

Figure 3.23 : Alignment of DA1 and it closets homologue DAR1
Multiple alignments were generated with Muscle 3.7. Amino acid similarity was determined according to BLOSUM62. In yellow: max similarity (3.0), in blue: medium similarity (1.5). The ubiquitin interaction motif is underlined (http://pfam.sanger.ac.uk), the predicted LIM domain is double underlined (http://pfam.sanger.ac.uk).

To examine whether *DA1* is involved in flg22-triggered signalling, I determined ROS production and seedling growth inhibition in the previously described *da1-1* mutant (kind gift from Prof. Michael Bevan, John Innes Centre) (Li et al., 2008). Notably, in both assays *da1-1* displayed altered responses. Compared to wild-type plants, this mutant produced significantly less ROS in response to flg22 treatment (Figure 3.24 B). In addition, *da1-1* plants also displayed reduced PAMP-sensitivity in seedling growth inhibition assays, especially after treatment with 50 and 100 nM flg22 (Figure 3.24 C). These results indicated that DA1 plays a role in flg22-triggered signalling. Therefore, I decided to further characterise this mutant in collaboration with Prof. Michael Bevan (John Innes Centre, UK).

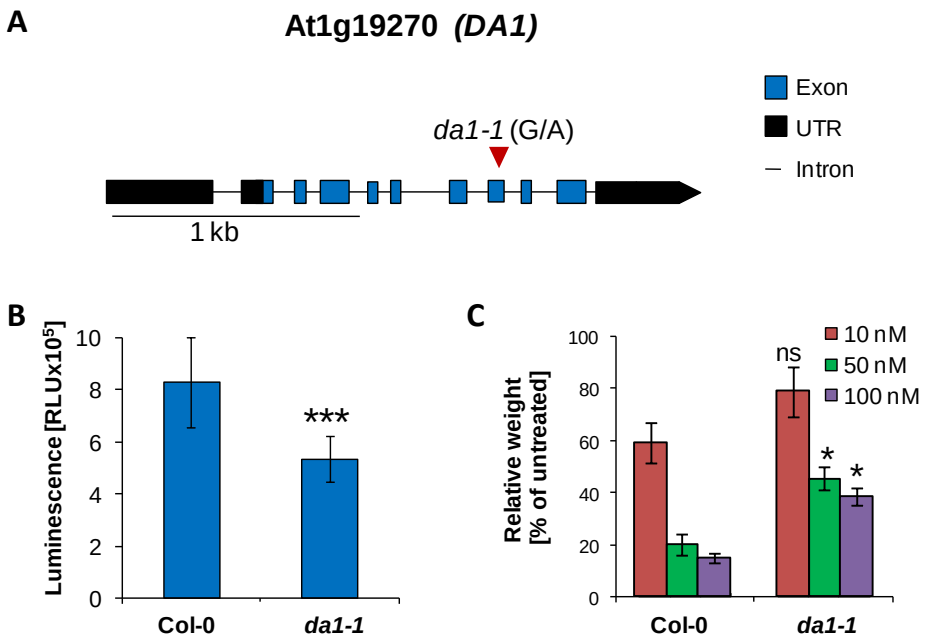

Figure 3.24: *da1-1* mutant displays reduced flg22-triggered responses in ROS production and seedling growth inhibition assay
(A) *da1-1* has a single-nucleotide G-to-A transition that causes a point mutation in a conserved amino acid (Li et al., 2008). (B) Seedling growth inhibition in response to increasing concentrations of flg22 in Columbia (Col-0) and *da1-1*. Results are represented as percentage of fresh weight of untreated seedlings. Results are average ± standard error with n=6. (C) Total ROS production represented as relative light units (RLU) in Columbia (Col-0) and *da1-1* after elicitation with 100nM flg22. Results are average ± standard error with n=8. These experiments were three times repeated with similar results. Asterisks indicate significant differences compared with wild-type values at P>0.05 (*) or P>0.001 (***). ns indicates that values were not significantly different from that of wild-type.

To validate that the *da1-1* mutation is causative for the observed impairment in flg22-triggered responses, seedling growth inhibition and ROS production were also determined in a *da1-1* mutant complemented with the genomic *DA1* sequence (*DA1COM,* kind gift from Prof. Michael Bevan, JIC) (Li et al., 2008). As expected, in this line the enhanced flg22-sensitivity was reverted, confirming that the observed effect was indeed caused by the *da1-1* mutation (Figure 3-25 A and C). Notably, *da1-1* also displayed a reduced sensitivity to elf18 in seedling growth inhibition and ROS assays, indicating that DA1 might also be involved in the regulation of the EFR signalling pathway (Figure 3-25 B and D).

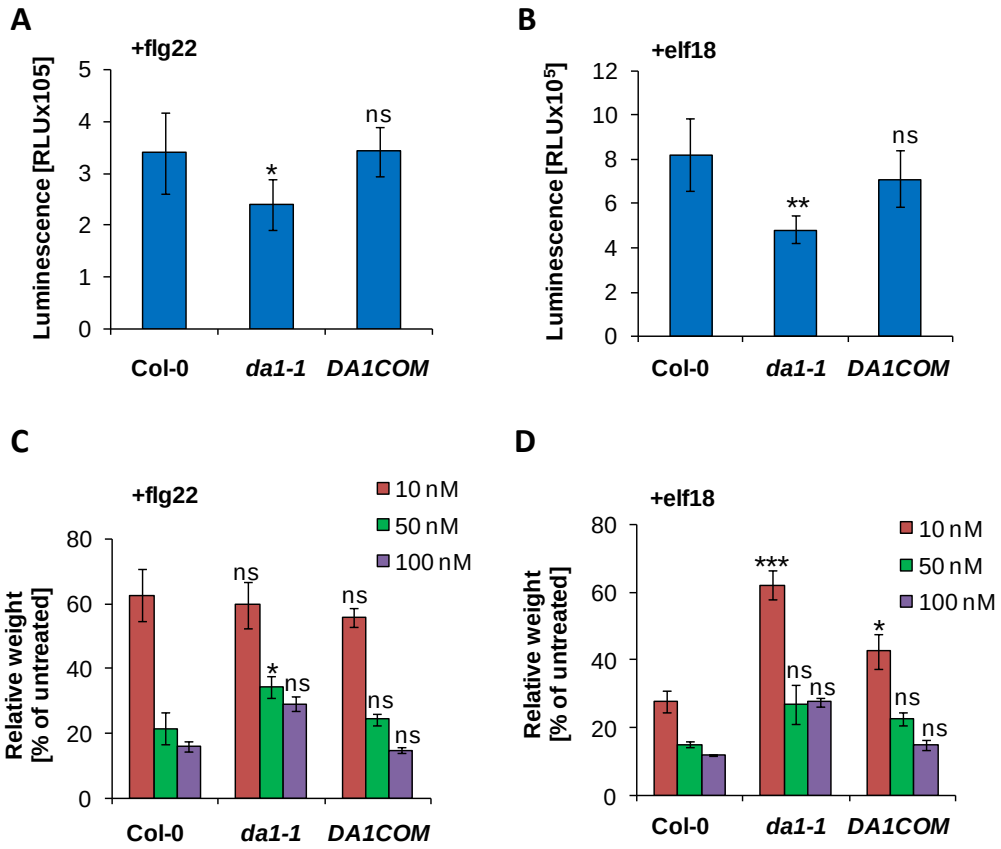

Figure 3.25: *da1-1* mutant displays reduced sensitivity to flg22 and elf18
(A) and (B) Total ROS production represented as relative light units (RLU) in Columbia (Col-0), *da1-1* and *DA1COM* after elicitation with 100 nM flg22 (A) and 100 nM elf18 (B). Results are average ± standard error with n=8. (C and D) Seedling growth inhibition in response to increasing concentrations of flg22 (C) and elf18 (D) in Columbia (Col-0), *da1-1* and *DA1COM*. Results are represented as percentage of fresh weight of untreated seedlings. Results are average ± standard error with n=6. Asterisks indicate significant differences compared with wild-type values at P>0.05 (*), P>0.01 (**) or P>0.001 (***). ns indicates that values were not significantly different from that of wild-type.

Ubiquitination of FLS2 plays an important role in receptor endocytosis and degradation (Haglund et al., 2003; Robatzek et al., 2006; Göhre et al., 2008; Lu et al., 2011). Since DA1 exhibits ubiquitin binding affinity and thus, might be involved in protein ubiquitination, we hypothesized that FLS2 endocytosis or degradation might be increased in *da1-1*, causing the reduced flg22-sensitivity. In order to test this, *FLS2* transcript and protein levels were determined by qRT-PCR and in α-FLS2 immunoblots. However, since no reproducible results could be obtained with the immunoblots, the FLS2 accumulation was additionally quantified by a radioactive flg22-binding assay (performed by Dr Delphine Chinchilla, University of Basel, Switzerland). Both assays revealed no difference in the *FLS2* expression and flg22-binding capacity in *da1-1* and wild-type plants, indicating that the FLS2 accumulation is not affected in *da1-1* (Figure 3.26 A and B).

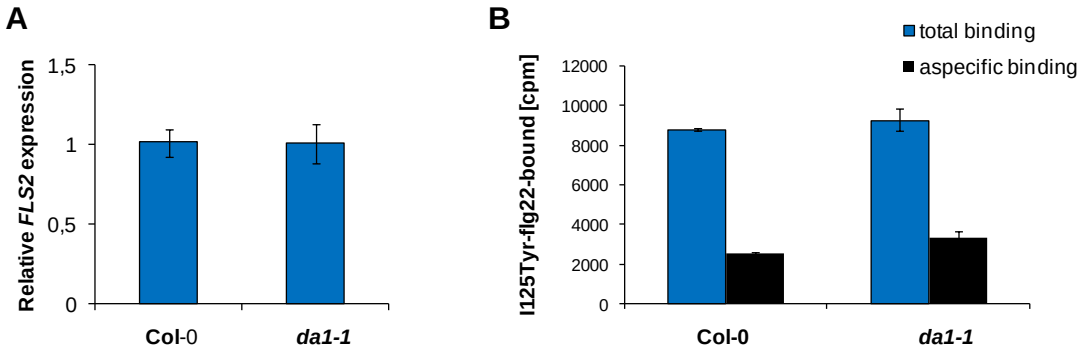

Figure 3.26*: da1-1* mutant shows *FLS2* expression and FLS2 protein levels similar to those of wild-type plants
(A) Relative *FLS2* expression level was determined by qRT-PCR using gene-specific primers and cDNA generated from 14-day-old *Arabidopsis* seedlings. Expression values were normalized to the expression of the housekeeping gene At5g15400 and plotted relative to the Col-0 expression level. Results are average ± standard error with n=4. This assay was repeated two times. (B) Specific flg22-binding was determined in 14-day old Col-0 and *da1-1* seedlings using radiolabeled ^{125}I-Tyr-flg22. Specific binding was competed for by adding an excess of unlabelled flg22 (assay carried out by Dr Delphine Chinchilla, University of Basel, Switzerland). This assay was carried out once.

In order to determine whether the decreased PAMP-induced responses observed in *da1-1* result in altered disease resistance, I tested the susceptibility of *da1-1* to bacterial infection. To this end, I spray-inoculated plants with the virulent *Pseudomonas syringae* pv. *tomato* DC3000. Plants were also inoculated with *Pto* DC3000 COR$^-$ and *Pto* DC3000

ΔAvrPto/ΔAvrPtoB. These weakly virulent bacterial strains lack the phytotoxin coronatine or the effectors AvrPto and AvrPtoB that are involved in PTI suppression (Melotto et al., 2006; Göhre et al., 2008; Shan et al., 2008; Xiang et al., 2008) and allow a more sensitive detection of PTI defects (Nekrasov et al., 2009). In all assays, bacterial growth was assessed three days after inoculation. To confirm the success of the bacterial infection, the *efr fls2* double mutant was included in all assays. As previously reported, this mutant displayed enhanced susceptibility to all bacterial strains tested (Figure 3.27 A-C) (Nekrasov et al., 2009). However, a significant difference was only observed with *Pto* DC3000 COR$^-$ and *Pto* DC3000 *ΔAvrPto/ΔAvrPtoB* (Figure 3.27 A-C).

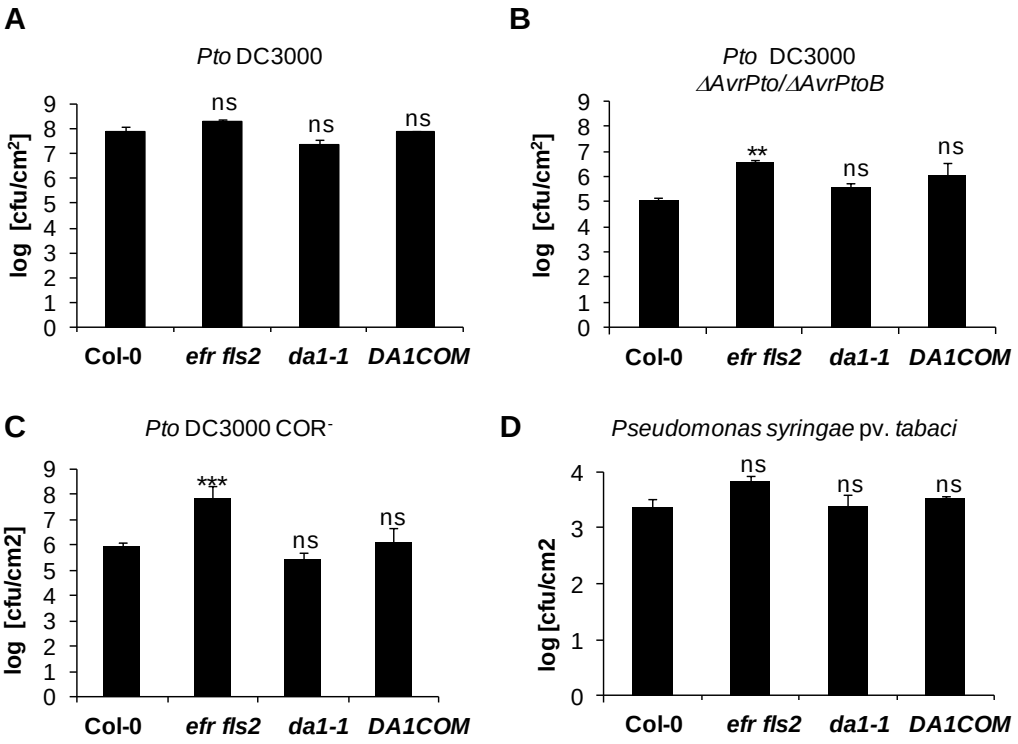

Figure 3.27*: da1-1* does not display altered susceptibility to different bacterial pathogens

(A) Four-week old plants (Col-0, *efr fls2, da1-1 and DA1COM*) were spray-inoculated with *Pseudomonas syringae* pv. *tomato* (*Pto*) DC3000 with OD_{600}= 0.02. (B) Four-week old plants (Col-0, *efr fls2, da1-1 and DA1COM*) were spray-inoculated with *Pto* DC3000 ***ΔAvrPto/ΔAvrPto*** with OD_{600}= 0.2 (C) Four-week old plants (Col-0, *efr fls2, da1-1 and DA1COM*) were spray-inoculated with *Pto* DC3000 COR$^-$ with OD_{600}=0.2. (D) Four-week old plants (Col-0, *efr fls2, da1-1 and DA1COM*) were syringe-infiltrated with *P. syringae* pv. *tabaci* 6605 OD_{600}=0.002. Bacterial growth was determined three days after infection and plotted as colony forming units per cm^2 leaf disc. Results are average ± standard error with n=4. Asterisks indicate significant differences compared with wild-type values at P>0.01 (**) or P>0.001 (***). ns indicates that values were not significantly different from that of wild-type.

In contrast, *da1-1* behaved in all bacterial assays like wild-type plants and therefore did not display an enhanced susceptibility (Figure 3.27 A-C).

Since leaves of *da1-1* plants are thicker than wild-type leaves and thus, might exhibit a natural barrier against pathogen infections, I also syringe-infiltrated plants with the hemibiotrophic bacterial pathogen *Pseudomonas syringae* pv. *tabaci (Pta),* which is non-adapated to *Arabidopsis.* Flg22-perception was previously shown to be involved in the non-host resistance to this bacterium in *Arabidopsis* and thus, infection with this strain again also allows a more sensitive detection of PTI defects (Li et al., 2005; Nekrasov et al., 2009). Consistent with the results obtained with spray-inoculated plants, the *da1-1* mutant did not display an altered resistance (Figure 3.27 D).

Thus, although I confirmed that some outputs of PAMP-triggered signalling are affected in *da1-1*, further investigations must be undertaken to decipher fully the involvement of DA1 in immunity.

3.4 Summary and discussion

Despite the high number of genes that are differentially expressed upon flg22 perception, little is known about the underlying transcriptional regulation of these genes. To gain further insight into these mechanisms, as well as to identify novel components of the FLS2 signalling pathway, expression data from plants treated with flg22 was used to build a putative transcriptional regulatory network, the so-called flg22-dependent gene expression network. Candidates of this network are predicted to regulate each other's expression in a flg22-dependent manner. In order to determine whether the seven predicted main regulators of the network are involved in the FLS2 signalling pathway, two outputs of this pathway, flg22-triggered ROS production and seedling growth inhibition, were examined in available mutants of these genes. Mutants of four candidates did not display altered responses in either of these assays. Although this indicates that *AtPP2-B6, G3Pp4, TCP15/TCP14* and *PP2C-73* might not be involved in PAMP-triggered signalling, these results should be considered cautiously. First, it is possible that these genes have close homologues that act redundantly in PAMP-triggered signalling. Therefore, to overcome gene redundancy, multiple

mutants or overexpression lines could be generated and characterised. Furthermore, only two outputs of the FLS2 signalling pathway were assessed and a potential effect on PTI could go unnoticed. Therefore, to assess an involvement of these genes in PTI, it would be essential to carry out a more comprehensive analysis by examining additional PAMP-induced responses, such as MAPK activation and PAMP-induced gene expression.

Interestingly, mutants of *RALFL23, DA1* and *GAI* displayed altered responses in seedling growth inhibition and ROS assays, indicating that they could be involved in flg22-mediated signalling. Notably, it had already been reported that *Arabidopsis* DELLA proteins, including GAI, are involved in the regulation of flg22-triggered seedling growth inhibition and our results are in agreement with this previously published data (Navarro et al., 2008). Moreover, the fact that GAI was identified as part of the flg22-dependent gene expression network further supports the validity of this approach.

It was previously shown that RALFL23 negatively regulates BR-triggered responses and *RALFL23* overexpression results in reduced BL-induced hypocotyl elongation (Srivastava et al., 2009). Furthermore, it had been reported that activation of the BR signalling pathway leads to inhibition of PTI, indicating a trade-off between plant growth and defence responses (Albrecht et al., 2012; Belkhadir et al., 2012). Thus, it would be anticipated that *ralfl23* mutants display reduced PAMP-triggered responses. However, all three tested mutants displayed increased flg22-induced responses in seedling growth inhibition and ROS assays suggesting that the role of RALFL23 in PTI is independent of its role in BR signalling. Therefore, further work is required to determine the function of RALFL23, and to investigate its involvement in PTI signalling.

DA1 had been described as a negative regulator of seed morphogenesis and organ growth and the *da1-1* mutant displays increased seed and organ size (Li et al., 2008). Interestingly, this mutant also displayed reduced flg22-triggered responses in seedling growth inhibition and ROS assays. Therefore, we decided to further characterise this mutant in collaboration with Prof. Michael Bevan. First, I confirmed that the reduced flg22-triggered sensitivity is caused by the *da1-1* mutation and therefore, reverted in mutants

complemented with the *DA1* genomic sequence. In addition, I showed that *da1-1* also displayed altered PTI responses after elf18 treatment, indicating that DA1 might also be involved in the EFR signalling pathway. Next, I tested whether *da1-1* displays an increased resistance to different bacterial pathogens. However, compared to wild-type plants no altered bacterial growth could be detected. Therefore, further investigations must be undertaken to understand to which extend DA1 is involved in PAMP-triggered immunity. For instance, the bacterial susceptibility could also be examined under different infection conditions e.g., by sampling at earlier time points or by spraying lower bacterial inoculums. Furthermore, it could be assessed whether the accumulation of hormones, such as ET, JA and SA, which are involved in defense responses, is altered in the *da1-1* mutant. In addition, the effect of DA1 might also be counterbalanced by a bacterial effector. To test this, *da1-1* plants could be inoculated with *Pto* DC3000 *hrcC*$^{-}$, a mutant strain lacking a functional type III-secretion system and that is therefore unable to deliver effector proteins into host cells.

In summary, the characterized flg22-dependent gene expression network presents a promising approach to discover novel components of the FLS2 signalling pathway. Thereby, a high number of candidates was identified in a both a cost- and time-efficient manner, and preliminary results indicate that three out of the seven selected candidates might be involved in PAMP-triggered signalling. However, microarrays only cover a certain percentage of the genome and it is likely that several important regulators of the flg22-dependent gene expression might not have been identified. Furthermore, another disadvantage of this method is that it is more time consuming to determine at which level of signalling the individual candidates play a role. Thus, a wide variety of signalling outputs might need to be assessed to identify the specific phenotypic contribution of each candidate. Consequently, since I only examined two different outputs of flg22-triggered signalling, I was not able to confirm whether all seven candidates are involved in the FLS2 signalling pathway. In contrast to candidates identified in protein or DNA-interaction screens, also no physical interaction between any of the

candidates and FLS2 signalling components is known *a priori*. Thus, it is more difficult to identify the mechanisms that cause the altered responses.

Chapter 4: Characterisation of potential EFR-interacting proteins

4.1 Introduction

An essential part of plant innate immunity is the perception of PAMPs by surface-localised PRRs. Two well-described bacterial PAMPs are flagellin and the bacterial elongation factor Tu that are recognised by the LRR-RLKs FLS2 and EFR, respectively (Gómez-Gómez et al., 1999; Gómez-Gómez and Boller, 2000; Zipfel et al., 2006). Both EFR and FLS2 require the association with the LRR-RLK BAK1, to form fully active receptor complexes (Chinchilla et al., 2007; Heese et al., 2007; Postel and Kemmerling, 2009; Roux et al., 2011). Recently, it has been reported that also BIK1 and BKK1 contribute to EFR- and FLS2-dependent signalling (Lu et al., 2010b; Lu et al., 2010a; Zhang et al., 2010; Roux et al., 2011). In turn, the closely related E3 ligases PUB12 and PUB13 catalyse specific ubiquitination of FLS2 to promote receptor degradation and attenuation of flg22-triggered signalling (Lu et al., 2011). This demonstrates that the activity of the two PRRs is under positive as well as negative regulation. However, although components, which regulate EFR and FLS2 upon PAMP perception, are described, it is still not understood how the activation of both receptors is blocked in the absence of ligand. In addition, the mechanism that links receptor activation and downstream responses are still mostly unknown. To gain further insight into these early signalling events, a yeast two-hybrid screen was performed to identify novel EFR-interacting proteins. Using this system, several important regulators of PRRs have been previously identified. For instance, yeast two-hybrid screens revealed that the two PP2Cs XB15 and KAPP interact with the PRRs XA21 and FLS2, respectively (Gómez-Gómez et al., 2001; Park et al., 2008). Furthermore, it was shown that both proteins negatively regulate XA21- or FLS2-dependent signalling pathway, confirming that both by yeast two-hybrid detected interactions are of biological relevance (Gómez-Gómez et al., 2001; Park et al., 2008).

4.2 Yeast two-hybrid screen- A general overview

The yeast two-hybrid system is a classical approach to identify protein-protein interactions *in vivo* (Fields and Song, 1989). Here, the protein of

interest (bait) is fused to the DNA-binding domain of a transcription factor (DB), while the potential interaction partner (prey) is fused to the activation domain (AD). Interaction of bait and prey leads to the reconstruction of the transcription factor that activates the expression of specific reporter genes (Figure 4.1). The fusion-proteins are generally expressed in auxotroph yeast strains that are unable to synthesise several amino acids but contain reporter genes that encode enzymes for their biosynthesis. Hence, only yeast cells that contain interacting bait and prey proteins can activate these reporter genes and are able to grow on selective media lacking these amino acids (Fields and Song, 1989).

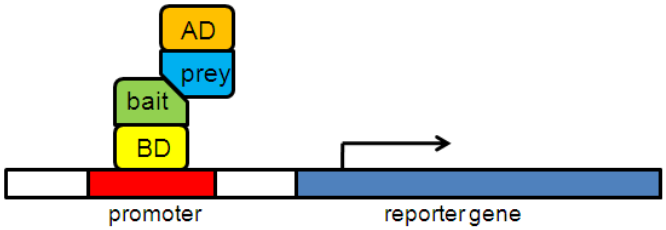

Figure 4.1: Overview of the yeast two-hybrid system
In the yeast two-hybrid system the bait protein is fused to the DNA-binding domain (BD), while the prey protein is fused to the activation domain (AD) of a transcription factor. Interaction of both proteins mediates the reconstruction of the transcription factor, which activates the expression of specific reporter genes (Fields and Song, 1989).

4.3 Results

4.3.1 Identification of novel EFR-interacting proteins by yeast two-hybrid screen

Note: The following described yeast two-hybrid screen was carried out by Dr Joachim Uhrig, University of Cologne, Germany. At the time I started my PhD, I was provided with a list of the identified interactors and the corresponding sequencing results.

To identify novel EFR-interacting proteins, a GAL4-based two-hybrid screen was carried out using the EFR cytoplasmic domain as a bait and a cDNA library generated from *Arabidopsis thaliana* seedlings treated with flg22 as a prey. Prey plasmids from yeast colonies able to grow on selective media were sequenced with a vector-specific primer, which was designed to anneal

upstream of the encoded DNA-binding domain. In total, 27 potential EFR-interacting proteins could be identified (Table A.3, in Appendix).

As a first step to validate the interactions, I determined which candidates were encoded in the right reading frame. Therefore, I translated the sequencing results of all candidates *in silico* starting at the N-terminally fused DNA-binding domain. I determined that 13 candidate genes were not encoded in a correct reading frame and thus, they were classified as potential false positive candidates. In addition, sequencing results from five candidates did not contain any vector-specific sequences and no conclusions about the frame could be made. In summary, I confirmed that nine of the 27 candidates were encoded in the right reading frame and only these proteins were considered as real candidates (Table 4.1).

Table 4.1: EFR-interacting proteins identified in the yeast two-hybrid screen
AGI number, gene name and the predicted function are indicated.

AGI	Name	Predicted function
At4g28400	PP2C-58	Predicted PP2C-type phosphatase
At3g12620	PP2C-38	Predicted PP2C-type phosphatase
At1g22410	-	3-deoxy-7-phosphoheptulonate synthase Potentially involved in aromatic amino acid biosynthesis
At3g11773	-	Electron carrier/ protein disulfide oxidoreductase
At5g63930	-	LRR-RLK (subfamily XI)
At2g20890	THF1, THYLAKOID FORMATION1	Involved in vesicle-mediated formation of thylakoid membranes
At1g51760	IAR3, IAA-ALANINE RESISTANT 3	IAA-Ala (indole-3-acetic acid alanine)-conjugate hydrolase
At2g17560	HMGB4, HIGH MOBILITY GROUP B4	Involved in the assembly of nucleoprotein complexes
At4g34990	MYB32, MYB DOMAIN PROTEIN 32	Transcription factor involved in pollen development

Initially, three of these candidates were selected for further characterisation: the two PP2C-type phosphatases, PP2C-58 and PP2C-38, and the predicted transcription factor MYB32.

It was recently reported that the activity of XA21, a rice PRR with close homology to EFR, is negatively regulated by the PP2C XB15 (Park et al.,

2008). Therefore, I hypothesised that the identified EFR-interacting proteins PP2C-58 and PP2C-38 could similarly regulate EFR activity. In addition, MYB4, a close homologue of MYB32, was found in a screen for potential novel regulator of PTI (Schwessinger and Zipfel, unpublished data), suggesting a possible involvement of MYB32 in immunity.

4.3.2 Characterisation of selected EFR-interacting proteins

Two strategies were used to assess whether the selected candidates, PP2C-38, PP2C-58 and MYB32, are true EFR interactors. First, I tested whether the candidates localise to the same subcellular compartment as EFR by determining the localisation of eGFP (enhanced green fluorescent protein)-tagged proteins *in planta*. As previously mentioned, EFR contains a transmembrane domain, which is inserted in the plasma membrane, as well as a cytoplasmic and an extracellular domain (Zipfel et al., 2006). Consistently, upon transient expression in *Nicotiana benthamiana,* EFR-GFP localises at the cell periphery (Roux, 2010). Thus, proteins that co-localise with EFR should be detected in the cytoplasm or at the plasma membrane. In addition, I tested by co-immunoprecipitation (Co-IP) whether the proteins associate with EFR-GFP *in planta.* Therefore, the candidates were expressed as FLAG and/or HA (haemagglutinin)-tagged recombinant proteins in *N. benthamiana* together with EFR-GFP.

4.3.2.1 MYB32 does not associate with EFR *in planta*

MYB32 belongs to the R2R3-MYB transcription factors, which carry two characteristic imperfect amino acid sequence repeats referred to as R2 and R3 (Kranz et al., 1998). Notably, several members of this family have been reported to regulate developmental processes and responses to biotic and abiotic stress (Stracke et al., 2007). Based on repeating amino acid motifs at the C-terminus, the *Arabidopsis* R2R3-type MYB family has been divided into 22 subgroups (Kranz et al., 1998). MYB32 as well as MYB3, MYB4 and MYB7 belong to subfamily 4 (Figure 4.2 and Figure 4.3) (Kranz et al., 1998; Stracke et al., 2001).

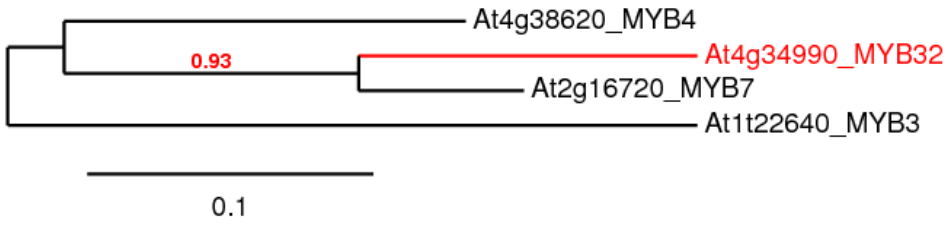

Figure 4.2: MYB32 belongs to subfamily 4 of MYB transcription factors
Phylogenetic tree of subfamily 4 of *Arabidopsis* MYB protein. MYB32 is indicated in red. The phylogenetic tree was generated using full-length amino acid sequences. MUSCLE was used for the alignment, PhyML for the phylogeny and TreeDyn for drawing the tree (www.phylogeny.fr). The horizontal branches are drawn to scale as indicated by the scale bar (bar = substitution/site rate of 0.1 %), and their length indicates the level of divergence among sequences. Bootstrap values are indicated in red above nodes.

```
MYB32           MGRSPCCEKDHTNKGAWTKEEDKLISYIKAHGEGCWRSLPRSAGLQRCGKSCRLRWINY 60
MYB7            MGRSPCCEKEHMNKGAWTKEEDERLVSYIKSHGEGCWRSLPRAAGLLRCGKSCRLRWINY 60
MYB4            MGRSPCCEKAHTNKGAWTKEEDERLVAYIKAHGEGCWRSLPKAAGLLRCGKSCRLRWINY 60
MYB3            MGRSPCCEKAHMNKGAWTKEEDQLLVDYIRKHGEGCWRSLPRAAGLQRCGKSCRLRWMNY 60

MYB32           LRPDLKRGNFTLEEDDLIIKLHSLLGNKWSLIATRLPGRTDNEIKNYWNTHVKRKLLRKG 120
MYB7            LRPDLKRGNFTHDEDELIIKLHSLLGNKWSLIAARLPGRTDNEIKNYWNTHIKRKLLSKG 120
MYB4            LRPDLKRGNFTEEEDELIIKLHSLLGNKWSLIAGRLPGRTDNEIKNYWNTHIRRKLINRG 120
MYB3            LRPDLKRGNFTEEEDELIIKLHSLLGNKWSLIAGRLPGRTDNEIKNYWNTHIKRKLLSRG 120

MYB32           IDPATHRPINETKTSQDSSDSSKTEDPLVK----ILSFG--PQLEKIANFG--DERIQKR 172
MYB7            IDPATHRGINEAKIS----DLKKTKDQIVK----DVSFV--TKFEETDKSG--DQKQNKY 168
MYB4            IDPTSHRPIQESSASQ---DSKPTQLEPVTSNTINISFTSAPKVETFHESISFPGKSEKI 177
MYB3            IDPNSHRLINESVVSP-----SSLQNDVVET--IHLDFSGPVKPEPVREEI---GMVNNC 170

MYB32           V--------EYSVVEERC-LDLNLELRISPPWQDKLHDERNLRFGRVKYRCSACRFGFGN 223
MYB7            IRNGLVCKEERVVVEEKIGPDLNLELRISPPWQNQ----------REISTCTASRFYMEN 218
MYB4            SMLTFKEEKDECPVQEKF-PDLNLELRISLPDDVDRLQGHG---KSTTPRCFKCSLGMIN 233
MYB3            ESSGTTSEKDYGNEEDWV---LNLELSVGPSYRYESTRKVSVVDSAESTRRWGSELFGAH 227

MYB32           GKECSCNNVKCQTEDSSSSSYSSTDISSS-IGYDFLGLNN---TRVLDFSTLEMK 274
MYB7            DMECSSETVKCQTENSSSISYSSIDISSSNVGYDFLGLK----TRILDFRSLEMK 269
MYB4            GMECRCGRMRCDVVGGSS---KGSDMSNG---FDFLGLAKKETTSLLGFRSLEMK 282
MYB3            ESDAVCLCCRIGLFRNES-------CRN---------------CRVSDVRTH--- 257
```

Figure 4.3: Amino acid alignment of subfamily 4 MYB transcription factors
Multiple alignments were generated with Muscle 3.7. Amino acid similarity was determined according to BLOSUM62. In yellow: max similarity (3.0), in blue medium similarity: (1.5). The R2 domain is underlined; the R3 domain is double underlined.

MYB4 was shown to regulate the accumulation of the UV-protecting compound sinapoylmalate by repressing the expression of *C4H (CINNAMATE 4-HYDROXYLASE),* which encodes a key enzyme of the phenylpropanoid biosynthetic pathway (Jin et al., 2000). Consistently, overexpression of *MYB4* decreases the level of UV-protecting agents and causes UV-B hypersensitivity (Jin et al., 2000; Schenke et al., 2011). Notably, the phenylpropanoid biosynthetic pathway is also repressed by biotic stress including treatment with flg22 (Saijo et al., 2009). Since the expression of *MYB4* is induced upon flg22 perception, it was implied that

MYB4 mediates attenuation of UV-B signalling in response to biotic stress (Schenke et al., 2011). Like MYB4, MYB32 regulates the expression of genes encoding enzymes of the phenylpropanoid biosynthetic pathway including DFR (DIHYDROFLAVONOL 4-REDUCTASE) and ANS (ANTHOCYANIDIN SYNTHASE), which catalyse anthocyanin production (Preston et al., 2004). MYB32 and MYB4 were also reported to regulate pollen development since *myb32* and *myb4* mutants exhibit irregular and collapsed pollen (Preston et al., 2004). Since both MYB proteins regulate the phenylpropanoid pathway, it was hypothesised that in *myb32* and *myb4* mutants structural components of the pollen wall, produced through this pathway, might be affected (Preston et al., 2004).

MYB32 was found to interact with EFR in yeast two-hybrid (Table 4.1). In order to confirm that this protein also interacts with EFR *in planta*, I first tested whether MYB32 localises to the same subcellular compartment as EFR. Therefore, MYB32-eGFP was transiently expressed under the control of the 35S promoter in *N. benthamiana* leaves. The localisation of MYB32-eGFP was determined by confocal laser scan microscopy. A fluorescent signal was only detected in the nucleus, indicating that MYB32 and EFR do not co-localise (Figure 4.4 A and B).

In order to test whether MYB32 could still associate with EFR *in planta*, I transiently co-expressed EFR-GFP and MYB32-HA under the control of the 35S promoter in *N. benthamiana*. Since the association of EFR with candidate proteins may occur in a ligand-dependent manner, infiltrated leaf tissues were treated with water or elf18 for 20 minutes. Total proteins were extracted and EFR-GFP was immunoprecipitated with GFP-Trap beads. Although, EFR-GFP was detectable in the IP extract, no co-immunoprecipitation of MYB32-HA was observed (Figure 4.4 C). Furthermore, no association was detected in the reciprocal IP after immunoprecipitating MYB32-HA (Figure 4.4 C). Together, these results indicate that MYB32 does not interact with EFR *in planta.*

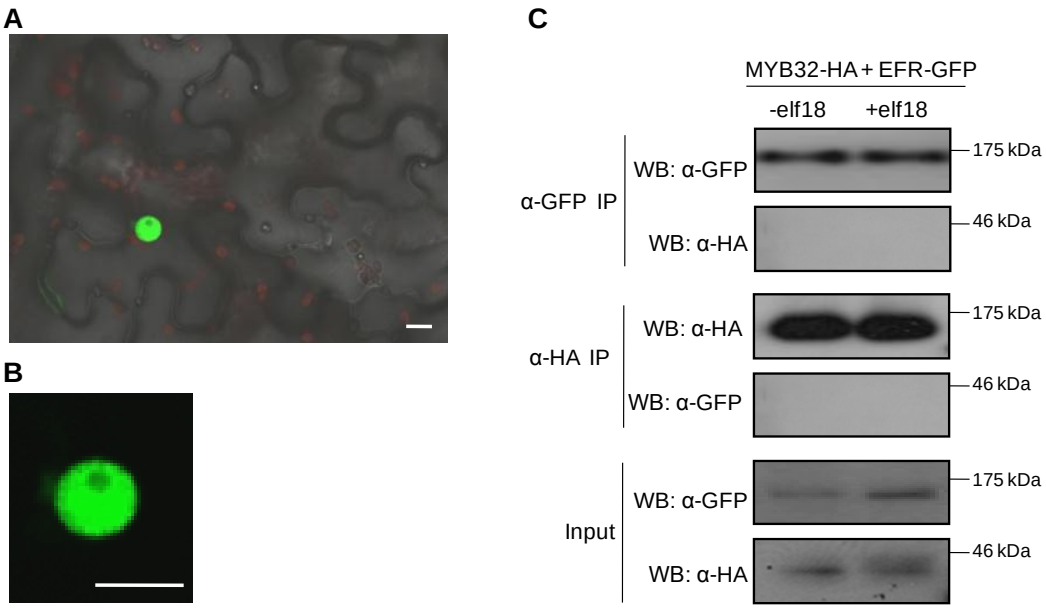

Figure 4.4: Transiently overexpressed MYB32 shows nuclear localisation and was not co-immunoprecipitated with EFR
(A) and (B) Confocal imaging of the leaf epidermis of *N. benthamiana* transiently expressing MYB32-eGFP under the control of the 35S promoter. (B) is a zoom in of the image in (A). Scale bar: 7.5 µm. (C) Co-immunoprecipitation of MYB32 and EFR. *N. benthamiana* leaves co-expressing MYB32-HA and EFR-GFP were treated (+) or not (-) with 100 nM elf18 for 20 minutes. Total proteins were extracted (Input) and EFR-GFP was immunoprecipitated with GFP-Trap beads (α-GFP IP). In the reciprocal IP MYB32-HA was immunoprecipitated with anti-HA Affinity Matrix (α-HA IP). HA- and GFP-tagged proteins were detected by immunoblot analysis with tag-specific antibodies. These experiments were two times repeated with similar results.

4.3.2.21 Characterisation of PP2C-58 and PP2C-38

PP2C-type protein phosphatases were previously named according to their chromosomal position (Xue et al., 2008), and I will refer to this nomenclature. Furthermore, PP2Cs have been clustered into 12 subfamilies, based on their amino acid sequence (Schweighofer et al., 2004). Since PP2C-58 and PP2C-38 have been placed in different families and thus, are not closely related, they were characterised independently.

4.3.2.2.1 PP2C-58 is closely related to protein phosphatases that are involved in defence responses

PP2C-58 belongs to the PP2C subfamily F (Schweighofer et al., 2004), which includes three characterised members: PAPP2C (PHYTOCHROME-ASSOCIATED PROTEIN PHOSPHATASE TYPE 2C) (Wang et al., 2012),

WIN2 (HOPW1-1-INTERACTING PROTEIN 2) (Lee et al., 2008) and PIA1 (PP2C INDUCED BY AVRRPM1) (Widjaja et al., 2010) (Figure 4.5).

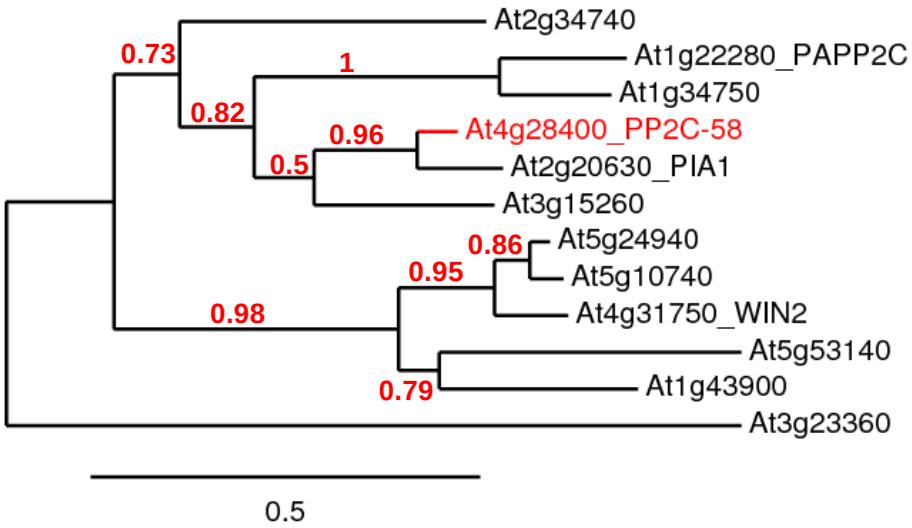

Figure 4.5: PP2C-58 belongs to the PP2C subfamily F, which also contains PAPP2C, PIA1 and WIN2
Phylogenetic tree of PP2C subfamily F. PP2C-58 is indicated in red. The phylogenetic tree was generated using full lengths amino acid sequences. MUSCLE was used for the alignment, PhyML for the phylogeny and TreeDyn for drawing the tree (www.phylogeny.fr). The horizontal branches are drawn to scale as indicated by the scale bar (bar = substitution/site rate of 0.5 %), and their length indicates the level of divergence among sequences. Bootstrap values are indicated in red above nodes.

PAPP2C has been shown to associate with the phytochromes phyA and phyB in the nucleus (Phee et al., 2008). Since both interactions and PAPP2C phosphatase activity are enhanced by red light, it was implied that PAPP2C plays a role in mediating phytochrome signalling (Phee et al., 2008). Recently, it has been shown that PAPP2C also associates with the R protein RPW8.2 (RESISTANCE TO POWDERY MILDEW 8.1), which confers resistance to powdery mildew (Xiao et al., 2003; Wang et al., 2012). Down-regulation of *PAPP2C* results in strong HR-like cell death, which correlates with elevated *RPW8.2* expression (Wang et al., 2012). Taken together, these results suggest that PAPP2C is also involved in RPW8.2-induced resistance (Wang et al., 2012). WIN2 was found to interact with the *Pseudomonas syringae* type III-secreted effector HopW1-1 in yeast two-hybrid assays (Lee et al., 2008). Knock-down of *WIN2* partially compromises HopW1-1-induced resistance, while overexpression of *WIN2* confers disease resistance to *Pto* DC3000 (Lee et al., 2008). WIN2 encodes an active

phosphatase (Lee et al., 2008); however, it is yet unclear whether it dephosphorylates HopW1-1. The third characterised member of subfamily F is PIA1, the closest homologue of PP2C-58. PIA1 was identified in a proteomic screen for proteins that accumulate upon recognition of the *P. syringae* type III-secreted effector AvrRpm1 (Widjaja et al., 2009). AvrRpm1 has been previously shown to suppress basal defence responses to promote bacterial infection (Kim et al., 2005). *pia1* loss-of-function mutants display enhanced disease resistance against *Pto* DC3000 expressing *avrRpm1*, but not against wild-type *Pto* DC3000, indicating that PIA1 is involved in AvrRpm1-induced responses (Widjaja et al., 2010).

PP2C-58 and PIA1 share 83 % amino acid sequence identity (Figure 4.5 and Figure 4.6). Nonetheless, only PIA1, but not PP2C-58, was found to accumulate upon AvrRpm1 recognition (Widjaja et al., 2010).

```
PP2C-58         MAGSNILHKIKLKAGFCGSAPDMGRGKSKMWKNITHGFHCVKGKSSHPMEDYVVSEFKKL 60
PIA1            MAGREILH--KMKVGLCGS--DTGRGKTKVWKNIAHGYDFVKGKAGHPMEDYVVSEFKKV 56

PP2C-58         EGHELGLFAIFDGHLGHDVAKYLQTNLFDNILKEKDFWTDTENAIRNAYRSTDAVILQQS 120
PIA1            DGHDLGLFAIFDGHLGHDVAKYLQTNLFDNILKEKDFWTDTKNAIRNAYISTDAVILEQS 116

PP2C-58         LKLGKGGSTAVTGILIDGKKLVVANVGDSRAVMSKNGVAHQLSVDHEPSKEKKEIESRGG 180
PIA1            LKLGKGGSTAVTGILIDGKTLVIANVGDSRAVMSKNGVASQLSVDHEPSKEQKEIESRGG 176

PP2C-58         FVSNIPGDVPRVDGQLAVARAFGDKSLKLHLSSEPDITHQTIDDHTEFILFASDGIWKVL 240
PIA1            FVSNIPGDVPRVDGQLAVARAFGDKSLKIHLSSDPDIRDENIDHETEFILFASDGVWKVM 236

PP2C-58         SNQEAVDAIKSIKDPHAAAKHLIEEAISRKSKDDISCIVVKFH---------- 283
PIA1            SNQEAVDLIKSIKDPQAAAKELIEEAVSKQSTDDISCIVPCFLRREALSERYCR 290
```

Figure 4.6: Alignment of PP2C-58 and its closest homologue PIA
Multiple alignments were generated with Muscle 3.7. Amino acid similarity was determined according to BLOSUM62. In yellow: max similarity (3.0), in blue medium similarity: (1.5). The predicted phosphate-binding loop [GXXXXGK(T)] is double underlined and the mutated amino acid is marked in red. The predicted PP2C-domain is underlined (http://pfam.sanger.ac.uk).

First, I tested whether the expression of *PP2C-58* and *PIA1* is regulated by PAMP treatment. qRT-PCR experiments with gene-specific primers revealed that *PP2C-58* is significantly induced upon flg22 and elf18 treatment, while the expression of *PIA1* is only weakly up-regulated (Figure 4.7). Thus, although both genes encode highly similar PP2Cs, I hypothesised that they might be involved in distinct processes based on their different expression profiles.

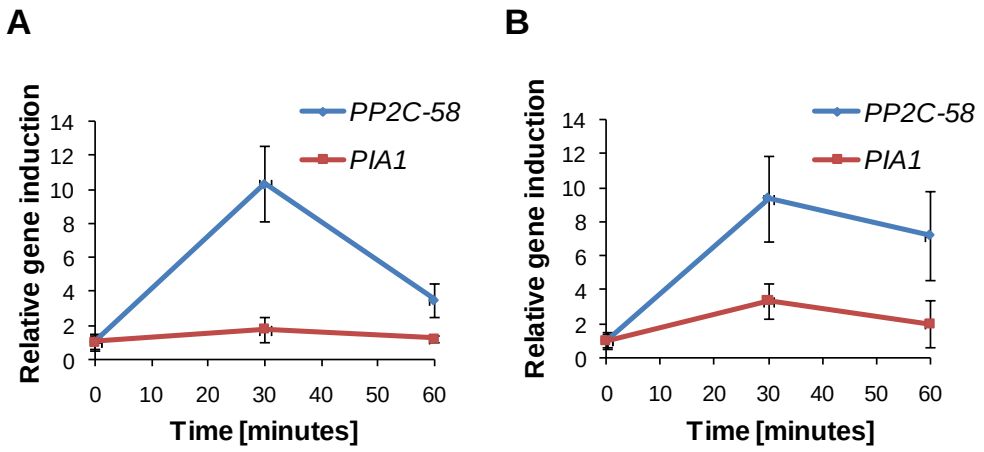

Figure 4.7: *PP2C-58* is significantly up-regulated upon PAMP treatment, while the expression of *PIA1* is only weakly induced
The gene induction was determined by qRT-PCR using gene-specific primers. cDNA was generated from 14-days old *Arabidopsis thaliana* seedlings treated with 100 nM elf18 (A) or 100 nM flg22 (B) for 0, 30 and 60 minutes. Expression values were normalized to the expression of the housekeeping gene At5g15400 and plotted relative to expression values at time point 0. Results are average ± standard error with n=4. The experiments were two times repeated with similar results.

Another difference between both PP2Cs can be found in their protein structure. While PIA1 carries a functional P-loop, this domain contains a point mutation in PP2C-58 (Figure 4.6; in red). P-loops are involved in binding of ATP and GTP, and mutagenesis of this domain can lead to a reduced activity, or even to loss of function (Evans et al., 1996; Ramakrishnan et al., 2002). Thus, it is possible that PP2C-58 is a weak or non-functional phosphatase.

4.3.2.2 An association of PP2C-58 with EFR was not detectable *in planta*

To determine whether the PP2C-58-EFR interaction, which was observed by yeast two-hybrid, could be of biological relevance, I examined the subcellular localisation of PP2C-58 after transiently expressing *PP2C-58-eGFP* under the control of the 35S promoter in *N. benthamiana*. Using confocal microscopy, I detected a fluorescent signal in the cytoplasm and the nucleus (Figure 4-8 A). However, since the same pattern is observed with free GFP (data not shown), it was possible that the eGFP-tag was cleaved off, thus explaining the apparent nucleo-cytoplasmic pattern of PP2C-58-eGFP. To test this, proteins were extracted and analysed in immunoblots with α-GFP

antibodies. Two specific bands were detected, which correspond to PP2C-58-eGFP (approximate molecular weight: 58 kDa) and eGFP alone (approximate molecular weight: 27 kDa) (Figure 4-8 B), indicating a partial cleavage of the tag. Thus, no clear conclusions can be made about the subcellular localisation of PP2C-58.

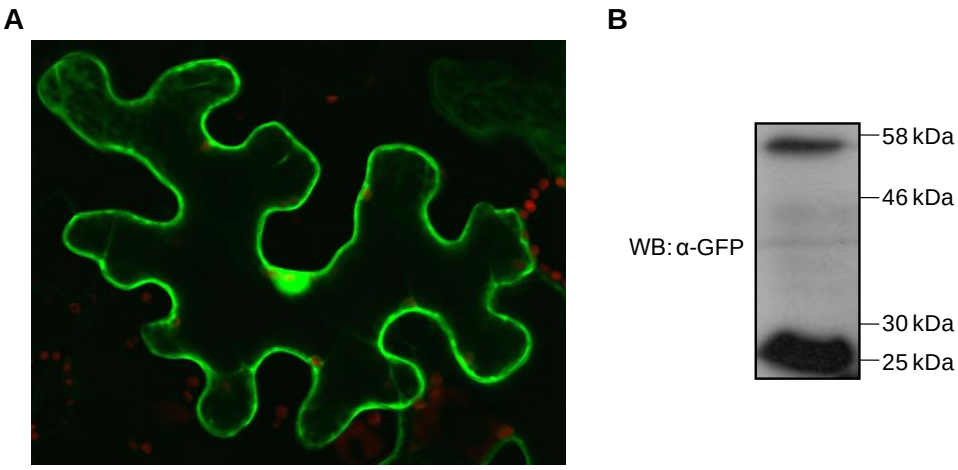

Figure 4.8: Cleavage of the eGFP-tag may mask the real subcellular localisation of PP2C-58-eGFP
(A) Confocal imaging of the leaf epidermis of *N. benthamiana* transiently expressing *PP2C-58-eGFP* under the control of the 35S promoter. (B) Crude protein extracts of the transformed *N. benthamiana* leaves were analysed in α-GFP immunoblots. This experiment was two times repeated with similar results.

To determine whether PP2C-58 associates with EFR *in planta*, I transiently co-expressed *EFR-GFP* and *PP2C-58-HA* under the control of the 35S promoter in *N. benthamiana*. Infiltrated leaf tissues were treated with water or elf18 for 20 minutes and EFR-GFP was subjected to immunoprecipitation. Since PP2C-58-HA was not detectable in the EFR-IP extract, an association could not be confirmed (Figure 4.9 A).

To further test for association, I also co-expressed *EFR-GFP* with *PP2C-58-FLAG* under the control of the 35S promoter. In contrast to what was found upon co-expression of EFR-GFP and PP2C-58-HA, PP2C-58-FLAG was detectable in EFR-IPs, and this equally in samples treated with water or elf18 (Figure 4.9 B). To exclude that PP2C-58-FLAG was non-specifically binding to the GFP-Trap beads or the eGFP-tag, PP2C-58-FLAG was co-expressed with eGFP alone. PP2C-58-FLAG was also detectable in this negative control, indicating that PP2C-58-FLAG was non-specifically co-immunoprecipitated (Figure 4.9 B). Thus, it was not possible to reach any

conclusions regarding the potential association between EFR and PP2C-58 *in planta* using the available fusion proteins in co-immunoprecipitation experiments.

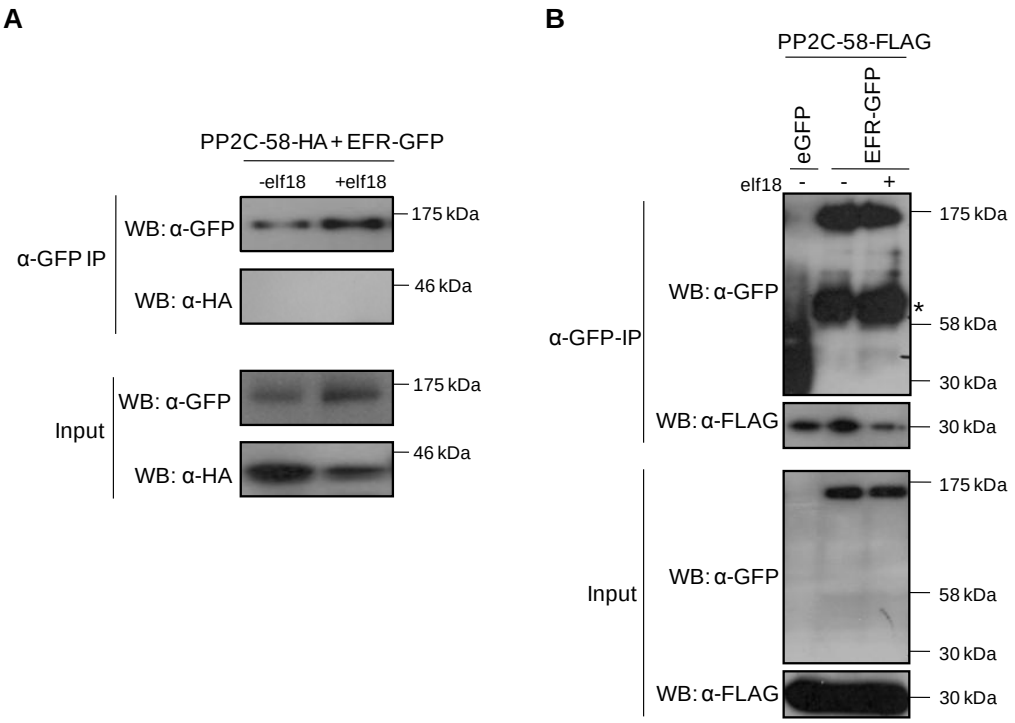

Figure 4.9: PP2C-58 shows non-specific binding and an association with EFR cannot be confirmed
Co-immunoprecipitation of PP2C-58 and EFR; *N. benthamiana* leaves co-expressing EFR-GFP and PP2C58-FLAG (A) or PP2C58-HA (B) were treated (+) or not (-) with 100 nM elf18 for 20 minutes. Total proteins were extracted (Input) and EFR-GFP was immunoprecipitated with GFP Trap beads (α-GFP IP). FLAG-, HA- and GFP-tagged proteins were detected by immunoblot analysis with tag-specific antibodies. Unspecific bands are indicated with a star. This experiment was two times repeated with similar results.

4.3.2.2.3 PP2C-38 belongs to a clade of uncharacterised PP2Cs

PP2C-38 is part of PP2C subfamily D (Schweighofer et al., 2004), a family with no characterised member (Figure 4.10). To determine whether *PP2C-38* could play a role in PAMP-triggered immunity, I tested if its expression is regulated by PAMP treatment. qRT-PCR experiments with gene-specific primers, revealed that *PP2C-38* expression is induced after flg22 and elf18 perception (Figure 4.11).

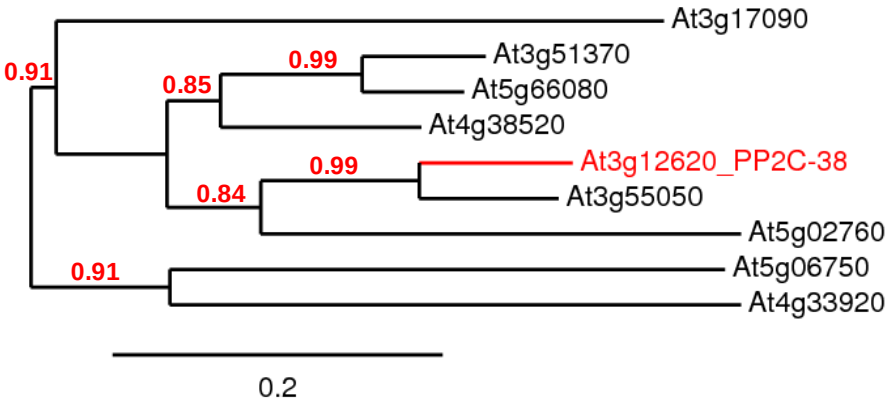

Figure 4.10: PP2C-38 belongs to a subfamily of uncharacterised PP2Cs
Phylogenetic tree of PP2C subfamily D. PP2C-38 is indicated in red. The phylogenetic tree was generated using full lengths amino acid sequences. MUSCLE was used for the alignment, PhyML for the phylogeny and TreeDyn for drawing the tree (www.phylogeny.fr). The horizontal branches are drawn to scale as indicated by the scale bar (bar = substitution/site rate of 0.2 %), and their length indicates the level of divergence among sequences. Bootstrap values are indicated in red above nodes.

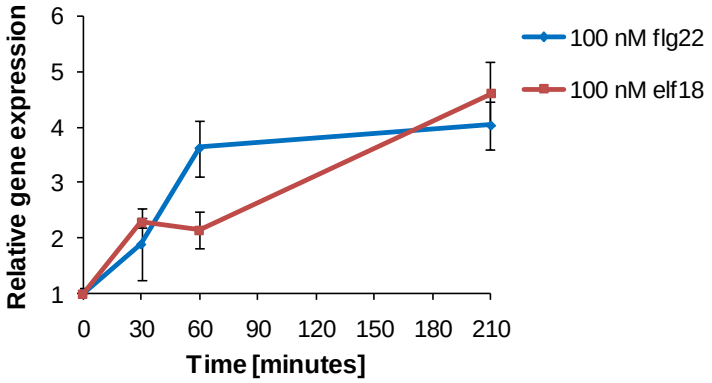

Figure 4.11: Expression of *PP2C-38* is induced by PAMP treatment
Gene induction was determined by qRT-PCR with gene-specific primers. cDNA was generated from 14-days old *Arabidopsis thaliana* seedlings treated with 100 nM elf18 or 100 nM flg22 for 30, 60 and 210 minutes. Expression values were normalized to the expression of the housekeeping gene At5g15400 and plotted relative to expression values at time point 0. Results are average ± standard error with n=4. This experiment was two times repeated with similar results.

4.3.2.2.4 PP2C-38 localises to the cell periphery and associates with EFR *in planta*

In order to determine whether PP2C-38 localises to the same subcellular compartment as EFR, PP2C-38-eGFP was transiently expressed under the control of the 35S promoter in *N. benthamiana*. Using confocal microscopy, I observed a signal at the cell periphery (Figure 4.12 A). Plasma membrane localisation was then confirmed by plasmolysis (Figure 4.12 B).

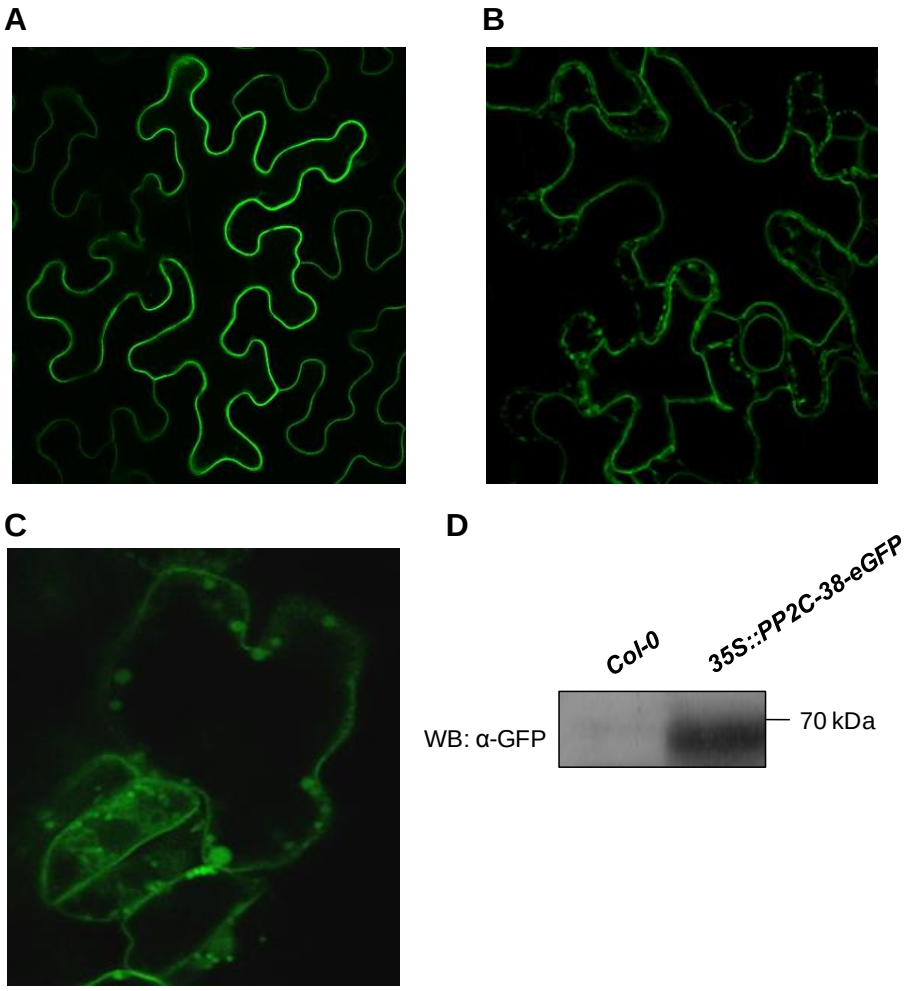

Figure 4.12: Overexpressed PP2C-38 localises to the cell periphery
(A and B) Confocal imaging of the leaf epidermis of *N. benthamiana* transiently expressing *PP2C-38-eGFP* under the control of the 35S promoter. (B) Plasmolysed tissue 5 minutes after infiltration of a 2 M Sucrose solution. (C) Confocal image of the leaf epidermis of stable transgenic *Arabidopsis thaliana* lines expressing *PP2C-38-eGFP* under the control of the 35S promoter. (D) Immunoblots with α-GFP antibodies confirmed that PP2C-38-eGFP is expressed. These experiments were two times repeated with similar results.

To test if the localisation is affected by PAMP perception, transformed tissue was treated with elf18 or flg22. The subcellular localisation of PP2C-38-eGFP was examined over a time course of 30 minutes, but no altered localisation was observed (data not shown). To further test if the detected localisation is not a consequence of *PP2C-38* overexpression, I also transiently expressed the genomic sequence of *PP2C-38* under the control of a 1 kb DNA region upstream of the open reading frame of this gene in *N. benthamiana*. No fluorescent signal could be detected, most likely due to low protein accumulation (data not shown). I further tested PP2C-38 localisation in stable transgenic *Arabidopsis* lines expressing *PP2C-38-eGFP* under the

control of the 35S promoter. In these lines, PP2C-38-eGFP was only weakly detectable by western blotting and fluorescent signals were only observed in small cells close to stomata (Figure 4.12 C and D). Although the results from confocal microscopy indicate that PIE localises at the cell periphery in *Arabidopsis*, the signal was too low to confirm membrane-association by plasmolysis.

Next, I tested whether PP2C-38-FLAG associates with EFR-GFP *in planta* upon transient co-expression in *N. benthamiana*. PP2C-38-FLAG was robustly detectable in the EFR-Immunoprecipitation, indicating that both proteins associate *in planta* (Figure 4.13). Interestingly, a reduced amount of PP2C-38 was co-immunoprecipitated from samples infiltrated with elf18 (Figure 4-13), indicating that PP2C-38 may dissociate from the EFR complex after elf18 perception.

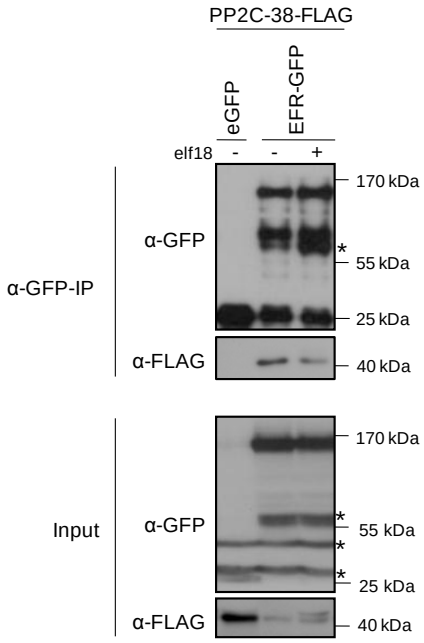

Figure 4.13: PP2C-38-FLAG associates with EFR-GFP *in planta* and dissociates from the EFR complex after elf18 perception
Co-immunoprecipitation of PP2C-38-FLAG and EFR-GFP. *N. benthamiana* leaves co-expressing PP2C-38-FLAG and EFR-GFP were treated (+) or not (-) with 100 nM elf18 for 20 minutes. Total proteins were extracted (Input) and EFR-GFP was immunoprecipitated with GFP-Trap beads (α-GFP IP). FLAG- and GFP-tagged proteins were detected by immunoblot analysis with tag-specific antibodies. This experiment was three times repeated with similar results.

4.4 Summary and discussion

To gain further insight into the early events of PAMP-triggered signalling, the yeast two-hybrid system was used to identify novel EFR-interacting proteins. In total, 27 potential EFR-interacting proteins were identified. However, only nine of these candidates were encoded in the correct reading frame, indicating that a high number of false positive interactions were detected in the screen. These were most likely caused by unspecific binding.

But also false negative interactions are commonly observed with the yeast two-hybrid system. Given that yeast lacks important chaperones needed for proper protein folding, as well as enzymes that would be required to catalyse specific post-translational modifications that may exist in plants, some proteins may not possess the for the specific interaction required configuration. Fusing bait and prey to the DNA-BD or AD of a transcription factor might also affect the protein configuration or even block the site of interaction and thus, interfere with the ability of the proteins to associate. Additionally, since this screen is based on the reconstruction of a transcription factor, all observed interactions have to occur in the nucleus. Consequently, extracellular proteins or proteins with stronger targeting signals might not successfully be imported into the nucleus and a potential interaction would not be observed. This could explain why none of the previously described EFR-associating proteins was found in the screen (Zhang et al., 2010; Roux et al., 2011; Schwessinger et al., 2011).

Three of the nine yeast two-hybrid candidates were selected for further characterisations: the predicted transcription factor MYB32 and the two predicted PP2Cs, PP2C-58 and PP2C-38. MYB32 was selected since its close homologue MYB4 has been previously identified in a screen for novel regulators of PTI (Schwessinger and Zipfel, unpublished data). Additionally, MYB4 was implied to play a role in flg22-mediated attenuation of UV-B signalling (Schenke et al., 2011). Thus, MYB32 might also be involved in PAMP-triggered responses.

Confocal microscopy analysis indicated that MYB32-eGFP localises exclusively in the nucleus. Consistent with the divergent localisation pattern,

an association between EFR and MYB32 *in planta* was not detected by co-immunoprecipitation. However, it cannot be ruled out that MYB32-eGFP may be mislocalized due to the addition of the tag, or that regulation of MYB32 localization may be altered due to overexpression of the protein. In addition, it has been shown very recently that XA21, a rice PRR with structural similarity to EFR, is cleaved upon ligand perception to release the intracellular kinase domain, which is then imported into the nucleus to interact with a WRKY transcription factor (Park and Ronald, 2012). A similar scenario might also be possible for EFR, and may explain a potential interaction with MYB32. Thus, although EFR cleavage has not been reported yet, this hypothesis could be tested by examining whether MYB32 associates with the cytoplasmic domain of EFR *in planta*.

In addition, the two PP2Cs identified in the screen were also selected for further characterisation. First, I characterised PP2C-58, which is closely related to the PP2Cs PAPP2C, WIN2 and PIA1 that are involved in the regulation of defence responses. PAPP2C was initially shown to play a role in mediating phytochrome signalling, but recent results suggest an additional role in RPW8.2-induced resistance (Phee et al., 2008; Wang et al., 2012). WIN2 was shown to associate with the *P. syringae* type III-secreted effector HopW1-1 and knock-down of *WIN2* partially compromises HopW1-1-induced resistance (Lee et al., 2008). Recently, PIA, the closest homologue of PP2C-58, has been reported to be involved in AvrRpm1-induced responses (Widjaja et al., 2010). Thus, it seems possible that PP2C-58 might as well play a role in the regulation of defence responses. Interestingly, I showed in qRT-PCR experiments that the expression of *PP2C-58* is induced by elf18 and flg22 treatment. Unfortunately, cleavage of the eGFP-tag of PP2C-58-eGFP made it impossible to reach any conclusion regarding the localisation of this protein by confocal microscopy. To overcome this, different approaches can be used. On one hand, cleavage of a fused tag might be avoided by using different tags. Alternatively, the subcellular localisation could be verified by cellular fractionation combined with mass-spectrometry to detect the endogenous protein.

In order to determine whether PP2C-58 associates with EFR *in planta*, I tested for protein interaction by Co-IP. However, since PP2C-58-FLAG was non-specifically co-immunoprecipitated, an association with EFR-GFP could not be assessed. In addition, no association between EFR-GFP and PP2C-58-HA was detectable. Thus, no conclusions can be reached as to whether PP2C-58 associates with EFR *in planta*. Alternatively, the EFR-PP2C-58 interaction could also be assessed by immunoprecipitating PP2C-58-FLAG and testing for co-immunoprecipitation of EFR.
To further investigate whether PP2C-58 is involved in elf18-triggered signalling the characterisation of loss- and gain-of-function lines could give additional indications.

The third characterised candidate, PP2C-38, belongs to a subfamily of uncharacterised PP2Cs. In qRT-PCR experiments I could demonstrate that the expression of *PP2C-38* is up-regulated by PAMP treatment. In addition, by expressing an eGFP-fusion protein in *N. benthamiana,* I showed that PP2C-38 localises to the cell periphery and thus potentially in close proximity to EFR. Co-IP experiments also confirmed that PP2C-38-FLAG associates with EFR-GFP *in planta*. This association was decreased upon elf18 treatment, indicating that PP2C-38 dissociates from the EFR complex upon ligand perception. In summary, these results indicate that PP2C-38 might play a role in EFR-dependent signalling. Therefore, I decided to further characterise this candidate. In the following chapters, I will refer to this PP2C as PIE, for PP2C interacting with EFR.

Chapter 5: PIE, a novel EFR-interacting PP2C-type phosphatase regulates PAMP receptor complexes

5.1 Introduction

Reversible protein phosphorylation, mediated by protein kinases and protein phosphatases, plays an important role in regulating many biological processes (Schweighofer et al., 2004). According to their substrate specificity, protein phosphatases have been divided into three major classes: protein tyrosine phosphatases, protein serine/threonine phosphatases and dual-specificity phosphatases, which dephosphorylate both tyrosine and serine/threonine residues (Cohen, 1989). Based on their structure and sensitivity to different inhibitors, serine/threonine phosphatases have been further sub-divided. The subgroup formed by phosphoprotein phosphatases (PPPs) includes type 1 (PP1), type 2A (PP2A), and type 2B (PP2B) protein phosphatases (Farkas et al., 2007). The subgroup formed by Mg^{2+}-dependent protein phosphatases (PPM) includes PP2Cs and pyruvate dehydrogenase phosphatases (Cohen, 1989). Notably, in contrast to the PPPs, which consist of catalytic subunits, PP2Cs are monomeric enzymes (Cohen, 1989). Regarding their sensitivity to different inhibitors, PP1s are inhibited by nanomolar concentrations of inhibitor-1 and 2, while PP2As are specifically inhibited by cantharidin (Huang and Glinsmann, 1976; Roach et al., 1985; Johansen and Ingebritsen, 1986; Li and Casida, 1992; Brüchert et al., 2008). In contrast, PP2Cs and PP2Bs require the divalent cations Mg^{2+} and Ca^{2+}, respectively, and consequently are inhibited by the chelators EDTA (Ethylene diamine tetraacetic acid) and EGTA (Ethylene glycol tetraacetic acid) (Luan, 2003).

The *Arabidopsis thaliana* genome encodes 76 putative PP2C-type phosphatases that were clustered into ten groups (A-J) based on their amino acid sequence (Schweighofer et al., 2004). Different members of the group A function as negative regulators of ABA signal transduction, including ABI1 and ABI2 (ABA-INSENSITIVE 1 AND 2), PP2CA (PROTEIN PHOSPHATASE 2CA) and HAB1 (HOMOLOGY TO ABI1) (Rodriguez et al., 1998; Gosti et al., 1999; Kuhn et al., 2006; Saez et al., 2006; Rubio et al., 2009).

The group B contains six PP2Cs named AP2Cs (ARABIDOPSIS PHOSPHATASE 2C), which are orthologous of MP2C (MEDICAGO PHOSPHATASE 2C), a PP2C that regulates MAPK signalling (Meskiene et al., 2003; Schweighofer et al., 2004). AP2C1, AP2C2, AP2C4 and AP2C3/*At*PP2C5 contain an N-terminal kinase interaction motif and inactivate *Arabidopsis* MPK6 and associate with MPK3, MPK4 and MPK6 (Schweighofer et al., 2007; Brock et al., 2010; Umbrasaite et al., 2010). AP2C1 regulates plant defence responses and consequently, *AP2C1* overexpression enhances susceptibility to the necrotrophic fungus *B. cinerea* (Schweighofer et al., 2007). *AP2C1* overexpression lines also display a significant reduction of wounding-induced ET and JA accumulation, indicating that AP2C1 additionally regulates stress-induced hormonal pathways (Schweighofer et al., 2007). Recently, AP2C3/*At*PP2C5 and AP2C1 were shown to regulate seed germination, stomatal closure and ABA-inducible gene expression in a partially redundant manner (Brock et al., 2010; Umbrasaite et al., 2010).

POLTERGEIST (POL) and POLTERGEIST-like (PLL) proteins belong to the group C and act redundantly to promote stem-cell identity (Yu et al., 2003; Schweighofer et al., 2004). In the shoot meristem, POL and PLL1 regulate the CLV3/WUS pathway and promote the expression of *WUSCHEL* (*WUS*), while in the root meristem POL and PLL1 are required for stem cell maintenance, presumably by participating in the CLE40/WOX5 pathway (Yu et al., 2000; Yu et al., 2003; Song et al., 2006; Gagne and Clark, 2007; Gagne et al., 2008; Song et al., 2008; Gagne and Clark, 2010).

An orthologue of *Arabidopsis* POL/PLLs, the rice PP2C XB15, associates with the PRR XA21 to induce receptor dephosphorylation and thereby attenuates XA21 signalling (Park et al., 2008). Consistently, transgenic lines overexpressing *Xb15* display compromised XA21-mediated resistance (Park et al., 2008). Like FLS2 and EFR, XA21 belongs to subfamily XII of LRR-RLKs (Boller and Felix, 2009). Interestingly, XA21 associates with a rice BAK1 orthologue that positively regulates XA21-mediated resistance (Pamela Ronalds, UC Davis, personal communication) (Monaghan and Zipfel, 2012), indicating that all three PRRs are regulated by similar mechanism.

Three PP2Cs of group F, PAPP2C, WIN2 and PIA1, play a role in plant defence responses. PAPP2C mediates phytochrome signalling but recent results suggest an additional role in RPW8.2-induced resistance (Phee et al., 2008; Wang et al., 2012). WIN2 associates with the *P. syringae* type III-secreted effector HopW1-1, and knock-down of *WIN2* partially compromises HopW1-1-induced resistance (Lee et al., 2008). PIA1 was identified in a proteomic screen for proteins that accumulate upon recognition of the *P. syringae* type III-secreted effector AvrRpm1 (Widjaja et al., 2009). *pia1* loss-of-function mutants display enhanced disease resistance against *Pto* DC3000 expressing *avrRpm1*, but not against *Pto* DC3000, indicating that PIA1 is specifically involved in AvrRpm1 induced responses (Widjaja et al., 2010). The target of PIA1 still remains elusive, but RIN4 phosphorylation does not appear to be affected in the *pia1* mutant (Widjaja et al., 2010).

KAPP, which regulates several RLKs, is not related to other PP2C groups and therefore, was placed as a singleton (Schweighofer et al., 2004). KAPP was first identified as an interactor of RLK5 (RECEPTOR-LIKE PROTEIN KINASE 5) (Stone et al., 1994), but has been shown to also associate with several other RLKs including CLAVATA1 and SERK1 (Stone et al., 1998; Trotochaud et al., 1999; Shah et al., 2002). In addition, KAPP interacts with the kinase domain of FLS2 in yeast two-hybrid assays, and *KAPP* overexpression decreases flg22 sensitivity (Gómez-Gómez et al., 2001). Surprisingly, *KAPP* overexpression was also reported to impair flg22 binding and thus, KAPP was initially implied to regulate ligand binding through FLS2 dephosphorylation (Gómez-Gómez et al., 2001). However, it had been later demonstrated that FLS2 kinase activity is not required for flg22 perception (Asai et al., 2002; Robatzek et al., 2006; Schulze et al., 2010; Schwessinger et al., 2011), and therefore, the previous hypothesis seems questionable.

To gain further insight into early signalling events of the EFR signalling pathway, a yeast two-hybrid screen was carried out to identify novel EFR-interacting proteins. This led to the identification of a yet uncharacterised putative PP2C, which was referred to as PIE (PP2C-INTERACTING WITH EFR). In the following chapter, I further examined the potential involvement of PIE in PTI.

5.2 Results

5.2.1 Characterisation of a novel PP2C-type phosphatase

5.2.1.1 PIE encodes a predicted PP2C-type phosphatase

The *Arabidopsis* Information Resource (TAIR) annotates two different splicing variants for *PIE* (At3g12620) (Swarbreck et al., 2008). Both carry a 1,158-bp open reading frame that consists of four exons. One splicing variant contains three introns, while the second variant carries an additional fourth intron in the 5'-UTR (Figure 5.1).

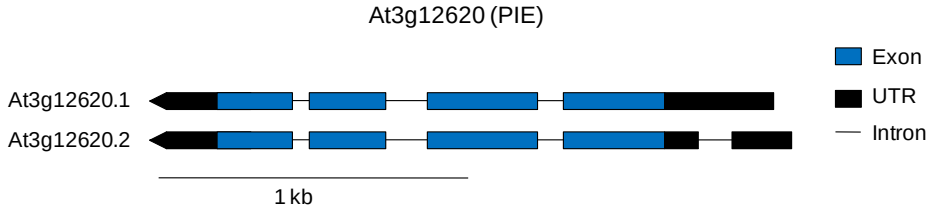

Figure 5.1: Schematic diagram showing the *PIE* gene structure
PIE structure is shown as annotated from The *Arabidopsis* Information Resource (TAIR) (www.arabidopsis.org)

Based on publicly available microarray data from the *Arabidopsis* eFP Browser database (http://bar.utoronto.ca/efp/cgi-bin/efpWeb.cgi) (Winter et al., 2007), *PIE* is expressed in most tissues, including leafs, stem, apex and flowers, while higher expression is detected in pollen. Interestingly, *PIE* expression is upregulated after treatment with the PAMPs flg22 (1.71 fold after 4 hours) and HrpZ (1.51 fold after 4 hours). In addition, qRT-PCR experiments with gene-specific primers revealed that *PIE* expression is also up-regulated after elf18 perception (Figure 4.11).

According to the database Pfam 26.0 (http://pfam.sanger.ac.uk) (Punta et al., 2012), *PIE* encodes a protein with a predicted molecular mass of 42.85 kDa, which carries a domain that is predicted to exhibit PP2C catalytic activity (Figure 5.2; underlined). This catalytic domain also contains the predicted metal-coordinating residues that interact with Mg^{2+} or Mn^{2+} ions to form a binuclear metal centre in *Arabidopsis* POL and human PP2Cα (Figure 5.2; in red) (Das et al., 1996; Yu et al., 2003). The databases Phobius and ARAMEMNON 7.0 (http://phobius.sbc.su.se; http://aramemnon.botanik.uni-

koeln.de) (Schwacke et al., 2003; Käll et al., 2004) predict that PIE contains a hydrophobic region, which presents a potential transmembrane domain (Figure 5.2; in green). However, according to SignalP 4.0 (http://www.cbs.dtu.dk/services/SignalP) (Petersen et al., 2011), the protein contains no signal peptide that could target the protein to the membrane. According to the database CSS-Palm 3.0 (http://csspalm.biocuckoo.org) (Zhou et al., 2006), PIE might be palmitoylated at cysteine 154 (Figure 5.2; in blue) and the database PhosPhAt 3.0 (http://phosphat.mpimp-golm.mpg.de) (Durek et al., 2009) predicts that PIE carries six potential phosphorylation sites (Figure 5.2; in orange).

```
  1 MVSSATILRMVAPCWRRPSVKGDHSTRDANGRCDGLLWYKDSGNHVAGEF
 51 SMSVIQANNLLEDHSKLESGPVSMFDSGPQATFVGVYDGHGGPEAARFVN
101 KHLFDNIRKFTSENHGMSANVITKAFLATEEDFLSLVRRQWQIKPQIASV
151 GACCLVGIICSGLLYIANAGDSRVVLGRLEKAFKIVKAVQLSSEHNASLE
201 SVREELRSLHPNDPQIVVLKHKVWRVKGIIQVSRSIGDAYLKKAEFNREP
251 LLAKFRVPEVFHKPILRAEPAITVHKIHPEDQFLIFASDGLWEHLSNQEA
301 VDIVNTCPRNGIARKLIKTALREAAKKREMRYSDLKKIDRGVRRHFHDDI
351 TVIVVFLDSHLVSRSTSRRPLLSISGGGDLAGPST
```

Figure 5.2: ***PIE* encodes a predicted PP2C-type phosphatase**
Deduced PIE amino acid sequence. The predicted PP2C catalytic domain is underlined (http://pfam.sanger.ac.uk), whereas metal coordinating residues are marked in red. The potential transmembrane domain is indicated in green and predicted phosphorylation sites are shown in orange. The predicted palmitoylation site is indicated in blue.

5.2.1.2 PIE belongs to a family of uncharacterised predicted PP2C-type phosphatases

In order to identify PIE orthologs, the amino acid sequence of PIE was compared to proteins from the plant species *Oryza sativa*, *Brachypodium distachyon, Populus trichocarpa*, *Glycine max, Arabidopsis lyrata, Vitis vinifera* and *Arabidopsis thaliana* (Figure 5.3). Interestingly, PIE shows significant similarity to other predicted plant PP2Cs. Yet, none of these proteins has been characterised, leaving the functional role of these proteins unknown.

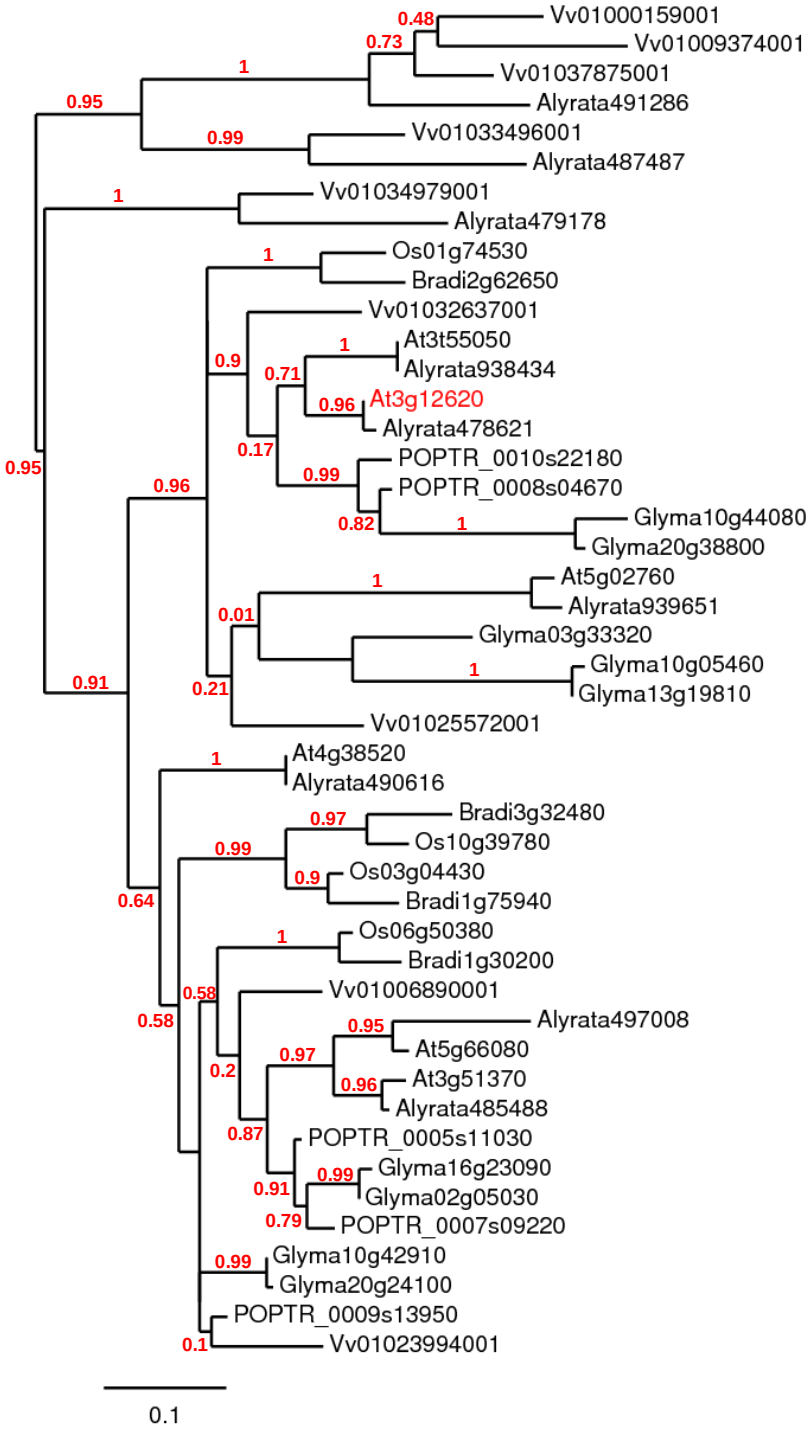

Figure 5.3: PIE shares sequence similarity with predicted PP2C-type phosphatases from different plant species

Phylogenetic tree of PIE and closely related proteins. PIE is indicated in red. Homologues from different plant species were identified using the BLAST search on the database Phytozome v8.0 (www.phytozome.net). The phylogenetic tree was generated using full-length amino acid sequences. MUSCLE was used for the alignment, PhyML for the phylogeny, and TreeDyn for drawing the tree (www.phylogeny.fr). The horizontal branches are drawn to scale as indicated by the scale bar (bar = substitution/site rate of 0.2 %), and their length indicates the level of divergence among sequences. Bootstrap values are indicated in red above nodes. At: *Arabidopsis thaliana*, Os: *Oryza sativa,* Bradi: *Brachypodium distachyon,* POPTR: Populus trichocarpa, Glyma: *Glycine max,* Vv: *Vitis vinifera,* Alyrata: *Arabidopsis lyrata.*

The closest *Arabidopsis* homologue of PIE is PP2C-48 (At3g55050) and both proteins share 75 % amino acid identity (Figure 5.4) (Schweighofer et al., 2004).

```
PIE             MVSSATILRMVAPCWRRPSVKGDHS--TRDANGRCDGLLWYKDSGNHVAGEFSMSVIQAN 58
PP2C-48         MVS-TTFRRIVSPCWRPFGIGEDSSPGSDDTNGRLDGLLWYKDSGNHITGEFSMAVVQAN 59

PIE             NLLEDHSKLESGPVSMFDSGPQATFVGVYDGHGGPEAARFVNKHLFDNIRKFTSENHGMS 118
PP2C-48         NLLEDHSQLESGPISLHESGPEATFVGVYDGHGGPEAARFVNDRLFYNIKRYTSEQRGMS 119

PIE             ANVITKAFLATEEDFLSLVRRQWQIKPQIASVGACCLVGIICSGLLYIANAGDSRVVLGR 178
PP2C-48         PDVITRGFVATEEEFLGLVQEQWKTKPQIASVGACCLVGIVCNGLLYVANAGDSRVVLGK 179

PIE             LEKAFKIVKAVQLSSEHNASLESVREELRSLHPNDPQIVVLKHKVWRVKGIIQVSRSIGD 238
PP2C-48         VANPFKELKAVQLSTEHNASIESVREELRLLHPDDPNIVVLKHKVWRVKGIIQVSRSIGD 239

PIE             AYLKKAEFNREPLLAKFRVPEVFHKPILRAEPAITVHKIHPEDQFLIFASDGLWEHLSNQ 298
PP2C-48         AYLKRAEFNQEPLLPKFRVPERFEKPIMRAEPTITVHKIHPEDQFLIFASDGLWEHLSNQ 299

PIE             EAVDIVNTCPRNGIARKLIKTALREAAKKREMRYSDLKKIDRGVRRHFHDDITVIVVFLD 358
PP2C-48         EAVDIVNSCPRNGVARKLVKAALQEAAKKREMRYSDLEKIERGIRRHFHDDITVIVVFLH 359

PIE             SHLVSRSTSRRPLLSISGGGDLAGPST-- 385
PP2C-48         ATNFATRTP----ISVKGGGLLSAHNPVL 384
```

Figure 5.4: Alignment of PIE and its closest homologue PP2C-48
Multiple alignments were generated with Muscle 3.7. Amino acid similarity was determined according to BLOSUM62. In yellow: max similarity (3.0), in blue medium similarity: (1.5). The predicted PP2C domains are underlined (http://pfam.sanger.ac.uk).

5.2.1.3 *PIE* encodes a functional PP2C-type phosphatase

(Note: The phosphatase assays were carried out with Dr Vardis Ntoukakis, The Sainsbury Laboratory).

To test if *PIE* encodes a functional PP2C, the enzymatic activity of PIE fusion proteins was examined. First we assessed whether PIE expressed in *Echerichia coli* has phosphatase activity. Therefore, PIE was expressed as a glutathione-S-transferase (GST) fusion protein and purified with GST-Trap columns. The phosphatase activity of PIE-GST was determined using a commercial Promega serine/threonine phosphatase assay system according to the manufacturer's instructions. In this assay phosphatase activity is calculated by measuring the release of phosphate from a phosphorylated synthetic peptide. PIE-GST catalysed the release of 30-40 pmol phosphate per minute in buffer containing $MgCl_2$ (Figure 5.5 A). This reaction was inhibited by the serine/threonine phosphatase inhibitor sodium fluoride (NaF) (Figure 5.5 A).

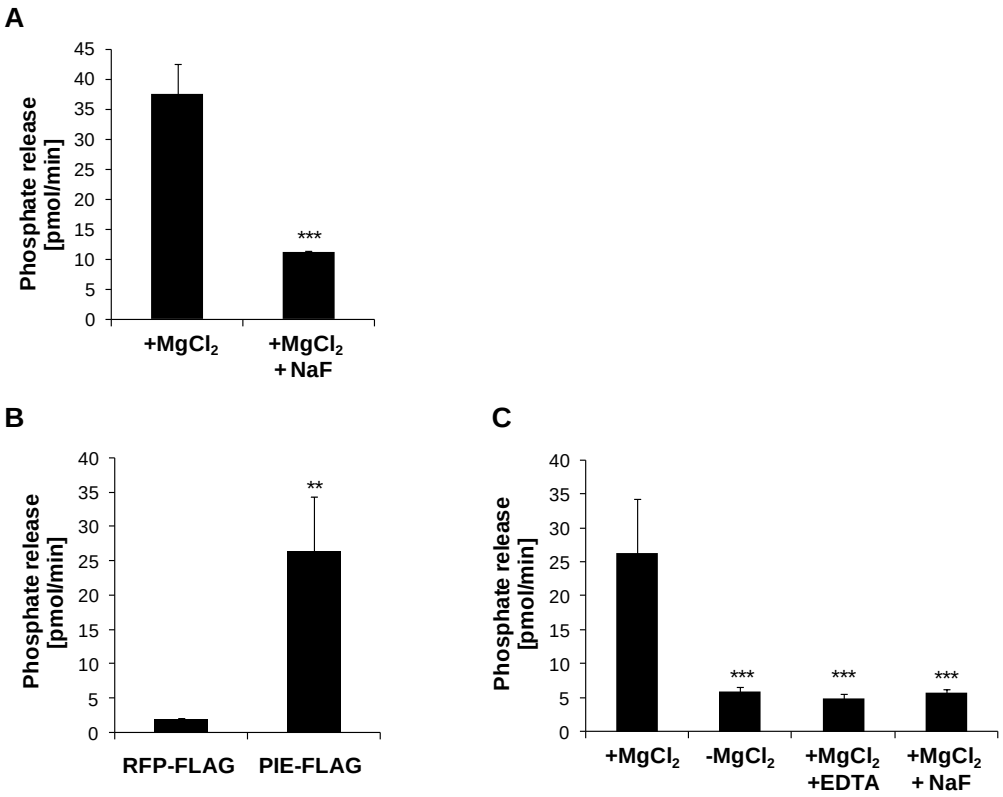

Figure 5.5: PIE possesses PP2C catalytic activity
(A) PIE expressed in *E. coli* exhibits serine/threonine phosphatase activity. PIE-GST was expressed in *E. coli* and purified with GST-Trap columns. Phosphatase activity was assayed by measuring the release of phosphate from a phosphorylated synthetic peptide. Phosphatase activity was assayed in buffer containing 50 mM NaF and/or 5 mM $MgCl_2$.
(B) PIE expressed *in planta* exhibits protein phosphatase activity. PIE-FLAG and RFP-FLAG, which was used as a negative control, were expressed in *Nicotiana benthamiana* and purified with ANTI-FLAG M2 Affinity Gel. Proteins were competitively eluted with FLAG peptides and phosphatase activity was assayed by measuring the release of phosphate from a phosphorylated synthetic peptide. (C) PIE is a PP2C-type phosphatase. PIE-FLAG was expressed and purified as described above. Phosphatase activity was assayed in buffer containing 5 mM $MgCl_2$ and 50 mM NaF or 25 mM EDTA. Results are average ± standard error with n=3. Asterisks indicate significant differences compared with wild-type values at P>0.001 (***) and P>0.005 (**). These assays were carried out by Dr Vardis Ntoukakis and repeated three times with similar results.

Next we tested if PIE expressed *in planta* exhibits phosphatase activity. To this end, PIE-FLAG and RFP-FLAG, which was used as a negative control, were expressed in *N. benthamiana* under the control of the 35S promoter. Proteins were purified with ANTI-FLAG M2 Affinity Gel and competitive eluted with FLAG-peptides. The phosphatase activity of PIE-FLAG and RFP-FLAG was again assayed by measuring the release of phosphate from a phosphorylated synthetic peptide. As expected, no considerable dephosphorylation could be detected in assays with RFP-FLAG (Figure 5.5 B). In contrast, PIE-FLAG catalysed the release of 25-35 pmol phosphate per

minute (Figure 5-5 B). The phosphatase activity was dependent on the presence of Mg^{2+} in the reaction buffer and a significantly reduced activity was measured in buffer lacking this cation (Figure 5.5 C). To further classify the detected phosphatase activity, the effect of the serine/threonine phosphatase inhibitor NaF and the PP2C-specific inhibitor EDTA was tested. Both inhibitors reduced PIE-mediated phosphate release significantly (Figure 5.5 C).
Together these results confirm that PIE exhibits PP2C activity.

5.2.2 PIE associates with PTI signalling components *in planta*

5.2.2.1 The association of PIE with EFR as well as the elf18-triggered dissociation do not require EFR kinase activity

BAK1, EFR and FLS2 possess intracellular kinase domains, and it has been shown that their kinase activity is required for several downstream signalling events (Asai et al., 2002; Robatzek et al., 2006; Schulze et al., 2010; Schwessinger et al., 2011). However, kinase activities of all three proteins are not required for the formation of the FLS2-BAK1 and FLS2-EFR complexes (Schulze et al., 2010; Schwessinger et al., 2011) and treatment with the general kinase inhibitor K-252a does not prevent complex formation in *Arabidopsis* cells (Schulze et al., 2010). Consistently, kinase-inactive mutants of EFR, FLS2 and BAK1 display full interaction capacities (Schwessinger et al., 2011). Hence, ligand-induced conformational changes may be sufficient to trigger the EFR-BAK1 and FLS2-BAK1 association (Boller and Felix, 2009).
In order to determine the importance of EFR kinase activity for the EFR-PIE association, PIE-FLAG was co-expressed with a GFP-tagged kinase-inactive mutant of EFR (EFR-KD) (Schwessinger et al., 2011) under the control of the 35S promoter in *N. benthamiana.* Infiltrated leaf tissues were treated with water or elf18 for 20 minutes and EFR-KD-GFP was immunoprecipitated. PIE associated with EFR-KD and dissociates after elf18 perception (Figure 5.6 A), as previously detected with EFR (Figure 4.13). This indicates that

both events are independent of EFR kinase activity. In contrast, no association between EFR and PIE-like (PP2C-48), the closest homologue of PIE, was detected (Figure 5.6 B).

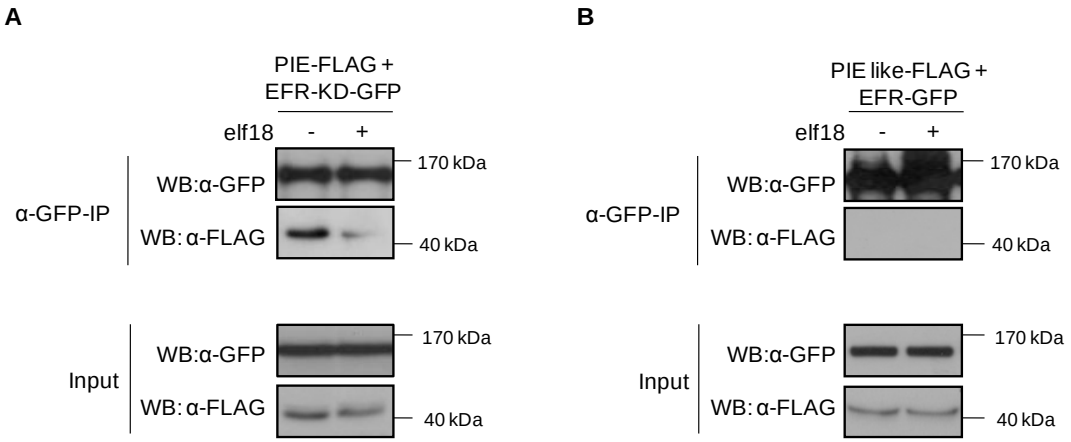

Figure 5.6: PIE associates with EFR and dissociates after elf18 perception independently of EFR kinase activity.
(A) Co-immunoprecipitation of PIE and kinase-dead EFR (EFR-KD). *N. benthamiana* leaves expressing PIE-FLAG and EFR-KD-GFP were treated (+) or not (-) with 100 nM elf18 for 20 minutes. Total proteins were extracted (Input) and GFP-tagged proteins were immunoprecipitated with GFP-Trap beads. FLAG- and GFP-tagged proteins were detected by immunoblot analysis with tag-specific antibodies. (B) Co-immunoprecipitation of PIE-like and EFR. *N. benthamiana* leaves expressing PIE-FLAG and EFR-KD-GFP were treated (+) or not (-) with 100 nM elf18 for 20 minutes. Total proteins were extracted (Input) and GFP-tagged proteins were immunoprecipitated with GFP-Trap beads. FLAG- and GFP-tagged proteins were detected by immunoblot analysis with tag-specific antibodies. These experiments were three times repeated with similar results.

5.2.2.2 PIE associates with FLS2 *in planta* and dissociates after flg22-perception

Since EFR and FLS2 share several signalling components, I tested whether PIE also associates with FLS2, by co-expressing FLS2-GFP and PIE-FLAG under the control of the 35S promoter in *N. benthamiana.* Infiltrated leaf tissues were treated with water or flg22 for 20 minutes and FLS2-GFP was immunoprecipitated. PIE was detectable in the FLS2-IP from leaf samples treated with water, confirming that both proteins associate *in planta* (Figure 5.7 A). In contrast, only a weak association could be detected in samples treated with flg22 (Figure 5.7 A), indicating that PIE dissociated from the FLS2 complex in a flg22-dependent manner. As in the case of EFR, PIE also associated with a kinase-inactive variant of FLS2 (FLS2-KD) (Schwessinger et al., 2011) (Figure 5.7 B). Since the flg22-induced dissociation was also

observed with FLS2-KD, both PIE steady-state association and flg22-dependent dissociation are independent of FLS2-kinase activity.

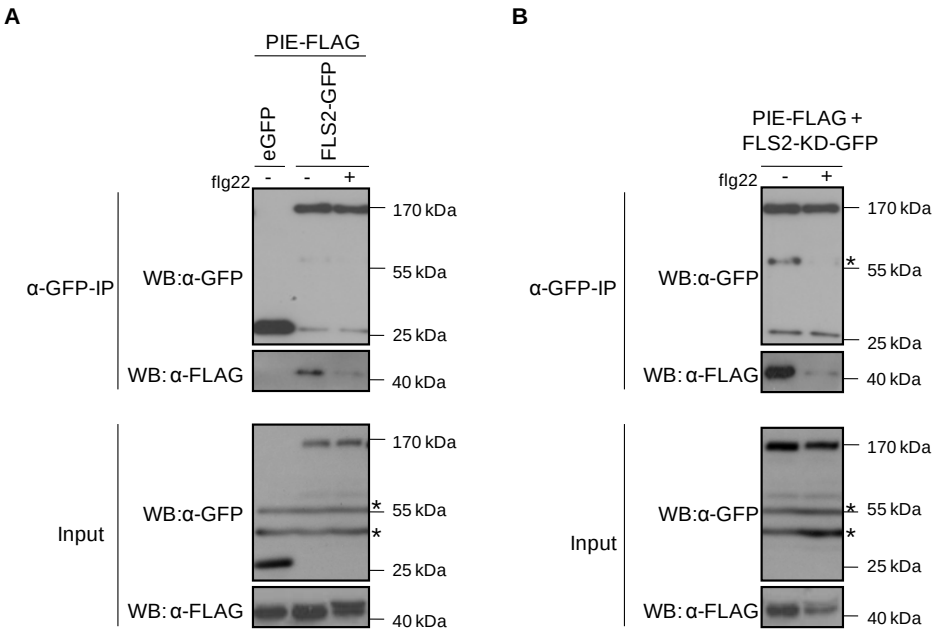

Figure 5.7: PIE associates with FLS2 and dissociates after flg22 perception independently of FLS2 kinase activity
Co-immunoprecipitation of PIE and wild-type (A) and kinase-dead FLS2 (B). *N. benthamiana* leaves expressing PIE-FLAG and FLS2-GFP or FLS2-KD-GFP were treated (+) or not (-) with 100 nM flg22 for 20 minutes. PIE-FLAG and eGFP was used as a negative control to test for non-specific binding. Total proteins were extracted (Input) and GFP-tagged proteins were immunoprecipitated with GFP-Trap beads. FLAG- and GFP-tagged proteins were detected by immunoblot analysis with tag-specific antibodies. Unspecific bands are indicated with a star. These experiments were three times repeated with similar results.

5.2.2.3 PIE associates with BRI1 but no BR-induced dissociation can be observed

In order to assess whether PIE interacts with other LRR-RLKs, I tested for association with the brassinosteroid-receptor BRI1. To this end, PIE-FLAG was co-expressed with BRI1-GFP under the control of the 35S promoter and infiltrated tissues were treated with water or brassinolide (BL, the most bioactive brassinosteroid) for three hours. PIE-FLAG was well detectable in the IP extract of BRI1-GFP, indicating that both proteins can associate *in planta* (Figure 5.8). However, in contrast to what was observed with EFR, FLS2 and BIK1, no ligand-induced dissociation of the BRI1-PIE complex was detected (Figure 5.8).

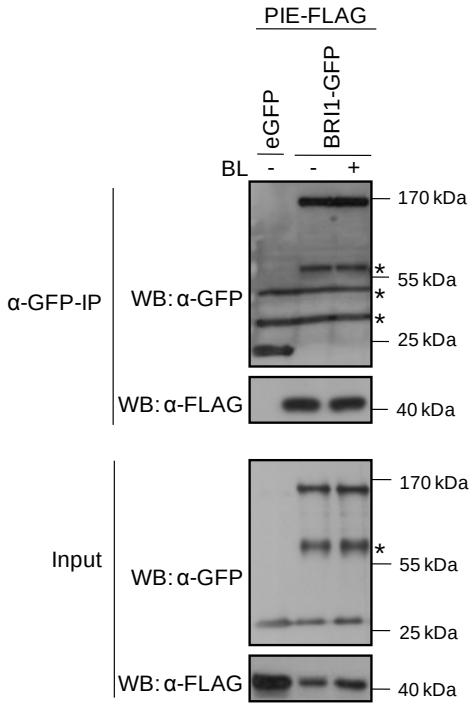

Figure 5.8: PIE associates with BRI1 *in planta* but no BR-induced dissociation can be detected
Co-immunoprecipitation of PIE and BRI1. *N. benthamiana* leaves expressing PIE-FLAG and BRI1-GFP were treated (+) or not (-) with 100 nM brassinolide (BL) for 3 hours. PIE-FLAG and eGFP was used as a negative control to test for non-specific binding. Total proteins were extracted (Input) and GFP-tagged proteins were immunoprecipitated with GFP Trap beads. FLAG- and GFP-tagged proteins were detected by immunoblot analysis with tag-specific antibodies. This experiment was three times repeated with similar results.

5.2.2.4 PIE associates with BIK1 *in planta* but not with BAK1

To assess whether PIE also associates with BIK1 and/or BAK1, PIE-FLAG was co-expressed with BAK1-GFP or BIK1-eGFP under the control of the 35S promoter, and infiltrated leaf tissues were treated with water or flg22 for 20 minutes. PIE associated with BIK1 and dissociated after flg22-perception (Figure 5.9). In contrast, no interaction was detected with BAK1 (Figure 5.9).

5.2.2.5 No interaction between PIE and PTI-signalling components was detected *in vitro*

I showed that PIE associates with EFR, FLS2 and BIK1 *in planta*. To determine whether these protein-protein interactions are direct or mediated through another protein, physical interaction was assessed in *in vitro* pull down assays.

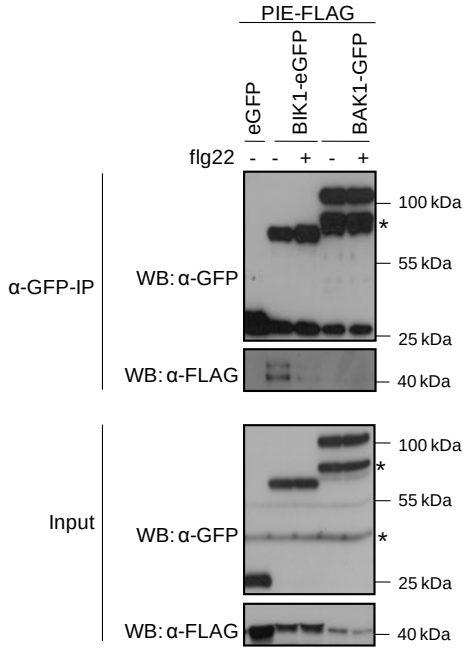

Figure 5.9: PIE associates with BIK1 *in planta* but not with BAK1
Co-immunoprecipitation of PIE and BIK1 or BAK1. *N. benthamiana* leaves expressing PIE-FLAG and BIK1-GFP or PIE-FLAG and BIK1-GFP were treated (+) or not (-) with 100 nM flg22 for 20 minutes. PIE-FLAG and eGFP was used as a negative control to test for non-specific binding. Total proteins were extracted (Input) and GFP-tagged proteins were immunoprecipitated with GFP-Trap beads. FLAG- and GFP-tagged proteins were detected by immunoblot analysis with tag-specific antibodies. This experiment was three times repeated with similar results.

To this end, the cytoplasmic domains of EFR, FLS2, BAK1 and BRI1, and full-length BIK1 were expressed as maltose binding protein-6xhistidine (MBP-6xHis) fusion proteins in *E. coli*, and purified using an amylose resin. In addition, MBP-6xHis was extracted and used as a negative control. Protein concentrations were determined by Bradford assay and 2 µg of each protein were incubated with equal amounts of purified GST or PIE-GST. MBP-tagged proteins were pulled down with amylose beads and protein extracts were analysed by SDS-PAGE (sodium dodecyl sulphate-polyacrylamide gel electrophoresis) and immunoblotting with tag-specific antibodies. PIE-GST was not pulled down with free MBP-6xHis. Hence, it can be excluded that the protein was non-specifically binding to the tag or the amylose resin (Figure 5.10). In addition, no interaction between PIE-GST and EFR, FLS2, BAK1 or BIK1 could be observed (Figure 5.10). However, PIE-GST was detectable in the BRI1-MBP pull-down, indicating that both proteins may interact physically (Figure 5.10).

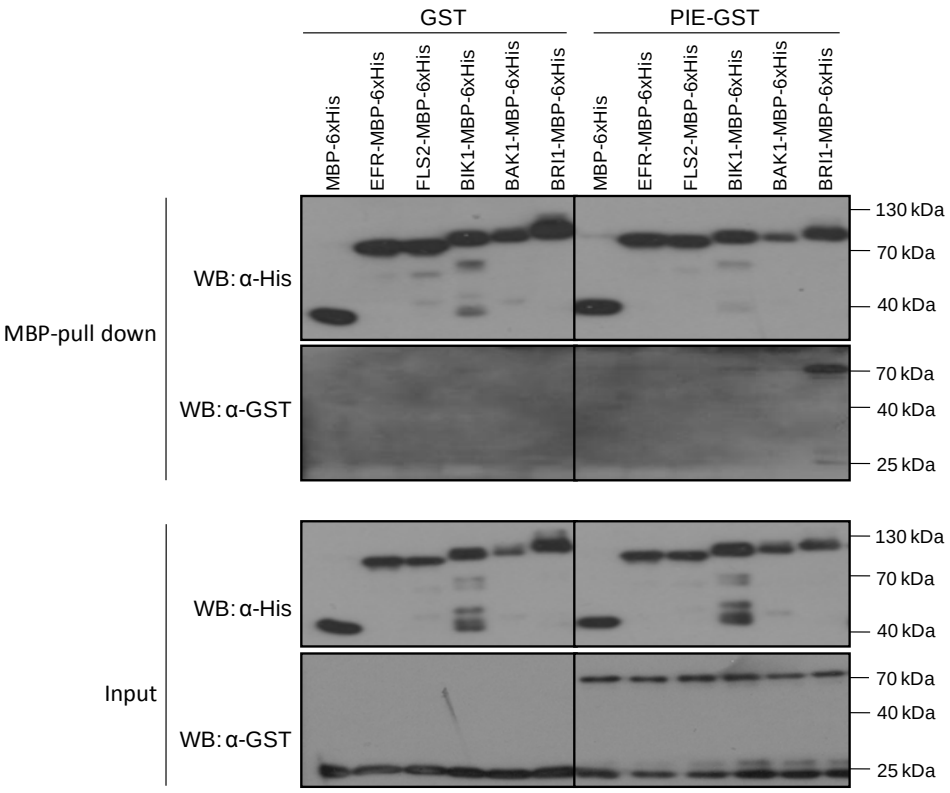

Figure 5.10: No interaction between PIE and PTI signalling components can be detected *in vitro*
Two micrograms of PIE-GST (right) or GST (left) were either incubated with 2 µg MBP-6xHis, EFR-MBP-6xHis, FLS2-MBP-6xHis, BIK1-MBP-6xHis, BAK1-MBP-6x His or BRI1-MBP-6xHis. MBP-6His-tagged proteins were pulled down with amylose beads. After washing three times, proteins were eluted with sample buffer, and analysed by SDS-PAGE and immunoblotting with α-GST or α-His antibodies. This experiment was repeated two times with similar results.

5.2.3 PIE dephosphorylates PTI signalling components *in vitro*

Note: These assays were carried out with Dr Vardis Ntoukakis (The Sainsbury Laboratory) and Dr Alberto Macho (The Sainsbury Laboratory).

PIE encodes an active PP2C that associates with EFR, FLS2 and BIK1 *in planta.* Since it had been shown that these proteins are phosphorylated in response to PAMP perception (Lu et al., 2010b; Schulze et al., 2010; Zhang et al., 2010; Schwessinger et al., 2011), I hypothesized that they could be potential substrates of PIE. To test this, protein dephosphorylation was assessed *in vitro* using recombinant proteins expressed in *E. coli*. Therefore,

MBP-6xHis tagged fusions proteins of full- length BIK and the cytoplasmic domains of EFR, FLS2 and BAK1 were expressed in *E. coli* and purified as described in section 5.2.2.5. Recombinant proteins were incubated with radiolabeled [γ-^{32}P]-ATP to enable detection of autophosphorylation. The proteins were then incubated with 2 µg purified PIE-GST or free GST and the phospho-status of EFR, FLS2, BIK1 and BAK1 was detected by autoradiography. Significant radioactive phosphate incorporation was observed in the samples with free GST (Figure 5.11 A), confirming that all proteins were autophosphorylated.

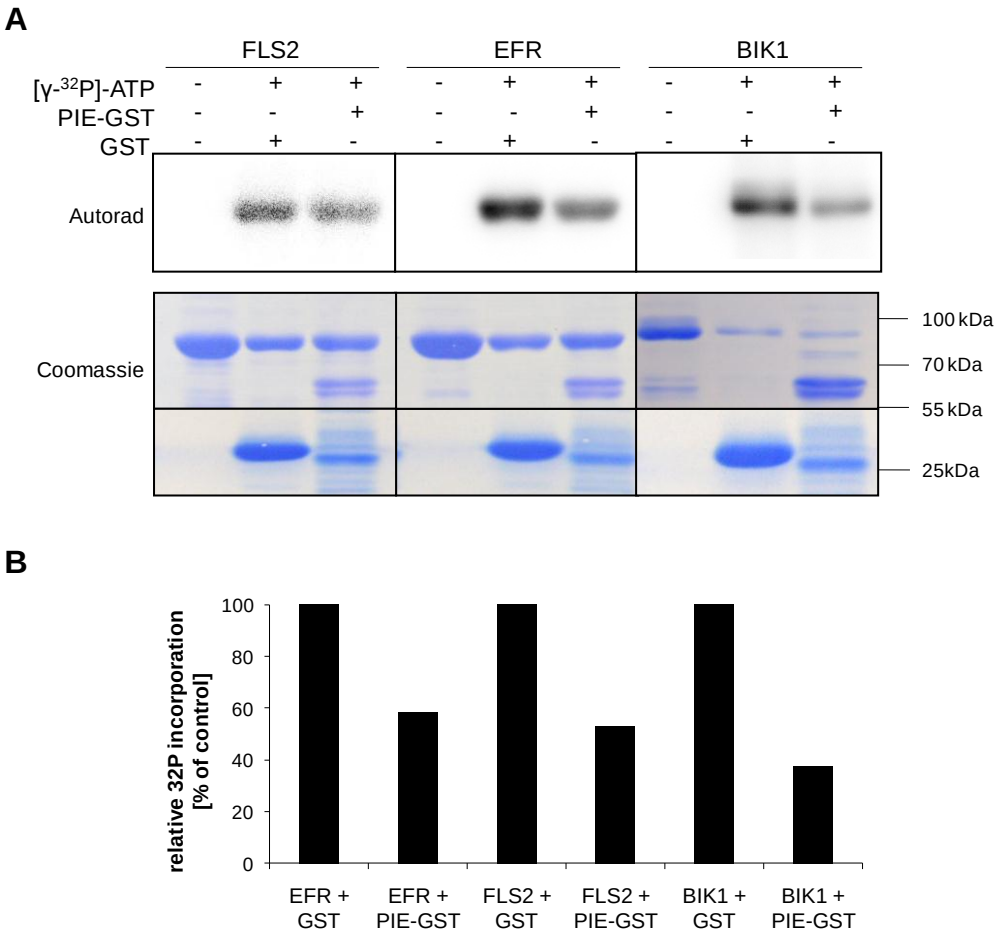

Figure 5.11: PIE dephosphorylates EFR, FLS2 and BIK1 *in vitro*
EFR-, FLS2- and BIK1-MBP were autophosphorylated with [γ-^{32}P]-ATP in kinase buffer for 30 minutes. ^{32}P-labeled proteins were washed with PP2C buffer and incubated with equal amounts of GST or PIE-GST for 30 minutes. The reactions were stopped by adding 2x Laemmli loading buffer and boiling for 5 minutes. Proteins were separated by SDS-PAGE. Gels were transferred to PVDF, which were stained with Coomassie brilliant blue and destained (Coomassie). For the autoradiography, the dried membrane was exposed to an image plate (Autorad) (A). The amount of incorporated ^{32}P was quantified using the AIDA image analysis software. Values are represented as percentage of the negative control (B). This experiment was three times repeated with similar results. This assay was carried out by Dr Alberto Macho.

Although I could not detect an interaction between PIE and PTI signalling components *in vitro*, EFR, FLS2 and BIK1 were dephosphorylated after incubation with PIE (Figure 5.11 A and B), indicating that they are substrate of the PP2C. In contrast, no clear results could be obtained with BAK1 and protein dephosphorylation was only detected in one out of three assays (data not shown).

5.2.4 PIE is phosphorylated upon PAMP perception

The database PhosPhAt 3.0 (Durek et al., 2009) predicts that PIE contains six potential phosphorylation sites. Phosphorylation has been shown to play a major role in regulating the enzymatic activity of many proteins (Johansen and Ingebritsen, 1986; Su et al., 2012). In addition, phosphorylation can affect the subcellular localisation and interaction properties of a protein, or can target it for degradation (Johansen and Ingebritsen, 1986; Vlach et al., 1997; Nambirajan et al., 2000; Pederson et al., 2001; Kuwahara et al., 2008). In order to test whether PIE is differentially phosphorylated upon PAMP perception, I examined PIE phosphorylation status prior and after elf18 and flg22 perception.

5.2.4.1 PAMP perception induces PIE mobility shift

To investigate whether PIE is phosphorylated upon PAMP perception, I tested whether the protein displays an altered mobility in SDS-PAGE upon elf18 and flg22 treatment. To this end, PIE-FLAG was co-expressed with EFR-GFP or FLS2-GFP under the 35S promoter in *N. benthamiana.* Infiltrated leaf tissues were treated with water, elf18 or flg22 for 20 minutes. Protein crude extracts were analysed by SDS-PAGE and immunoblotting with tag-specific antibodies. Strikingly, PIE extracted from tissue treated with flg22 or elf18 migrated as a double band on SDS-PAGE, while proteins extracted from tissue treated with water ran as a single band (Figure 5.12 A). The band shift is reduced but still detectable in protein extracts from tissue co-expressing PIE and EFR-KD or FLS2-KD (Figure 5.12 A). In contrast, no

mobility shift of PIE-like (PP2C-48), the closest homologue of PIE, could be observed after PAMP-perception (Figure 5.12 B).

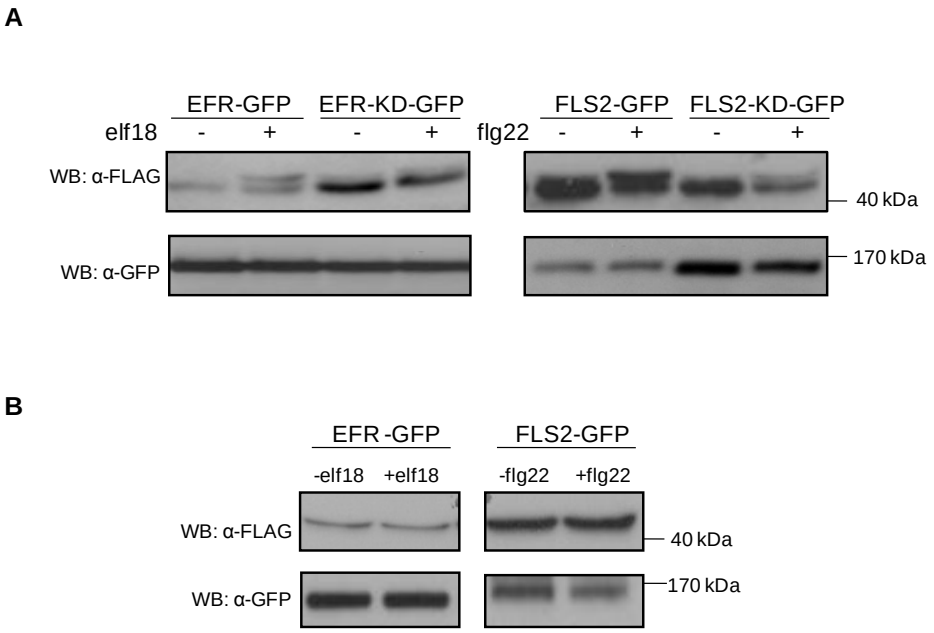

Figure 5.12: PAMP perception induces PIE mobility shift after transient expression in *Nicotiana benthamiana*
(A) PAMP perception induces PIE mobility shift on SDS-PAGE. *N. benthamiana* leaves expressing PIE-FLAG and EFR-GFP or EFR-KD-GFP were treated with 100 nM elf18 for 20 minutes. *N. benthamiana* leaves expressing PIE-FLAG and FLS2-GFP or FLS2-KD-GFP were extracted and analysed by SDS-PAGE and immunoblotting with α-FLAG and α-GFP antibodies. (B) No mobility shift of PIE-like (PP2C-48) was detected upon PAMP perception. *N. benthamiana* leaves expressing PIE-like-FLAG and EFR-GFP were treated with 100 nM elf18 for 20 minutes. *N. benthamiana* leaves expressing PIE-FLAG and FLS2-GFP were treted with 100 nM flg22 for 20 minutes. Proteins were extracted and analysed by SDS-PAGE and immunoblotting with α-FLAG and α-GFP antibodies. These experiments were three times repeated with similar results.

To further validate these observations, an *35S::PIE-FLAG* construct was transformed in *Arabidopsis* to generate stable transgenic plants. qRT-PCR experiments with gene-specific primers confirmed that several of the transformed lines overexpress *PIE* (Figure 5.13 A). However, accumulation of PIE-FLAG fusion proteins was not detectable in any of these lines in α-FLAG immunoblots (Figure 5.13 B). Therefore, stable transgenic *Arabidopsis* lines expressing *PIE-eGFP* under the control of the 35S promoter were generated (for further details see Chapter 5.5). Fourteen days old seedlings from homozygous transgenic lines were treated with water or flg22 for 20 minutes and proteins were extracted.

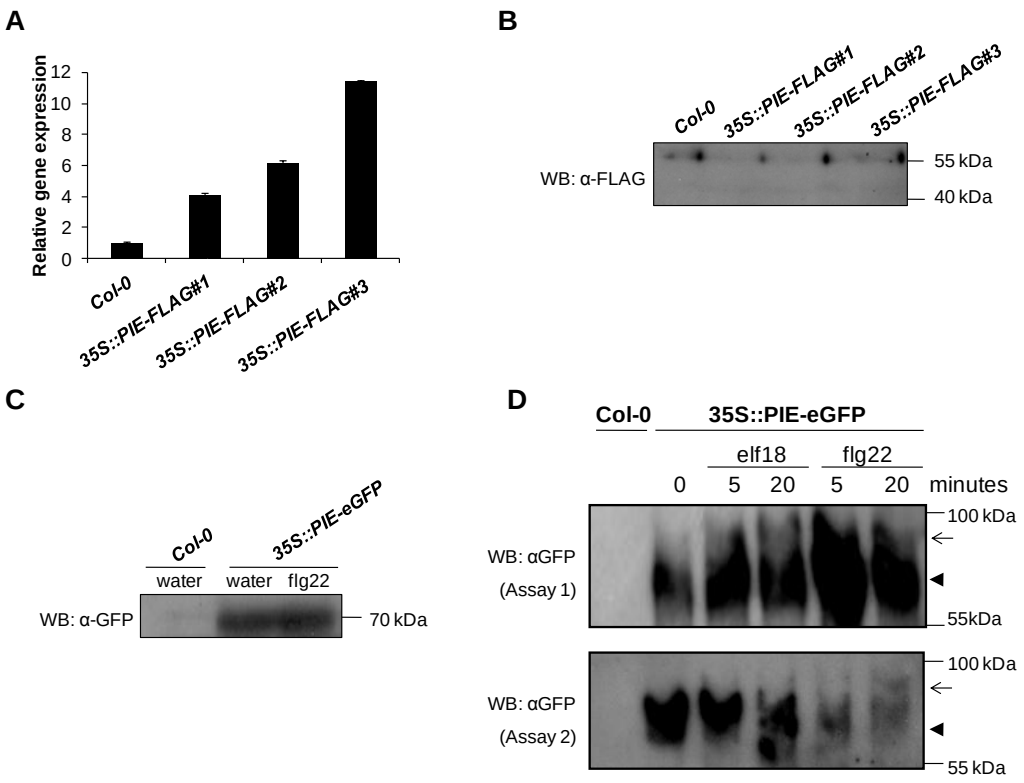

Figure 5.13: No PIE mobility shift can be detected after PAMP perception in stable transgenic *Arabidopsis thaliana* lines
(A) Stable transgenic *Arabidopsis* lines expressing PIE-FLAG under the control of the 35S promoter were generated. *PIE* expression level was tested in 14-day old homozygous F3 seedlings by qRT-PCR with gene-specific primers. (B) PIE-FLAG protein level was determined in 14-day old homozygous F3 seedlings. Protein crude extracts were analysed by SDS-PAGE and immunoblotting with an α-FLAG antibody. (C and D) PIE band shift was tested in *Arabidopsis* in 14-day old homozygous F3 seedlings that were treated with water or 100 nM flg22 for 20 minutes (C) or flg22 and elf18 for 5, 10 or 20 minutes (D). Protein extracts were analysed by SDS-PAGE (C) or SDS-PAGE containing Phos-tag (D) and immunoblotting with an α-FLAG antibody. PIE-eGFP is indicated with triangles, a potential PIE band shift is indicated by arrows. These experiments were three times repeated with similar results.

Although PIE-eGFP was detectable in α-GFP immunoblots, a PAMP-induced mobility shift was not observed (Figure 5.13 C). PIE-eGFP is approximately 25 kDa bigger than PIE-FLAG. Thus, an altered mobility might be harder to detect. To increase the separation of phosphorylated proteins, protein extracts were analysed in SDS-PAGE containing the phosphate-binding molecule Phos-tag. Phos-tag specifically binds phosphorylated proteins and thus, decreases their mobility (Kinoshita et al., 2006). Protein separation in Phos-tag gels is often affected by high concentrations of inorganic salts and detergents in the samples. In order to minimize the disorder, PIE-eGFP was immunoprecipitated with GFP-Trap beads, and the beads were washed four-

times with Tris-buffer. Proteins were eluted and separated in Phos-tag gels. Although a potential band shift was detectable in samples that were treated with elf18 and flg22 for 20 minutes, the quality of the separation was not sufficient to allow clear interpretations (Figure 5.13 D). Thus, I could not reach any conclusions as to whether PIE is also phosphorylated in *Arabidopsis* upon PAMP perception. Consequently, I continued to characterise PIE phosphorylation in *N. benthamiana* upon transient expression of PIE.

5.2.4.2 PIE is phosphorylated upon PAMP perception

To test if the observed PIE mobility shift was caused by protein phosphorylation, I determined whether the altered migration could be restored by phosphatase treatment. Therefore, PIE-FLAG was co-expressed with EFR-GFP in *N. benthamiana* and the transformed leaf tissue was treated with elf18. PIE-FLAG was immunoprecipitated with ANTI-FLAG M2 Affinity Gel and incubated with calf alkaline intestinal phosphatase (CIP). This treatment reverted PIE mobility shift, and the reversion was blocked by co-treatment with a cocktail of the phosphatase inhibitors NaF, EDTA and $NaVO_3$ (Sodium metavanadate) (Figure 5.14 A). Together these results indicate that the observed band shift results from phosphorylation and therefore, that PIE is phosphorylated upon PAMP perception.

The database PhospAt predicts that PIE contains six potential phosphorylation sites: two serines, three threonines and one tyrosine phosphorylation site. In order to determine on which amino acids PIE is phosphorylated, protein extracts were analysed in immunoblots with α-Phospho-Threonine, α-Phospho-Serine and α-Phospho-Tyrosine antibodies. However, under the here used conditions, in all three blots no signal corresponding to PIE-FLAG was detected (Figure 5.14 B). Thus, it still remains unclear on which amino acids PIE is phosphorylated.

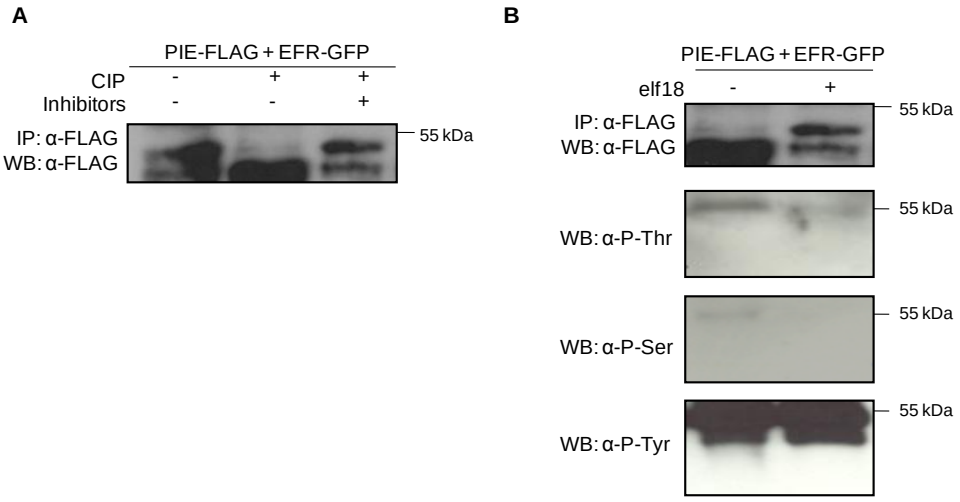

Figure 5.14: PIE is phosphorylated upon PAMP-perception
(A) Elf18-induced PIE mobility shift is restored by treatment with calf intestinal phosphatase (CIP). *N. benthamiana* leaves expressing PIE-FLAG and EFR-GFP were treated with 100 nM elf18 for 20 minutes. Total proteins were subjected to immunoprecipitation with ANTI-FLAG M2 Affinity Gel. Beads were washed three times and PIE-FLAG conjugated to the beads was treated or not with calf alkaline intestinal phosphatase and with or without phosphatase inhibitors (NaF, EDTA, $NaVO_3$). Proteins were eluted with 2×sample buffer and analysed by SDS-PAGE and immunoblotting with α-FLAG antibodies.
(B) No specific phosphorylation was detected with α-phospho-antibodies. *N. benthamiana* leaves expressing PIE-FLAG and EFR-GFP were treated with 100 nM elf18 for 20 minutes. Total proteins were subjected to immunoprecipitation with ANTI-FLAG M2 Affinity Gel. Proteins were eluted with 2× sample buffer and analysed by SDS-PAGE and immunoblotting with α-FLAG, α-Phospho-Threonine, α-Phospho-Serine and α-Phospho-Tyrosine antibodies.

5.2.4.3 Phosphorylation potentially increases PIE enzymatic activity

Next, we examined whether PIE phosphatase activity is altered upon PAMP-induced phosphorylation. Therefore, the Michaelis constant (Km), which indicates the substrate affinity of an enzyme, was calculated to compare PIE enzymatic activity prior and after PAMP perception. To this end, PIE-FLAG was transiently expressed in *N. benthamiana* and infiltrated tissues were treated with water or 100 nM flg22. PIE-FLAG was co-immunoprecipitated as described in section 5.3.1.3. and competitively eluted with FLAG peptides. Phosphatase activity of PIE was determined by measuring the phosphate release from a phosphorylated synthetic peptide as described in section 5.3.1.3. The time-dependent phosphate release was measured with increasing substrate concentrations. The reaction rates and substrate concentrations were fitted in a Michaelis-Menten plot by non-linear regression (Figure 5.15 A) and the Michaelis constant was calculated using the Prism 5.01 Software (GraphPad Software, La Jolla California USA)

(Figure 5.15 B). In three biological repeats a lower Km was measured with PIE immunoprecipitated from samples treated with flg22 compared to control samples treated with water (Figure 5.15 B). This indicates that upon PAMP perception PIE substrate affinity, and thus potentially also the catalytic activity, is increased. However, although this result was highly reproducible, the difference was not always significant.

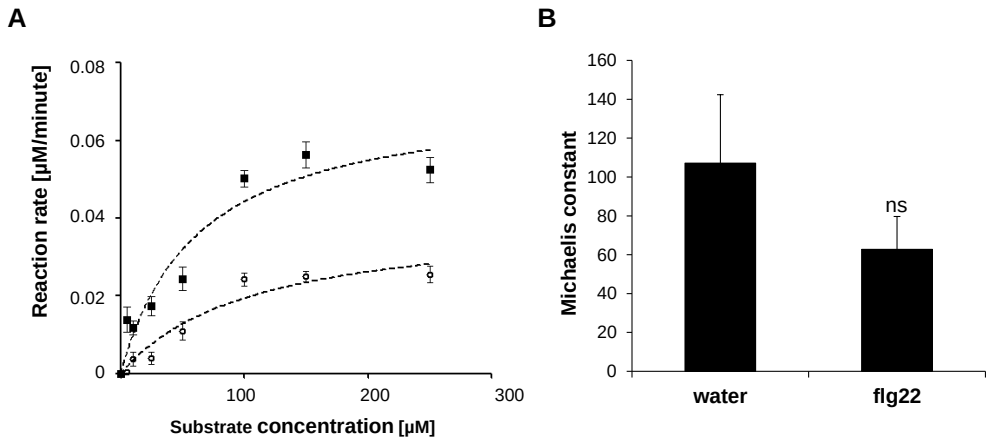

Figure 5.15: PIE substrate affinity is increased upon PAMP perception
PIE-FLAG was transiently expressed in *Nicotiana benthamiana* under the control of the 35S promoter and infiltrated tissues were treated with water (o) or 100 nM flg22 (■) for 20 minutes. PIE-FLAG was purified with FLAG M2 Affinity Gel and competitively eluted with FLAG peptides. Phosphatase activity was determined using different concentrations of a phosphorylated synthetic peptide. (A) The time-dependent phosphatase release (reaction rate) was plotted against the substrate concentrations. (B) Calculation of the Michaelis constant was performed with the Graphpad Prism software. Results are average ± standard error with n=3. This experiment was three times repeated with similar results. ns indicates that values were not significantly different from that of the control.

5.2.5 PIE might act as a negative regulator of PAMP-triggered signalling

5.2.5.1 General characterisation of *PIE* loss-of-function and overexpression lines

To explore the contribution of PIE to PTI signalling, *PIE* overexpression and loss-of-function lines were characterised. To generate stable transgenic *PIE* overexpression lines, *Arabidopsis thaliana* was transformed with a *35S::PIE-eGFP* construct. Homozygous T3 plants were selected and *PIE* overexpression was confirmed by qRT-PCR with gene-specific primers (Figure 5.16A). In addition, PIE-eGFP accumulation was quantified in α-GFP immunoblots. Since PIE-eGFP was only weakly detectable in protein crude

extracts, the protein level was additionally quantified after specific enrichment by α-GFP IP (Figure 5.16 B). Only one out of the three tested lines displayed a significantly increased PIE level, while in the two other tested lines *PIE* was only weakly overexpressed (Figure 5.16). To examine the effect of *PIE* overexpression in a dose-dependent manner, I selected the strong overexpression line *35S::PIE-eGFP#2* and the weak overexpression line *35S::PIE-eGFP#4* for further characterisations.

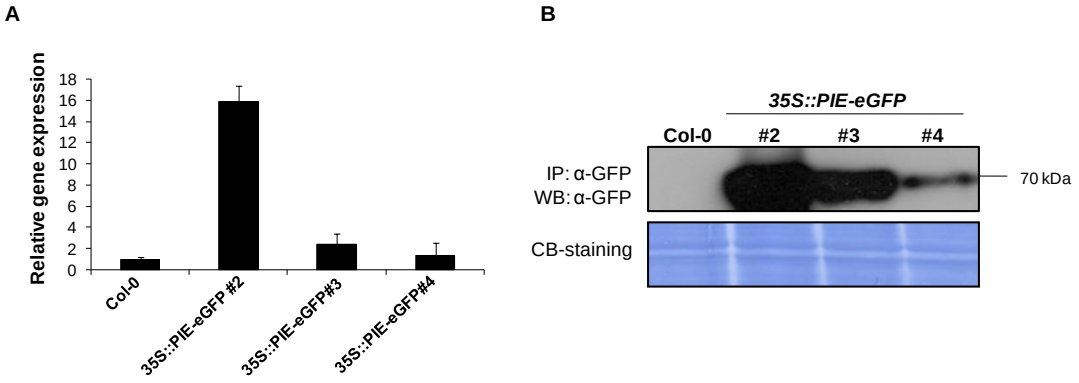

Figure 5.16: *PIE* expression and PIE-GFP protein level in different *PIE* overexpression lines
(A) *PIE* expression level was determined by qRT-PCR with gene-specific primers. cDNA was generated from 14-day old seedlings. Expression values were normalized to the expression of the housekeeping gene At4g15400 and plotted relative to the expression of Col-0. (B) PIE-GFP was purified from 14-day old seedlings and purified with GFP-Trap beads. Proteins were analysed by SDS-PAGE and immunoblotting with an α-GFP antibody.

In addition, I obtained different *PIE* T-DNA insertion lines from NASC and *PIE* expression was determined in homozygous lines by quantitative and semi-quantitative RT-PCR. In all three tested lines, the T-DNA insertion did not completely abolish *PIE* expression (Figure 5.17 A-C). However, in *pie-1* and *pie-2* reduced *PIE* expression could be detected (Figure 5.17 C), and both lines were selected for further characterisation.

The selected *35S::PIE* and *pie* lines were grown under short-day and long-day conditions. Notably, under both growth conditions all lines appeared phenotypically similar to wild-type (Col-0) plants (Figure 5.18). This indicates that PIE action is likely to be linked to specific environmental conditions.

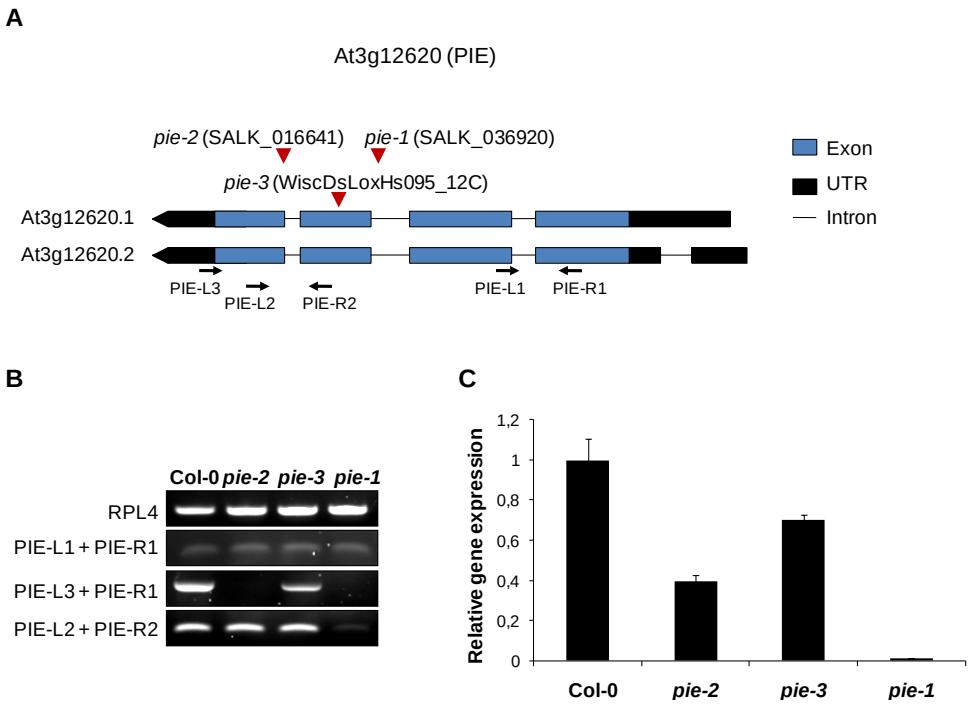

Figure 5.17: *PIE* expression level in different T-DNA insertion lines
(A) *pie-1* and *pie-2* carry a T-DNA insertion in an exon of *PIE* while *pie-3* carries a T-DNA insertion in an intron. (B) *PIE* expression was determined by semi-quantitative RT-PCR using gene-specific primers (as indicated in A). RPL4 primers were used to quantify the overall cDNA concentration in each sample. (C) *PIE* expression level was determined by qRT-PCR using the gene-specific primers PIE-L2 and PIE-R2. Expression values were normalized to the expression of the housekeeping gene At4g15400 and plotted relative to the expression of Col-0.

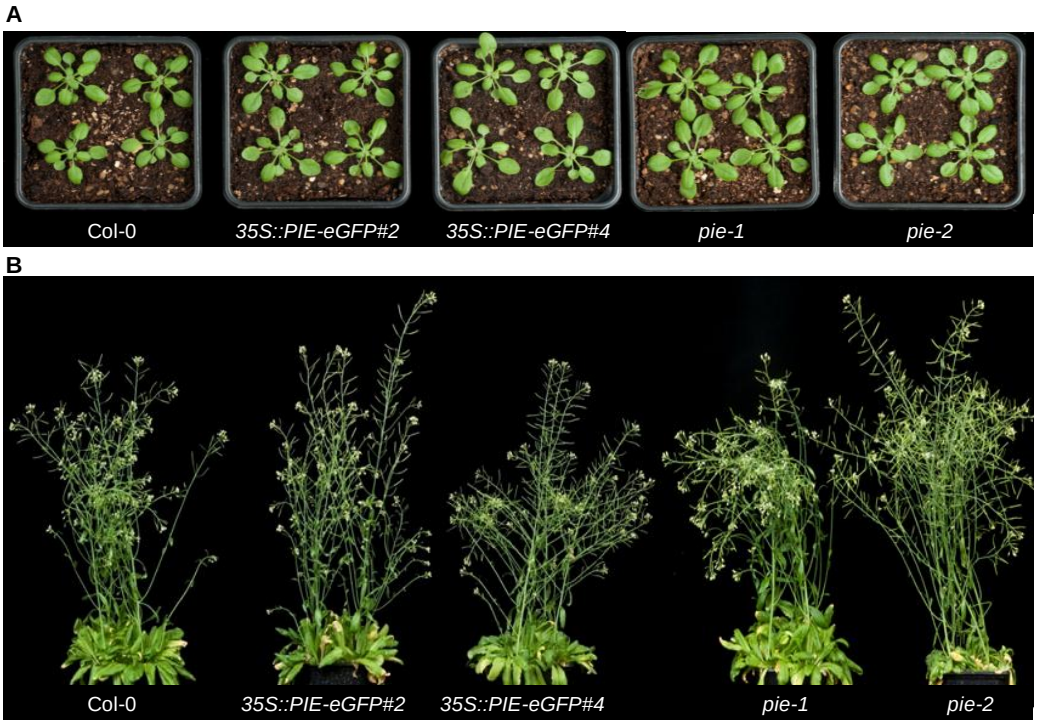

Figure 5.18: *PIE* overexpression and *pie* T-DNA insertion lines do not display an altered developmental phenotype
Col-0, *35S::PIE-eGFP#2*, *35S::PIE-eGFP#4*, *pie-1* and *pie-2* plants were for 4 weeks grown under short-day conditions (A) followed by 3 weeks under long-day conditions (B).

5.5.2.1. Altered *PIE* expression affects PAMP-triggered ROS burst and seedling growth inhibition

To test whether PIE regulates PAMP-triggered responses, I determined elf18- and flg22-induced ROS production in different *PIE* lines. In order to obtain some preliminary results while the stable transgenic *Arabidopsis* lines were generated, the effect of *PIE* overexpression was first examined in *N. benthamiana* by transient overexpression. As *Arabidopsis,* the *N. benthamiana* genome encodes a functional FLS2 receptor, but in contrast lacks an EF-Tu perception system (Kunze et al., 2004; Zipfel et al., 2006; Hann and Rathjen, 2007). However, it has been shown that transient expression of *AtEFR* confers elf18-responsiveness, indicating that downstream signalling components are conserved between *Arabidopsis* and *Nicotiana* (Zipfel et al., 2006). For the ROS assay with flg22, PIE-FLAG or eGFP, which was used as a negative control, were expressed in *N. benthamiana*, while for the assay with elf18, EFR-GFP was co-expressed with either eGFP or PIE-FLAG. Interestingly, expression of PIE led in both assays to a significantly reduced PAMP sensitivity (Figure 5.19). This result indicates that PIE negatively regulates elf18- and flg22-triggered ROS production.

To further validate this result, ROS production was determined in two independent *Arabidopsis 35S::PIE* transgenic lines. In both tested lines elf18- and flg22-triggered ROS production was significantly decreased (Figure 5.20). Notably, the reduction correlated with the *PIE* expression level, and thus, the strongest effect was detected in *35S:PIE-eGFP#2* (Figure 5.20), which displayed the higher *PIE* expression (Figure 5.16 A). This indicates that PIE regulates the ROS production in a dose-dependent manner. Surprisingly, the PAMP-induced ROS production was also reduced in *pie* loss-of-function lines. However, the observed differences were not significant (Figure 5.21).

Consistent with the reduced PAMP sensitivity observed in the ROS assay, *35S::PIE* displayed reduced seedling growth inhibition with different concentrations of flg22 and elf18 (Figure 5.22 A and B). Again, the strength

of the effect was correlating with the *PIE* expression level. In contrast, *pie* mutants displayed wild-type responses in this assay (Figure 5.22 C and D).

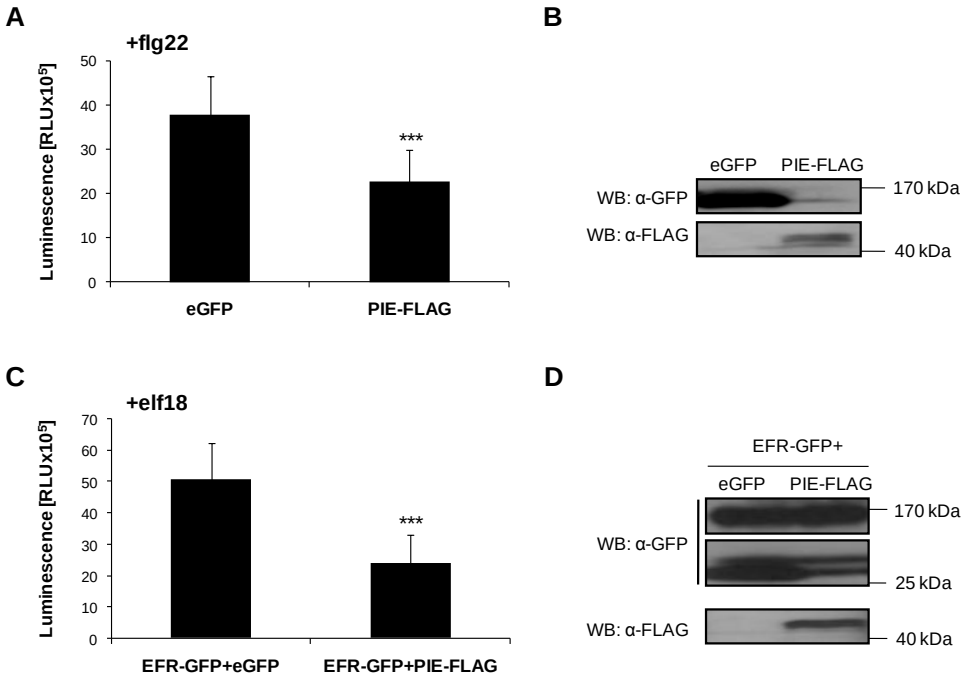

Figure 5.19: Transient overexpression of *PIE* in *Nicotiana benthamiana* reduces elf18- and flg22-triggered ROS production
(A) Time-dependent ROS production represented as relative light units (RLU) in *Nicotiana benthamiana* transiently expressing PIE-FLAG or eGFP after elicitation with 100 nM flg22. (B) Time-dependent ROS production represented as relative light units (RLU) in *Nicotiana benthamiana* transiently expressing PIE-FLAG and EFR-GFP or eGFP and EFR-GFP after elicitation with 100 nM elf18. Results are shown as sum ± standard error with n=8. Asterisks indicate significant differences compared to wild-type values at P< 0.001 (***). (C and D) To confirm that eGFP, PIE-FLAG and EFR-GFP were equally expressed, proteins were extracted from the ROS samples and analysed in immunoblots with tag-specific antibodies. These experiments were three times repeated with similar results.

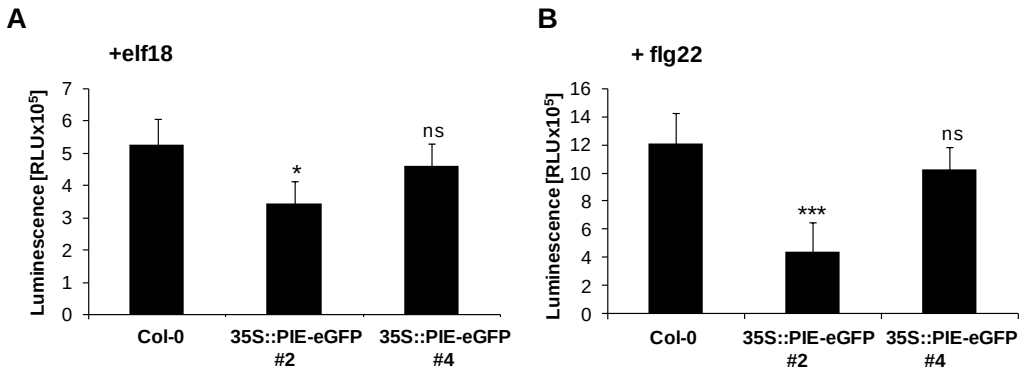

Figure 5.20: *PIE* overexpression in *Arabidopsis thaliana* reduced elf18- and flg22-triggered ROS production
Total ROS production represented as relative light units (RLU) in Col-0, *35S::PIE-eGFP#2* and *35S::PIE-eGFP#4* after elicitation with 10 nM elf18 (A) or 10 nM flg22 (B). Results are shown as sum ± standard error with n=8. All experiments were performed three times with similar results. Asterisks indicate significant differences compared to wild-type values at P< 0.05 (*) or P>0.001 (***), not significant differences are indicated with ns. These experiments were three times repeated with similar results.

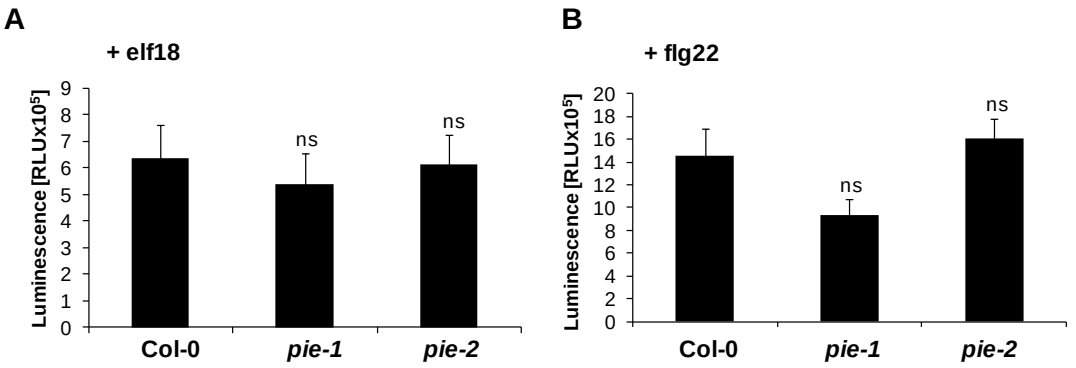

Figure 5.21: *pie* lines display wild-type flg22- and elf18-triggered ROS production.
Total ROS production represented as relative light units (RLU) in Col-0, *pie-1* and *pie-2* after elicitation with 100 nM elf18 (A) or 10 nM flg22 (B). Results are shown as sum ± standard error with n=8. ns indicates non significant differences compared to wild-type. These experiments were three times repeated with similar results.

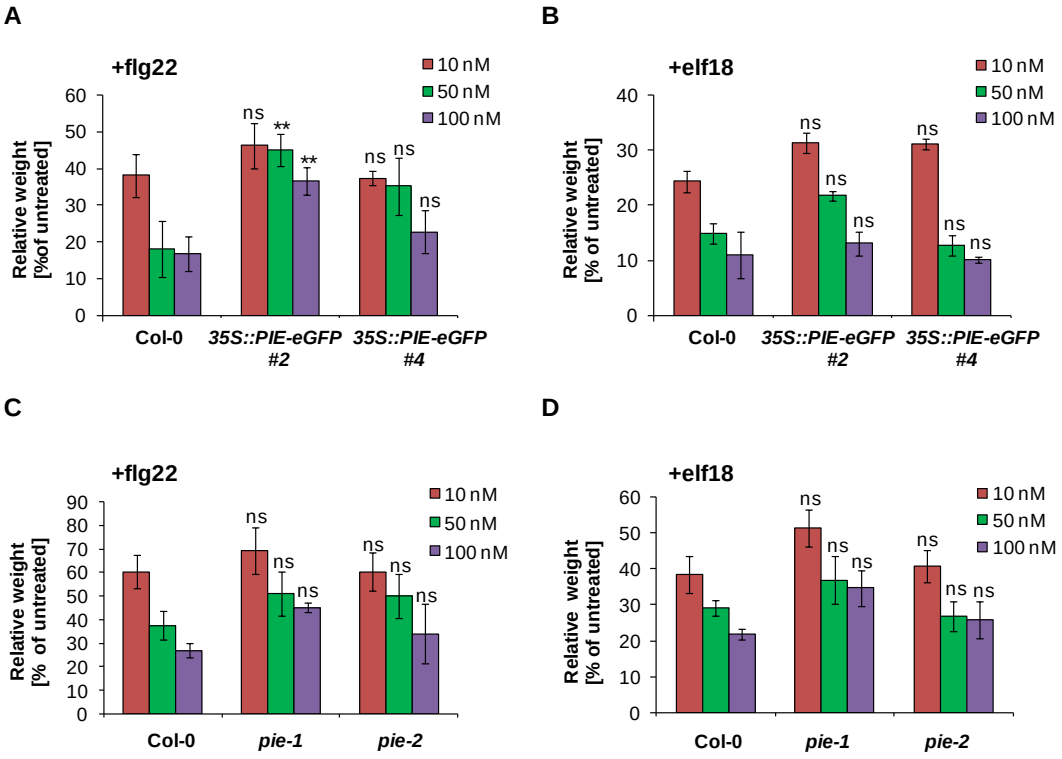

Figure 5.22: *PIE* over expression lines display reduced sensitivity to flg22 and elf18 in seedling growth inhibition
Seedling growth inhibition in response to increasing concentrations of flg22 and elf18 in Col-0, *35S::PIE-eGFP#2* and *35S::PIE-eGFP#4* (A and B) or *pie-1* and *pie-2* (C and D). Results are represented as seedling fresh weight (A and C) and percentage relative to untreated seedlings (B and D). Results are average ± standard error with n=6. All experiments were performed three times with similar results. Asterisks indicate significant differences compared to wild-type values at P<0.01 (**), not significant differences are indicated with ns. These experiments were two times repeated with similar results.

5.2.5.2 Reduced *PIE* expression enhances susceptibility to bacterial pathogens

Next, I tested the contribution of PIE to disease resistance. To this end, *35S::PIE* lines were spray-inoculated with the virulent bacterium *P. syringae* pv. *tomato* (*Pto*) DC3000. In addition, plants were inoculated with the weakly virulent strain *Pto* DC3000 COR$^-$, which lacks the phytotoxin coronatine. The bacterial growth was assessed three days after inoculation. To confirm the success of the bacterial infection, the *efr fls2* double mutant was included in all assays. As previously reported, this mutant displayed increased susceptibility to all tested bacterial strains (Figure 5.23) (Nekrasov et al., 2009). However, no altered bacterial growth could be observed in the tested *35S::PIE* lines (Figure 5.23). Thus, although I confirmed that *PIE* overexpression affects several outputs of PAMP-triggered signalling, I could not detect an altered bacterial resistance in *35S::PIE* lines.

Next, I determined bacterial susceptibility in *pie* mutants. Both mutants displayed no altered susceptibility to *Pto* DC3000 (Figure 5.24 A). However, an increased bacterial titer was detected in *pie-1* after inoculation with *Pto* DC3000 COR$^-$, and the plants were as hyper-susceptible as *efr fls2* (Figure 5.24 A).

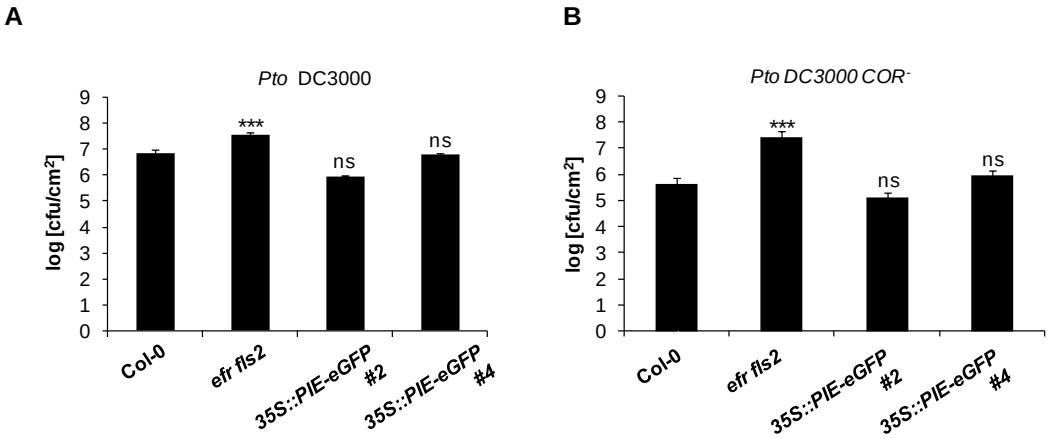

Figure 5.23: *PIE* overexpression mutants do not display altered susceptibility to *P. syringae* pv. *tomato* (*Pto*) DC3000

(A) Four-week old plants (Col-0, *efr fls2, 35S::PIE-eGFP#2 and 35S::PIE-eGFP#4*) were spray-inoculated with *Pseudomonas syringae* pv. *tomato* (*Pto*) DC3000 (OD_{600}= 0.02). (B) Four-week old plants (Col-0, *efr fls2, 35S::PIE-eGFP#2 and 35S::PIE-eGFP#4*) were spray-inoculated with *Pto* DC3000 COR$^-$ (OD_{600}= 0.2). Bacterial growth was determined three days after infection and plotted as colony forming units per cm^2 leaf disc. Results are average ± standard error with n=4. Asterisks indicate significant differences compared to wild-type values at P>0.001 (***), not significant differences are indicated with ns. These experiments were three times repeated with similar results.

.

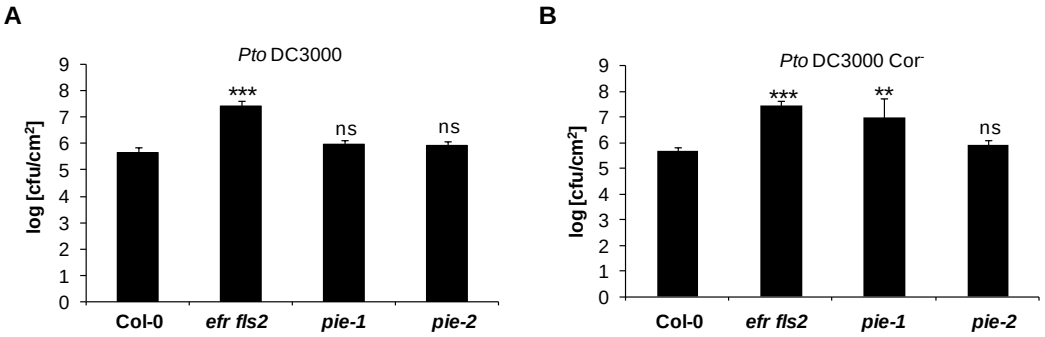

Figure 5.24: *pie-1* displays enhanced susceptibility to *P. syringae* pv. *tomato* (*Pto*) DC3000 COR⁻ but not to *Pto* DC3000
(A) Four-week old plants (Col-0, *efr fls2, pie-1 and pie-2*) were spray-inoculated with *Pseudomonas syringae* pv. *tomato* (*Pto*) DC3000 (OD_{600}= 0.02). (B) Four-week old plants (Col-0, *efr fls2, pie-1 and pie-2*) were spray-inoculated with *Pto* DC3000 COR⁻ (OD_{600}= 0.2). Bacterial growth was determined three days after infection and plotted as colony forming units per cm^2 leaf disc. Results are average ± standard error with n=4. Asterisks indicate significant differences compared to wild-type values at P< 0.01 (**) or P>0.001 (***), not significant differences are indicated with ns. These experiments were three times repeated with similar results.

5.3 Summary and discussion

5.3.1 Characterisation of a novel PP2C type phosphatase

PIE expression is up-regulated after treatment with various PAMPs, indicating a potential role in PAMP-triggered signalling. To assess the function of this protein, the amino acid sequence was analysed using publicly available prediction databases.

According to the database Pfam 26.0 (http://pfam.sanger.ac.uk), PIE contains a predicted PP2C domain. To determine whether PIE exhibits phosphatase activity, I expressed recombinant fusion proteins *in planta* and in *E. coli*. Both PIE-GST, expressed in *E. coli*, and PIE-FLAG, expressed *in planta*, catalysed phosphate release from a phosphorylated synthetic peptide. The phosphatase activity is Mg^{2+}-dependent and was reduced in presence of the serine/threonine phosphatase inhibitor NaF and the PP2C-specific inhibitor EDTA. Together, these results confirm that *PIE* encodes an active PP2C.

I showed that upon transient expression in *N. benthamiana* PIE-eGFP localises to the plasma membrane (Figure 4.12). This localisation was not

affected by PAMP perception, and thus appears to be constitutive. Yet, it remains unclear how PIE is targeted to the cell periphery. A significant number of proteins are covalently attached to the membrane via post-translational modification like palmitoylation, myristoylation or glycosylphosphatidyl-inositol (GPI)-anchor (Sherrier et al., 1999; Peter et al., 2004; Tsugama et al., 2012).

PIE is not predicted to contain a myristoylation site or to carry a (GPI)-anchor as determined using the databases Myristoylator and PredGPI (http://gpcr.biocomp.unibo.it/predgpi; http://web.expasy.org/myristoylator) (Bologna et al., 2004; Pierleoni et al., 2008). However, the database CSS-Palm 3.0 (Zhou et al., 2006) predicts that PIE carries a potential palmitoylation site at cysteine 154 and covalent attachment of fatty acids on this amino acid could mediate the localisation of PIE at the plasma membrane. This hypothesis could be tested by examining the localisation of PIE^{C154A}.

PIE also contains a potential transmembrane domain that could attach the protein to the membrane. Nevertheless, a signal peptide that could target PIE to the plasma membrane was not identified. Furthermore, the predicted transmembrane domain is enclosed in the PP2C domain and thus, if the domain would be inserted in the membrane, the enzymatic activity would be affected. Since PIE associates with EFR, a plasma membrane localised protein, this interaction could also be responsible for the localisation of PIE at the cell periphery. In summary, these observations suggest that the predicted transmembrane domain is not responsible for PIE localisation, but rather a post-translational modifications or the interaction with transmembrane proteins.

Depending on their attachment properties, membrane-associated proteins can be differentially solubilised. Proteins that are integrated in the membrane can only be extracted with detergents, while peripheral proteins dissociate following treatment with polar reagents, including solutions with an elevated pH or high salt concentrations. Thus, further biochemical characterisation could shed light on the specific attachment mechanism that localises PIE to the membrane.

5.3.2 PIE associates with PTI-signalling components *in planta*

Using Co-IP experiments I showed that PIE associates with EFR and FLS2 upon transient overexpression *in planta.* Notably, the association was decreased upon PAMP perception, indication that PIE was dissociating from the receptor complexes. Association with EFR and FLS2, as well as PAMP-triggered dissociation, were independent of the kinase activities of the receptors. However, it is unclear which mechanisms induce this dissociation. In the current model, upon ligand binding the LRR domain of EFR and FLS2 undergo a conformation change allowing the receptors to heteromerise with BAK1 (Boller and Felix, 2009). This association then triggers specific phosphorylation events that induce downstream signalling (Schulze et al., 2010). Since any of these events could trigger PIE dissociation, further investigation must be undertaken to explain this observation. First, to test whether the heteromerization with BAK1 affects the PIE-EFR and PIE-FLS2 association, the interactions could be assessed in *bak1* knock-out mutants or BAK1/SERK3 silenced *N. benthamiana* plants. To rule out that phosphorylation events have an impact on the dissociation, pre-treating plant tissue with kinase inhibitors prior the Co-IP could give further indications.

Notably, I detected an interaction between PIE and the BR-receptor BRI1 *in planta* and *in vitro*. But, in contrast to the association of PIE with EFR and FLS2, the BRI1-PIE association was not decreased after ligand perception. Thus, it is questionable whether this association is of biological relevance or caused by non-specific binding.

I confirmed that PIE also associates with BIK1 *in planta*. Notably, BIK1 had been previously shown to associate with EFR and FLS2 (Lu et al., 2010b; Zhang et al., 2010). Thus, it is possible that the association between PIE and BIK1 is mediated through the receptors. However, since I could not detect a direct interaction between PIE and EFR, FLS2 or BIK1 by *in vitro* pull down, this hypothesis could so far not be confirmed. Alternatively, to test whether EFR and FLS2 mediate the PIE-BIK1 association, the interaction could also be examined in the *efr fls2* background.

Notably, I could not detect and association between PIE and BAK1. Although this indicates that both proteins might not associate *in planta*, it was recently

shown that C-terminally tagged version of BAK1 are not fully functional (Ntoukakis et al., 2011). Therefore, to confirm this initial result, it should also be assessed whether PIE associates with un-tagged BAK1.

In summary, I have shown that PIE associates with EFR, FLS2 and BIK1 *in planta*. However, further investigations are needed to identify the mechanisms that regulate these interactions. Moreover, since these interactions were observed upon transient protein overexpression in *N. benthamiana*, I am also currently aiming to confirm them in stable transgenic *Arabidopsis thaliana* lines expressing PIE-FLAG.

5.3.3 PIE dephosphorylates PTI signalling components *in vitro*

Although, I could not detect an association of PIE and EFR, FLS2 or BIK1 *in vitro*, we showed that EFR, FLS2 and BIK1 are dephosphorylated by PIE *in vitro*. Therefore, I concluded that the for the *in vitro* pull downs used conditions might not be suitable to conserve and or detect the protein-protein interactions.

Since for the dephosphorylation assay the proteins were expressed in *E. coli* and autophosphorylated *in vitro*, EFR, FLS2 and BIK1 may be differentially phosphorylated than proteins, which were expressed and auto- and transphosphorylated *in planta*. Therefore, in order to further validate these observations, the phosphorylation status of EFR, FLS2 and BIK1 will be tested in *Arabidopsis* wild-type plants and transgenic *PIE* overexpression lines. To this end, the proteins will be extracted and their kinase activity, which is correlated with their phospo-status, will be determined in *in vitro* kinase assays.

Notably, it was shown that different potential phosphorylation sites of several PRRs can regulate distinct processes. For instance, $FLS2^{T867V}$, $FLS2^{T1040A}$, $FLS2^{T1072A}$ and $FLS2^{S878A}$ are not affected in their flg22-binding capacity, but display altered PAMP-triggered responses (Robatzek et al., 2006). Furthermore, flg22-mediated endocytosis of $FLS2^{T867V}$ is strongly reduced (Robatzek et al., 2006). Therefore, in order to determine the effect of PIE-

mediated dephosphorylation on FLS2, EFR and BIK1, it would be of high interest to identify the specific phosphorylation sites, which are targeted by PIE. Site-directed mutagenesis of these sites could then give further indications about their biological function.

Note: This part of the project will be continued by Dr Alberto Macho and Daniel Couto, The Sainsbury Laboratory.

5.3.4 PIE is phosphorylated upon PAMP perception

PIE carries six predicted phosphorylation sites and I confirmed that the protein is phosphorylated upon elf18 and flg22 perception. Kinase activities of EFR and FLS2 were partially required for PIE phosphorylation. This indicates that both receptors might directly phosphorylate PIE. However, EFR and FLS2 have been shown to regulate BIK1 and BAK1 activity through phosphorylation and thus, their kinase activity might only indirectly affect PIE phospho-status. Considering that PIE associates with EFR, FLS2 and BIK1 *in planta,* all three proteins could potentially phosphorylate PIE. This hypothesis is currently tested using *in vitro* kinase assays. In addition, the importance of BIK1 and BAK1 for PIE phosphorylation will also be investigated *in planta.* Therefore, PIE phosphorylation-status will be analysed in *Arabidopsis* wild-type and *bak1-5* or *bik1 pbl1* background. However, since no clear results could be obtained using the mobility shift assays in *Arabidopsis*, mass spectrometry will be used as an alternative technique to detect PIE phosphorylation. This could additionally lead to the identification of specific phosphorylation sites. In addition, a site-directed mutagenesis approach is currently used to identify potential PIE phosphorylation sites (Daniel Couto, The Sainsbury Laboratory).

Furthermore, the molecular function of PIE phosphorylation is yet to be determined. It was demonstrated that phosphorylation can affect the interaction properties of a protein, alter its localization or affect its enzymatic activity. Consequently, I speculated that PIE phosphorylation might regulate the conformation of the protein to induce its dissociation from the receptor complex. However, while PIE phosphorylation partially requires kinase active EFR and FLS2, PIE dissociation from the receptor complex was independent

of the kinase activity of both PRRs. Alternatively, this modification could affect the subcellular localization of PIE. For instance, it was shown that BKI1 (BRI1 KINASE INHIBITOR 1), which associate with BRI1 to block receptor activation in absence of ligand, is phosphorylated upon brassinosteroid perception (Wang and Chory, 2006). Consequently, BKI1 dissociates from the plasma membrane and thereby relieves BRI1 inhibition (Wang and Chory, 2006). But since the localization of PIE was not altered upon PAMP treatment, this hypothesis could so far not be confirmed. Notably, initial results imply that PIE phosphatase activity is increased upon phosphorylation. To confirm this observation the phosphatase activity of the by site-directed mutagenesis generated phospho-mutants is currently tested *in vitro*. Considering that PIE dissociates from the receptor complex, this observation might indicate that PIE may have further targets in addition to EFR, FLS2 in BIK1. Here, a screen for novel PIE interactors might lead to the identification of potential downstream targets.

Note: This part of the project will be continued by Daniel Couto, a PhD student in the group.

5.3.5 PIE might act as a negative regulator of PAMP-triggered signalling

In order to test whether PIE affects PAMP-triggered responses, I characterised *PIE* overexpression and loss-of-function lines. Notably, I showed that *PIE* overexpression significantly reduced elf18- and flg22-triggered ROS production in both *Nicotiana benthamiana* and *Arabidopsis*. Furthermore, *Arabidopsis 35S::PIE* lines also displayed reduced PAMP sensitivity in seedling growth inhibition. Surprisingly, reduced responses were also detected in *pie* lines. Altogether, these results might suggest that *PIE* must be maintained at an optimal expression level to allow proper activation of signalling. Thus, in overexpression lines PIE might block receptor activation through increased dephosphorylation of EFR, FLS2 and BIK1. In contrast, in *pie* loss-of-function lines signalling might be constantly switched on, leading to a depletion of the system. Alternatively, the induction threshold might be increased in these mutants. Consequently, in *pie* mutants

the proper activation of PAMP-triggered responses would be impaired. In summary, these results indicate that an optimal level of PIE is required for proper PTI signalling. A similar effect has been recently reported for *ERF104 (ETHYLENE RESPONSE FACTOR 104)* mutants (Bethke et al., 2009), where both *erf104* loss-of-function and *ERF104* overexpression lines showed reduced immunity against *B. cinerea* and *P. syringae* pv. *phaseolicola* (Bethke et al., 2009). Furthermore, both lines displayed enhanced flg22-triggered seedling growth inhibition (Bethke et al., 2009). To further confirm that altered *PIE* expression levels reduce PAMP-triggered responses, it is currently determined whether MAPK activation and PAMP-induced gene expression are also affected in the different mutants (Daniel Couto, The Sainsbury Laboratory).

I also tested the contribution of PIE to disease resistance. Notably, *35S::PIE* transgenic lines did not display altered susceptibility to different *Pto* DC3000 strains. In order to test whether bacterial resistance could be affected by altered accumulation of the defence related hormone SA, it is currently being tested whether *35S::PIE* transgenic lines display elevated levels of this hormone (Daniel Couto, The Sainsbury Laboratory). Similarly, it was shown that *bik1* displays reduced PAMP-triggered responses but an increased resistance to *Pto* DC3000 (Veronese et al., 2006; Lu et al., 2010b; Zhang et al., 2010). Here, further investigation revealed that the altered resistance is likely caused by elevated SA levels (Veronese et al., 2006).

I showed that *pie-1* displays increased susceptibility to *Pto* DC3000 COR$^-$ but not to wild type *Pto* DC3000. The phytotoxin coronatine (COR) has been shown to suppress PAMP-induced stomatal closure (Melotto et al., 2006). Upon infection with *Pto* DC3000 COR$^-$, perception of bacterial PAMPs triggers stomatal closure and blocks bacterial entry in the leaf apoplast. Therefore, the reduced bacterial resistance of *pie-1* might be a consequence of the decreased PAMP-sensitivity of this mutant. Notably, *pie-2* did not display an altered susceptibility to *Pto* DC3000 COR$^-$. Since *PIE* expression is less affected in this mutant than in *pie-1*, this observation further indicates that the altered resistance in *pie-1* might be caused by a decreased *PIE* expression level. Preliminary results indicate that *pie-1* also displays increased susceptibility to *Pto* DC3000 *ΔAvrPto/ΔAvrPtoB*, which lacks the

type III-secreted effectors AvrPto and AvrPtoB, and we currently aim to confirm this result. AvrPtoB has been reported to associate with FLS2 to induce receptor degradation, while AvrPto was implied to inhibit the kinase activities of FLS2 and EFR (Göhre et al., 2008; Xiang et al., 2008; Xiang et al., 2010). Thus, the observed reduced resistance to the *Pto* strain lacking both effectors might again be correlated with the altered PAMP-triggered responses. In summary, these results indicate that an optimal *PIE* expression is required for proper PAMP-triggered signalling. However, further investigations must be undertaken to confirm these initial observations.

A potential model, which illustrating how PIE regulates PTI signalling is shown in Figure 5.25.

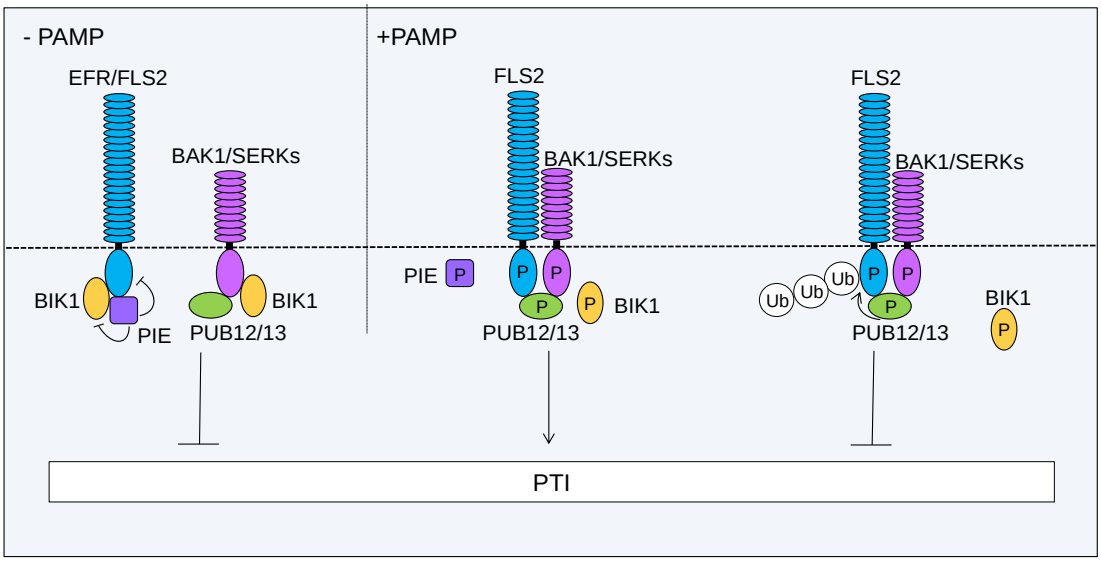

Figure 5.25: PIE negatively regulates the two PRRs FLS2 and EFR in absence of ligand
PIE associates with EFR, FLS2 and BIK1 in absence of ligand and blocks constitutive receptor activation by keeping EFR, FLS2 and BIK1 in the dephosphorylated state. Upon PAMP perception, PIE is phosphorylated and dissociates from the receptor complex. EFR and FLS2 associate with BAK1 and subsequently, auto- and transphosphorylation events trigger the formation of active receptor complexes and induce downstream signalling.
FLS2 signalling is in turn attenuated by PUB12 and PUB13 which catalyse FLS2 ubiquitination and thereby promote its degradation. Phosphorylated proteins are indicated with a P, poly-ubiquitinated proteins are indicated with Ub.

Chapter 6: General conclusions and final remarks

Microbes, plants and animals have one thing in common: they are able to perceive and respond to internal and environmental changes. Signal transduction pathways play a crucial role in initiating these responses. The disruption of signalling pathways can have severe consequences and was shown to cause a variety of human diseases including cancer and cardiac diseases (Vogelstein and Kinzler, 2004; Eroles et al., 2012; Ling and Kumar, 2012; Portbury et al., 2012).

As for animals, signal transduction pathways also play an important role in plant immunity. For instance, in *Arabidopsis* the two PRRs EFR and FLS2 perceive the bacterial PAMPs EF-Tu and flagellin, respectively, and induce a variety of defence responses that ultimately lead to PAMP-triggered immunity (Boller and Felix, 2009). However, only few components of both signalling pathways have been described so far.

In order to identify novel signalling components of EFR- and FLS2-dependent signalling, I used two very different approaches. First, I characterised a predicted flg22-dependent gene expression network that was generated using publicly available microarray data. Candidates of this network are predicted to regulate each other's expression in a flg22-dependent manner and thus, are potentially involved in the FLS2 signalling pathway. Notably, one of the seven predicted main regulators of this network, the DELLA transcription factor GAI, has already been reported to regulate flg22-triggered signalling (Achard et al., 2008; Navarro et al., 2008). This nicely supports the validity of this approach. Furthermore, I showed that mutation of at least two other candidate genes was affecting PTI signalling. Thus, I could demonstrate that the characterisation of the main regulators of the predicted flg22-dependent gene expression network presents a promising approach to identify novel components of the FLS2 signalling pathway. However, further investigation must be undertaken to decipher the underlying mechanism, by which these candidates regulate flg22-triggered responses.

Notably, the three candidates, which displayed altered PTI responses, were previously shown to regulate developmental processes. As they were not clearly linked to PTI, I might not have selected them for characterisation if

they would have been identified in a protein-protein interaction screen. This illustrates the difficulty when it comes to selecting promising candidate for further characterisations.

I therefore used a more targeted approach to study how signalling is regulated at the receptor level. Several PRRs require the association with co-regulators for initiation of downstream signalling. For instance, EFR and FLS2 signalling is positively regulated by the SERKs BAK1 and BKK1, as well as BIK1 (Chinchilla et al., 2007; Lu et al., 2010b; Zhang et al., 2010; Roux et al., 2011; Schwessinger et al., 2011). In contrast, negative regulation of receptors blocks constitutive signalling in the absence of ligand or attenuates activated signalling pathways. A well described example is the Ax21 receptor XA21, which associates with the ATPase XB24 in absence of its ligand (Chen et al., 2010b). XB24 promotes phosphorylation of XA21 on specific serine and threonine residues and thereby keeps the PRR in an inactive state (Chen et al., 2010b). Upon Ax21 perception, XB24 dissociates from the XA21 complex to facilitate receptor activation and induction of downstream responses (Chen et al., 2010b). In contrast, Ax21-induced signalling is attenuated by the PP2C XB15 (Park et al., 2008). XB15 associates with XA21 upon ligand perception to promote its dephosphorylation and consequently inactivation (Park et al., 2008). Similarly, the PP2C KAPP was shown to associate with several RLKs, including FLS2, and is thought to attenuate downstream signalling through RLK dephosphorylation (Braun et al., 1997; Williams et al., 1997; Gómez-Gómez et al., 2001; Shah et al., 2002). In addition, the two closely related E3 ubiquitin ligases PUB12 and PUB13 associate with FLS2 upon flg22 perception to promote its ubiquitination and thereby degradation (Lu et al., 2011). Consequently, PUB12 and PUB13 effectively attenuate the FLS2 signalling pathway (Lu et al., 2011).

However, while mechanism that deactivate FLS2-dependent signalling upon flg22 perception have been described, signalling components that block constitutive activation of FLS2 and EFR in absence of their ligand are still unknown. Therefore, in order to understand how signal transduction is regulated at the receptor level, I characterised novel EFR-interacting

proteins, which were identified in a yeast two-hybrid screen. I could confirm that at least one of the selected candidates, a predicted PP2C, which is referred to as PIE (PP2C-interacting with EFR), localises in the same subcellular compartment as EFR and associates with the receptor *in planta*. Consequently, this protein was selected for further characterisation. Next, I showed that PIE also associates with FLS2 and BIK1 *in planta.* Notably, PIE dissociates from both the EFR and FLS2 receptor complexes upon ligand-perception. Therefore, I concluded that PIE might regulate the EFR and FLS2 phosphorylation-status in absence of ligand. Consistent with this hypothesis, we showed that PIE dephosphorylates EFR, FLS2 and BIK1 *in vitro*. However, further investigations are required to confirm these initial results. Additional work is also needed to draw clear conclusions about the genetic requirement of PIE for the EFR and FLS2 signalling pathway.

In summary, these results indicate that the activation of EFR- and FLS2-dependent signalling is, as previously shown for XA21, under negative regulation to block constitutive signalling in absence of their ligand.

Notably, I also demonstrated that PIE is phosphorylated upon PAMP perception and preliminary results imply that PIE phosphatase activity is increased by this post-translational modification. Considering that PIE dissociates from the receptor complex, this observation indicates that PIE might have further targets in addition to EFR, FLS2 and BIK1. Interestingly, it was recently reported that BKI1, which associates with BRI1 to block receptor activation in the absence of ligand, is phosphorylated upon brassinosteroid perception (Wang and Chory, 2006). Subsequently, BKI1 dissociates from the BRI1 complex and associates with a 14-3-3 protein, which in turn leads to the expression of BR-responsive genes (Wang et al., 2011). Thus, BKI1 functions as both a negative and positive regulator of BR-mediated signalling. However, it still needs to be determined whether a similar scenario is also possible for PIE. Here, the characterization of PIE phospho-mutants or the identification of novel PIE interactors could give further indications.

In summary, both approaches allowed me to identify novel components of flg22- and elf18-triggered signalling, despite the constraints of the systems

used. Here, addition to gene redundancies and subtle phenotypes, a major challenge was the characterisation of the PIE-EFR/FLS2 association. Based on its transient character, several modifications to the Co-IP protocols commonly used in the lab were required, to confirm the PIE-RLK association *in planta*. Thus, looking back the most difficult challenge during my PhD was to decide for how long it is worth to try to obtain a certain result and when it is time to “move-on”.

Appendix

Table A.1: Overview of primers that were used to validate the flg22-depenedent gene expression network
(* primer with good amplification efficiency that were used to test the gene expression)

gene	Primer pair number	Efficiency calculated (excepted range: 1.95-2.05)
At2g02310	P1	1.75
	P2	No result
	P3	2.33
	P4	2.27
	P5	2.161
	P6	1.86
	P7	3.67
At4g17550	P1	2.05*
	P2	7.82
	P3	1.91
At1g19270	P1	2.19
	P2	2.00*
	P3	1.997
At1g69690	P1	1.92
	P2	2.12
	P3	1.45
	P4	2.025*
	P5	2.42
	P6	2.175
At5g27930	P1	2.04*
	P2	2.08
At3g16570	P1	2.12
	P2	1.80
	P3	1.74
	P4	2.077
	P5	2.023*
At1g14920	P1	1.86
	P2	2.27
	P3	1.87
	P4	2.22
	P5	2.023*

Table A.2: Flg22-dependent induction values of the flg22-dependent gene expression network determined by microarray or qRT-PCR

gene	data source	time after flg22 treatment [minutes]		
		0	60	240
At1g14920	AtGene Express	1	0.473634	0.542466
	eFP Browser	1	0.47	0.56
	qRT-PCR	1	0.416318	0.757888
	error qRT-PCR	0.117202	0.041764	0.05077
At3g16570	AtGene Express	1	0.45722	0.4705
	eFP Browser	1	0.49	0.52
	qRT-PCR	1	0.589933	0.639241
	error qRT-PCR	0.160374	0.124508	0.10494
At1g69690	AtGene Express	1	0.299525	0.507735
	eFP Browser	1	0.43	0.57
	qRT-PCR	1	0.60131	0.483747
	error qRT-PCR	0.111353	0.253269	0.144403
At5g27930	AtGene Express	1	0.589263	0.486911
	eFP Browser	1	0.68	0.58
	qRT-PCR	1	0.589225	0.451326
	error qRT-PCR	0.08287	0.083706	0.070484
At1g19270	AtGene Express	1	2.840712	2.509071
	eFP Browser	1	2.27	2.3
	qRT-PCR	1	1.776305	2.295179
	error qRT-PCR	0.389742	0.069122	0.037863
At4g17550	AtGene Express	1	0.5347	0.386467
	eFP Browser	1	0.47	0.42
	qRT-PCR	1	0.944486	0.534708
	error qRT-PCR	0.224302	0.298078	0.237591
At2g02310	AtGene Express	1	16.80294	16.18642
	eFP Browser	1	4.01	7.52
	qRT-PCR	1	7.182456	11.74752
	error qRT-PCR	0.222112	1.35923	1.08893

Table A.3: Yeast two-hybrid interactors identified in a screen with the EFR cytoplasmic domain

AGI	Name	Function/domain (from TAIR/pubmed)	Number of times found in the screen	Encoded in frame
At4g28400	PP2C-58	Predicted PP2C-type phosphatase	6	yes
At5g39510	SGR4, SHOOT GRAVITROPSIM 4	V-SNARE domain, involved in vesicle transport	2	no vector specific sequence
At1g10630	ARFA1f, ADP-ribosylation factor A1F	Involved in GTP binding	2	no
At5g14660	PDF1B, PEPTIDE DEFORMYLASE 1B	Peptide deformylase domain	1	no vector specific sequence
AtMg00090	RPS3, ribosomal protein S3	Ribosomal protein S3	4	no vector specific sequence
At5g56200	-	Putative C2H2 zinc finger transcription factor	1	no
At2g35240	DAG	Plastid developmental protein	1	no
At1g54290	SUI1	Eukaryotic translation initiation factor	1	no
At1g14130	-	2-oxoglutarate (2OG) and Fe(II)-dependent oxygenase-like protein	1	no
At4g26410	-	unknown	1	no
At4g32530	VHA-c”	Vacuolar ATP synthase subunit c	1	no
At3g12620	PP2C-38	{redicted PP2C-type phosphatase	3	yes
At3g61480	-	Quinoprotein amine dehydrogenase	1	no
At1g22410	-	3-deoxy-7-phosphoheptulonate synthase activity Potentially involved in aromatic amino acid family biosynthesis	1	yes
At3g11773	-	Electron carrier/ protein disulfide oxidoreductase	1	yes
At3g20330	PYRB, PYRIMIDINE B	Aspartate carbamoyltransferase, involved in pyrimidine ribonucleotide biosynthesis	4	no vector specific sequence

Table A.3 ***continued***

At2g41430	ERD15, EARLY RESPONSIVE TO DEHYDRATION 15	Small acidic protein involved in various stress signalling	1	no
At3g18640	-	Zinc finger CCCH domain-containing	1	no vector specific sequence
At5g63930	-	Leucine-rich repeat protein kinase family protein subfamily XI	1	yes
At2g20890	THF1, THYLAKOID FORMATION1	Involved in vesicle-mediated formation of thylakoid membranes	4	yes
At1g30510	RFNR2, root-type ferredoxin:NADP(H) oxidoreductase	NADPH oxidoreductase	1	no
At1g05720	-	Selenoprotein family protein	1	no
At1g51760	IAR3, IAA-ALANINE RESISTANT 3	IAA-Ala conjugate hydrolase activity	2	IAR3
At5g14550	-	Core-2/I-branching beta-1,6-N-acetylglucosaminyltransferase family protein	1	no
At2g17560	HMGB4, HIGH MOBILITY GROUP B4	Involved in the assembly of nucleoprotein complexes	1	yes
At4g34990	MYB32, MYB DOMAIN PROTEIN 32	Transcription factor involved in pollen development	1	yes
At3g50380	-	Similar to vacuolar protein sorting-associated protein vps13	1	no

Table A.3: Primer used for genotyping, sequencing, cloning primer and qRT-PCR

primer name	sequence	used for
LB_SAIL	TAGCATCTGAATTTCATAACCAATCTCG ATACAC	genotyping
LBb1.3 (SALK)	ATTTTGCCGATTTCGGAAC	genotyping
Wisc_LB	AATAGCCTTTACTTGAGTTGGCGTAAAA G	genotyping
SALK_036920L	CCTCTTCGACAACATCAGGAG	genotyping
SALK_036920R	TTGCTGCCTCTCTTAGAGCTG	genotyping
SALK_016641L	TCCATGTCCTTGCTCATAACC	genotyping
SALK_016641R	AAGCCCATCCTTAGAGCAGAG	genotyping
SALK_026517L	GAGGCTGAACGCACTATTGTC	genotyping
SALK_026517R	TTCAACTTTGACCCATCAACC	genotyping
SALK_069824L	GCAGACCCTACACAAACAAGC	genotyping
SALK_069824R	AGCTGCATTACAAGAAGCAGC	genotyping
WiscDsLoxHs095_12C_L	CTTAGGCCATGAAAAGCAATG	genotyping
WiscDsLoxHs095_12C_R	ACAAAGTTTGGCGTGTCAAAG	genotyping
SALK_064440L	AATGTCGTCCACTCGTTAACG	genotyping
SALK_064440R	AAGAGTGGCCAAAGAAGAAGC	genotyping
SALK_107367L	AATGTCGTCCACTCGTTAACG	genotyping
SALK_107367R	ATGAACGTCATGGCTTACGAG	genotyping
SALK_071338L	ATGGTTTCTGTTCACACTGCC	genotyping
SALK_071338R	CATCTGTTGTGGCTGTTGTTG	genotyping
SALK_059283L	ACTAACCCCCATGACATCTCC	genotyping
SALK_059283R	GAATTCATCGCCATCTCTCAC	genotyping
SALK_130757L	GATGATTGCGTAGGGTTTCTG	genotyping
SALK_130757R	ACGATGCAACAAAACCTCATC	genotyping
SALK_011491L	AGAACCACGTAAGCCCATCTC	genotyping
SALK_011491R	TCAAATGAACTCCACTACCGC	genotyping

Table A.3 *continued*

SALK_042824L	ATGGGACATTTCTCATCGATG	genotyping
SALK_042824R	GGACGGAAGTTAAAACTTCCG	genotyping
SALK_028649L	CATTAACCATCATGGCGATTC	genotyping
SALK_028649R	TTTGGTTCGATTTGAATCGAC	genotyping
SALK_048861L	GTAAGAATCGATCTTGCGGTG	genotyping
SALK_048861R	TTTCCCTGAAAAAGCAAAAGAG	genotyping
SALK_064994L	AGGATTCGAACCTTCGAAAAC	genotyping
SALK_064994R	TCGGTGGATTGAGAAGATACG	genotyping
SALK_000027L	TGTTGCTTTGTGTCGTTATGC	genotyping
SALK_000027R	CAGCCACGAGAGTAAGGATTG	genotyping
SALK_135682L	CAAATCATGGAAGGAGACCAC	genotyping
SALK_135682R	CAGCCACGAGAGTAAGGATTG	genotyping
M13_forward	GTAAAACGACGGCCAG	sequencing
M13_reverse	CAGGAAACAGCTATGAC	sequencing
pACT-F	TATAACGCGTTTGGAATCAC	sequencing
pACT-R	GTTACATGGCCAAGATTGAA	sequencing
pAS-F	GATTTTTCCTCGAGAAGACC	sequencing
pAS-R	CAGGAAACAGCTATGAC	sequencing
pGEX4T1-At3g12620-F-*Bam*HI	GGATCCGTATCATCGGCAACTATATTGCG	cloning
pGEX4T1_F	GGGCTGGCAAGCCACGTTTGGTG	sequencing
pGEX4T1_R	CCGGGAGCTGCATGTGTCAGAGG	sequencing
pB42AD-At3g1620-*Mfe*I-720on	CAATTGTTAAAGAAAGCAGAATTCAA	Y2H cloning
At3g12620-own-promoter-F	CACCGAGACGCGTTTCCATCTC	GATEWAY cloning
At3g12620-CDS-F	CACCATGGTATCATCGGCAAC	GATEWAY cloning
At3g12620-Rstop	TCAAGTAGAAGGTCCAGCTAAATC	GATEWAY cloning

Table A.3 *continued*

At3g12620-Rnostop	AGTAGAAGGTCCAGCTAAATC	GATEWAY cloning
At4g28400C-F	CACCATGGCAGGCAGTAATATTCTCC	GATEWAY cloning
At4g28400-Rnostop	GTGGAACTTTACAACGATACA	GATEWAY cloning
At4g34990C-F	CACCATGGGAAGGTCTCCTTG	GATEWAY cloning
At4g34990-Rnostop	TTTCATTTCCAAAGTGCTAAAAT	GATEWAY cloning
AT3G55050-CDS_caccF	caccATGGTATCTACAACATTTAG	GATEWAY cloning
AT3G55050-CDS_R	CTATAAAACGGGATTATGGGC	GATEWAY cloning
At3g12620_R	AATGTCTCCGCACTCCTCTATC	qRT-PCR
At3g12620_1_F	AGAGCCGGCAATTACAGTACAC	qRT-PCR
At3g12620_1_R	AATGTCTCCGCACTCCTCTATC	qRT-PCR
At3g12620_2_F	GAGCCGGCAATTACAGTACAC	qRT-PCR
At3g12620_2_R	ATGTCTCCGCACTCCTCTATC	qRT-PCR
At4g28400_F	GACTCCAGAGCAGTGATGTCTAAG	qRT-PCR
At4g28400_R	ATGCTCTTGCAACCGCTAAC	qRT-PCR
At4g28400_1_F	GACTCCAGAGCAGTGATGTCTAAG	qRT-PCR
At4g28400_1_R	TGCTCTTGCAACCGCTAAC	qRT-PCR
At4g28400_2_F	AGACTCCAGAGCAGTGATGTCTAAG	qRT-PCR
At4g28400_2_R	ATGCTCTTGCAACCGCTAAC	qRT-PCR
At3g55050pPCR1f	GGAGGAGTTTCTCGGTTTAGTG	qRT-PCR
At3g55050pPCR1r	CTCCTGCGTTTGCAACATAC	qRT-PCR
At3g55050pPCR2f	GATCCATTGGTGACGCATAC	qRT-PCR
At3g55050pPCR2r	AACAGCTTCCTGGTTGCTTAG	qRT-PCR
At3g55050pPCR3f	AGGAGGAGTTTCTCGGTTTAGTG	qRT-PCR
At3g55050pPCR3r	CTCCTGCGTTTGCAACATAC	qRT-PCR
At1g19270qPCR-P1F	tgggggtttcgtgaagcttattgg	qRT-PCR
At1g19270qPCR-P1R	caacccggagcctttggttagag	qRT-PCR
At1g19270qPCR-P2F	ggcacatccttttgggttcagaag	qRT-PCR
At1g19270qPCR-P2R	ctcaaggcaaagtttccgtccatc	qRT-PCR
At1g19270qPCR-P3F	gtgggggtttcgtgaagcttattgg	qRT-PCR

Table A.3 *continued*

At1g19270qPCR-P3R	CCGGAGCCTTTGGTTAGAGCCTTT	qRT-PCR
At2g02310qPCR-P1F	TTAGCTGCAAAGGAACTGTGGATCA	qRT-PCR
At2g02310qPCR-P1/2R	ACTACCACCCATCTGGAAAGAACGA	qRT-PCR
At4g17550qPCR-P1/3F	TTTTGACCCGTCTGGTTATTGCTG	qRT-PCR
At4g17550qPCR-P1R	TTGCGCAAACAATGGTTTCTGTTC	qRT-PCR
At4g17550qPCR-P2F	CTTTTGACCCGTCTGGTTATTGCTG	qRT-PCR
At4g17550qPCR-P2R	CTTGCGCAAACAATGGTTTCTGTTC	qRT-PCR
At4g17550qPCR-P3R	TGCGCAAACAATGGTTTCTGTTC	qRT-PCR
At5g27930qPCR-P1F	CAAGAGCGGTACTAGCCATGGAGTC	qRT-PCR
At5g27930qPCRP1/2R	CTTTGCAGCCAATTATCCGCTCCT	qRT-PCR
At5g27930qPCR2-P2R	TCAAGAGCGGTACTAGCCATGGAGT	qRT-PCR
At1g69690qPCR-P1R	TTTCTGGACAGCCTTTGGCTTCTG	qRT-PCR
At1g69690qPCR-P1F	GCAGCATTCAACGCCGCTAAAACT	qRT-PCR
At1g14920qPCR-P1F	ATGAAGAAGACGACGGTAAC	qRT-PCR
At1g14920qPCR-P1R	TAGCGAACTGATTGAGAATCG	qRT-PCR
At1g14920qPCR-P2R	CATGACGCTCAACTCGGTCA	qRT-PCR
At1g14920qPCR-P2F	TGTTTGACTCGTTGGAAGGT	qRT-PCR
At1g14920qPCR-P3R	CGCACCAGGTCGTCCCAAGA	qRT-PCR
At1g14920qPCR-P3F	TGGCTCATTTAGCTGAGGCG	qRT-PCR
At1g69690qPCR-P2R	ATGGCTATGTTCTCCACCGC	qRT-PCR
At1g69690qPCR-P2F	AGTGGCGGCGGTAGTGGAGT	qRT-PCR
At1g69690qPCR-P3R	ACTCCACTACCGCCGCCACT	qRT-PCR
At1g69690qPCR-P3F	TCAGCATCAGGTTCGTCCCA	qRT-PCR
At3g16570qPCR-P1F	ACCGGCGCATATTAGCTACG	qRT-PCR
At3g16570qPCR-P2F	TCTCAATCCACCGAATTCGC	qRT-PCR
At3g16570qPCR-P1R	GCTGCAGCCACGAGAGTAAG	qRT-PCR
At3g16570qPCR-P2R	GTCCATCTCGAACTCCTCTC	qRT-PCR
U-Box F	TGCGTGCCAGATAATACACTATT	qRT-PCR
U-Box R	TGCTGCCCAACATCAGGT	qRT-PCR

Literature

Aarts, N., Metz, M., Holub, E., Staskawicz, B.J., Daniels, M.J., and Parker, J.E. (1998). Different requirements for EDS1 and NDR1 by disease resistance genes define at least two R gene-mediated signaling pathways in Arabidopsis. Proceedings of the National Academy of Sciences **95,** 10306-10311.

Achard, P., Renou, J.-P., Berthomé, R., Harberd, N.P., and Genschik, P. (2008). Plant DELLAs Restrain Growth and Promote Survival of Adversity by Reducing the Levels of Reactive Oxygen Species. Current Biology **18,** 656-660.

Albert, M., K. Jehle, A., Lipschis, M., Mueller, K., Zeng, Y., and Felix, G. (2010a). Regulation of cell behaviour by plant receptor kinases: Pattern recognition receptors as prototypical models. European Journal of Cell Biology **89,** 200-207.

Albert, M., Jehle, A.K., Mueller, K., Eisele, C., Lipschis, M., and Felix, G. (2010b). *Arabidopsis thaliana* Pattern Recognition Receptors for Bacterial Elongation Factor Tu and Flagellin Can Be Combined to Form Functional Chimeric Receptors. Journal of Biological Chemistry **285,** 19035-19042.

Albrecht, C., Russinova, E., Kemmerling, B., Kwaaitaal, M., and de Vries, S.C. (2008). *Arabidopsis* SOMATIC EMBRYOGENESIS RECEPTOR KINASE Proteins Serve Brassinosteroid-Dependent and -Independent Signaling Pathways. Plant Physiology **148,** 611-619.

Albrecht, C., Boutrot, F., Segonzac, C., Schwessinger, B., Gimenez-Ibanez, S., Chinchilla, D., Rathjen, J.P., de Vries, S.C., and Zipfel, C. (2012). Brassinosteroids inhibit pathogen-associated molecular pattern–triggered immune signaling independent of the receptor kinase BAK1. Proceedings of the National Academy of Sciences **109,** 303-308.

Ali, R., Ma, W., Lemtiri-Chlieh, F., Tsaltas, D., Leng, Q., von Bodman, S., and Berkowitz, G.A. (2007). Death Don't Have No Mercy and Neither Does Calcium: *Arabidopsis* CYCLIC NUCLEOTIDE GATED CHANNEL2 and Innate Immunity. The Plant Cell Online **19,** 1081-1095.

Anderson, J.C., Bartels, S., Besteiro, M.A.G., Shahollari, B., Ulm, R., and Peck, S.C. (2011). *Arabidopsis* MAP Kinase Phosphatase 1 (AtMKP1) negatively regulates MPK6-mediated PAMP responses and resistance against bacteria. The Plant Journal **67,** 258-268.

Apel, K., and Hirt, H. (2004). REACTIVE OXYGEN SPECIES: Metabolism, Oxidative Stress, and Signal Transduction. Annual Review of Plant Biology **55,** 373-399.

Asai, T., Tena, G., Plotnikova, J., Willmann, M.R., Chiu, W., Gomez-Gomez, L., Boller, T., Ausubel, F.M., and Sheen, J. (2002). MAP kinase signalling cascade in *Arabidopsis* innate immunity. Nature **415,** 977-983.

Ausubel, F.M. (2005). Are innate immune signaling pathways in plants and animals conserved? Nat Immunol **6,** 973-979.

Axtell, M.J., and Staskawicz, B.J. (2003). Initiation of RPS2-Specified Disease Resistance in *Arabidopsis* Is Coupled to the AvrRpt2-Directed Elimination of RIN4. Cell **112,** 369-377.

Aziz, A., Heyraud, A., and Lambert, B. (2004). Oligogalacturonide signal transduction, induction of defense-related responses and protection of grapevine against *Botrytis cinerea*. Planta **218,** 767-774.

Bach, I. (2000). The LIM domain: regulation by association. Mechanisms of Development **91,** 5-17.

Bailey, B.A., Dean, J.F.D., and Anderson, J.D. (1990). An Ethylene Biosynthesis-Inducing Endoxylanase Elicits Electrolyte Leakage and Necrosis in *Nicotiana tabacum* cv *Xanthi* Leaves. Plant Physiology **94,** 1849-1854.

Bailey, B.A., Korcak, R.F., and Anderson, J.D. (1993). Sensitivity to an Ethylene Biosynthesis-Inducing Endoxylanase in *Nicotiana tabacum L.* cv *Xanthi* Is Controlled by a Single Dominant Gene. Plant Physiology **101,** 1081-1088.

Bar, M., and Avni, A. (2009). EHD2 inhibits ligand-induced endocytosis and signaling of the leucine-rich repeat receptor-like protein LeEix2. The Plant Journal **59,** 600-611.

Bar, M., Sharfman, M., Ron, M., and Avni, A. (2010). BAK1 is required for the attenuation of ethylene-inducing xylanase (Eix)-induced defense responses by the decoy receptor LeEix1. The Plant Journal **63,** 791-800.

Bartels, S., Besteiro, M.A.G., Lang, D., and Ulm, R. (2010). Emerging functions for plant MAP kinase phosphatases. Trends in Plant Science **15,** 322-329.

Bartels, S., Anderson, J.C., González Besteiro, M.A., Carreri, A., Hirt, H., Buchala, A., Métraux, J.-P., Peck, S.C., and Ulm, R. (2009). MAP KINASE PHOSPHATASE1 and PROTEIN TYROSINE PHOSPHATASE1 Are Repressors of Salicylic Acid Synthesis and SNC1-Mediated Responses in *Arabidopsis*. The Plant Cell Online **21,** 2884-2897.

Beckers, G.J.M., and Spoel, S.H. (2006). Fine-Tuning Plant Defence Signalling: Salicylate versus Jasmonate. Plant Biology **8,** 1-10.

Bedinger, P.A., Pearce, G., and Covey, P.A. (2010). RALFs: Peptide regulators of plant growth. Plant Signaling & Behavior **5,** 1342-1346.

Belkhadir, Y., Jaillais, Y., Epple, P., Balsemão-Pires, E., Dangl, J.L., and Chory, J. (2012). Brassinosteroids modulate the efficiency of plant immune responses to microbe-associated molecular patterns. Proceedings of the National Academy of Sciences **109,** 297-302.

Bellincampi, D., Salvi, G., De Lorenzo, G., Cervone, F., Marfà, V., Eberhard, S., Darvill, A., and Albersheim, P. (1993). Oligogalacturonides inhibit the formation of roots on tobacco explants. The Plant Journal **4,** 207-213.

Benschop, J.J., Mohammed, S., O'Flaherty, M., Heck, A.J.R., Slijper, M., and Menke, F.L.H. (2007). Quantitative Phosphoproteomics of Early Elicitor Signaling in *Arabidopsis*. Molecular & Cellular Proteomics **6,** 1198-1214.

Bethke, G., Unthan, T., Uhrig, J.F., Pöschl, Y., Gust, A.A., Scheel, D., and Lee, J. (2009). Flg22 regulates the release of an ethylene

response factor substrate from MAP kinase 6 in *Arabidopsis thaliana* via ethylene signaling. Proceedings of the National Academy of Sciences **106,** 8067-8072.

Bethke, G., Pecher, P., Eschen-Lippold, L., Tsuda, K., Katagiri, F., Glazebrook, J., Scheel, D., and Lee, J. (2011). Activation of the *Arabidopsis thaliana* Mitogen-Activated Protein Kinase MPK11 by the Flagellin-Derived Elicitor Peptide, flg22. Molecular Plant-Microbe Interactions **25,** 471-480.

Bhattacharjee, S., Halane, M.K., Kim, S.H., and Gassmann, W. (2011). Pathogen Effectors Target Arabidopsis EDS1 and Alter Its Interactions with Immune Regulators. Science **334,** 1405-1408.

Bisgrove, S.R., Simonich, M.T., Smith, N.M., Sattler, A., and Innes, R.W. (1994). A disease resistance gene in *Arabidopsis* with specificity for two different pathogen avirulence genes. The Plant Cell Online **6,** 927-933.

Boch, J., and Bonas, U. (2010). *Xanthomonas* AvrBs3 Family-Type III Effectors: Discovery and Function. Annual Review of Phytopathology **48,** 419-436.

Boch, J., Scholze, H., Schornack, S., Landgraf, A., Hahn, S., Kay, S., Lahaye, T., Nickstadt, A., and Bonas, U. (2009). Breaking the Code of DNA Binding Specificity of TAL-Type III Effectors. Science **326,** 1509-1512.

Boller, T., and Felix, G. (2009). A Renaissance of Elicitors: Perception of Microbe-Associated Molecular Patterns and Danger Signals by Pattern-Recognition Receptors. Annual Review of Plant Biology **60,** 379-406.

Bologna, G., Yvon, C., Duvaud, S., and Veuthey, A.-L. (2004). N-terminal Myristoylation Predictions by Ensembles of Neural Networks. Proteomics **4,** 1626-1632.

Boudsocq, M., Willmann, M.R., McCormack, M., Lee, H., Shan, L., He, P., Bush, J., Cheng, S.H., and Sheen, J. (2010). Differential innate immune signalling via Ca(2+) sensor protein kinases. Nature **464,** 418-422.

Boutrot, F., Segonzac, C., Chang, K.N., Qiao, H., Ecker, J.R., Zipfel, C., and Rathjen, J.P. (2010). Direct transcriptional control of the *Arabidopsis* immune receptor FLS2 by the ethylene-dependent transcription factors EIN3 and EIL1. Proceedings of the National Academy of Sciences **107,** 14502-14507.

Braun, D.M., Stone, J.M., and Walker, J.C. (1997). Interaction of the maize and Arabidopsis kinase interaction domains with a subset of receptor-like protein kinases: implications for transmembrane signaling in plants. The Plant Journal **12,** 83-95.

Brock, A.K., Willmann, R., Kolb, D., Grefen, L., Lajunen, H.M., Bethke, G., Lee, J., Nürnberger, T., and Gust, A.A. (2010). The *Arabidopsis* Mitogen-Activated Protein Kinase Phosphatase PP2C5 Affects Seed Germination, Stomatal Aperture, and Abscisic Acid-Inducible Gene Expression. Plant Physiology **153,** 1098-1111.

Brodersen, P., Petersen, M., Bjørn Nielsen, H., Zhu, S., Newman, M.-A., Shokat, K.M., Rietz, S., Parker, J., and Mundy, J. (2006). *Arabidopsis* MAP kinase 4 regulates salicylic acid- and jasmonic

acid/ethylene-dependent responses via EDS1 and PAD4. The Plant Journal **47,** 532-546.

Brooks, D.M., Bender, C.L., and Kunkel, B.N. (2005). The *Pseudomonas syringae* phytotoxin coronatine promotes virulence by overcoming salicylic acid-dependent defences in *Arabidopsis thaliana*. Molecular Plant Pathology **6,** 629-639.

Browse, J. (2009). Jasmonate Passes Muster: A Receptor and Targets for the Defense Hormone. Annual Review of Plant Biology **60,** 183-205.

Brüchert, N., Mavila, N., Boknik, P., Baba, H.A., Fabritz, L., Gergs, U., Kirchhefer, U., Kirchhof, P., Matus, M., Schmitz, W., DePaoli-Roach, A.A., and Neumann, J. (2008). Inhibitor-2 prevents protein phosphatase 1-induced cardiac hypertrophy and mortality. American Journal of Physiology - Heart and Circulatory Physiology **295,** 1539-1546.

Brunner, F., Rosahl, S., Lee, J., Rudd, J.J., Geiler, C., Kauppinen, S., Rasmussen, G., Scheel, D., and Nurnberger, T. (2002). Pep-13, a plant defense-inducing pathogen-associated pattern from *Phytophthora* transglutaminases. EMBO Journal **21,** 6681-6688.

Brutus, A., Sicilia, F., Macone, A., Cervone, F., and De Lorenzo, G. (2010). A domain swap approach reveals a role of the plant wall-associated kinase 1 (WAK1) as a receptor of oligogalacturonides. Proceedings of the National Academy of Sciences **107,** 9452-9457.

Canonne, J., Marino, D., Jauneau, A., Pouzet, C., Brière, C., Roby, D., and Rivas, S. (2011). The *Xanthomonas* Type III Effector XopD Targets the Arabidopsis Transcription Factor MYB30 to Suppress Plant Defense. The Plant Cell Online **23,** 3498-3511.

Cao, J., and Shi, F. (2012). Evolution of the RALF Gene Family in Plants: Gene Duplication and Selection Patterns. Evolutionary Bioinformatics **8,** 271.

Caplan, J., Padmanabhan, M., and Dinesh-Kumar, S.P. (2008). Plant NB-LRR Immune Receptors: From Recognition to Transcriptional Reprogramming. Cell Host & Microbe **3,** 126-135.

Century, K.S., Holub, E.B., and Staskawicz, B.J. (1995). NDR1, a locus of Arabidopsis thaliana that is required for disease resistance to both a bacterial and a fungal pathogen. Proceedings of the National Academy of Sciences **92,** 6597-6601.

Che, F.-S., Nakajima, Y., Tanaka, N., Iwano, M., Yoshida, T., Takayama, S., Kadota, I., and Isogai, A. (2000). Flagellin from an Incompatible Strain of *Pseudomonas avenae* Induces a Resistance Response in Cultured Rice Cells. Journal of Biological Chemistry **275,** 32347-32356.

Chen, F., Gao, M.-J., Miao, Y.-S., Yuan, Y.-X., Wang, M.-Y., Li, Q., Mao, B.-Z., Jiang, L.-W., and He, Z.-H. (2010a). Plasma Membrane Localization and Potential Endocytosis of Constitutively Expressed XA21 Proteins in Transgenic Rice. Molecular Plant **3,** 917-926.

Chen, H., Xue, L., Chintamanani, S., Germain, H., Lin, H., Cui, H., Cai, R., Zuo, J., Tang, X., Li, X., Guo, H., and Zhou, J.-M. (2009). ETHYLENE INSENSITIVE3 and ETHYLENE INSENSITIVE3-LIKE1 Repress SALICYLIC ACID INDUCTION DEFICIENT2 Expression to

Negatively Regulate Plant Innate Immunity in Arabidopsis. The Plant Cell Online **21,** 2527-2540.

Chen, X., Chern, M., Canlas, P.E., Ruan, D., Jiang, C., and Ronald, P.C. (2010b). An ATPase promotes autophosphorylation of the pattern recognition receptor XA21 and inhibits XA21-mediated immunity. Proceedings of the National Academy of Sciences **107,** 8029-8034.

Chen, Y.-C., Siems, W.F., Pearce, G., and Ryan, C.A. (2008). Six Peptide Wound Signals Derived from a Single Precursor Protein in Ipomoea batatas Leaves Activate the Expression of the Defense Gene Sporamin. Journal of Biological Chemistry **283,** 11469-11476.

Cheng, H., Qin, L., Lee, S., Fu, X., Richards, D.E., Cao, D., Luo, D., Harberd, N.P., and Peng, J. (2004). Gibberellin regulates *Arabidopsis* floral development via suppression of DELLA protein function. Development **131,** 1055-1064.

Cheng, W., Munkvold, Kathy R., Gao, H., Mathieu, J., Schwizer, S., Wang, S., Yan, Y.-b., Wang, J., Martin, Gregory B., and Chai, J. (2011). Structural Analysis of Pseudomonas syringae AvrPtoB Bound to Host BAK1 Reveals Two Similar Kinase-Interacting Domains in a Type III Effector. Cell host & microbe **10,** 616-626.

Chinchilla, D., Bauer, Z., Regenass, M., Boller, T., and Felix, G. (2006). The *Arabidopsis* Receptor Kinase FLS2 Binds flg22 and Determines the Specificity of Flagellin Perception. The Plant Cell Online **18,** 465-476.

Chinchilla, D., Zipfel, C., Robatzek, S., Kemmerling, B., Nurnberger, T., Jones, J.D.G., Felix, G., and Boller, T. (2007). A flagellin-induced complex of the receptor FLS2 and BAK1 initiates plant defence. Nature **448,** 497-500.

Chini, A., Fonseca, S., Chico, J.M., Fernández-Calvo, P., and Solano, R. (2009). The ZIM domain mediates homo- and heteromeric interactions between *Arabidopsis* JAZ proteins. The Plant Journal **59,** 77-87.

Chisholm, S.T., Coaker, G., Day, B., and Staskawicz, B.J. (2006). Host-Microbe Interactions: Shaping the Evolution of the Plant Immune Response. Cell **124,** 803-814.

Clough, S.J., Fengler, K.A., Yu, I.-c., Lippok, B., Smith, R.K., and Bent, A.F. (2000). The Arabidopsis dnd1 “defense, no death” gene encodes a mutated cyclic nucleotide-gated ion channel. Proceedings of the National Academy of Sciences **97,** 9323-9328.

Coca, M., and San Segundo, B. (2010). AtCPK1 calcium-dependent protein kinase mediates pathogen resistance in *Arabidopsis*. The Plant Journal **63,** 526-540.

Cohen, P. (1989). Structure and regulation of protein phosphatases. Biochemical Journal **58,** 453-508.

Constabel, C.P., Yip, L., and Ryan, C.A. (1998). Prosystemin from potato, black nightshade, and bell pepper: primary structure and biological activity of predicted systemin polypeptides. Plant Molecular Biology **36,** 55-62.

Covey, P.A., Subbaiah, C.C., Parsons, R.L., Pearce, G., Lay, F.T., Anderson, M.A., Ryan, C.A., and Bedinger, P.A. (2010). A Pollen-Specific RALF from Tomato That Regulates Pollen Tube Elongation. Plant Physiology **153,** 703-715.

Cubas, P., Lauter, N., Doebley, J., and Coen, E. (1999). The TCP domain: a motif found in proteins regulating plant growth and development. The Plant Journal **18,** 215-222.

Cui, H., Wang, Y., Xue, L., Chu, J., Yan, C., Fu, J., Chen, M., Innes, R.W., and Zhou, J.-M. (2010). *Pseudomonas syringae* Effector Protein AvrB Perturbs *Arabidopsis* Hormone Signaling by Activating MAP Kinase 4. Cell Host & Microbe **7,** 164-175.

da Silva, F.G., Shen, Y., Dardick, C., Burdman, S., Yadav, R.C., de Leon, A.L., and Ronald, P.C. (2004). Bacterial Genes Involved in Type I Secretion and Sulfation Are Required to Elicit the Rice Xa21-Mediated Innate Immune Response. Molecular Plant-Microbe Interactions **17,** 593-601.

Dangl, J.L., and Jones, J.D.G. (2001). Plant pathogens and integrated defence responses to infection. Nature **411,** 826-833.

Danna, C.H., Millet, Y.A., Koller, T., Han, S.-W., Bent, A.F., Ronald, P.C., and Ausubel, F.M. (2011). The Arabidopsis flagellin receptor FLS2 mediates the perception of Xanthomonas Ax21 secreted peptides. Proceedings of the National Academy of Sciences **108,** 9286-9291.

Darvill, A., Augur, C., Bergmann, C., Carlson, R.W., Cheong, J.-J., Eberhard, S., Hahn, M.G., Ló, V.-M., Marfa, V., Meyer, B., Mohnen, D., O'Neill, M.A., Spiro, M.D., van Halbeek, H., York, W.S., and Albersheim, P. (1992). Oligosaccharins—oligosaccharides that regulate growth, development and defence responses in plants. Glycobiology **2,** 181-198.

Das, A.K., Helps, N.R., Cohen, P.T., and Barford, D. (1996). Crystal structure of the protein serine/threonine phosphatase 2C at 2.0 A resolution. The EMBO Journal **15,** 6798-6809.

Day, B., Dahlbeck, D., and Staskawicz, B.J. (2006). NDR1 Interaction with RIN4 Mediates the Differential Activation of Multiple Disease Resistance Pathways in Arabidopsis. The Plant Cell Online **18,** 2782-2791.

De Lorenzo, G., Brutus, A., Savatin, D.V., Sicilia, F., and Cervone, F. (2011). Engineering plant resistance by constructing chimeric receptors that recognize damage-associated molecular patterns (DAMPs). FEBS Letters **585,** 1521-1528.

Decreux, A., Thomas, A., Spies, B., Brasseur, R., Cutsem, P.V., and Messiaen, J. (2006). *In vitro* characterization of the homogalacturonan-binding domain of the wall-associated kinase WAK1 using site-directed mutagenesis. Phytochemistry **67,** 1068-1079.

Denoux, C., Galletti, R., Mammarella, N., Gopalan, S., Werck, D., De Lorenzo, G., Ferrari, S., Ausubel, F.M., and Dewdney, J. (2008). Activation of Defense Response Pathways by OGs and Flg22 Elicitors in *Arabidopsis* Seedlings. Molecular Plant **1,** 423-445.

Desclos-Theveniau, M., Arnaud, D., Huang, T.-Y., Lin, G.J.-C., Chen, W.-Y., Lin, Y.-C., and Zimmerli, L. (2012). The *Arabidopsis* Lectin Receptor Kinase LecRK-V.5 Represses Stomatal Immunity Induced by *Pseudomonas syringae* pv. . PLoS Pathogens **8**.

Dill, A., and Sun, T.-P. (2001). Synergistic Derepression of Gibberellin Signaling by Removing RGA and GAI Function in *Arabidopsis thaliana*. Genetics **159,** 777-785.

Dinant, S., Clark, A.M., Zhu, Y., Vilaine, F., Palauqui, J.-C., Kusiak, C., and Thompson, G.A. (2003). Diversity of the Superfamily of Phloem Lectins (Phloem Protein 2) in Angiosperms. Plant Physiology **131,** 114-128.

Dodds, P.N., and Rathjen, J.P. (2010). Plant immunity: towards an integrated view of plant–pathogen interactions
Nature Reviews Genetics **11,** 539-548.

Dodds, P.N., Lawrence, G.J., Catanzariti, A.-M., Teh, T., Wang, C.-I.A., Ayliffe, M.A., Kobe, B., and Ellis, J.G. (2006). Direct protein interaction underlies gene-for-gene specificity and coevolution of the flax resistance genes and flax rust avirulence genes. Proceedings of the National Academy of Sciences **103,** 8888-8893.

Dong, X. (2004). NPR1, all things considered. Current Opinion in Plant Biology **7,** 547-552.

Dunning, F.M., Sun, W., Jansen, K.L., Helft, L., and Bent, A.F. (2007). Identification and Mutational Analysis of Arabidopsis FLS2 Leucine-Rich Repeat Domain Residues That Contribute to Flagellin Perception. The Plant Cell Online **19,** 3297-3313.

Durek, P., Schmidt, R., Heazlewood, J.L., Jones, A., MacLean, D., Nagel, A., Kersten, B., and Schulze, W.X. (2009). PhosPhAt: the *Arabidopsis thaliana* phosphorylation site database. Nucleic Acids Research.

Eitas, T.K., and Dangl, J.L. (2010). NB-LRR proteins: pairs, pieces, perception, partners, and pathways. Current Opinion in Plant Biology **13,** 472-477.

Elbaz, M., Avni, A., and Weil, M. (2002). Constitutive caspase-like machinery executes programmed cell death in plant cells. Cell Death Differentiation **9,** 726-733.

Enkerli, J., Felix, G., and Boller, T. (1999). The Enzymatic Activity of Fungal Xylanase Is Not Necessary for Its Elicitor Activity. Plant Physiology **121,** 391-398.

Eroles, P., Bosch, A., Alejandro Pérez-Fidalgo, J., and Lluch, A. (2012). Molecular biology in breast cancer: Intrinsic subtypes and signaling pathways. Cancer treatment reviews **38,** 698-707.

Eulgem, T., and Somssich, I.E. (2007). Networks of WRKY transcription factors in defense signaling. Current Opinion in Plant Biology **10,** 366-371.

Evans, B., Tishmack, P.A., Pokalsky, C., Zhang, M., and Van Etten, R.L. (1996). Site-Directed Mutagenesis, Kinetic, and Spectroscopic Studies of the P-Loop Residues in a Low Molecular Weight Protein Tyrosine Phosphatase. Biochemistry **35,** 13609-13617.

Farkas, I., Dombrádi, V., Miskei, M., Szabados, L., and Koncz, C. (2007). Arabidopsis PPP family of serine/threonine phosphatases. Trends in Plant Science **12,** 169-176.

Farras, R., Ferrando, A., Jasik, J., Kleinow, T., Okresz, L., Tiburcio, A., Salchert, K., del Pozo, C., Schell, J., and Koncz, C. (2001). SKP1-

SnRK protein kinase interactions mediate proteasomal binding of a plant SCF ubiquitin ligase. EMBO J **20,** 2742-2756.

Felix, G., and Boller, T. (2003). Molecular Sensing of Bacteria in Plants. Journal of Biological Chemistry **278,** 6201-6208.

Felix, G., Regenass, M., and Boller, T. (1993). Specific perception of subnanomolar concentrations of chitin fragments by tomato cells: induction of extracellular alkalinization, changes in protein phosphorylation, and establishment of a refractory state. The Plant Journal **4,** 307-316.

Felix, G., Grosskopf, D.G., Regenass, M., and Boller, T. (1991). Rapid changes of protein phosphorylation are involved in transduction of the elicitor signal in plant cells. Proceedings of the National Academy of Sciences **88,** 8831-8834.

Felix, G., Regenass, M., Spanu, P., and Boller, T. (1994). The protein phosphatase inhibitor calyculin A mimics elicitor action in plant cells and induces rapid hyperphosphorylation of specific proteins as revealed by pulse labeling with $^{[33P]}$phosphate. Proceedings of the National Academy of Sciences **91,** 952-956.

Felix, G., Duran, J.D., Volko, S., and Boller, T. (1999). Plants have a sensitive perception system for the most conserved domain of bacterial flagellin. The Plant Journal **18,** 265-276.

Feng, F., and Zhou, J.-M. (2012). Plant–bacterial pathogen interactions mediated by type III effectors. Current Opinion in Plant Biology **15,** 469-476.

Ferrari, S., Galletti, R., Denoux, C., De Lorenzo, G., Ausubel, F.M., and Dewdney, J. (2007). Resistance to *Botrytis cinerea* Induced in *Arabidopsis* by Elicitors Is Independent of Salicylic Acid, Ethylene, or Jasmonate Signaling But Requires PHYTOALEXIN DEFICIENT3. Plant Physiology **144,** 367-379.

Feys, B.J., Wiermer, M., Bhat, R.A., Moisan, L.J., Medina-Escobar, N., Neu, C., Cabral, A., and Parker, J.E. (2005). Arabidopsis SENESCENCE-ASSOCIATED GENE101 Stabilizes and Signals within an ENHANCED DISEASE SUSCEPTIBILITY1 Complex in Plant Innate Immunity. The Plant Cell Online **17,** 2601-2613.

Fields, S., and Song, O. (1989). A novel genetic system to detect protein protein interactions. Nature **340,** 245-246.

Fliegmann, J., Mithöfer, A., Wanner, G., and Ebel, J. (2004). An Ancient Enzyme Domain Hidden in the Putative β-Glucan Elicitor Receptor of Soybean May Play an Active Part in the Perception of Pathogen-associated Molecular Patterns during Broad Host Resistance. Journal of Biological Chemistry **279,** 1132-1140.

Fliegmann, J., Montel, E., Djulić, A., Cottaz, S., Driguez, H., and Ebel, J. (2005). Catalytic properties of the bifunctional soybean β-glucan-binding protein, a member of family 81 glycoside hydrolases. FEBS Letters **579,** 6647-6652.

Flor, H.H. (1971). Current Status of the Gene-For-Gene Concept. Annual Review of Phytopathology **9,** 275-296.

Fonseca, S., Chini, A., Hamberg, M., Adie, B., Porzel, A., Kramell, R., Miersch, O., Wasternack, C., and Solano, R. (2009). (+)-7-iso-

Jasmonoyl-L-isoleucine is the endogenous bioactive jasmonate. Nat Chem Biol **5,** 344-350.

Fouts, D.E., Badel, J.L., Ramos, A.R., Rapp, R.A., and Collmer, A. (2003). A Pseudomonas syringae pv. tomato DC3000 Hrp (Type III Secretion) Deletion Mutant Expressing the Hrp System of Bean Pathogen P. syringae pv. syringae 61 Retains Normal Host Specificity for Tomato. Molecular Plant-Microbe Interactions **16,** 43-52.

Frei dit Frey, N., Mbengue, M., Kwaaitaal, M., Nitsch, L., Altenbach, D., Häweker, H., Lozano-Duran, R., Njo, M.F., Beeckman, T., Huettel, B., Borst, J.W., Panstruga, R., and Robatzek, S. (2012). Plasma Membrane Calcium ATPases Are Important Components of Receptor-Mediated Signaling in Plant Immune Responses and Development. Plant Physiology **159,** 798-809.

Fritz-Laylin, L.K., Krishnamurthy, N., Tör, M., Sjölander, K.V., and Jones, J.D.G. (2005). Phylogenomic Analysis of the Receptor-Like Proteins of Rice and *Arabidopsis*. Plant Physiology **138,** 611-623.

Fu, X., Richards, D.E., Fleck, B., Xie, D., Burton, N., and Harberd, N.P. (2004). The *Arabidopsis* Mutant *sleepy1 gar2-1* Protein Promotes Plant Growth by Increasing the Affinity of the SCFSLY1 E3 Ubiquitin Ligase for DELLA Protein Substrates. The Plant Cell Online **16,** 1406-1418.

Fu, Z.Q., Yan, S., Saleh, A., Wang, W., Ruble, J., Oka, N., Mohan, R., Spoel, S.H., Tada, Y., Zheng, N., and Dong, X. (2012). NPR3 and NPR4 are receptors for the immune signal salicylic acid in plants. Nature **486,** 228-232.

Fuchs, Y., Saxena, A., Gamble, H.R., and Anderson, J.D. (1989). Ethylene Biosynthesis-Inducing Protein from Cellulysin Is an Endoxylanase. Plant Physiology **89,** 138-143.

Furman-Matarasso, N., Cohen, E., Du, Q., Chejanovsky, N., Hanania, U., and Avni, A. (1999). A Point Mutation in the Ethylene-Inducing Xylanase Elicitor Inhibits the β-1-4-Endoxylanase Activity But Not the Elicitation Activity. Plant Physiology **121,** 345-352.

Gagne, J.M., and Clark, S.E. (2007). The Protein Phosphatases POL and PLL1 are Signaling Intermediates for Multiple Pathways in Arabidopsis. Plant Signaling & Behavior **2,** 245-246.

Gagne, J.M., and Clark, S.E. (2010). The Arabidopsis Stem Cell Factor POLTERGEIST Is Membrane Localized and Phospholipid Stimulated. The Plant Cell Online **22,** 729-743.

Gagne, J.M., Song, S.-K., and Clark, S.E. (2008). POLTERGEIST and PLL1 are required for stem cell function with potential roles in cell asymmetry and auxin signaling. Communicative & Integrative Biology **1,** 53-55.

Galletti, R., Denoux, C., Gambetta, S., Dewdney, J., Ausubel, F.M., De Lorenzo, G., and Ferrari, S. (2008). The AtrbohD-Mediated Oxidative Burst Elicited by Oligogalacturonides in Arabidopsis Is Dispensable for the Activation of Defense Responses Effective against Botrytis cinerea. Plant Physiology **148,** 1695-1706.

Gao, M., Liu, J., Bi, D., Zhang, Z., Cheng, F., Chen, S., and Zhang, Y. (2008). MEKK1, MKK1/MKK2 and MPK4 function together in a

mitogen-activated protein kinase cascade to regulate innate immunity in plants. Cell Research **18,** 1190-1198.

Garcia-Brugger, A., Lamotte, O., Vandelle, E., Bourque, S., Lecourieux, D., Poinssot, B., Wendehenne, D., and Pugin, A. (2006). Early Signaling Events Induced by Elicitors of Plant Defenses. Molecular Plant-Microbe Interactions **19,** 711-724.

García, A.V., Blanvillain-Baufumé, S., Huibers, R.P., Wiermer, M., Li, G., Gobbato, E., Rietz, S., and Parker, J.E. (2010). Balanced Nuclear and Cytoplasmic Activities of EDS1 Are Required for a Complete Plant Innate Immune Response. PLoS Pathog **6,** e1000970.

Geldner, N., and Robatzek, S. (2008). Plant Receptors Go Endosomal: A Moving View on Signal Transduction. Plant Physiology **147,** 1565-1574.

Genger, R.K., Jurkowski, G.I., McDowell, J.M., Lu, H., Jung, H.W., Greenberg, J.T., and Bent, A.F. (2008). Signaling Pathways That Regulate the Enhanced Disease Resistance of Arabidopsis "Defense, No Death" Mutants. Molecular Plant-Microbe Interactions **21,** 1285-1296.

Gimenez-Ibanez, S., Hann, D.R., Ntoukakis, V., Petutschnig, E., Lipka, V., and Rathjen, J.P. (2009). AvrPtoB Targets the LysM Receptor Kinase CERK1 to Promote Bacterial Virulence on Plants. Current biology **19,** 423-429.

Glazebrook, J. (2005). Contrasting Mechanisms of Defense Against Biotrophic and Necrotrophic Pathogens. Annual Review of Phytopathology **43,** 205-227.

Göhre, V., Spallek, T., Häweker, H., Mersmann, S., Mentzel, T., Boller, T., de Torres, M., Mansfield, J.W., and Robatzek, S. (2008). Plant Pattern-Recognition Receptor FLS2 Is Directed for Degradation by the Bacterial Ubiquitin Ligase AvrPtoB. Current biology **18,** 1824-1832.

Gómez-Gómez, L., and Boller, T. (2000). FLS2: An LRR Receptor like Kinase Involved in the Perception of the Bacterial Elicitor Flagellin in *Arabidopsis*. Molecular Cell **5,** 1003-1011.

Gómez-Gómez, L., Felix, G., and Boller, T. (1999). A single locus determines sensitivity to bacterial flagellin in *Arabidopsis thaliana*. The Plant Journal **18,** 277-284.

Gómez-Gómez, L., Bauer, Z., and Boller, T. (2001). Both the Extracellular Leucine-Rich Repeat Domain and the Kinase Activity of FLS2 Are Required for Flagellin Binding and Signaling in *Arabidopsis*. The Plant Cell Online **13,** 1155-1163.

González Besteiro, M.A., Bartels, S., Albert, A., and Ulm, R. (2011). *Arabidopsis* MAP kinase phosphatase 1 and its target MAP kinases 3 and 6 antagonistically determine UV-B stress tolerance, independent of the UVR8 photoreceptor pathway. The Plant Journal **68,** 727-737.

Gosti, F., Beaudoin, N., Serizet, C., Webb, A.A.R., Vartanian, N., and Giraudat, J. (1999). ABI1 protein phosphatase 2C is a negative regulator of abscisic acid signaling. Plant Cell **11**.

Grant, M., and Lamb, C. (2006). Systemic immunity. Current Opinion in Plant Biology **9,** 414-420.

Grant, M., Godiard, L., Straube, E., Ashfield, T., Lewald, J., Sattler, A., Innes, R., and Dangl, J. (1995). Structure of the *Arabidopsis* RPM1

gene enabling dual specificity disease resistance. Science **269,** 843-846.

Grgurina, I., Mariotti, F., Fogliano, V., Gallo, M., Scaloni, A., Iacobellis, N.S., Lo Cantore, P., Mannina, L., van Axel Castelli, V., Greco, M.L., and Graniti, A. (2002). A new syringopeptin produced by bean strains of *Pseudomonas syringae* pv. *syringae*. Biochimica et Biophysica Acta **1597,** 81-89.

Gudesblat, G.E., Torres, P.S., and Vojnov, A.A. (2009). Xanthomonas campestris Overcomes Arabidopsis Stomatal Innate Immunity through a DSF Cell-to-Cell Signal-Regulated Virulence Factor. Plant Physiology **149,** 1017-1027.

Gust, A.A., Biswas, R., Lenz, H.D., Rauhut, T., Ranf, S., Kemmerling, B., Götz, F., Glawischnig, E., Lee, J., Felix, G., and Nürnberger, T. (2007). Bacteria-derived Peptidoglycans Constitute Pathogen-associated Molecular Patterns Triggering Innate Immunity in *Arabidopsis*. Journal of Biological Chemistry **282,** 32338-32348.

Haglund, K., Di Fiore, P.P., and Dikic, I. (2003). Distinct monoubiquitin signals in receptor endocytosis. Trends in biochemical sciences **28,** 598-604.

Ham, J.H., Kim, M.G., Lee, S.Y., and Mackey, D. (2007). Layered basal defenses underlie non-host resistance of Arabidopsis to *Pseudomonas syringae* pv. *phaseolicola*. The Plant Journal **51,** 604-616.

Hammond-Kosack, K.E., and Jones, J.D.G. (1997). Plant Disease Resistance Genes. Annual Review of Plant Physiology and Plant Molecular Biology **48,** 575-607.

Han, S.-W., Lee, S.-W., and Ronald, P.C. (2011a). Secretion, modification, and regulation of Ax21. Current Opinion in Microbiology **14,** 62-67.

Han, S.-W., Sriariyanun, M., Lee, S.-W., Sharma, M., Bahar, O., Bower, Z., and Ronald, P.C. (2011b). Small Protein-Mediated Quorum Sensing in a Gram-Negative Bacterium. PLos ONE **6,** e29192.

Hann, D.R., and Rathjen, J.P. (2007). Early events in the pathogenicity of *Pseudomonas syringae* on *Nicotiana benthamiana*. The Plant Journal **49,** 607-618.

Harberd, N.P., Belfield, E., and Yasumura, Y. (2009). The Angiosperm Gibberellin-GID1-DELLA Growth Regulatory Mechanism: How an "Inhibitor of an Inhibitor" Enables Flexible Response to Fluctuating Environments. The Plant Cell Online **21,** 1328-1339.

Haruta, M., Burch, H.L., Nelson, R.B., Barrett-Wilt, G., Kline, K.G., Mohsin, S.B., Young, J.C., Otegui, M.S., and Sussman, M.R. (2010). Molecular Characterization of Mutant *Arabidopsis* Plants with Reduced Plasma Membrane Proton Pump Activity. Journal of Biological Chemistry **285,** 17918-17929.

Häweker, H., Rips, S., Koiwa, H., Salomon, S., Saijo, Y., Chinchilla, D., Robatzek, S., and von Schaewen, A. (2010). Pattern Recognition Receptors Require N-Glycosylation to Mediate Plant Immunity. Journal of Biological Chemistry **285,** 4629-4636.

He, P., Shan, L., and Sheen, J. (2007). Elicitation and suppression of microbe-associated molecular pattern-triggered immunity in plant–microbe interactions. Cellular Microbiology **9,** 1385-1396.

Hecht, V., Vielle-Calzada, J.-P., Hartog, M.V., Schmidt, E.D.L., Boutilier, K., Grossniklaus, U., and de Vries, S.C. (2001). The *Arabidopsis* Somatic Embryogenesis Receptor Kinase 1 Gene Is Expressed in Developing Ovules and Embryos and Enhances Embryogenic Competence in Culture. Plant Physiology **127,** 803-816.

Heese, A., Hann, D.R., Gimenez-Ibanez, S., Jones, A.M.E., He, K., Li, J., , Schroeder, J.I., Peck, S.C., and Rathjen, J.P. (2007). The receptor-like kinase SERK3/BAK1 is a central regulator of innate immunity in plants. Proceedings of the National Academy of Sciences **104,** 12217-12222.

Heidrich, K., Wirthmueller, L., Tasset, C., Pouzet, C., Deslandes, L., and Parker, J.E. (2011). Arabidopsis EDS1 Connects Pathogen Effector Recognition to Cell Compartment–Specific Immune Responses. Science **334,** 1401-1404.

Heijenoort, J.v. (2001). Formation of the glycan chains in the synthesis of bacterial peptidoglycan. Glycobiology **11,** 25R-36R.

Helft, L., Reddy, V., Chen, X., Koller, T., Federici, L., Fernández-Recio, J., Gupta, R., and Bent, A. (2011). LRR Conservation Mapping to Predict Functional Sites within Protein Leucine-Rich Repeat Domains. PLos ONE **6,** e21614.

Hinsch, M., and Staskawicz, B. (1996). Identification of a new *Arabidopsis* disease resistance locus, RPs4, and cloning of the corresponding avirulence gene, avrRps4, from *Pseudomonas syringae* pv. *pisi.* Molecular Plant Microbe Interaction **9,** 55-61.

Hiroki, S., Satoshi, K., Nobuhiko, M., Tomoko, T., Etsuko, H., Norihiro, M., and Chikara, O. (2010). Characterization of a Novel Isoform of *Arabidopsis* PP2C, *At*PP2CF1. 21st International conference on *Arabidopsis* research

Holton, N., Caño-Delgado, A., Harrison, K., Montoya, T., Chory, J., and Bishop, G.J. (2007). Tomato BRASSINOSTEROID INSENSITIVE1 Is Required for Systemin-Induced Root Elongation in *Solanum pimpinellifolium* but Is Not Essential for Wound Signaling. The Plant Cell **19,** 1709-1717.

Huang, F.L., and Glinsmann, W.H. (1976). Separation and characterization of two phosphorylase phosphatase inhibitors from rabbit skeletal muscle. Eur J Biochem **70,** 419–426.

Huffaker, A., Pearce, G., and Ryan, C.A. (2006). An endogenous peptide signal in *Arabidopsis* activates components of the innate immune response. Proceedings of the National Academy of Sciences **103,** 10098-10103.

Huffaker, A., Dafoe, N.J., and Schmelz, E.A. (2011). ZmPep1, an Ortholog of Arabidopsis Elicitor Peptide 1, Regulates Maize Innate Immunity and Enhances Disease Resistance. Plant Physiology **155,** 1325-1338.

Ichimura, K., Casais, C., Peck, S.C., Shinozaki, K., and Shirasu, K. (2006). MEKK1 Is Required for MPK4 Activation and Regulates Tissue-specific and Temperature-dependent Cell Death in *Arabidopsis*. Journal of Biological Chemistry **281,** 36969-36976.

Iizasa, E.i., Mitsutomi, M., and Nagano, Y. (2010). Direct Binding of a Plant LysM Receptor-like Kinase, LysM RLK1/CERK1, to Chitin in Vitro. Journal of Biological Chemistry **285,** 2996-3004.

Jabs, T., Tschöpe, M., Colling, C., Hahlbrock, K., and Scheel, D. (1997). Elicitor-stimulated ion fluxes and O2− from the oxidative burst are essential components in triggering defense gene activation and phytoalexin synthesis in parsley. Proceedings of the National Academy of Sciences **94,** 4800-4805.

Jacobs, A.K., Lipka, V., Burton, R.A., Panstruga, R., Strizhov, N., Schulze-Lefert, P., and Fincher, G.B. (2003). An *Arabidopsis* Callose Synthase, GSL5, Is Required for Wound and Papillary Callose Formation. The Plant Cell **15,** 2503-2513.

Jeppesen, M.G., Navratil, T., Spremulli, L.L., and Nyborg, J. (2005). Crystal Structure of the Bovine Mitochondrial Elongation Factor Tu·Ts Complex. Journal of Biological Chemistry **280,** 5071-5081.

Jeworutzki, E., Roelfsema, M.R.G., Anschütz, U., Krol, E., Elzenga, J.T.M., Felix, G., Boller, T., Hedrich, R., and Becker, D. (2010). Early signaling through the *Arabidopsis* pattern recognition receptors FLS2 and EFR involves Ca2+-associated opening of plasma membrane anion channels. The Plant Journal **62,** 367-378.

Jin, H., Cominelli, E., Bailey, P., Parr, A., Mehrtens, F., Jones, J., Tonelli, C., Weisshaar, B., and Martin, C. (2000). Transcriptional repression by AtMYB4 controls production of UV-protecting sunscreens in *Arabidopsis*. EMBO Journal **19,** 6150-6161.

Johansen, J.W., and Ingebritsen, T.S. (1986). Phosphorylation and inactivation of protein phosphatase 1 by pp60v-src. Proceedings of the National Academy of Sciences **83,** 207-211.

Jones, J.D.G., and Dangl, J.L. (2006). The plant immune system. Nature **444,** 323-329.

Jurkowski, G.I., Smith, R.K., Yu, I.c., Ham, J.H., Sharma, S.B., Klessig, D.F., Fengler, K.A., and Bent, A.F. (2004). Arabidopsis DND2, a Second Cyclic Nucleotide-Gated Ion Channel Gene for Which Mutation Causes the “Defense, No Death” Phenotype. Molecular Plant-Microbe Interactions **17,** 511-520.

Kadota, Y., Goh, T., Tomatsu, H., Tamauchi, R., Higashi, K., Muto, S., and Kuchitsu, K. (2004). Cryptogein-Induced Initial Events in Tobacco BY-2 Cells: Pharmacological Characterization of Molecular Relationship among Cytosolic Ca2+ Transients, Anion Efflux and Production of Reactive Oxygen Species. Plant and Cell Physiology **45,** 160-170.

Kaku, H., Nishizawa, Y., Ishii-Minami, N., Akimoto-Tomiyama, C., Dohmae, N., Takio, K., Minami, E., and Shibuya, N. (2006). Plant cells recognize chitin fragments for defense signaling through a plasma membrane receptor. Proceedings of the National Academy of Sciences **103,** 11086-11091.

Käll, L., Krogh, A., and Sonnhammer, E.L.L. (2004). A Combined Transmembrane Topology and Signal Peptide Prediction Method. Journal of Molecular Biology **338,** 1027-1036.

Katsir, L., Schilmiller, A.L., Staswick, P.E., He, S.Y., and Howe, G.A. (2008). COI1 is a critical component of a receptor for jasmonate and the bacterial virulence factor coronatine. Proceedings of the National Academy of Sciences **105,** 7100-7105.

Kay, S., Hahn, S., Marois, E., Hause, G., and Bonas, U. (2007). A Bacterial Effector Acts as a Plant Transcription Factor and Induces a Cell Size Regulator. Science **318,** 648-651.

Kieffer, M., Master, V., Waites, R., and Davies, B. (2011). TCP14 and TCP15 affect internode length and leaf shape in *Arabidopsis*. The Plant Journal **68,** 147-158.

Kim, J.-G., Taylor, K.W., Hotson, A., Keegan, M., Schmelz, E.A., and Mudgett, M.B. (2008). XopD SUMO Protease Affects Host Transcription, Promotes Pathogen Growth, and Delays Symptom Development in *Xanthomonas*-Infected Tomato Leaves. The Plant Cell Online **20,** 1915-1929.

Kim, M.G., da Cunha, L., McFall, A.J., Belkhadir, Y., DebRoy, S., Dangl, J.L., and Mackey, D. (2005). Two *Pseudomonas syringae* Type III Effectors Inhibit RIN4-Regulated Basal Defense in *Arabidopsis*. Cell **121,** 749-759.

King, K.E., Moritz, T., and Harberd, N.P. (2001). Gibberellins Are Not Required for Normal Stem Growth in *Arabidopsis thaliana* in the Absence of GAI and RGA. Genetics **159,** 767-776.

Kinoshita, E., Kinoshita-Kikuta, E., Takiyama, K., and Koike, T. (2006). Phosphate-binding Tag, a New Tool to Visualize Phosphorylated Proteins. Molecular & Cellular Proteomics **5,** 749-757.

Kloek, A.P., Verbsky, M.L., Sharma, S.B., Schoelz, J.E., Vogel, J., Klessig, D.F., and Kunkel, B.N. (2001). Resistance to *Pseudomonas syringae* conferred by an *Arabidopsis thaliana* coronatine-insensitive (coi1) mutation occurs through two distinct mechanisms. The Plant Journal **26,** 509-522.

Kong, Q., Qu, N., Gao, M., Zhang, Z., Ding, X., Yang, F., Li, Y., Dong, O.X., Chen, S., Li, X., and Zhang, Y. (2012). The MEKK1-MKK1/MKK2-MPK4 Kinase Cascade Negatively Regulates Immunity Mediated by a Mitogen-Activated Protein Kinase Kinase Kinase in Arabidopsis. The Plant Cell Online **24,** 2225-2236.

Kranz, H.D., Denekamp, M., Greco, R., Jin, H., Leyva, A., Meissner, R.C., Petroni, K., Urzainqui, A., Bevan, M., Martin, C., Smeekens, S., Tonelli, C., Paz-Ares, J., and Weisshaar, B. (1998). Towards functional characterisation of the members of the R2R3-MYB gene family from *Arabidopsis thaliana*. The Plant Journal **16,** 263-276.

Krol, E., Mentzel, T., Chinchilla, D., Boller, T., Felix, G., Kemmerling, B., Postel, S., Arents, M., Jeworutzki, E., Al-Rasheid, K.A.S., Becker, D., and Hedrich, R. (2010). Perception of the *Arabidopsis* Danger Signal Peptide 1 Involves the Pattern Recognition Receptor AtPEPR1 and Its Close Homologue AtPEPR2. Journal of Biological Chemistry **285,** 13471-13479.

Kuhn, J.M., Boisson-Dernier, A., Dizon, M.B., Maktabi, M.H., and Schroeder, J.I. (2006). The Protein Phosphatase AtPP2CA Negatively Regulates Abscisic Acid Signal Transduction in *Arabidopsis*, and Effects of *abh1* on AtPP2CA mRNA. Plant Physiology **140,** 127-139.

Kunkel, B.N., and Brooks, D.M. (2002). Cross talk between signaling pathways in pathogen defense. Current Opinion in Plant Biology **5,** 325-331.

Kunze, G., Zipfel, C., Robatzek, S., Niehaus, K., Boller, T., and Felix, G. (2004). The N Terminus of Bacterial Elongation Factor Tu Elicits Innate Immunity in *Arabidopsis* Plants. The Plant Cell Online **16,** 3496-3507.

Kuwahara, H., Nishizaki, M., and Kanazawa, H. (2008). Nuclear Localization Signal and Phosphorylation of Serine350 Specify Intracellular Localization of DRAK2. Journal of Biochemistry **143,** 349-358.

Kwaaitaal, M., Huisman, R., Maintz, J., Reinstädler, A., and Panstruga, R. (2011). Ionotropic glutamate receptor (iGluR)-like channels mediate MAMP-induced calcium influx in Arabidopsis thaliana. Biochemical Journal **440,** 355-365.

Lacombe, S., Rougon-Cardoso, A., Sherwood, E., Peeters, N., Dahlbeck, D., van Esse, H.P., Smoker, M., Rallapalli, G., Thomma, B.P.H.J., Staskawicz, B., Jones, J.D.G., and Zipfel, C. (2010). Interfamily transfer of a plant pattern-recognition receptor confers broad-spectrum bacterial resistance. Nat Biotech **28,** 365-369.

Laluk, K., Luo, H., Chai, M., Dhawan, R., Lai, Z., and Mengiste, T. (2011). Biochemical and Genetic Requirements for Function of the Immune Response Regulator BOTRYTIS-INDUCED KINASE1 in Plant Growth, Ethylene Signaling, and PAMP-Triggered Immunity in Arabidopsis. The Plant Cell Online **23,** 2831-2849.

Lanfermeijer, F.C., Staal, M., Malinowski, R., Stratmann, J.W., and Elzenga, J.T.M. (2008). Micro-Electrode Flux Estimation Confirms That the Solanum pimpinellifolium cu3 Mutant Still Responds to Systemin. Plant Physiology **146,** 129-139.

Lee, H., Chah, O.-K., and Sheen, J. (2011). Stem-cell-triggered immunity through CLV3p-FLS2 signalling. Nature **473,** 376-379.

Lee, M.W., Jelenska, J., and Greenberg, J.T. (2008). *Arabidopsis* proteins important for modulating defense responses to *Pseudomonas syringae* that secrete HopW1-1. The Plant Journal **54,** 452-465.

Lee, S.-W., Han, S.-W., Sririyanum, M., Park, C.-J., Seo, Y.-S., and Ronald, P.C. (2009). A Type I–Secreted, Sulfated Peptide Triggers XA21-Mediated Innate Immunity. Science **326,** 850-853.

Lee, S., Cheng, H., King, K.E., Wang, W., He, Y., Hussain, A., Lo, J., Harberd, N.P., and Peng, J. (2002). Gibberellin regulates *Arabidopsis* seed germination via RGL2, a GAI/RGA-like gene whose expression is up-regulated following imbibition. Genes & Development **16,** 646-658.

Li, G., Meng, X., Wang, R., Mao, G., Han, L., Liu, Y., and Zhang, S. (2012a). Dual-Level Regulation of ACC Synthase Activity by MPK3/MPK6 Cascade and Its Downstream WRKY Transcription Factor during Ethylene Induction in Arabidopsis. PLoS Genet **8,** e1002767.

Li, J., Wen, J., Lease, K.A., Doke, J.T., Tax, F.E., and Walker, J.C. (2002). BAK1, an *Arabidopsis* LRR Receptor-like Protein Kinase, Interacts with BRI1 and Modulates Brassinosteroid Signaling. Cell **110,** 213-222.

Li, J., Zhao-Hui, C., Batoux, M., Nekrasov, V., Roux, M., Chinchilla, D., Zipfel, C., and Jones, J.D.G. (2009). Specific ER quality control

components required for biogenesis of the plant innate immune receptor EFR. Proceedings of the National Academy of Sciences **106,** 15973-15978.

Li, W., Ahn, I.-P., Ning, Y., Park, C.-H., Zeng, L., Whitehill, J.G.A., Lu, H., Zhao, Q., Ding, B., Xie, Q., Zhou, J.-M., Dai, L., and Wang, G.-L. (2012b). The U-Box/ARM E3 Ligase PUB13 Regulates Cell Death, Defense, and Flowering Time in Arabidopsis. Plant Physiology **159,** 239-250.

Li, X., Lin, H., Zhang, W., Zou, Y., Zhang, J., Tang, X., and Zhou, J.-M. (2005). Flagellin induces innate immunity in nonhost interactions that is suppressed by Pseudomonas syringae effectors. Proceedings of the National Academy of Sciences of the United States of America **102,** 12990-12995.

Li, Y., Zheng, L., Corke, F., Smith, C., and Bevan, M.W. (2008). Control of final seed and organ size by the DA1 gene family in *Arabidopsis thaliana*. Genes & Development **22,** 1331-1336.

Li, Y.M., and Casida, J.E. (1992). Cantharidin binding protein identification as protein phosphatase 2A. Proceedings of the National Academy of Sciences **89,** 11867-11870.

Li, Z.-Y., Li, B., and Dong, A.-W. (2012c). The Arabidopsis Transcription Factor AtTCP15 Regulates Endoreduplication by Modulating Expression of Key Cell-cycle Genes. Molecular Plant **5,** 270-280.

Ling, J., and Kumar, R. (2012). Crosstalk between NFkB and glucocorticoid signaling: A potential target of breast cancer therapy. Cancer letters **322,** 119-126.

Liu, J., Elmore, J.M., Fuglsang, A.T., Palmgren, M.G., Staskawicz, B.J., and Coaker, G. (2009). RIN4 Functions with Plasma Membrane H^+-ATPases to Regulate Stomatal Apertures during Pathogen Attack. PLoS Biology. **7,** e1000139.

Liu, T., Liu, Z., Song, C., Hu, Y., Han, Z., She, J., Fan, F., Wang, J., Jin, C., Chang, J., Zhou, J.-M., and Chai, J. (2012). Chitin-Induced Dimerization Activates a Plant Immune Receptor. Science **336,** 1160-1164.

Liu, Y., and Zhang, S. (2004). Phosphorylation of 1-Aminocyclopropane-1-Carboxylic Acid Synthase by MPK6, a Stress-Responsive Mitogen-Activated Protein Kinase, Induces Ethylene Biosynthesis in *Arabidopsis*. The Plant Cell Online **16,** 3386-3399.

Lotze, M.T., Zeh, H.J., Rubartelli, A., Sparvero, L.J., Amoscato, A.A., Washburn, N.R., DeVera, M.E., Liang, X., Tör, M., and Billiar, T. (2007). The grateful dead: damage-associated molecular pattern molecules and reduction/oxidation regulate immunity. Immunological Reviews **220,** 60-81.

Lu, D., Wu, S., He, P., and Shan, L. (2010a). Phosphorylation of receptor-like cytoplasmic kinases by bacterial flagellin. Plant Signaling & Behavior **5,** 598-600.

Lu, D., Wu, S., Gao, X., Zhang, Y., Shan, L., and He, P. (2010b). A receptor-like cytoplasmic kinase, BIK1, associates with a flagellin receptor complex to initiate plant innate immunity. Proceedings of the National Academy of Sciences **107,** 496-501.

Lu, D., Lin, W., Gao, X., Wu, S., Cheng, C., Avila, J., Heese, A., Devarenne, T.P., He, P., and Shan, L. (2011). Direct Ubiquitination of Pattern Recognition Receptor FLS2 Attenuates Plant Innate Immunity. Science **332,** 1439-1442.

Lu, X., Tintor, N., Mentzel, T., Kombrink, E., Boller, T., Robatzek, S., Schulze-Lefert, P., and Saijo, Y. (2009). Uncoupling of sustained MAMP receptor signaling from early outputs in an Arabidopsis endoplasmic reticulum glucosidase II allele. Proceedings of the National Academy of Sciences **106,** 22522-22527.

Luan, S. (2003). Protein Phosphatases in Plants. Annual Review of Plant Biology **54,** 63-92.

Lukasik, E., and Takken, F.L.W. (2009). STANDing strong, resistance proteins instigators of plant defence. Current Opinion in Plant Biology **12,** 427-436.

Lumbreras, V., Vilela, B., Irar, S., Solé, M., Capellades, M., Valls, M., Coca, M., and Pagès, M. (2010). MAPK phosphatase MKP2 mediates disease responses in *Arabidopsis* and functionally interacts with MPK3 and MPK6. The Plant Journal **63,** 1017-1030.

Ma, W., and Berkowitz, G.A. (2007). The grateful dead: calcium and cell death in plant innate immunity. Cellular Microbiology **9,** 2571-2585.

Macho, A.P., Boutrot, F., Rathjen, J.P., and Zipfel, C. (2012). ASPARTATE OXIDASE Plays an Important Role in Arabidopsis Stomatal Immunity. Plant Physiology **159,** 1845-1856.

Mackey, D., and McFall, A.J. (2006). MAMPs and MIMPs: proposed classifications for inducers of innate immunity. Molecular Microbiology **61,** 1365-1371.

Mackey, D., Holt, B.F., Wiig, A., and Dangl, J.L. (2002). RIN4 Interacts with *Pseudomonas syringae* Type III Effector Molecules and Is Required for RPM1-Mediated Resistance in *Arabidopsis*. Cell **108,** 743-754.

Mackey, D., Belkhadir, Y., Alonso, J.M., Ecker, J.R., and Dangl, J.L. (2003). Arabidopsis RIN4 Is a Target of the Type III Virulence Effector AvrRpt2 and Modulates RPS2-Mediated Resistance. Cell **112,** 379-389.

Malinowski, R., Higgins, R., Luo, Y., Piper, L., Nazir, A., Bajwa, V., Clouse, S., Thompson, P., and Stratmann, J. (2009). The tomato brassinosteroid receptor BRI1 increases binding of systemin to tobacco plasma membranes, but is not involved in systemin signaling. Plant Molecular Biology **70,** 603-616.

Marfà, V., Gollin, D.J., Eberhard, S., Mohnen, D., Dan/ill, A., and Albersheim, P. (1991). Oligogalacturonides are able to induce flowers to form on tobacco explants. The Plant Journal **1,** 217-225.

Marois, E., Van den Ackerveken, G., and Bonas, U. (2002). The *Xanthomonas* Type III Effector Protein AvrBs3 Modulates Plant Gene Expression and Induces Cell Hypertrophy in the Susceptible Host. Molecular Plant-Microbe Interactions **15,** 637-646.

Matzinger, P. (2002). The Danger Model: A Renewed Sense of Self. Science **296,** 301-305.

Medzhitov, R., and Janeway, C.A. (2002). Decoding the Patterns of Self and Nonself by the Innate Immune System. Science **296,** 298-300.

Melotto, M., Underwood, W., and He, S.Y. (2008). Role of Stomata in Plant Innate Immunity and Foliar Bacterial Diseases. Annual Review of Phytopathology **46,** 101-122.

Melotto, M., Underwood, W., Koczan, J., Nomura, K., and He, S.Y. (2006). Plant Stomata Function in Innate Immunity against Bacterial Invasion. Cell **126,** 969-980.

Merlot, S., Mustilli, A.-C., Genty, B., North, H., Lefebvre, V., Sotta, B., Vavasseur, A., and Giraudat, J. (2002). Use of infrared thermal imaging to isolate *Arabidopsis* mutants defective in stomatal regulation. The Plant Journal **30,** 601-609.

Merlot, S., Leonhardt, N., Fenzi, F., Valon, C., Costa, M., Piette, L., Vavasseur, A., Genty, B., Boivin, K., Muller, A., Giraudat, J., and Leung, J. (2007). Constitutive activation of a plasma membrane H^+-ATPase prevents abscisic acid-mediated stomatal closure. EMBO Journal **26,** 3216-3226.

Mersmann, S., Bourdais, G., Rietz, S., and Robatzek, S. (2010). Ethylene Signaling Regulates Accumulation of the FLS2 Receptor and Is Required for the Oxidative Burst Contributing to Plant Immunity. Plant Physiology **154,** 391-400.

Meskiene, I., Baudouin, E., Schweighofer, A., Liwosz, A., Jonak, C., Rodriguez, P.L., Jelinek, H., and Hirt, H. (2003). Stress-induced Protein Phosphatase 2C Is a Negative Regulator of a Mitogen-activated Protein Kinase. Journal of Biological Chemistry **278,** 18945-18952.

Mészáros, T., Helfer, A., Hatzimasoura, E., Magyar, Z., Serazetdinova, L., Rios, G., Bardóczy, V., Teige, M., Koncz, C., Peck, S., and Bögre, L. (2006). The *Arabidopsis* MAP kinase kinase MKK1 participates in defence responses to the bacterial elicitor flagellin. The Plant Journal **48,** 485-498.

Miaczynska, M., Pelkmans, L., and Zerial, M. (2004). Not just a sink: endosomes in control of signal transduction. Current Opinion in Cell Biology **16,** 400-406.

Mingossi, F., Matos, J., Rizzato, A., Medeiros, A., Falco, M., Silva-Filho, M., and Moura, D. (2010). SacRALF1, a peptide signal from the grass sugarcane *Saccharum spp*., is potentially involved in the regulation of tissue expansion. Plant Molecular Biology **73,** 271-281.

Mithöfer, A., Fliegmann, J., Neuhaus-Url, G., Schwarz, H., and Ebel, J. (2000). The Hepta-Glucoside Elicitor-Binding Proteins from Legumes Represent a Putative Receptor Family. In Biological Chemistry, pp. 705.

Miya, A., Albert, P., Shinya, T., Desaki, Y., Ichimura, K., Shirasu, K., Narusaka, Y., Kawakami, N., Kaku, H., and Shibuya, N. (2007). CERK1, a LysM receptor kinase, is essential for chitin elicitor signaling in *Arabidopsis*. Proceedings of the National Academy of Sciences **104,** 19613-19618.

Monaghan, J., and Zipfel, C. (2012). Plant pattern recognition receptor complexes at the plasma membrane. Current Opinion in Plant Biology **in press**.

Moscou, M.J., and Bogdanove, A.J. (2009). A Simple Cipher Governs DNA Recognition by TAL Effectors. Science **326,** 1501.

Mucyn, T.S., Clemente, A., Andriotis, V.M.E., Balmuth, A.L., Oldroyd, G.E.D., Staskawicz, B.J., and Rathjen, J.P. (2006). The Tomato NBARC-LRR Protein Prf Interacts with Pto Kinase in Vivo to Regulate Specific Plant Immunity. The Plant Cell Online **18,** 2792-2806.

Mueller, K., Bittel, P., Chinchilla, D., Jehle, A.K., Albert, M., Boller, T., and Felix, G. (2012). Chimeric FLS2 Receptors Reveal the Basis for Differential Flagellin Perception in Arabidopsis and Tomato. The Plant Cell Online **24,** 2213-2224.

Mur, L.A.J., Kenton, P., Lloyd, A.J., Ougham, H., and Prats, E. (2008). The hypersensitive response; the centenary is upon us but how much do we know? Journal of Experimental Botany **59,** 501-520.

Naito, K., Taguchi, F., Suzuki, T., Inagaki, Y., Toyoda, K., Shiraishi, T., and Ichinose, Y. (2008). Amino Acid Sequence of Bacterial Microbe-Associated Molecular Pattern flg22 Is Required for Virulence. Molecular Plant-Microbe Interactions **21,** 1165-1174.

Nakagami, H., Soukupová, H., Schikora, A., Zárský, V., and Hirt, H. (2006). A Mitogen-activated Protein Kinase Kinase Kinase Mediates Reactive Oxygen Species Homeostasis in *Arabidopsis*. Journal of Biological Chemistry **281,** 38697-38704.

Nam, K.H., and Li, J. (2002). BRI1/BAK1, a Receptor Kinase Pair Mediating Brassinosteroid Signaling. Cell **110,** 203-212.

Nambirajan, S., Radha, V., Kamatkar, S., and Swarup, G. (2000). PTP-S2, a nuclear tyrosine phosphatase, is phosphorylated and excluded from condensed chromosomes during mitosis. Journal of Biosciences **25,** 33-40.

Navarro, L., Zipfel, C., Rowland, O., Keller, I., Robatzek, S., Boller, T., and Jones, J.D.G. (2004). The Transcriptional Innate Immune Response to flg22. Interplay and Overlap with Avr Gene-Dependent Defense Responses and Bacterial Pathogenesis. Plant Physiology **135,** 1113-1128.

Navarro, L., Bari, R., Achard, P., Lisón, P., Nemri, A., Harberd, N.P., and Jones, J.D.G. (2008). DELLAs Control Plant Immune Responses by Modulating the Balance of Jasmonic Acid and Salicylic Acid Signaling. Current Biology **18,** 650-655.

Nekrasov, V., Li, J., Batoux, M., Roux, M., Chu, Z.-H., Lacombe, S., Rougon, A., Bittel, P., Kiss-Papp, M., Chinchilla, D., van Esse, H.P., Jorda, L., Schwessinger, B., Nicaise, V., Thomma, B.P.H.J., Molina, A., Jones, J.D.G., and Zipfel, C. (2009). Control of the pattern-recognition receptor EFR by an ER protein complex in plant immunity. EMBO Journal **28,** 3428-3438.

Nicaise, V., Roux, M., and Zipfel, C. (2009). Recent Advances in PAMP-Triggered Immunity against Bacteria: Pattern Recognition Receptors Watch over and Raise the Alarm. Plant Physiology **150,** 1638-1647.

Nishimura, M.T., Stein, M., Hou, B.-H., Vogel, J.P., Edwards, H., and Somerville, S.C. (2003). Loss of a Callose Synthase Results in Salicylic Acid-Dependent Disease Resistance. Science **301,** 969-972.

Nomura, K., DebRoy, S., Lee, Y.H., Pumplin, N., Jones, J., and He, S.Y. (2006). A Bacterial Virulence Protein Suppresses Host Innate Immunity to Cause Plant Disease. Science **313,** 220-223.

Nomura, K., Mecey, C., Lee, Y.-N., Imboden, L.A., Chang, J.H., and He, S.Y. (2011). Effector-triggered immunity blocks pathogen degradation of an immunity-associated vesicle traffic regulator in *Arabidopsis*. Proceedings of the National Academy of Sciences **108,** 10774-10779.

Ntoukakis, V., Schwessinger, B., Segonzac, C., and Zipfel, C. (2011). Cautionary Notes on the Use of C-Terminal BAK1 Fusion Proteins for Functional Studies. The Plant Cell Online **23,** 3871-3878.

Nuernberger, T., and Lipka, V. (2005). Non-host resistance in plants: new insights into an old phenomenon. Molecular Plant Pathology **6,** 335-345.

Nühse, T.S., Peck, S.C., Hirt, H., and Boller, T. (2000). Microbial Elicitors Induce Activation and Dual Phosphorylation of the Arabidopsis thaliana MAPK 6. Journal of Biological Chemistry **275,** 7521-7526.

Nühse, T.S., Stensballe, A., Jensen, O.N., and Peck, S.C. (2004). Phosphoproteomics of the *Arabidopsis* Plasma Membrane and a New Phosphorylation Site Database. The Plant Cell Online **16,** 2394-2405.

Nühse, T.S., Bottrill, A.R., Jones, A.M.E., and Peck, S.C. (2007). Quantitative phosphoproteomic analysis of plasma membrane proteins reveals regulatory mechanisms of plant innate immune responses. The Plant Journal **51,** 931-940.

Nürnberger, T., Nennstiel, D., Jabs, T., Sacks, W.R., Hahlbrock, K., and Scheel, D. (1994). High affinity binding of a fungal oligopeptide elicitor to parsley plasma membranes triggers multiple defense responses. Cell **78,** 449-460.

Olsen, A.N., Mundy, J., and Skriver, K. (2002). Peptomics, identification of novel cationic *Arabidopsis* peptides with conserved sequence motifs In Silico Biology **2**.

Opgen-Rhein, R., and Strimmer, K. (2007). From correlation to causation networks: a simple approximate learning algorithm and its application to high-dimensional plant gene expression data. BMC Systems Biology **1,** 37.

Pandey, S.P., and Somssich, I.E. (2009). The Role of WRKY Transcription Factors in Plant Immunity. Plant Physiology **150,** 1648-1655.

Pandey, S.P., Roccaro, M., Schön, M., Logemann, E., and Somssich, I.E. (2010). Transcriptional reprogramming regulated by WRKY18 and WRKY40 facilitates powdery mildew infection of *Arabidopsis*. The Plant Journal **64,** 912-923.

Park, C.-J., and Ronald, P.C. (2012). Cleavage and nuclear localization of the rice XA21 immune receptor. Nature **3,** 920.

Park, C.-J., Bart, R., Chern, M., Canlas, P.E., Bai, W., and Ronald, P.C. (2010). Overexpression of the Endoplasmic Reticulum Chaperone BiP3 Regulates XA21-Mediated Innate Immunity in Rice. PLos ONE **5,** e9262.

Park, C.J., Peng, Y., Chen, X., Dardick, C., Ruan, D., Bart, R., Canlas, P.E., and Ronald, P.C. (2008). Rice XB15, a protein phosphatase 2C, negatively regulates cell death and XA21-mediated innate immunity. PLoS Biology **6,** e231.

Pearce, G., and Ryan, C.A. (2003). Systemic Signaling in Tomato Plants for Defense against Herbivores. Journal of Biological Chemistry **278,** 30044-30050.

Pearce, G., Moura, D.S., Stratmann, J., and Ryan, C.A. (2001a). RALF, a 5-kDa ubiquitous polypeptide in plants, arrests root growth and development. Proceedings of the National Academy of Sciences **98,** 12843-12847.

Pearce, G., Moura, D.S., Stratmann, J., and Ryan, C.A. (2001b). Production of multiple plant hormones from a single polyprotein precursor. Nature **411,** 817-820.

Pearce, G., Siems, W.F., Bhattacharya, R., Chen, Y.-C., and Ryan, C.A. (2007). Three Hydroxyproline-rich Glycopeptides Derived from a Single Petunia Polyprotein Precursor Activate defensin I, a Pathogen Defense Response Gene. Journal of Biological Chemistry **282,** 17777-17784.

Pearce, G., Bhattacharya, R., Chen, Y.-C., Barona, G., Yamaguchi, Y., and Ryan, C.A. (2009). Isolation and Characterization of Hydroxyproline-Rich Glycopeptide Signals in Black Nightshade Leaves. Plant Physiology **150,** 1422-1433.

Pederson, T.M., Kramer, D.L., and Rondinone, C.M. (2001). Serine/Threonine Phosphorylation of IRS-1 Triggers Its Degradation. Diabetes **50,** 24-31.

Pedley, K.F., and Martin, G.B. (2005). Role of mitogen-activated protein kinases in plant immunity. Current Opinion in Plant Biology **8,** 514-517.

Peng, Y., Bartley, L.E., Chen, X., Dardick, C., Chern, M., Ruan, R., Canlas, P.E., and Ronald, P.C. (2008). OsWRKY62 is a Negative Regulator of Basal and Xa21-Mediated Defense against Xanthomonas oryzae pv. oryzae in Rice. Molecular Plant **1,** 446-458.

Peter, C., Repetti, P.P., Day, B., Dahlbeck, D., Mehlert, A., and Staskawicz, B.J. (2004). Overexpression of the plasma membrane-localized NDR1 protein results in enhanced bacterial disease resistance in *Arabidopsis* thaliana. The Plant Journal **40,** 225-237.

Petersen, M., Brodersen, P., Naested, H., Andreasson, E., Lindhart, U., Johansen, B., Nielsen, H.B., Lacy, M., Austin, M.J., Parker, J.E., Sharma, S.B., Klessig, D.F., Martienssen, R., Mattsson, O., Jensen, A.B., and Mundy, J. (2000). *Arabidopsis* MAP Kinase 4 Negatively Regulates Systemic Acquired Resistance. Cell **103,** 1111-1120.

Petersen, T.N., Brunak, S., von Heijne, G., and Nielsen, H. (2011). SignalP 4.0: discriminating signal peptides from transmembrane regions. Nat Meth **8,** 785-786.

Petutschnig, E.K., Jones, A.M.E., Serazetdinova, L., Lipka, U., and Lipka, V. (2010). The Lysin Motif Receptor-like Kinase (LysM-RLK) CERK1 Is a Major Chitin-binding Protein in *Arabidopsis thaliana* and Subject to Chitin-induced Phosphorylation. Journal of Biological Chemistry **285,** 28902-28911.

Phee, B.-K., Kim, J.-I., Shin, D.H., Yoo, J., Park, K.-J., Han, Y.-J., Kwon, Y.-K., Cho, M.-H., Jeon, J.-S., Bhoo, S.H., and Hahn, T.-R. (2008). A novel protein phosphatase indirectly regulates phytochrome-interacting factor 3 via phytochrome. Biochem J **415,** 247-255.

Pierleoni, A., Martelli, P., and Casadio, R. (2008). PredGPI: a GPI-anchor predictor. BMC Bioinformatics **9,** 392.

Portbury, A.L., Ronnebaum, S.M., Zungu, M., Patterson, C., and Willis, M.S. (2012). Back to your heart: Ubiquitin proteasome system-regulated signal transduction. Journal of Molecular and Cellular Cardiology **52,** 526-537.

Postel, S., and Kemmerling, B. (2009). Plant systems for recognition of pathogen-associated molecular patterns. Seminars in Cell & Developmental Biology **20,** 1025-1031.

Postel, S., Küfner, I., Beuter, C., Mazzotta, S., Schwedt, A., Borlotti, A., Halter, T., Kemmerling, B., and Nürnberger, T. (2010). The multifunctional leucine-rich repeat receptor kinase BAK1 is implicated in *Arabidopsis* development and immunity. European Journal of Cell Biology **89,** 169-174.

Preston, J., Wheeler, J., Heazlewood, J., Li, S.F., and Parish, R.W. (2004). AtMYB32 is required for normal pollen development in *Arabidopsis thaliana*. The Plant Journal **40,** 979-995.

Promega. (2009). Serine/Threonine Phosphatase Assay System Technical Bulletin. TB218.

Pugin, A., Frachisse, J.M., Tavernier, E., Bligny, R., Gout, E., Douce, R., and Guern, J. (1997). Early Events Induced by the Elicitor Cryptogein in Tobacco Cells: Involvement of a Plasma Membrane NADPH Oxidase and Activation of Glycolysis and the Pentose Phosphate Pathway. The Plant Cell Online **9,** 2077-2091.

Punta, M., Coggill, P.C., Eberhardt, R.Y., Mistry, J., Tate, J., Boursnell, C., Pang, N., Forslund, K., Ceric, G., Clements, J., Heger, A., Holm, L., Sonnhammer, E.L.L., Eddy, S.R., Bateman, A., and Finn, R.D. (2012). The Pfam protein families database. Nucleic Acids Research **40,** 290-301.

Qi, Z., Verma, R., Gehring, C., Yamaguchi, Y., Zhao, Y., Ryan, C.A., and Berkowitz, G.A. (2010). Ca2+ signaling by plant *Arabidopsis thaliana* Pep peptides depends on AtPepR1, a receptor with guanylyl cyclase activity, and cGMP-activated Ca2+ channels. Proceedings of the National Academy of Sciences **107,** 21193-21198.

Qiu, J., Fiil, B., Petersen, K., Nielsen, H., Botanga, C., Thorgrimsen, S., Palma, K., Suarez-Rodriguez, M., Sandbech-Clausen, S., Lichota, J., Brodersen, P., Grasser, K.D., Mattsson, O., Glazebrook, J., Mundy, J., and Petersen, M. (2008). *Arabidopsis* MAP kinase 4 regulates gene expression through transcription factor release in the nucleus. EMBO Journal **27,** 2214-2221.

Raffaele, S., Vailleau, F., Léger, A., Joubès, J., Miersch, O., Huard, C., Blée, E., Mongrand, S., Domergue, F., and Roby, D. (2008). A MYB Transcription Factor Regulates Very-Long-Chain Fatty Acid Biosynthesis for Activation of the Hypersensitive Cell Death Response in *Arabidopsis*. The Plant Cell Online **20,** 752-767.

Ramaiah, M., Jain, A., Baldwin, J.C., Karthikeyan, A.S., and Raghothama, K.G. (2011). Characterization of the Phosphate Starvation-Induced Glycerol-3-phosphate permease Gene Family in *Arabidopsis*. Plant Physiology **157,** 279-291.

Ramakrishnan, C., Dani, V.S., and Ramasarma, T. (2002). A conformational analysis of Walker motif A [GXXXXGKT (S)] in

nucleotide-binding and other proteins. Protein Engineering **15,** 783-798.

Ramos, H.C., Rumbo, M., and Sirard, J.-C. (2004). Bacterial flagellins: mediators of pathogenicity and host immune responses in mucosa. Trends in Microbiology **12,** 509-517.

Ranf, S., Eschen-Lippold, L., Pecher, P., Lee, J., and Scheel, D. (2011). Interplay between calcium signalling and early signalling elements during defence responses to microbe- or damage-associated molecular patterns. The Plant Journal **68,** 100-113.

Raz, V., and Fluhr, R. (1993). Ethylene Signal Is Transduced via Protein Phosphorylation Events in Plants. The Plant Cell Online **5,** 523-530.

Reddy, V.S., and Reddy, A.S.N. (2004). Proteomics of calcium-signaling components in plants. Phytochemistry **65,** 1745-1776.

Ren, F., and Lu, Y.-T. (2006). Overexpression of tobacco hydroxyproline-rich glycopeptide systemin precursor A gene in transgenic tobacco enhances resistance against *Helicoverpa armigera* larvae. Plant Science **171,** 286-292.

Rivas, S. (2012). Nuclear Dynamics during Plant Innate Immunity. Plant Physiology **158,** 87-94.

Rivas, S., and Thomas, C.M. (2002). Recent advances in the study of tomato *Cf* resistance genes. Molecular Plant Pathology **3,** 277-282.

Roach, P., Roach, P.J., and DePaoli-Roach, A.A. (1985). Phosphoprotein phosphatase inhibitor-2. Identification as a species of molecular weight 31,000 in rabbit muscle, liver, and other tissues. Journal of Biological Chemistry **260,** 6314-6317.

Robatzek, S., Chinchilla, D., and Boller, T. (2006). Ligand-induced endocytosis of the pattern recognition receptor FLS2 in *Arabidopsis*. Genes & Development **20,** 537-542.

Robatzek, S., Bittel, P., Chinchilla, D., Köchner, P., Felix, G., Shiu, S.-H., and Boller, T. (2007). Molecular identification and characterization of the tomato flagellin receptor LeFLS2, an orthologue of <i>Arabidopsis</i> FLS2 exhibiting characteristically different perception specificities. Plant Molecular Biology **64,** 539-547.

Robert-Seilaniantz, A., Grant, M., and Jones, J.D.G. (2011). Hormone Crosstalk in Plant Disease and Defense: More Than Just JASMONATE-SALICYLATE Antagonism. Annual Review of Phytopathology **49,** 317-343.

Rodriguez, P.L., Benning, G., and Grill, E. (1998). ABI2, a second protein phosphatase 2C involved in abscisic acid signal transduction in *Arabidopsis*. FEBS Letters **421,** 185-190.

Romeis, T., Piedras, P., and Jones, J.D.G. (2000). Resistance Gene-Dependent Activation of a Calcium-Dependent Protein Kinase in the Plant Defense Response. The Plant Cell Online **12,** 803-815.

Romeis, T., Ludwig, A.A., Martin, R., and Jones, J.D.G. (2001). Calcium-dependent protein kinases play an essential role in a plant defence response. EMBO Journal **20,** 5556-5567.

Römer, P., Hahn, S., Jordan, T., Strauß, T., Bonas, U., and Lahaye, T. (2007). Plant Pathogen Recognition Mediated by Promoter Activation of the Pepper *Bs3* Resistance Gene. Science **318,** 645-648.

Römer, P., Strauss, T., Hahn, S., Scholze, H., Morbitzer, R., Grau, J., Bonas, U., and Lahaye, T. (2009). Recognition of AvrBs3-Like Proteins Is Mediated by Specific Binding to Promoters of Matching Pepper *Bs3* Alleles. Plant Physiology **150,** 1697-1712.

Ron, M., and Avni, A. (2004). The Receptor for the Fungal Elicitor Ethylene-Inducing Xylanase Is a Member of a Resistance-Like Gene Family in Tomato. The Plant Cell Online **16,** 1604-1615.

Ron, M., Kantety, R., Martin, G.B., Avidan, N., Eshed, Y., Zamir, D., and Avni, A. (2000). High-resolution linkage analysis and physical characterization of the EIX-responding locus in tomato. TAG Theoretical and Applied Genetics **100,** 184-189.

Roux, M., Schwessinger, B., Albrecht, C., Chinchilla, D., Jones, A., Holton, N., Malinovsky, F.G., Tör, M., de Vries, S., and Zipfel, C. (2011). The *Arabidopsis* Leucine-Rich Repeat Receptor–Like Kinases BAK1/SERK3 and BKK1/SERK4 Are Required for Innate Immunity to Hemibiotrophic and Biotrophic Pathogens. The Plant Cell Online **23,** 2440-2455.

Rubio, S., Rodrigues, A., Saez, A., Dizon, M.B., Galle, A., Kim, T., Santiago, J., Flexas, J., Schroeder, J.I., and Rodriguez, P.L. (2009). Triple Loss of Function of Protein Phosphatases Type 2C Leads to Partial Constitutive Response to Endogenous Abscisic Acid. Plant Physiology **150,** 1345-1355.

Saez, A., Robert, N., Maktabi, M.H., Schroeder, J.I., Serrano, R., and Rodriguez, P.L. (2006). Enhancement of Abscisic Acid Sensitivity and Reduction of Water Consumption in *Arabidopsis* by Combined Inactivation of the Protein Phosphatases Type 2C ABI1 and HAB1. Plant Physiology **141,** 1389-1399.

Saijo, Y., Tintor, N., Lu, X., Rauf, P., Pajerowska-Mukhtar, K., Haweker, H., Dong, X., Robatzek, S., and Schulze-Lefert, P. (2009). Receptor quality control in the endoplasmic reticulum for plant innate immunity. EMBO Journal **28,** 3439-3449.

Sakai, J., Rawson, R.B., Espenshade, P.J., Cheng, D., Seegmiller, A.C., Goldstein, J.L., and Brown, M.S. (1998). Molecular Identification of the Sterol-Regulated Luminal Protease that Cleaves SREBPs and Controls Lipid Composition of Animal Cells. Molecular Cell **2,** 505-514.

Scheer, J.M., and Ryan, C.A. (2002). The systemin receptor SR160 from *Lycopersicon peruvianum* is a member of the LRR receptor kinase family. Proceedings of the National Academy of Sciences **99,** 9585-9590.

Scheer, J.M., Pearce, G., and Ryan, A.C. (2005). LeRALF, a plant peptide that regulates root growth and development, specifically binds to 25 and 120 kDa cell surface membrane proteins of *Lycopersicon peruvianum* Planta **221,** 667-674.

Schenk, P.M., Kazan, K., Wilson, I., Anderson, J.P., Richmond, T., Somerville, S.C., and Manners, J.M. (2000). Coordinated plant defense responses in *Arabidopsis* revealed by microarray analysis. Proceedings of the National Academy of Sciences **97,** 11655-11660.

Schenke, D., Boettcher, C., and Scheel, D. (2011). Crosstalk between abiotic ultraviolet-B stress and biotic (flg22) stress signalling in *Arabidopsis* prevents flavonol accumulation in favor of pathogen

defence compound production. Plant, Cell & Environment **34,** 1849-1864.

Schmid, M., Davison, T.S., Henz, S.R., Pape, U.J., Demar, M., Vingron, M., Schölkopf, B., Weigel, D., and Lohmann, J. (2005). A gene expression map of *Arabidopsis* development. Nature Genetics **37,** 501-506.

Scholze, H., and Boch, J. (2011). TAL effectors are remote controls for gene activation. Current Opinion in Microbiology **14,** 47-53.

Schulze, B., Mentzel, T., Jehle, A.K., Mueller, K., Beeler, S., Boller, T., Felix, G., and Chinchilla, D. (2010). Rapid Heteromerization and Phosphorylation of Ligand-activated Plant Transmembrane Receptors and Their Associated Kinase BAK1. Journal of Biological Chemistry **285,** 9444-9451.

Schwacke, R., Schneider, A., van der Graaff, E., Fischer, K., Catoni, E., Desimone, M., Frommer, W.B., Flügge, U.-I., and Kunze, R. (2003). ARAMEMNON, a Novel Database for *Arabidopsis* Integral Membrane Proteins. Plant Physiology **131,** 16-26.

Schweighofer, A., Hirt, H., and Meskiene, I. (2004). Plant PP2C phosphatases: emerging functions in stress signaling. Trends in Plant Science **9,** 236-243.

Schweighofer, A., K, azanaviciute, V., Scheikl, E., Teige, M., Doczi, R., Hirt, H., Schwanninger, M., Kant, M., Schuurink, R., Mauch, F., Buchala, A., Cardinale, F., and Meskiene, I. (2007). The PP2C-Type Phosphatase AP2C1, Which Negatively Regulates MPK4 and MPK6, Modulates Innate Immunity, Jasmonic Acid, and Ethylene Levels in *Arabidopsis*. The Plant Cell Online **19,** 2213-2224.

Schwessinger, B., Roux, M., Kadota, Y., Ntoukakis, V., Sklenar, J., Jones, A., and C., Z. (2011). Phosphorylation-Dependent Differential Regulation of Plant Growth, Cell Death, and Innate Immunity by the Regulatory Receptor-Like Kinase BAK1. . 7 **4**.

Segonzac, C., Feike, D., Gimenez-Ibanez, S., Hann, D.R., Zipfel, C., and Rathjen, J.P. (2011). Hierarchy and Roles of Pathogen-Associated Molecular Pattern-Induced Responses in *Nicotiana benthamiana*. Plant Physiology **156,** 687-699.

Segonzac, C., Nimchuk, Z.L., Beck, M., Tarr, P.T., Robatzek, S., Meyerowitz, E.M., and Zipfel, C. (2012). The Shoot Apical Meristem Regulatory Peptide CLV3 Does Not Activate Innate Immunity. The Plant Cell Online.

Servet, C., Benhamed, M., Latrasse, D., Kim, W., Delarue, M., and Zhou, D.-X. (2008). Characterization of a phosphatase 2C protein as an interacting partner of the histone acetyltransferase GCN5 in *Arabidopsis*. Biochimica et Biophysica Acta **1779,** 376-382.

Shah, K., Russinova, E., Gadella, T.W.J., Willemse, J., and de Vries, S.C. (2002). The *Arabidopsis* kinase-associated protein phosphatase controls internalization of the somatic embryogenesis receptor kinase 1. Genes & Development **16,** 1707-1720.

Shan, L., He, P., Li, J., Heese, A., Peck, S.C., Nürnberger, T., Martin, G.B., and Sheen, J. (2008). Bacterial Effectors Target the Common Signaling Partner BAK1 to Disrupt Multiple MAMP Receptor-Signaling

Complexes and Impede Plant Immunity. Cell host & microbes **4,** 17-27.

Sharfman, M., Bar, M., Ehrlich, M., Schuster, S., Melech-Bonfil, S., Ezer, R., Sessa, G., and Avni, A. (2011). Endosomal signaling of the tomato leucine-rich repeat receptor-like protein LeEix2. The Plant Journal **68,** 413-423.

Sheard, L.B., Tan, X., Mao, H., Withers, J., Ben-Nissan, G., Hinds, T.R., Kobayashi, Y., Hsu, F.-F., Sharon, M., Browse, J., He, S.Y., Rizo, J., Howe, G.A., and Zheng, N. (2010). Jasmonate perception by inositol-phosphate-potentiated COI1-JAZ co-receptor. Nature **468,** 400-405.

Sherrier, D.J., Prime, T.A., and Dupree, P. (1999). Glycosylphosphatidylinositol-anchored cell-surface proteins from *Arabidopsis*. Electrophoresis **20,** 2027-2035.

Shibuya, N., and Minami, E. (2001). Oligosaccharide signalling for defence responses in plant. Physiological and Molecular Plant Pathology **59,** 223-233.

Shimizu, T., Nakano, T., Takamizawa, D., Desaki, Y., Ishii-Minami, N., Nishizawa, Y., Minami, E., Okada, K., Yamane, H., Kaku, H., and Shibuya, N. (2010). Two LysM receptor molecules, CEBiP and OsCERK1, cooperatively regulate chitin elicitor signaling in rice. The Plant Journal **64,** 204-214.

Shinya, T., Motoyama, N., Ikeda, A., Wada, M., Kamiya, K., Hayafune, M., Kaku, H., and Naoto, S. (2012). Functional characterization of CEBiP and CERK1 homologs in Arabidopsis and rice reveals the presence of different chitin receptor systems in plants. Plant and Cell Physiology.

Shiu, S.-H., and Bleecker, A.B. (2001). Plant Receptor-Like Kinase Gene Family: Diversity, Function, and Signaling. Sci. STKE **2001,** re22-.

Silipo, A., Erbs, G., Shinya, T., Dow, J.M., Parrilli, M., Lanzetta, R., Shibuya, N., Newman, M.-A., and Molinaro, A. (2010). Glyco-conjugates as elicitors or suppressors of plant innate immunity. Glycobiology **20,** 406-419.

Singh, P., Kuo, Y.-C., Mishra, S., Tsai, C.-H., Chien, C.-C., Chen, C.-W., Desclos-Theveniau, M., Chu, P.-W., Schulze, B., Chinchilla, D., Boller, T., and Zimmerli, L. (2012). The Lectin Receptor Kinase-VI.2 Is Required for Priming and Positively Regulates Arabidopsis Pattern-Triggered Immunity. The Plant Cell Online **24,** 1256-1270.

Song, S.-K., Lee, M.M., and Clark, S.E. (2006). POL and PLL1 phosphatases are CLAVATA1 signaling intermediates required for Arabidopsis shoot and floral stem cells. Development **133,** 4691-4698.

Song, S., Hofhuis, H., Lee, M.M., and Clark, S.E. (2008). Key Divisions in the Early *Arabidopsis* Embryo Require POL and PLL1 Phosphatases to Establish the Root Stem Cell Organizer and Vascular Axis. Developmental cell **15,** 98-109.

Song, W.-Y., Wang, G.-L., Chen, L.-L., Kim, H.-S., Pi, L.-Y., Holsten, T., Gardner, J., Wang, B., Zhai, W.-X., Zhu, L.-H., Fauquet, C., and Ronald, P. (1995). A Receptor Kinase-Like Protein Encoded by the Rice Disease Resistance Gene, Xa21. Science **270,** 1804-1806.

Srivastava, R., Liu, J.-X., Guo, H., Yin, Y., and Howell, S.H. (2009). Regulation and processing of a plant peptide hormone, AtRALF23, in *Arabidopsis*. The Plant Journal **59,** 930-939.

Stepanova, A.N., and Alonso, J.M. (2009). Ethylene signaling and response: where different regulatory modules meet. Current Opinion in Plant Biology **12,** 548-555.

Stone, J.M., Trotochaud, A.E., Walker, J.C., and Clark, S.E. (1998). Control of meristem development by CLAVATA1 receptor kinase and kinase-associated protein phosphatase interactions. Plant Physiology **117,** 1217-1225.

Stone, J.M., Collinge, M.A., Smith, R.D., Horn, M.A., and Walker, J.C. (1994). Interaction of a protein phosphatase with an *Arabidopsis* serine-threonine receptor kinase. Science **266,** 793-795.

Stracke, R., Werber, M., and Weisshaar, B. (2001). The R2R3-MYB gene family in *Arabidopsis thaliana*. Current Opinion in Plant Biology **4,** 447-456.

Stracke, R., Ishihara, H., Huep, G., Barsch, A., Mehrtens, F., Niehaus, K., and Weisshaar, B. (2007). Differential regulation of closely related R2R3-MYB transcription factors controls flavonol accumulation in different parts of the *Arabidopsis thaliana* seedling. The Plant Journal **50,** 660–677.

Su, Y.-F., Yang, T., Huang., H., Liu, L.F., and Hwang, J. (2012). Phosphorylation of Ubc9 by Cdk1 Enhances SUMOylation Activity. PLoS ONE **7**.

Suarez-Rodriguez, M.C., Adams-Phillips, L., Liu, Y., Wang, H., Su, S.-H., Jester, P.J., Zhang, S., Bent, A.F., and Krysan, P.J. (2007). MEKK1 Is Required for flg22-Induced MPK4 Activation in *Arabidopsis* Plants. Plant Physiology **143,** 661-669.

Sugimoto, H., Kondo, S., Muramoto, N., Tanaka, T., Hattori, E., Ogawa, K., Mitsukawa, N., and Ohto, C. (2011). AtPPCF Encodes a Functional *Arabidopsis* PP2C Which Belongs to Group E. 22ND INTERNATIONAL CONFERENCE ON ARABIDOPSIS RESEARCH.

Swarbreck, D., Wilks, C., Lamesch, P., Berardini, T.Z., Garcia-Hernandez, M., Foerster, H., Li, D., Meyer, T., Muller, R., Ploetz, L., Radenbaugh, A., Singh, S., Swing, V., Tissier, C., Zhang, P., and Huala, E. (2008). The *Arabidopsis* Information Resource (TAIR): gene structure and function annotation. Nucleic Acids Research **36,** D1009-D1014.

Taguchi, F., Shimizu, R., Nakajima, R., Toyoda, K., Shiraishi, T., and Ichinose, Y. (2003). Differential effects of flagellins from *Pseudomonas syringae* pv. *tabaci, tomato* and *glycinea* on plant defense response. Plant Physiology and Biochemistry **41,** 165-174.

Takai, R., Isogai, A., Takayama, S., and Che, F.-S. (2008). Analysis of Flagellin Perception Mediated by flg22 Receptor OsFLS2 in Rice. Molecular Plant-Microbe Interactions **21,** 1635-1642.

Takken, F.L.W., and Goverse, A. (2012). How to build a pathogen detector: structural basis of NB-LRR function. Current Opinion in Plant Biology **15,** 375-384.

Tanaka, H., Kitakura, S., De Rycke, R., De Groodt, R., and Friml, J. (2009). Fluorescence Imaging-Based Screen Identifies ARF GEF

Component of Early Endosomal Trafficking. Current Biology **19,** 391-397.

Tavernier, E., Wendehenne, D., Blein, J.P., and Pugin, A. (1995). Involvement of Free Calcium in Action of Cryptogein, a Proteinaceous Elicitor of Hypersensitive Reaction in Tobacco Cells. Plant Physiology **109,** 1025-1031.

Thines, B., Katsir, L., Melotto, M., Niu, Y., Mandaokar, A., Liu, G., Nomura, K., He, S.Y., Howe, G.A., and Browse, J. (2007). JAZ repressor proteins are targets of the SCFCOI1 complex during jasmonate signalling. Nature **448,** 661-665.

Thomma, B.P.H.J., Eggermont, K., Penninckx, I.A.M.A., Mauch-Mani, B., Vogelsang, R., Cammue, B.P.A., and Broekaert, W.F. (1998). Separate jasmonate-dependent and salicylate-dependent defense-response pathways in *Arabidopsis* are essential for resistance to distinct microbial pathogens. Proceedings of the National Academy of Sciences **95,** 15107-15111.

Thordal-Christensen, H. (2003). Fresh insights into processes of nonhost resistance. Current Opinion in Plant Biology **6,** 351-357.

Trotochaud, A.E., Hao, T., Wu, G., Yang, Z., and Clark, S.E. (1999). The CLAVATA1 receptor-like kinase requires CLAVATA3 for its assembly into a signaling complex that includes KAPP and a Rho-related protein. Plant Cell **11,** 393-405.

Tsugama, D., Liu, S., and Takano, T. (2012). A putative myristoylated 2C-type protein phosphatase, PP2C74, interacts with SnRK1 in *Arabidopsis*. FEBS Letters **586,** 693-698.

Tyler, L., Thomas, S.G., Hu, J., Dill, A., Alonso, J.M., Ecker, J.R., and Sun, T.-P. (2004). DELLA Proteins and Gibberellin-Regulated Seed Germination and Floral Development in *Arabidopsis*. Plant Physiology **135,** 1008-1019.

Uberti-Manassero, N.G., Lucero, L.E., Viola, I.L., Vegetti, A.C., and Gonzalez, D.H. (2012). The class I protein AtTCP15 modulates plant development through a pathway that overlaps with the one affected by CIN-like TCP proteins. Journal of Experimental Botany **63,** 809-823.

Umbrasaite, J., Schweighofer, A., Kazanaviciute, V., Magyar, Z., Ayatollahi, Z., Unterwurzacher, V., Choopayak, C., Boniecka, J., Murray, J.A.H., Bogre, L., and Meskiene, I. (2010). MAPK Phosphatase AP2C3 Induces Ectopic Proliferation of Epidermal Cells Leading to Stomata Development in *Arabidopsis*. PLos ONE **5,** e15357.

van der Hoorn, R.A.L., and Kamoun, S. (2008). From Guard to Decoy: A New Model for Perception of Plant Pathogen Effectors. The Plant Cell Online **20,** 2009-2017.

Veronese, P., Nakagami, H., Bluhm, B., AbuQamar, S., Chen, X., Salmeron, J., Dietrich, R.A., Hirt, H., and Mengiste, T. (2006). The Membrane-Anchored BOTRYTIS-INDUCED KINASE1 Plays Distinct Roles in Arabidopsis Resistance to Necrotrophic and Biotrophic Pathogens. The Plant Cell Online **18,** 257-273.

Vlach, J., Hennecke, S., and Amati, B. (1997). Phosphorylation-dependent degradation of the cyclin-dependent kinase inhibitor p27Kip1. EMBO Journal **16,** 5334-5344.

Vogelstein, B., and Kinzler, K.W. (2004). Cancer genes and the pathways they control. Nat Med **10,** 789-799.

Wagner, T.A., and Kohorn, B.D. (2001). Wall-Associated Kinases Are Expressed throughout Plant Development and Are Required for Cell Expansion. The Plant Cell Online **13,** 303-318.

Wan, J., Tanaka, K., Zhang, X.-C., Son, G.H., Brechenmacher, L., Nguyen, T.H.N., and Stacey, G. (2012). LYK4, a LysM receptor-like kinase, is important for chitin signaling and plant innate immunity in *Arabidopsis*. Plant Physiology.

Wan, J., Zhang, X.-C., Neece, D., Ramonell, K.M., Clough, S., Kim, S.-y., Stacey, M.G., and Stacey, G. (2008). A LysM Receptor-Like Kinase Plays a Critical Role in Chitin Signaling and Fungal Resistance in *Arabidopsis*. The Plant Cell Online **20,** 471-481.

Wang, H., Yang, C., Zhang, C., Wang, N., Lu, D., Wang, J., Zhang, S., Wang, Z.-X., Ma, H., and Wang, X. (2011). Dual Role of BKI1 and 14-3-3 s in Brassinosteroid Signaling to Link Receptor with Transcription Factors. Developmental cell **21,** 825-834.

Wang, W.-M., Ma, X.-F., Zhang, Y., Luo, M.-C., Wang, G.-L., Bellizzi, M., Xiong, X.-Y., and Xiao, S.-Y. (2012). PAPP2C Interacts with the Atypical Disease Resistance Protein RPW8.2 and Negatively Regulates Salicylic Acid-Dependent Defense Responses in *Arabidopsis*. Molecular Plant.

Wang, X., and Chory, J. (2006). Brassinosteroids Regulate Dissociation of BKI1, a Negative Regulator of BRI1 Signaling, from the Plasma Membrane. Science **313,** 1118-1122.

Wang, Y.-S., Pi, L.-Y., Chen, X., Chakrabarty, P.K., Jiang, J., De Leon, A.L., Liu, G.-Z., Li, L., Benny, U., Oard, J., Ronald, P.C., and Song, W.-Y. (2006). Rice XA21 Binding Protein 3 Is a Ubiquitin Ligase Required for Full Xa21-Mediated Disease Resistance. The Plant Cell Online **18,** 3635-3646.

Wang, Y., Li, J., Hou, S., Wang, X., Li, Y., Ren, D., Chen, S., Tang, X., and Zhou, J.-M. (2010). A Pseudomonas syringae ADP-Ribosyltransferase Inhibits *Arabidopsis* Mitogen-Activated Protein Kinase Kinases. The Plant Cell Online **22,** 2033-2044.

Widjaja, I., Naumann, K., Roth, U., Wolf, N., Mackey, D., Dangl, J.L., Scheel, D., and Lee, J. (2009). Combining subproteome enrichment and Rubisco depletion enables identification of low abundance proteins differentially regulated during plant defense. PROTEOMICS **9,** 138-147.

Widjaja, I., Lassowskat, I., Bethke, G., Eschen-Lippold, L., Long, H.-H., Naumann, K., Dangl, J.L., Scheel, D., and Lee, J. (2010). A protein phosphatase 2C, responsive to the bacterial effector AvrRpm1 but not to the AvrB effector, regulates defense responses in *Arabidopsis*. The Plant Journal **61,** 249-258.

Wiermer, M., Feys, B.J., and Parker, J.E. (2005). Plant immunity: the EDS1 regulatory node. Current Opinion in Plant Biology **8,** 383-389.

Williams, R.W., Wilson, J.M., and Meyerowitz, E.M. (1997). A possible role for kinase-associated protein phosphatase in the Arabidopsis CLAVATA1 signaling pathway. Proceedings of the National Academy of Sciences **94,** 10467-10472.

Willmann, R., Lajunen, H.M., Erbs, G., Newman, M.-A., Kolb, D., Tsuda, K., Katagiri, F., Fliegmann, J., Bono, J.-J., Cullimore, J.V., Jehle, A.K., Götz, F., Kulik, A., Molinaro, A., Lipka, V., Gust, A.A., and Nürnberger, T. (2011). *Arabidopsis* lysin-motif proteins LYM1 LYM3 CERK1 mediate bacterial peptidoglycan sensing and immunity to bacterial infection. Proceedings of the National Academy of Sciences **108,** 19824-19829.

Winter, D., Vinegar, B., Nahal, H., Ammar, R., and Wilson, G.V. (2007). An "Electronic Fluorescent Pictograph" Browser for Exploring and Analyzing Large-Scale Biological Data Sets. PLos ONE **2**.

Wu, J., Kurten, E.L., Monshausen, G., Hummel, G.M., Gilroy, S., and Baldwin, I.T. (2007). NaRALF, a peptide signal essential for the regulation of root hair tip apoplastic pH in Nicotiana attenuata, is required for root hair development and plant growth in native soils. The Plant Journal **52,** 877-890.

Wu, S., Lu, D., Kabbage, M., Wei, H.-L., Swingle, B., Records, A.R., Dickman, M., He, P., and Shan, L. (2011). Bacterial Effector HopF2 Suppresses *Arabidopsis* Innate Immunity at the Plasma Membrane. Molecular Plant-Microbe Interactions **24,** 585-593.

Wu, Y., Zhang, D., Chu, Jee Y., Boyle, P., Wang, Y., Brindle, Ian D., De Luca, V., and Després, C. (2012). The *Arabidopsis* NPR1 Protein Is a Receptor for the Plant Defense Hormone Salicylic Acid. Cell Reports **1,** 639-647.

Wurzinger, B., Mair, A., Pfister, B., and Teige, M. (2011). Cross-talk of calcium-dependent protein kinase and MAP kinase signaling. Plant Signaling & Behavior **6,** 8-12.

Xiang, T., Zong, N., Zhang, J., Chen, J., Chen, M., and Zhou, J.-M. (2010). BAK1 Is Not a Target of the *Pseudomonas syringae* Effector AvrPto. Molecular Plant-Microbe Interactions **24,** 100-107.

Xiang, T., Zong, N., Zou, Y., Wu, Y., Zhang, J., Xing, W., Li, Y., Tang, X., Zhu, L., Chai, J., and Zhou, J.-M. (2008). *Pseudomonas syringae* Effector AvrPto Blocks Innate Immunity by Targeting Receptor Kinases. Current biology **18,** 74-80.

Xiao, S., Charoenwattana, P., Holcombe, L., and Turner, J.G. (2003). The *Arabidopsis* Genes RPW8.1 and RPW8.2 Confer Induced Resistance to Powdery Mildew Diseases in Tobacco. Molecular Plant-Microbe Interactions **16,** 289-294.

Xie, D.-X., Feys, B.F., James, S., Nieto-Rostro, M., and Turner, J.G. (1998). COI1: An *Arabidopsis* Gene Required for Jasmonate-Regulated Defense and Fertility. Science **280,** 1091-1094.

Xing, W., Zou, Y., Liu, Q., Liu, J., Luo, X., Huang, Q., Chen, S., Zhu, L., Bi, R., Hao, Q., Wu, J.-W., Zhou, J.-M., and Chai, J. (2007). The structural basis for activation of plant immunity by bacterial effector protein AvrPto. Nature **449,** 243-247.

Xu, W.-H., Wang, Y.-S., Liu, G.-Z., Chen, X., Tinjuangjun, P., Pi, L.-Y., and Song, W.-Y. (2006a). The autophosphorylated Ser686, Thr688, and Ser689 residues in the intracellular juxtamembrane domain of XA21 are implicated in stability control of rice receptor-like kinase. The Plant Journal **45,** 740-751.

Xu, X., Chen, C., Fan, B., and Chen, Z. (2006b). Physical and Functional Interactions between Pathogen-Induced *Arabidopsis* WRKY18, WRKY40, and WRKY60 Transcription Factors. The Plant Cell Online **18,** 1310-1326.

Xue, T., Wang, D., Zhang, S., Ehlting, J., Ni, F., Jakab, S., Zheng, C., and Zhong, Y. (2008). Genome-wide and expression analysis of protein phosphatase 2C in rice and Arabidopsis. BMC genomics **9,** 550.

Yamaguchi, Y., and Huffaker, A. (2011). Endogenous peptide elicitors in higher plants. Current Opinion in Plant Biology **14,** 351-357.

Yamaguchi, Y., Pearce, G., and Ryan, C.A. (2006). The cell surface leucine-rich repeat receptor for AtPep1, an endogenous peptide elicitor in *Arabidopsis*, is functional in transgenic tobacco cells. Proceedings of the National Academy of Sciences **103,** 10104-10109.

Yamaguchi, Y., Huffaker, A., Bryan, A.C., Tax, F.E., and Ryan, C.A. (2010). PEPR2 Is a Second Receptor for the Pep1 and Pep2 Peptides and Contributes to Defense Responses in *Arabidopsis*. The Plant Cell Online **22,** 508-522.

Yan, Y., Stolz, S., Chételat, A., Reymond, P., Pagni, M., Dubugnon, L., and Farmer, E.E. (2007). A Downstream Mediator in the Growth Repression Limb of the Jasmonate Pathway. The Plant Cell Online **19,** 2470-2483.

Yang, C.-J., Zhang, C., Lu, Y.-N., Jin, J.-Q., and Wang, X.-L. (2011). The Mechanisms of Brassinosteroids' Action: From Signal Transduction to Plant Development. Molecular Plant **4,** 588-600.

Yoo, S.-D., Cho, Y.-H., Tena, G., Xiong, Y., and Sheen, J. (2008). Dual control of nuclear EIN3 by bifurcate MAPK cascades in C2H4 signalling. Nature **451,** 789-795.

Yu, H., Ito, T., Zhao, Y., Peng, J., Kumar, P., and Meyerowitz, E.M. (2004). Floral homeotic genes are targets of gibberellin signaling in flower development. Proceedings of the National Academy of Sciences **101,** 7827-7832.

Yu, L.P., Miller, A.K., and Clark, S.E. (2003). POLTERGEIST Encodes a Protein Phosphatase 2C that Regulates CLAVATA Pathways Controlling Stem Cell Identity at *Arabidopsis* Shoot and Flower Meristems. Current biology **13,** 179-188.

Yu, L.P., Simon, E.J., Trotochaud, A.E., and Clark, S.E. (2000). POLTERGEIST functions to regulate meristem development downstream of the *CLAVATA* loci. 127 **8**.

Zaltsman, A., Krichevsky, A., Loyter, A., and Citovsky, V. (2010). *Agrobacterium* Induces Expression of a Host F-Box Protein Required for Tumorigenicity. Cell Host & Microbe **7,** 197-209.

Zeng, W., and He, S.Y. (2010). A Prominent Role of the Flagellin Receptor FLAGELLIN-SENSING2 in Mediating Stomatal Response to *Pseudomonas syringae* pv *tomato* DC3000 in *Arabidopsis*. Plant Physiology **153,** 1188-1198.

Zhang, J., Shao, F., Li, Y., Cui, H., Chen, L., Li, H., Zou, Y., Long, C., Lan, L., Chai, J., Chen, S., Tang, X., and Zhou, J. (2007). A *Pseudomonas syringae* Effector Inactivates MAPKs to Suppress PAMP-Induced Immunity in Plants. Cell Host & Microbe **1,** 175-185.

Zhang, J., Li, W., , Xiang, T., Liu, Z., Laluk, K., Ding, X., Zou, Y., Gao, M., Zhang, X., Chen, S., Mengiste, T., Zhang, Y., and Zhou, J.M. (2010). Receptor-like Cytoplasmic Kinases Integrate Signaling from Multiple Plant Immune Receptors and Are Targeted by a *Pseudomonas syringae* Effector. Cell Host & Microbe **7,** 290-301.

Zhang, Z., Wu, Y., Gao, M., Zhang, J., Kong, Q., Liu, Y., Ba, H., Zhou, J., and Zhang, Y. (2012). Disruption of PAMP-Induced MAP Kinase Cascade by a *Pseudomonas syringae* Effector Activates Plant Immunity Mediated by the NB-LRR Protein SUMM2. Cell Host & Microbe **11,** 253-263.

Zheng, X.-y., Spivey, Natalie W., Zeng, W., Liu, P.-P., Fu, Zheng Q., Klessig, Daniel F., He, Sheng Y., and Dong, X. (2012). Coronatine Promotes *Pseudomonas syringae* Virulence in Plants by Activating a Signaling Cascade that Inhibits Salicylic Acid Accumulation. Cell Host & Microbe **11,** 587-596.

Zheng, Z., Mosher, S., Fan, B., Klessig, D., and Chen, Z. (2007). Functional analysis of Arabidopsis WRKY25 transcription factor in plant defense against *Pseudomonas syringae*. BMC Plant Biology **7,** 2.

Zhou, F., Xue, Y., Yao, X., and Xu, Y. (2006). CSS-Palm: palmitoylation site prediction with a clustering and scoring strategy (CSS). Bioinformatics **22,** 894-896.

Zipfel, C., and Felix, G. (2005). Plants and animals: a different taste for microbes? Current Opinion in Plant Biology **8,** 353-360.

Zipfel, C., and Rathjen, J.P. (2008). Plant Immunity: AvrPto Targets the Frontline. Current biology **18,** R218-R220.

Zipfel, C., Robatzek, S., Navarro, L., Oakeley, E.J., Jones, J.D.G., Felix, G., and Boller, T. (2004). Bacterial disease resistance in *Arabidopsis* through flagellin perception. Nature **428,** 764-767.

Zipfel, C., Kunze, G., Chinchilla, D., Caniard, A., Jones, J.D.G., Boller, T., and Felix, G. (2006). Perception of the Bacterial PAMP EF-Tu by the Receptor EFR Restricts *Agrobacterium*-Mediated Transformation. Cell **125,** 749-760.